PARAMETRIC STUDY OF A CABLE-STAYED BRIDGE UNDER SEISMIC LOADS

By
Sven Mayer
Steven L. McCabe

Structural Engineering and Engineering Materials
SM Report No. 52
September 1998

THE UNIVERSITY OF KANSAS CENTER FOR RESEARCH, INC.
2291 Irving Hill Drive - Campus West, Lawrence, Kansas 66045

Parametric Study of a Cable-Stayed Bridge under Seismic Loads

By
Sven Mayer
Steven L. McCabe

Structural Engineering and Engineering Materials
SM Report No. 52

UNIVERSITY OF KANSAS CENTER FOR RESEARCH, INC.
LAWRENCE, KANSAS
September 1998

ACKNOWLEDGEMENTS

We wish to thank Mr. Maury Miller and Mr. Steve Hague of HNTB Corporation, and the Missouri Department of Transportation for providing the necessary documents and information about the Cape Girardeau bridge. Their helpful assistance and cooperation during this project is greatly appreciated. Without their support this project would not have been possible.

Appreciation is also to be given to the Department of Civil and Environmental Engineering at the University of Kansas for supporting Mr. Mayer and allowing the use of their equipment. We also would like to thank Mr. Ken Pearce, Director of the Engineering Computing Services at Learned Hall for providing high performance computing capabilities during the entire project.

ABSTRACT

The topic of this paper is a parametric study of a cable-stayed bridge under seismic loads. The bridge modeled in this study is the Bill Emerson Bridge crossing the Mississippi River at Gape Girardeau in Missouri. A description of the development of the 3-D finite element model for both a linear and nonlinear dynamic analysis is given by using the original bridge design. Then a collection of parameters was studied as to their effect on the dynamic response. Different deck elements (e.g. girder box, slab, etc.), pylons (e.g. A-shape, H-shape, etc), cable areas, and material properties are used. Linear and nonlinear multiple, single response spectrum analyses with an emphasis on the nonlinear cable behavior are performed in this parametric study.

The study showed that a composite concrete steel girder and a concrete box performed the best. Further it showed that A-shape towers stabilized the structure horizontally and increased the torsional stiffness. The doubling of the cable area decreased the vertical displacements up to 30 %. Therefore, a doubling of the cable area might be reasonable depending on the applications.

The multiple response-spectrum analysis lead to higher displacements than the single response-spectrum analysis. Consequently a multiple response spectrum analysis is preferable, if multiple excitation-input data are available.

The comparison between the non-linear and linear analysis demonstrated that for this bridge the non-linear effects of the cables were small and could be ignored. Nevertheless, for long span cable stayed bridges, the nonlinear effects of the cables should be considered.

TABLE OF CONTENTS

LIST OF TABLES

LIST OF FIGURES

Page

CHAPTER 1: INTRODUCTION

1.1 General

In recent years, medium and long span cable-stayed bridges have become increasingly popular. Their aesthetic appearance and economic design make them interesting for engineers and State Transportation Departments.

The Bill Emerson Bridge at Cape Girardeau, located 100 miles south of St. Louis, is a good example of this type of bridge, see Fig. 1. The original narrow truss bridge was not suitable for the steadily increasing traffic loads. This situation called for a new and wider bridge. A cable-stayed bridge was selected by MODOT, as the most economic and aesthetic alternative.

While the designers considered the financial aspects of the bridge, the structure's performance during seismic activity also had to be considered, because the bridge is located only 50 miles south of the New Madrid seismic zone, see Fig. 1.2. The geotechnical report indicated that there is a 90 percent chance that an earthquake with a magnitude up to 8.5 might occur in the next 250 years. Therefore, the engineers designed the bridge to resist an earthquake up to this magnitude.

The development of a 3-D finite element model is described and then results from the parametric study (with an emphasis of the deck, pylons, cables and material properties) are discussed, because the overall stiffness, stability and serviceability are mainly controlled by their performance. The results are compared and help to

understand the basic behavior of cable-stayed bridges under seismic loads. At the end, design recommendations are given which should improve the design of future cable-stayed bridges in high seismic zones.

1.2 Description of the Bill Emerson Bridge at Cape Girardeau

The Bill Emerson Bridge, shown in Fig. 1.1, was designed in 1994. Construction started in 1997 and the structure is not yet completed. The main span of the bridge is 1150-ft (345 m); then there are two equal side spans of 485-ft (140 m) which make a total length of 2086-ft (625 m), shown in Fig. 1.3. The bridge consists of two H-shaped concrete towers, double-plane fan type cables, and a composite concrete–steel girder bridge deck. The towers are 320-ft (96 m) high above the water level, and the deck is 96-ft (29 m) wide. A total of 128 cables, 64 supporting the main span and 64 supporting each side span, are anchored to the towers and to the deck.

The road deck consists of two 11-in (275 mm) precast concrete slabs with a 3-in (75 mm) silica fume concrete wearing surface and three non-structural traffic barriers. A typical cross-section of the bridge deck is shown in Fig. 1.4. Each of the precast concrete slabs is 17.5-ft (5.25 m) wide and 48-ft (14.5 m) long. Two non-structural traffic barriers sit on the edges of the road lanes and one barrier is in the center to divide the traffic lanes.

The deck's floor beams are equally spaced longitudinally in intervals of 17.5-ft (5.25 m) and transport the deck loads to the edge girders. At the outer edge of the

deck, the two edge girders are 92-ft (27.6 m) apart from each other in the transverse direction. Both consist of structural steel ASTM A 572 Grade 50. The cables are connected every 35-ft (10.5 m) to the top flanges of the edge girders and to the towers.

The two towers are shown in Fig. 1.5 and 1.6. Each of them consists of two concrete legs, which are 12-ft (3.6 m) long in the transverse direction and 22-ft (6.6 m) long in the longitudinal direction, one lower strut supporting the deck and an upper strut connected to the upper legs. The dimensions of the two legs are variable throughout the height of the towers. From the foundation up to the lower strut the two legs have the above mentioned dimensions and are connected by a solid 8-ft (2.4 m) thick concrete wall, as can be seen in Fig. 1.5 and 1.6 in cross section E-E. The lower strut itself is 13-ft (3.9 m) wide and has an average height of 12-ft (3.6 m), see cross-section D-D in Fig. 1.5 and 1.6. From the lower strut upward to the upper struts, the two legs are 22-ft (6.6 m) long in the longitudinal direction. The transverse direction becomes narrower toward the upper strut. It starts with 12-ft (3.6 m) at the lower strut and ends with 9-ft (2.7 m) at the upper strut.

In addition, a rectangular access passageway that starts with 8.5-ft x 16-ft (2.55 m x 4.8 m) and ends with 5.5-ft x 16-ft (1.65 m x 4.8 m) is provided in both towers, as shown by cross-section B-B in Fig. 1.5 and 1.6. The upper strut is 17-ft (5.1 m) wide and has an average height of 15-ft (4.5 m), see cross-section C-C in Fig. 1.5 and 1.6. The third section change occurs above the upper strut to the top of the towers. The

legs are 22-ft (6.6 m) long in the longitudinal direction and 9-ft (2.7 m) wide in the transverse direction. A rectangular access hole is located in the two legs with dimensions of 5.5-ft x 13-ft (1.65 m x 3.9 m), which can be seen in cross-section A-A in Fig. 1.5 and 1.6.

At both towers, vertical steel bearings are provided that allow sliding in the horizontal plane, see Fig. 1.7 and 1.8. In the horizontal direction, an earthquake shock transmission device is installed to allow some movement in the transverse direction during such an occurrence, see Fig. 1.9. At the ends of the bridge are tie-down links to the piers, which are illustrated in Fig. 1.10 and 1.11.

Next, the cables are constructed of 0.6-in (15 mm) diameter ASTM A 416 strands and have varying cross section areas from 4.34 in^2 to 11.72 in^2 (2712.5 mm^2 to 7325 mm^2), as shown in Fig. 1.12. and Table 2.2. They are wrapped hellically with a polyethylene covering and are grouted and sealed, see Fig. 1.16. The cables are anchored every 35-ft (10.5 m) to the edge girders and floor beams throughout approximately the entire length of the bridge. The first five cables at each end of the bridge are anchored every 12-ft (3.6 m) At the upper part of the towers the first 12 cables are anchored in 5-ft (1.5 m) intervals. The other four cables are anchored in 6-ft, 7-ft, 8-ft and 14-ft (1.8 m, 2.1 m, 2.4 m, and 4.2 m) intervals, as can be seen in Fig. 1.14 and 1.15.

1.3 Project Description and Objectives

The scope of this project is to examine a cable stayed bridge with varying performances under the effects of seismic loads. Cable non-linearities are considered and different types of analyses, e.g. single response spectrum and multiple response spectrum analyses are performed to determine the response of the bridge to seismic loads. This study will lead to an understanding of the basic behavior of cable-stayed bridges under seismic loads.

This project's work is performed in four major phases. The first phase is to use all the available geometric information about the bridge and to develop a 3-D finite element model. After that, a parametric study is performed with an emphasis on the main structural elements, deck, cables, and towers. The third phase is to evaluate and compare those results. In the last phase conclusions are made and design recommendations or design guidelines are given for future designs of cable-stayed bridges in high seismic zones.

CHAPTER 2: FINITE ELEMENT MODELING

2.1 General

The modeling process was divided into three phases. First one has to determine whether a 2-D or a 3-D model should be used. Previous investigations by Wilson [29,28] have shown that 2-D models were too conservative and not accurate enough. For example, in investigations by Nazmy [19] no coupled modes occurred in the 2-D modal analyses, indicating that there were only vertical and transverse modes. Coupled modes were not present, which is not accurate according to Nazmy [19]. The 3-D modal analyses showed that coupled modes do exist and that there are not only vertical and transverse modes present, but also torsional and torsional coupled with transverse modes. Therefore, it was determined to use a 3-D finite element model for this study.

The second phase involved geometric considerations for the bridge. After an examination of the drawings, the structure was divided into the three main parts, deck, cables and pylons and for each part, a suitable 3-D finite element model was developed.

During the third phase, constraints were determined and applied to the model. Both the second and third phases are described in more detail later in this chapter.

The finite element program ANSYS 5.3 was used to create the models and to perform the following analysis.

Five models emerged from the considerations from the scope of the parametric study. Those five models are presented in the following material. The first model was modeled after the original design. The other four models were developed for the parametric study and represent alternatives to the original design. During the modeling of the alternatives most of the elements of the original model were conserved with a few changes in these models.

2.2 Model 1

As mentioned earlier, this model represented the original design of the Bill Emerson Bridge. The modeling of the three main structural parts of the bridge is explained below.

2.2.1 Deck

The deck is a composite concrete–steel girder bridge deck, as shown in Fig. 1.4. It consists of steel floor beams, steel edge girders and a precast concrete slab. As described, earlier the floor beams are spaced in 17.5-ft (5.25 m) intervals and the cables are anchored every 35-ft (10.50 m) to the top flange of the edge girders. This made it convenient to model a 35-ft (10.50 m) long and 96-ft (28.8 m) wide section. Later this section was inserted over the whole length of the deck. It consisted of one slab; two edge girders at the outer edges of the slab and three floor beams spaced equally 17.5-ft (5.25 m) in the transverse direction, see Fig. 2.4. The thickness of

those elements were small, e.g. the webs were up to one inch (25 mm) thick and the flanges were up to 2.5-in (62.5 mm) thick, as can be seen in Fig. 1.4. Therefore, elastic shell elements with six degrees of freedom were used for all the elements, because shell elements proved to be accurate for analyses of thin structures. Concrete properties such as Modulus of Elasticity, Density, and Poisson's ratio were assigned to the slab, and steel properties were assigned to the beams and girders. Overall, 58 deck sections were used to model the whole deck. Nodes were placed at the connection points to the towers, at the connection points to the piers, the anchor points of the cables, and at locations where results were needed.

2.2.2 Towers

The towers consist of concrete legs, struts and walls, as described earlier and shown in Fig. 1.5 and 1.6. The legs and struts were assumed to behave like beams and were expected to act like beams. Therefore, elastic 3-D beam elements with six degrees of freedom were used. As mentioned in Chapter One, the cross-section of the legs and struts changed over the height and length of the towers. This was considered by dividing the towers in six sections and calculating the gross cross section properties for each section. All material properties and gross cross section properties for the legs and struts are shown in Table 2. The concrete wall between the two legs was modeled with the same elastic shell elements that were used for the deck elements. The reason for that was that 3-D elements and shell elements are

compatible and interact well, which leads to accurate results.

Overall 450 beam elements and 150 shell elements were used for the two towers. Nodes were mainly placed at section changes, connection points to the deck, and the anchor locations at the upper parts of the towers.

2.2.3 Cables

The cables consist of 0.6-in (15 mm) diameter strands with varying cross sectional areas from 4.34 in^2 to 11.72 in^2 (2712.5 mm^2 to 7325 mm^2), as shown in Fig. 1.12. These elements were modeled as linear elastic 3-D link elements with three degrees of freedom. Investigations by Wilson [29] showed that it is appropriate to use link elements with a special equivalent Modulus of Elasticity to consider the sag effect of cables. Under certain circumstances this approximation works well according to Wilson [29]. A definition and explanation of the equivalent Modulus of Elasticity will be given later in Chapter Three.

Just a single link element with Nodes at the ends, where the cables are connected to the deck and towers, was used to model each of the 128 cables. Each link was modeled by using all the geometric and material property information, e.g. length, cable area, etc. from the drawings or the accompanying papers. An overview of all those material and geometric properties for each cable is given in Table 2.2 and Fig. 1.13.

2.2.4 Deck-Tower Bearings

Figures 1.7, 1.8 and 1.9 show the deck tower bearings. Their elements were designed to allow sliding in the longitudinal direction and some movement in the transverse direction to decrease the seismic forces in the deck. The vertical direction was assumed to be fixed. This situation required a special solution. Publications by Khali [15] indicated that the easiest and most appropriate way to model the bearings would be by using elastic 3-D link elements in the vertical and horizontal direction. This allows an adjustment of the stiffness of the links, to simulate the free movement in the longitudinal direction, limiting movement in transverse direction, and fixation in vertical direction. Therefore, it was chosen for the modeling process. Four link elements two on each side of the towers were used, one in the vertical direction and one in the longitudinal direction, as can be seen in Fig. 2.2 The material and geometric properties were selected according to the determined stiffness of the links, which is explained in 4.7. and 5.5.6.

2.2.5 Piers and Abutments

The towers are founded on bedrock, which means the tower base can be treated as being fixed. The ends of the deck are connected to the piers by a tension-link mechanism, which can be seen in Fig. 1.10 and 1.11. This allows the deck to rotate freely about the vertical axis and the transverse axis. The transational degrees of freedom are fixed in transverse and vertical directions on both abutments. The

longitudinal translation is fixed on one abutment only, which allows the deck to move in longitudinal direction during an earthquake. As a result, the rotation about the longitudinal axis, and the movement in transverse and vertical directions, were constrained at both abutments. In addition the movement in the longitudinal direction was fixed at one abutment. This constraint case was determined as the best in this study and, therefore, it was used for all models.

2.3 Model 2

The second model was not significantly different from the first, with only the deck configuration differing from the first. The towers, cables, and constraints were the same.

For the deck a prestressed concrete slab was used, which is a lesser-known alternative to the composite design and is shown in Fig. 2.

2.3.1 Deck

For the slab a precast concrete slab with a average thickness of 18-in (450 mm) was used, which favored shell elements as the best choice. Therefore, 3-D elastic shell elements with six degrees of freedom were selected. The same modeling procedure used for the first model was employed here. One deck element 35-ft (10.5 m) x 96-ft (28.8 m) was created and inserted 58 times across the whole deck length. Nodes were

created at the connection points to the towers and at the anchor locations of the cables.

2.4 Model 3

This model used a popular alternative for the deck, a prestressed concrete box, which can be seen in Fig. 2.1. A 10-in (250 mm) thick slab on the top, two vertical 8-in (200 mm) thick walls under the slab, one 8-in (200 mm) thick slab on the bottom, and two 8-in (200 mm) thick slabs on the sides that connected the bottom to the top slab were used. Again the towers, cables and constraints were the same, as for Model 1.

2.4.1 Deck

As mentioned above, the slab thicknesses were small and favored the same elastic 3-D shell elements with six degrees of freedom that were used for the slabs in Models 1 and 2. The deck was modeled the same way as in the previous two cases mentioned. One deck element was created and inserted as often as necessary over the whole length of the bridge. This one deck element consisted of one slab on the top, two walls sitting at the third points of the slab, one connected to the ends of the vertical walls, and two slabs on each side that connected top to bottom. Nodes were created at the connection points to the towers and at the anchor location of the cables.

2.5 Model 4

In this model, the tower configuration was changed. An A-shaped tower with two concrete legs, one lower strut supporting the deck, and two upper struts connected to the legs, see Fig. 2.3, was used instead of an H-shape tower. The dimensions of the concrete legs changed in three sections over the height of the towers. The first section extended from the foundation up to the first strut. The legs were 22-ft (6.6 m) long in the longitudinal direction and 12-ft (3.60 m) in the transverse direction. Above the strut the legs became narrower toward the first upper strut. With dimensions mentioned above, the struts ended up with 22-ft (6.6 m) in the longitudinal direction and 9-ft (2.7 m) in the transverse direction. In addition, a rectangular passageway 8.5-ft (2.55 m) x 16-ft (4.8 m) and 5.5-ft (1.65 m) x 16-ft (4.8 m) was located in the center of the legs. The third section started above the first upper strut and went until the strut at the top of the tower. The legs maintained this dimension. Only the rectangular passageway became narrower in the longitudinal direction, and decreased to 13-ft (3.9 m). The two upper struts had the same dimensions 17-ft (5.1 m) wide and 15-ft (4.5 m) high with a rectangular access hole of 13-ft (3.9 m) x 11-ft (3.3 m). The lower strut was solid concrete 13-ft (3.9m) x 14-ft (4.2 m). The deck, cables and constraints were the same as in the other models.

2.5.1 Towers

The modeling process of the A-shape towers was similar to the one of the H-shape

towers. The struts and legs were modeled as elastic 3-D beam elements with six degrees of freedom. As described in 2.5, the tower had several section changes in the height. That meant that each section had different gross cross-section properties. To each section, different gross-cross section properties were applied. Those gross cross-section properties were calculated and are shown in Table 2.1. Overall the tower consisted of 596 beam elements. Nodes were placed at the points that were connected to the deck, and at the cable anchor point at the upper part of the tower.

2.6 Model 5

The fifth model was a combination of the second and the fourth models. The towers were A-shaped towers, as described in 2.5. The deck consisted of a prestressed concrete slab, which was used for Model 2. The cables and the constraints remained the same as in all the previous models.

2.61 Deck

The modeling process was the same, as used for Model 2 and is described in 2.3.1.

2.62 Tower

The towers were modeled as described in 2.5.1.

CHAPTER 3: ANALYSIS DESCRIPTION

3.1 General

The topic of this study was to investigate the dynamic behavior of cable-stayed bridges under seismic loads. Therefore, a linear and non-linear dynamic analysis was performed. Publications by Abdel-Ghaffar [1,2,3] indicated that the non-linear behavior of cables should be considered during a dynamic analysis, especially for medium to long span cable-stayed bridges. The procedure to be used will be explained later in more detail. The results of both linear and non linear analysis types will be compared and conclusions will be drawn.

Two methods of seismic analysis were used, the single response spectrum analysis and multiple response spectrum analysis. Investigations by Nazmy [19] showed that the results from the multiple response spectrum analysis were significantly different from the single response spectrum analysis results. Therefore, in this study single and multiple excitations were applied at the base of the towers and at the pier abutments. The results will show how much these two methods differ from each other.

Those methods of analyses were performed first on Model 1, which represented the original design. Then they were used for the parametric study and the results were compared. The following paragraphs explain the different analysis methods in more detail.

3.2 Linear Dynamic Analysis

In the linear dynamic analysis it was assumed that the behavior was linear. Small deflections and no material or geometrical non-linearities were assumed. The deformations of all elements remain in the elastic range.

3.2.1 Single Response Spectrum Analysis

A single response spectrum analysis was used to calculate the response to random loading conditions such as earthquake and wind. The results of the necessary preceding modal analysis were used with a specified spectrum to calculate the displacements and stresses in the model.

As mentioned above, at first a modal analysis was performed to determine the natural frequencies of the model. According to Wilson [29,30] 20 to 30 modes in the range between 0.2 hz and 2 hz should give an accurate response for structures of this size. Therefore twenty to thirty modes were used in the range mentioned above.

After the controlling natural frequencies of the models were determined response spectra were applied to determine the maximum response of the structure. Figures 3.2, 3.3, and 3.4 show the two horizontal and the one vertical response spectra for pier one. Figures 3.5, 3.6, and 3.7 show the response spectra for pier two, and Figs. 3.8 to 3.13 show the response spectra for pier three and four.

In a single response spectrum analysis, just one spectrum curve could be applied to all base excitations. Therefore, the largest spectrum curve was used for the single

response spectrum analysis. Figure 3.14 shows which spectra curve was the largest. This curve was then applied to all base excitation, see Fig. 3 with a constant damping factor of five percent, which is a commonly used damping factor according to Khali [15]. In order to get the maximum response for the structure the square root of sum of squares (SRSS) mode combination was used.

3.2.2 Multiple Response Spectrum Analysis

The multiple response spectrum analysis is similar to the single response spectrum analysis with the difference being that various spectrum curves were applied at different points in the structure, as shown in Fig. 3.1. As mentioned earlier, the twelve spectrum curves for the piers can be seen in Figs. 3.2 to 3.13. Spectrum curves one to three were applied to the base of pier one. Spectrum curves four to six were applied to tower one. Spectrum curves seven to nine were applied to tower two and spectrum curves ten to twelve were applied to pier two, see Fig. 3.1. A damping factor of five percent was also used here. As mentioned in 3.2.1, in order to get the maximum response of the structure, a SRSS mode combination was used.

3.3 Nonlinear Dynamic Analysis

As described earlier the non-linear behavior of the cables was a main concern. Therefore, the non-linear analysis was limited to the sag effect of the cables, which is highly non-linear. No geometric non-linearity or large deflections were considered in

this analysis. Several investigations concerning the non-linear behavior of cables found in cable-stayed bridges have already been done. Ernst [5] was the first person who introduced an equivalent Modulus of Elasticity for the cables. His work resulted in the following expression:

$$Eq = E/(1+ (\gamma l)^2)/12\ \sigma^3 \qquad \text{(Eq. 3.1)}$$

Where σ = stress in the cable, l = horizontal length of the cable, γ = density (weight per unit volume), E = Modulus of Elasticity of steel, and Eq = Equivalent Modulus of Elasticity. This formulation was valid for a single value of stress. Therefore Ernst developed a second expression:

$$Eq = E/(1+ [(\gamma l)^2 *(1+\mu)^4 *E] /12\ \sigma m^3\ 16\mu^2 \qquad \text{(Eq. 3.2)}$$

Where $\mu = \sigma_{low}/\sigma_{up}$, and $\sigma_m = (\sigma_{low} + \sigma_{up})/2$. This equation was used in this study to determine the equivalent Modulus of Elasticity. It is valid for a cable that works between two stress levels, σ_{low} and σ_{up}.

Leonhardt [16] presented a derivative of Ernst's equations. Leonhardt considered a simple supported inclined cable with $E = \infty$, see Fig. 3.15. By increasing the value of the force N that acts on both ends of the cable towards infinity, the shape of the cable approaches a straight line. An increase of the force from N to N1 = N +ΔN

caused an extension $\Delta\Delta s$ of the cable. An apparent specific extension $\varepsilon f = \Delta\Delta s/s$ can be defined and from there an apparent Modulus of Elasticity, E_f can be defined:

$$Ef = \sigma/\varepsilon f \qquad \text{(Eq. 3.3)}$$

The specific stress-strain relationship of a cable is characterized by its Modulus of Elasticity $E = \sigma/\varepsilon$. An equivalent Modulus of Elasticity that considers the two above-mentioned phenomena can be defined.

$$Eq = \sigma/(\varepsilon + \varepsilon_f) \Rightarrow E_f E/ E_f + E \Rightarrow E/(1+E/ E_f) \qquad \text{(Eq. 3.4)}$$

If the ratio between the sag f and the length of the inclined cable is low, a parabola can be used as an approximation for the catenary. For this case Ernst established the following equation:

$$Ef = 12\ \sigma^3 /(\gamma l)^2) \qquad \text{(Eq. 3.5)}$$

Using Eq. 3.5 with Eq. 3.4 gives Eq. 3.1. Eq. 3.2. can be derived by using Ernst's secant modulus in Eq. 3.6 with Eq. 3.4.

$$Ef = 12\ \sigma m^3 * 16\mu^2 /(\gamma l)^2 * (1+\mu)^4 \qquad \text{(Eq. 3.6)}$$

Figure 3.16 show the equivalent Modulus of Elasticity and its dependence on the cable length and the stress level. The shorter the cable and the higher the stress level, the smaller the difference between the equivalent Modulus of Elasticity and the normal value. If the force increases toward infinity, the cable behaves more like a straight steel bar.

Figure 1.13 and 1.14 show the necessary cable properties that were needed for the calculation of the equivalent Modulus of Elasticity. The results of the calculations are shown in Table 3. The short cables had an Eq that was close to 29000 ksi, which was used for the linear analysis; even the longest cable had an Eq with 28763 ksi that was close to the one used in the linear analysis, which is shown in Table 3.

The explanation might be that the lengths of the cables are short and the stress levels are high. Ernst's chart in Fig. 3.16 supports this assumption. It shows the equivalent Modulus of Elasticity as a function of stress and cable length. Clearly the equivalent Modulus of Elasticity drops with an increase of cable length and decrease of stress level. The longest cable that was used in this study was 400-ft (138 m), and the stress level was between 80 and 118 ksi. The Eq in Fig 3.16 for those data is close to 29000 ksi. Therefore, the nonlinear effects of the cable are negligible for this case. This behavior is discussed more in Chapter Five when the results of the linear and non-linear analyses are considered.

CHAPTER 4: PARAMETRIC STUDY

4.1 Description of Parametric Study

Former investigations by Walther [28] have shown that the static behavior of a cable-stayed bridge is influenced mainly by the interaction between the principal characteristics of the bridge, e.g. deck inertia, cable area, tower layout and connection between the pylons and the deck. There have been few studies on the dynamic behavior of cables-stayed bridges. Therefore, this parametric study investigated the dynamic behavior of cable-stayed bridges with the emphasis on the main structural elements: deck, towers, and cables.

Different deck elements, tower shapes, and cable areas were used and the results compared. Later, the parametric study was extended to include material properties, slab thicknesses, tower-deck bearings, and the piers and abutments constraints. For example, instead of concrete properties, steel properties were applied to the model or different constraints were used at the abutments. All results from those cases helped explain the basic dynamic behavior of cable-stayed bridges and to find the most favorable configuration. The main elements of the parametric study are explained separately and in detail in the following:

4.2 Deck

Three different types of deck configurations were considered in this study: a composite concrete-steel deck, a concrete box, and a prestressed precast concrete slab shown in Figs. 1.4, 2, and 2.1. A detailed description of each deck configuration was given in Chapter Two and can be reviewed there. These three cases represent different moments of inertia categories: the slab had the lowest moment of inertia with an I of 1500000 in^4, followed by the box design with an I of 124757805 in^4 and the composite design with an I of 128633270 in^4. The results provide an idea of the level of influence of the value of the deck moment of inertia in a dynamic analysis of a cable-stayed bridge. Their values will also show which deck configuration performs the best in combination with the other structural elements, such as cables and towers.

4.3 Towers

Two different types of towers were used, an A-shape tower and an H-shape tower. The H-shape tower was part of the original design. Both tower configurations are shown in Figs. 1.5, 1.6, and 2.3. A detailed description of the configuration of both towers was given in Chapter Two.

Many researchers, as Walther [28] have indicated that the A-shape towers are a better choice because of their higher torsional stiffness, especially if used for long cable-stayed bridges. The advantage of the H-shape tower, which was used in the design of the Bill Emerson bridge was that the 8-ft (2.4 m) thick wall at the base of

the towers added a great deal of stiffness to the towers. Conversely, the legs were not connected at the top of the tower and could cause large displacements at the top of the tower. In addition, the construction costs may be higher because of the additional concrete wall between the lower legs of the towers. The results in Chapter Five will show which tower configuration performed better.

4.4 Cables

As mentioned earlier in Chapter Three, a cable behaves in a non-linear way. It can take just tension and loses stiffness the more it sags. Therefore, a comparison between a linear analysis and a non-linear analysis, which considers just the non-linear behavior of the cables, was performed. The results of that comparison are shown and discussed in detail in Chapter Five.

Another interesting aspect that was examined was the area of the cables. Four cases, including the original one were created. The first case used half of the cable area of the original design. The second one used the original design data. In the third case the cable area was doubled, and in the fourth case it was tripled. This range showed how changing of the cable area affected the behavior of the structure. Chapter Five will give results and answers to these cases.

4.5 Material Properties

One main question posed in the beginning stage of almost every design process is

whether steel, concrete or other material should be used. Thus, it is necessary to determine which material is most suitable under the present configurations and loads.

At first, a dynamic analysis with a concrete box was performed. This concrete box is shown in Fig. 2.1. Then the concrete was exchanged for a combination of steel and concrete, where the slab remains in concrete and the superstructure was in steel. Fig. 4 shows this box configuration. The results of those calculations are shown in Chapter Five and will show which material performs the best.

4.6 Slab Thickness

In 4.2 it was mentioned that a simple prestressed precast concrete slab was used for the deck. Previously, the goal was to determine the best deck configuration out from the three mentioned. A more comprehensive look is taken at the slab thickness here. Three slab thicknesses were used 14-in (350 mm), 18-in (450 mm), and 25-in (625 mm). The results showed which was the most appropriate slab thickness to use. The optimum slab thickness was used for the prestressed precast concrete slab case in 4.2.

4.7 Tower-Deck Bearings

The type of connection between the deck and the towers has a significant effect on the structure under seismic loads, as already mentioned in the description of the modeling of the deck-tower bearings in Chapter Two. Many investigators, as Wilson [29,30] have already studied this problem. In this study only the effects of deck-tower

bearings on the original design of the Bill Emerson Bridge were investigated. As described in Chapter Two, the connections were modeled by using vertical and horizontal link elements. The stiffness of those elements was increased and decreased to simulate a fixed, half-fixed, or movable connection. Since the area and the Modulus of Elasticity mainly control the stiffness of those link elements; an infinitive high Modulus of Elasticity was used for the fixed case to simulate the high stiffness. On the other hand a low Modulus of Elasticity was used to simulate the low stiffness for the movable case. The area of the link elements was chosen according to the size of the real tower bearings. The results of this investigation should determine which connection type is the most favorable for a cable-stayed bridge under seismic loads. This connection type was then used for all the other models and the rest of the study.

4.8 Pier and Abutments Constraints

Several investigations by Leonhardt [16], Wilson [29,30] and Abdel-Ghaffar [1,2,3] have shown that the choice of the constraints can have a considerable influence on the behavior of cable-stayed bridges under seismic loads.

The influence of different constraints on the original design was investigated in this study. Longitudinal constraint changes have had the largest effect on cable-stayed-bridges according to previous investigations. In this study only the constraints in the longitudinal direction were changed. Three different constraint cases were created. In case one, both ends could move in the longitudinal direction. In case two,

both ends were fixed in the longitudinal direction, and in case three, one end was free and the other end was fixed in the longitudinal direction. All the other constraints were the same, as described in 2.2.5.

The results of this study showed which constraint case was the most preferable. This optimum case was then used for all the other models and for all other cases that were involved in this parametric study.

CHAPTER 5: EVALUATION AND COMPARISON OF RESULTS

5.1 General

In the following, the results of several analyses are described, discussed, evaluated and compared. At first the Modal Analysis results are presented and evaluated. Then a comparison between linear/non-linear dynamic analysis results and single/multiple response spectrum analysis results is performed and the results are discussed. After, that the results of the parametric study are presented and examined. In the end follows a summary and evaluation of all results.

5.2 Comparison of Modal Analyses Results

Table 5 shows the natural frequencies for the five models from the modal analysis, which is necessary in order to perform the response spectrum analysis, as mentioned in Chapter Three.

As expected, the A-slab and the Slab design proved to be flexible and had the lowest natural frequencies starting with 0.24 hz and ending with 1.2 hz. Because of the large torsional stiffness, the box had the largest natural frequencies between 1.34 hz and 1.90 hz. The A-shape and the composite models were inbetween and showed almost the same frequencies in the lower range with 0.34 hz and 0.3 hz. In the higher range, the A-shape model topped the composite model with 1.81 hz compared to 1.66 hz. This result also was expected, because the A-shape tower-configuration was

supposed to give the structure a larger torsional and horizontal stiffness, which would lead to higher natural frequencies. Altogether, the results from the modal analysis were reasonable and therefore, could be used for the response spectrum analysis.

In Figs. 5 to 5.29 the first 30 modes of the composite design are illustrated. The figures clearly indicate that the first two modes are only transverse modes followed by a torsional mode. This result was anticipated because according to Wilson [28] the first modes are transverse modes. The first torsional-transverse coupled mode occurred in the fifth mode, see Fig. 5.5. As mentioned earlier in Chapter Two, these coupled modes occur only in 3-D modal analyses and are important for accurate investigations. After the fifth mode, mainly transverse modes occurred. Only in modes 6,16,18,21,22,25,29, and 30, did torsional and coupled modes occur. The rest of the modes were horizontal, longitudinal or vertical modes only, as can be seen in Figs. 5 to 5.29.

5.3 Comparison of Linear and Non-Linear Dynamic Analyses Results

In the following, the linear and non-linear results of the five models are presented separately in charts, as can be seen in Figs. 5.31 to 5.36. For each model the non-liner and linear results are summarized in a comparison chart to demonstrate clearly the differences between the two different analyses types, see Figs. 5.37 to 5.51.

5.3.1 Linear Analyses Results

The results are presented in 3-D Column charts, where the y-axis indicates the displacements in inches and the x-axis, the locations of the response displacements considered in this investigation, which are illustrated in Fig. 5.30. The locations were selected according to other studies, such as the study from Abdel-Ghaffar [3]. In addition, results were collected at locations that seemed to give important information on the behavior of the structure. The columns are color-coded and represent the five models that were used in this analysis.

The single linear response spectrum analysis produced vertical, horizontal, and longitudinal single response spectrum displacements, which are illustrated in Figs. 5.31 to 5.33.

The vertical displacements showed that the A-shape model had the least displacements of all models in the center of the main span with 11.67 inches, followed by the original design with 12.16 inches, the A-slab design (13.5inches), the box design (14.19 inches), and the slab design (16.36 inches), see Fig. 5.31. At joint 2, the order changed. The original design had the least displacement at this location, followed by the A-shape, box, A-slab, and slab design. The displacements here were in the range from 12.3 inches to 15.3 inches.

As expected, the vertical displacements of the towers were small. Therefore, no comprehensive statement can be made about the displacements at those locations. The displacements at the center of the side span followed almost the same

pattern as the displacements at the center of the main span. This time the box design had the least displacements with 10.31 inches, followed by the composite design. The rest were ranked in the same order as before.

The horizontal displacements were lower than the vertical displacements and are shown in Fig. 5.32. The ranking of the results at the center of the main span differed a little bit from the ranking of the vertical displacements. The original design had the least displacements with 8.6 inches, followed by the A-shape model with 8.9 inches, the box with 9.11 inches, the A-slab with 9.6 inches and the slab model with 9.7 inches.

Again the longitudinal displacements were, lower than the horizontal displacements and are presented in Fig. 5.33. The ranking at the center of the main slab did not change either. The original design had again the lowest displacements with 1.89 inches and the slab model had the highest displacements with 2.31 inches.

5.3.2 Non Linear Analyses Results

The results of the nonlinear single response spectrum analysis were similar to the linear response spectrum analysis. They followed exactly the same pattern as the linear response spectrum analysis results, and are presented in Figs. 5.34 to 5.36.

5.3.3 Summary and Comparison of Results

The comparison between the linear and nonlinear analysis was done separately for each model, and is illustrated in the Figs. 5.37 to 5.51. As mentioned earlier, the results were similar and there was almost no observable difference between the linear and non-linear results. The numbers differed only at the second decimal place, and could be seen as almost identical. For example, see Fig. 5.37. The non-linear response displacements were 12.194 inches at the main span center. At the same location the linear response displacements differed with 12.164 inches only slightly from the non-linear response displacements. This result leads to the conclusion that the non-linear behavior of the cables could be neglected in this investigation. This supposition is reasonable for several reasons. The cable length is only 400-ft, which is not long according to Ernst [5] concerning the equivalent Modulus of Elasticity, and the stress level is high with 80 ksi to 118 ksi. As mentioned in Chapter Three, the shorter the cable and the larger, the force acting on the cable, the more the cable behaves like a straight bar. This conclusion means that the behavior is linear and the Modulus of Elasticity does not change significantly. The results of this investigation and the results of the aforementioned investigations by Ernst [5] and Leonardt [16] indicated this clearly.

Although this and many previous investigations showed that non-linear effects can be neglected for this type of bridge, this study still continued to consider the non-linear behavior of the cables for the rest of the study to get more accurate results and

to investigate the influence on other parameter changes.

5.4 Comparison between Single and Multiple Response Spectrum Analyses

As mentioned in Chapter Three, many investigators as, Abdel-Ghaffar [1,2,3], indicated that multiple response spectrum analyses should be performed, if multiple excitation-input data are available. For this, bridge multiple excitation data were available, therefore a multiple response spectrum analysis was performed and the results were compared with a single response spectrum analysis to compare the differences.

In the following, the single response spectrum displacements and member forces for each model are discussed first, see Figs. 5.34 to 5.36 and 5.52 to 5.53. Then the multiple response spectrum displacements and member forces are explained in Figs. 5.54 to 5.59. Figures 5.60 to 5.84 then summarize the results from both analysis types to point out the differences.

5.4.1 Single Response Spectrum Results

The results are presented in the same manner, as already described in 5.3.1. Figures 5.34 to 5.36 show the vertical, horizontal and longitudinal response spectrum displacements. In addition, Figs. 5.52 to 5.53 show the member forces for the investigated models. The y-axis indicates the member force in kips. The location of the elements can be seen on the x-axis. The columns are color-coded and each column

represents one model. Since the results of the single response spectrum analysis were already described, only the element results are discussed in the following.

The element results did not yield in any significantly different results. The ranking of the results was approximately the same, as for the displacements. The original design showed in most cases the lowest forces with the box design followed by the A-shape design. Only the low cable forces of the slab designs disturbed the ranking a little bit. This is mostly attributable to to the low dead load in those designs. Overall, the forces in the cables were in the range between 84 ksi for the short cables and 342 ksi for the longer cables, see Fig. 5.52. The forces in the tower legs at the base of the towers were between 7177 kips and 8507 kips, see Fig. 5.53.

5.4.2 Multiple Response Spectrum Results

The multiple response displacements are shown in the Figs. 5.54 to 5.56. From these figures it is evident that the multiple response spectrum analysis yielded in higher results than the single response spectrum analysis. The vertical displacements were between 0.0865 inches at the upper strut joint for the composite model and 45.77 inches at the center of the main slab for the slab model, see Fig. 5.54. The horizontal displacements were in the range of 0.144 inches at the lower strut joint and 15.081 inches at the tower top, see Fig. 5.55. In the longitudinal direction the displacements were between 1.39 inches at mid span and 15.77 inches at the tower top, which can be seen in Fig. 5.56.

The member forces and bending moments are displayed in Figs. 5.57 to 5.59. The results followed the same pattern as for the single response force members. Again, only the values were obviously different. The cable forces were between 74.73 kips and 456 kips, see Fig. 5.57. The minimum bending moment at the base of the tower legs was 107058 ft-kips and the minimum force was 9611 kips, see Fig 5.58 and 5.59. The maximum bending moment was 187008 ft-kips and the maximum member force was 14572 kips.

5.4.3 Evaluation and Comparison of Results

The comparisons between the single response spectrum and multiple response-spectrum displacements and member forces were performed the same way as the comparison between the linear and non-linear analysis and are presented in the Figs. 5.60 to 5.84. The charts indicate that the results differed from each other. For example, Fig. 5.60 shows the single and multiple vertical displacements for the composite design. At the center of the main slab the single-response analysis resulted in a deflection of 12.19 inches. The multiple response spectrum analysis on the other hand resulted in a vertical deflection of 23.87 inches, which was twice as much. The comparison of the other models showed equal results or even more severe differences as in Fig. 5.72, where the multiple response spectrum displacements with 45.77 inches were even three times larger than the single response spectrum displacements with only 16.36 inches.

The comparison of the element forces is presented in Figs. 5.75 to 5.84 and showed the same picture, but the differences were not as severe as they were for the displacements. The multiple response spectrum results were less than twice as large as the single response spectrum results. For example, in Fig. 5.83 the multiple response cable force for the long cable is 382 kips and the single response cable force is just 205 kips.

Altogether this showed that if multiple-excitation input data are available, a multiple-response spectrum analysis is to be preferred, if not mandatory.

5.5 Results of Parametric Study

In the following, summaries of figures are presented that summarize the results of the parametric study, which were described in detail in Chapter Four.

As mentioned in the paragraphs above, the charts are set up the same way, color-coded column-charts with displacements, member forces or bending moments along the y-axis and the location of the nodes and elements along the x-axis.

5.5.1 Deck

As mentioned earlier, one of the main goals of this study was to determine which deck configuration is the most favorable for cable-stayed bridges under seismic loads. The response spectrum results of the investigation of the deck are summarized in Figs. 5.112 to 5.117.

First the vertical displacements of the three deck configurations were compared, which are presented in Fig. 5.112. The box had the lowest displacements with 23.67 inches at the center of the main span, followed by the original composite design with 23.87 inches and the slab model with 45.77 inches. Noticeable was that the slab configuration came up with high displacements compared to the other two deck configurations. The differences were between 10 to 20 inches. That indicated that the slab design might not be a good choice for this kind of bridge under seismic loads.

The horizontal displacements, illustrated in Fig. 5.113, were in favor of the original design at almost all locations. The displacements were lower than those of the other deck configurations. The differences were between 1 and 2 inches.

In the longitudinal direction at the center of the main and side span all deck configurations had displacements around 1.5 and 1.8 inches, as can be seen in Fig. 5.114. At the top of the tower the differences got larger in favor of the box design. The box design displayed the lowest displacements with 7.7 inches compared to the highest displacements of the slab design with 15.76 inches. Overall this showed that the box design performed slightly better than the composite design, at least according to the response displacements.

The response member forces and bending moments are illustrated in Figs. 5.115 to 5.117. Overall, the results confirmed the above conclusions. The cable forces were the lowest for the box design with 74 kips, followed by the original design with 86 kips and the slab design with 91 kips, see Fig. 5.115. The forces at the base of the

tower and in the main slab also were the lowest for the box design, followed by the original design, see Fig. 5.116. The member force and bending moment at the tower legs were with 9611 kips and 107058 ft-kips in favor of the composite design. Overall the results showed that the box design had the least amount of forces, bending moments, and displacements at almost all locations.

5.5.2 Towers

The comparison of the vertical displacements of the two tower configurations showed that the H-shape tower configuration had 2 inches less displacement at the center of the main slab and the side slab, as can be seen in Fig. 5.85. It seemed that the H-shape tower performed better.

The horizontal displacements in Fig. 5.86 corrected the first impression. The A-shape tower, with it's larger stiffness in horizontal direction, had fewer displacements at the top of the tower compared to the H-shape tower. The displacements for the A-shape tower were 5 inches and for the H-shape tower they were 14 inches.

The longitudinal displacements then showed the same picture as the vertical displacements. The H-shape tower configuration showed slightly smaller displacements, now even smaller than the first time. For example, the H-shape configuration had a longitudinal deflection of 1.45 inches at the center of the main span. The A-shape configuration resulted in a deflection of 1.51 inches at the same place. The difference was an insignificant 0.06 inches, see Fig. 5.87. Overall, the A-

shape configuration is more favorable than the H-shape configuration, especially for larger span bridges, where the horizontal stiffness is more important.

Another interesting point became evident as well. The slab design with an H-shape tower performed badly. It showed large displacements in horizontal (14.19 inches) and longitudinal (15.76 inches) direction at the top of the tower, as can be seen in Figs. 5.86 and 5.87. As a result, it is not desirable to use the slab design with an H-shape tower configuration.

5.5.3 Cables

The response spectrum displacements for the cable area comparison are shown in Figs. 5.88 to 5.90. From these figures it can be seen that with an increasing of the cable area, the displacements decreased; with a decreasing cable area the displacements increased. For example, the vertical deflection of the original design for the center of the main span was 23.8 inches. A doubling of the cable area lead to a decrease of the deflection to 17.97 inches. A tripling of the cable area produced a displacement of 15.09 inches. On the other hand, half of the cable area increased the deflection to 33.14 inches, see Fig. 5.88. The horizontal and longitudinal displacements, presented in Figs. 5.89 and 5.90, showed similar results. The results also favored the doubling case, but the differences were not as severe anymore. For example, for the horizontal displacements at center span the doubling case came up with 11.34 inches compared to 12.56 inches for the normal case, see Fig 5.89.

Overall, these results showed that a doubling of cable area was the most favorable option of the three discussed options, because it decreased the displacements about 30 percent and increased the stiffness of the structure. The halving on the other side lead to an increase of the displacements of almost 50 percent. The tripling of the cable area did not noticeably decrease the displacements when compared to doubling the area. Doubling of the cable area appears to be the better option.

The comparison of the element member forces, and bending moments, presented in Figs. 5.91 to 5.93, showed an increase of the forces in the cables from 255 kips to 503 kips with an increasing of the cable area, while the forces in the deck slab, decreased from 454 kips to 388 kips. These results seem reasonable, because high stiffness attracts high forces. Other parts of the bridge, as for example the deck, can be designed for less loads. Therefore, an increasing of the cable area is desirable. The doubling of the area also seemed more preferable than the tripling of the area, because the differences between both options were not severe, as can be seen in Figs. 5.91 to 5.93.

5.5.4 Material Properties

As mentioned in Chapter Four, a popular question in every project is whether steel or concrete should be used. In this study a comparison between a concrete box and a steel box with a concrete slab on the top was performed and the results are presented in Figs. 5.94 to 5.96.

As can be seen in Figs. 5.94 to 5.96 all the response displacement results indicated clearly that the concrete option yielded better results. The vertical displacements of the concrete option were 10 inches less than the displacements of the steel option, see Fig. 5.94. The difference decreased to 2 inches for the horizontal displacements, as shown in Fig. 5.95. The longitudinal displacements were in close proximity, e.g. the center of the main slab had displacements of 1.3 to 1.5 inches, as can be seen in Fig. 5.96. This leads to the conclusion that the particular steel box with the concrete slab is not a good choice for the cable-stayed bridge discussed in this study. The concrete box is more suitable and more effective and is, therefore, the better choice.

5.5.5 Slab Thickness

The results of the slab thickness comparison for the slab models are presented in Figs. 5.97 to 5.99. The results of the vertical displacements in Fig. 5.97 showed that the 18-inch slab performed surprisingly the best. It had the least vertical displacements in the center of the main span with 16.36 inches and 15.12 inches at the center of the side span. At the cable joint in the center of the main slab it had a slightly higher deflection of 15.32 inches compared to that of the 14-inch slab.

The horizontal displacements of the three slab thicknesses, presented in Fig. 5.98, did not differ very much from each other. The results were all in the same range. For example, at the center of the main slab all three slab thicknesses had a deflection of 8.6 inches, see Fig. 5.98.

The longitudinal displacements favored the 14-inch thick slab. At all locations it had lower deflections compared to the 18-inch thick slab, however, the differences were small. For example, at the top of the towers the 14-inch slab showed a 6.11-inch deflection compared to a 6.23-inch deflection of the 18-inch slab; Fig. 5.99. Consequently, an 18-inch thick slab was used for the rest of the parametric study, since it performed well and practical reasons, such as reinforcement, favor thicker slabs

5.5.6 Tower-Deck Bearings

As explained in 4.7, the purpose of this investigation was to examine the influence of the tower bearings of the performance of the structure under seismic loads. Three cases were investigated: a movable connection, a half-fixed connection, and a fixed connection.

The results of this investigation are presented in Figs. 5.100 to 5.105. The results confirmed the expected behavior of the bridge. The movable bearings logically allow movement, and therefore, the highest longitudinal displacements (1.95 inches) occurred in this case. The fixed case on the other hand showed the lowest displacement (1.87 inches), see Fig. 5.102. The half-fixed case settled right between the movable and fixed case with 1.89 inches, as is illustrated in Fig. 5.102. The results did not differ much from each other. For example, the horizontal displacements at the top of the tower differed just 0.10 inches from each other, as can be seen in Fig. 5.101.

The member forces and bending moments are shown in Figs. 5.103 to 5.105. The results also were in favor of the half-fixed tower connection. The fixed connection produced high forces (7114 kips) and high bending moments (152208 ft-kips) in the tower, which can be seen in Fig. 5.105. In this case the connection is so rigid that all the seismic forces are completely transferred. The movable connection came up with low forces of 5345 kips in the tower. The problem with this connection type was that under static loads it introduced high forces (107830 kips) in the deck and in the towers, as can be seen in Fig. 5.104. The half-fixed type connection produced decent forces (6583 kips) in the towers under seismic and static loads. It seemed that this kind of connection is the most desirable of all the three types that were investigated in this study. Therefore, it was selected and used for all the other models and for the rest of the parametric study.

5.5.7 Piers and Abutments Constraints

The vertical, horizontal, and longitudinal response spectrum displacements of the three constraints cases, described in 4.8, are presented in Figs. 5.106 to 5.111. The vertical displacements in Fig. 5.106 showed that case one with one end fixed and one end free had the least vertical displacement compared to the other cases. For example at the center of the main slab case one had a vertical deflection of 12.2 inches. Case two had 12.73 inches and case three 13.05 inches. The differences were not large, but still they indicated that case one performed the best. The horizontal displacements

were similar. Case one still had the least displacements at almost all locations, but the differences between the cases decreased to 0.1 inches, as can be seen in Fig. 5.107. The longitudinal displacements showed a different picture. At almost all locations the fixed case had the least displacements with 1.25 inches, followed closely by the fixed and free case, as is illustrated in Fig. 5.108. This was expected, because no movements are possible at a fixed constraint. On the other hand, this created large stresses in the deck and towers, which can be seen in the member forces and bending moment results in Figs. 5.109 to 5.111. The highest bending moments occurred in the fixed case and were 275 ft-kips at the center of the main slab and 181433 ft-kips at the base of the tower legs. On the other hand the lowest bending moments (85041 ft-kips) occurred in the free case. The one end free and other end fixed case came up with 107058 ft-Kips, which is right between the other cases and can be seen in Fig. 5.111.

The forces in the cables, which are presented in Fig. 5.109, were in favor of the fixed case. The highest force (370 kips) appeared in the no constraints case. The lowest force (259 kips) occurred in the fixed case, see Fig. 5.109. It was expected that the fixed case would have the lowest cable force, because the deck elements get more support from the fixed constraints and lower the force in the cables.

Based on the above mentioned results, the case with one end fixed and one end free seemed to be most favorable. The vertical displacements are kept to a minimum with this configuration and the forces and bending moments are still in a reasonable

range compared to the other two cases. For the rest of the parametric study the first constraint case was employed.

5.6 Summary and Evaluation of Results

The modal analysis, as described in the beginning of this chapter, already set a trend for the following investigations. It indicated that the box design might be the stiffest, and the slab designs the most flexible; it also showed that the A-shape tower configuration added stiffness and stability to the structure. All these indications were reasonable according to previous investigations by Wilson [30] and were helpful in determining the response displacements, member forces and bending moments.

The results of the comparison between the non-linear analysis and the linear analysis were not very surprising. They showed and confirmed what several previous investigators, as Fleming [7], already stated, that for small and medium bridges, the non-linear effects of the cables are negligible. A linear dynamic analysis is, therefore, more than sufficient and accurate.

The comparison between the multiple and single response spectrum analysis indicated that the multiple response spectrum analysis results in larger and more accurate results than the single response spectrum analysis. This result confirmed the statements made by Nazmy [19] in his investigations and enforced the recommendation that if multiple-excitation data are available, a multiple response-spectrum analysis should be performed.

The parametric study resulted in partially surprising and anticipated results, which gave some deep insights into the basic behavior of cable stayed bridges under seismic loads.

The deck study showed that the box deck configuration was the best alternative. This result was not necessarily expected but it was suspected, because of the known large torsional stiffness of the box.

The tower comparison did not result in any surprising results either. The A-shape tower performed the best, because of his larger horizontal stiffness compared to the H-shape tower.

The cable area study produced some interesting results. The doubling of the cable area resulted in a decrease of the vertical displacements by 30 % in the center of the main span. Such large reduction was not expected. It showed that a doubling of the cable area should be considered, if displacements are to be decreased and stability increased.

The comparison of the slab thicknesses resulted in helpful results for the deck configuration study. Surprisingly it determined that the 18-inch thick slab performed the best and should be used for the slab models. This result was not anticipated. It seemed more reasonable that the 25-inch slab would have the least displacements. The reason for this might be that the dead load was too large and, therefore, produced large displacements. No similar investigations have been done before. In Leonhard's work [16] only slab thicknesses for static loads are investigated. Slab thicknesses of

15 to 20 inches are the recommended values according to those investigations. Therefore, the determined 18-inches seemed acceptable.

The material property comparison resulted in favor of the concrete design, but the comparison was not comprehensive and was just limited to a particular deck configuration. Therefore, no comprehensive statements can be made about the influence of material properties of cable stayed-bridges under seismic loads.

The constraints study showed surprising results. It did not favor the case with any longitudinal constraints at both ends, which is the recommended configuration according to Walther [28]. The results favored the case with one end constraint longitudinally and one end free. This case showed the lowest displacements, forces and moments for the bridge studied in this investigation. No publications could be found that confirmed those results. So, in order to apply those results to other bridges, more comprehensive research has to be done.

The tower-deck bearing comparison did not show any surprising or new results. As expected according to Yamada [30], the half-fixed case performed the best. It settled between the fixed and movable case, which were too extreme in their results.

Overall the results were reasonable, provided meaningful insights about the basic behavior of cable stayed bridges under seismic loads, and gave some ideas and recommendations for future research and designs. For example, the study showed that doubling of the cable area increases the stiffness and decreases the displacements. It also indicated that the A-shape tower and the box deck configuration results in less

response displacements and, therefore are very favorable. A summary of these results and all the other results with a comparison between the investigated results and current knowledge is given in Table 5.2.

Concerning the evaluation of the original design, the results showed that the original design performed well compared to all the other models. Still the results indicated that some improvements might improve the stability, stiffness and serviceability of the bridge. For example, an exchange of the tower configuration or a doubling of the cable area would add more stiffness and stability to the structure. All the suggested improvements are presented in Table 5.1.

CHAPTER 6: CONCLUSIONS AND RECOMMENDATIONS

6.1 General

The purpose of this study was to investigate the behavior cable-stayed bridges during sesmic activity, and to perform a parametric study of the dynamic performance analysis of cable-stayed bridges. In the following, the resulting conclusions and recommendations are summarized.

6.2 Linear Non-Linear Analysis Comparison

As described in detail in 5.3.3, the results of the linear and non-linear analysis were almost identical. In most cases the values differed only after the third decimal place. These results, together with work by Fleming [7], lead to the conclusion that for the bridge studied in this investigation, and for bridges with similar geometric properties, the non-linear effects of the cables are negligible. This observation means that linear dynamic analysis, without consideration of the non-linear effects of the cables, are accurate enough for bridges with medium span length, as the bridge in this study.

6.3 Single-Multiple Response Spectrum Analysis Comparison

The comparison between the results of the two analysis types in 5.4.3, clearly highlighted the significant differences between the results. The multiple response

spectrum analysis resulted in larger displacements, member forces and bending moments than the single response spectrum analysis, as described in 5.4.3. The single response spectrum analysis is not accurate enough and yields in unrepresentative response, which can be unsafe and undesirable, thus multiple response spectrum analyses should be carried out. This result is also confirmed by Nazmy's investigations [19].

6.4 Deck

The results in 5.5.1 were slightly in favor of the box deck configuration, but followed closely by the original design with a composite concrete-steel girder bridge deck. Therefore, only a slight recommendation for using box deck elements rather than composite concrete-steel girder bridge deck elements can be given here.

6.5 Towers

The tower comparison results showed a noteworthy picture. For vertical and longitudinal displacements there was not much of a difference between the two tower types, but for the horizontal displacements the results differed in favor of the A-shape tower type. The conclusion is that A-shape towers should be used instead of H-shape towers. It strongly decreases the horizontal displacements of the towers and it adds stiffness and stability to the whole structure. According to Gimsing [11], for existing

cable-stayed bridges, especially long-span cable-stayed bridges, A-shape towers are effective. Therefore, the above conclusion also is relevant for bridges other than the one mentioned in this study. It can be extended towards long-span cable-stayed bridges, as well.

6.6 Cables

The cable area study showed that an increase of the cable area, had a significant influence of the responses of the structure to seismic loads; the displacements dropped significantly. A doubling of the area emerged out of the study as the most favorable. The conclusion is that an increase of the cable area is strongly recommended for decreasing the displacements and establishing more stability for the structure.

6.7 Slab Thickness

The slab thickness investigation showed that the 18-inch thick slab performed the best compared to the other slab thicknesses. It was more of a sub-investigation, because the results were needed in order to perform the other investigations. As a result, no specific conclusion could be drawn. The only conclusion made was that the vertical displacements do not decrease linearly with a linearly increase of the slab thickness.

6.8 Material Properties

As already indicated in 5.5.4 and 5.6, there is little that can be said about this comparison, other than that for the bridge studied in this study, a box constructed completely out of concrete is strongly preferred over a box with steel walls and a concrete slab on the top.

6.9 Tower-Deck Bearings

As mentioned in 5.5.6. and 5.6, the tower-deck bearing study did not reveal significant results. The results were similar to results in previous investigations from Khali [15]. The conclusion is made that half-fixed tower deck bearings should be used for bridges that are located in high seismic zones to decrease the forces and moments in the towers during an earthquake. Shock device dampers or rubber block bearings are good choices to accommodate this requirement.

6.10 Pier Abutment Constraints

The results of the constraint comparison brought up some interesting points. It showed that none longitudinal constraints are not the optimal configuration in every case. It turned out that one end constraint and the other end free was the better option. This result alone does not lead to a strong conclusion. More research has to be done on this topic before a conclusive statement can be made. But so far one can conclude

that the special mentioned constraint case should be at least considered as an alternative.

6.11 Summary of Conclusions

Overall most of the conclusions that emerge from this study are reasonable and have been confirmed by previous investigations by Khali [15], Abdel-Ghaffar [1,2,3], Wilson [29,30], Fleming [6,7,8] or common engineering knowledge. The conclusions should help to understand the basic behavior of cable-stayed bridges under seismic loads and improve the design process for future projects. A short summary of all the made conclusions is given in Table 5.3.

6.12 Design Recommendations

According to the above conclusions the following design recommendations were formulated:

- The non-linear behavior of cables does not have to be considered for medium span-bridges.
- Multiple response spectrum analysis should be carried out if multiple excitation data are available.
- An A-shape tower should be selected, especially for long-span structures.
- A concrete box or a composite concrete-steel girder bridge deck is prefered for the deck.

- The doubling of the cable area should be considered to decrease displacements and to increase the stability of the structure.
- A longitudinally fixation of one end of the bridge should be considered for the constraints.

6.13 Concluded Suggestions for Improvement of Original Design

According to the design recommendations a improvement table for the original design was created, which can be seen in Table 5.1. The table shows that the composite deck could be replaced by the concrete box, the H-shape towers should be exchanged for A-shape towers, the cable area should be doubled, and one end of the bridge should be constrained longitudinally. Those suggestions emerged from the study and should improve the performance of the bridge during an earthquake.

6.14 Future Research

As mentioned in the paragraph above, this study showed several areas, where future research is needed to confirm results or to obtain greater insights. The pier constraints are a good example. Do the conclusions from this study apply to other cases? More research must be done to transfer conclusions from this study to other cases.

The material properties are another good example. How do material changes

affect the performance of the structure under an earthquake? Do steel towers perform better than concrete towers? The cables are also interesting. How much does the cable arrangement affect the performance? Is a fan or harp pattern more favorable during an earthquake? Another big question is, how far can all the conclusions for this medium size bridge be transferred to long-span bridges? All these questions might serve as an impetus for researchers to look for answers.

References

1. Abdel-Ghaffar, A.M. and Nazmy, A. S., "Earthquake Resistant Analysis of Cable-Stayed Bridges in Eastern and Central United States," *Proceedings of the Third U.S. National Conference on Earthquake Engineering*, Charleston South Carolina, August 24-28, 1986, 2085-2096.
2. Abdel-Ghaffar, Ahmed M. and Nazmy, Aly S., "Non-Linear Earthquake-Response Analysis of Long-Span Cable-Stayed Bridges: Theory," *Earthquake Engineering and Structural Dynamics,* Vol. 19, 1990, 45-62.
3. Abdel-Ghaffar, Ahmed M. and Nazmy, Aly S., "Non-Linear Earthquake-Response Analysis of Long-Span Cable-Stayed Bridges: Applications, "*Earthquake Engineering and Structural Dynamics,* Vol. 19, 1990, 63-76.
4. Chopra, Anil K, *Dynamics of Structures, Theory and Applications to Earthquake Engineering*, Prentice Hall, Englewood Cliffs, N.J., 1995.
5. Ernst, H. J., "Der E-Modul von Seilen unter Beruecksichtigung des Durchhanges," *Bauingenieur,* No. 2, 1965, 52-55.
6. Fleming, J. F., Egeseli, E. A., "Dynamic Behavior of a Cable-Stayed Bridge," *Earthquake Engineering and Structural Dynamics,* Vol. 8, 1982, 1-16.
7. Fleming, J. F., "Linear Versus Nonlinear Behavior of Cable-Stayed Bridges," *Wind Seismic Effects, Proeedings 14th Joint Panel Conerence. U.S.-Japan Cooperative Program Natural Resources, 1983, 343-*28.

8. Fleming, J. F., "Static and Dynamic Analysis of Cable-Stayed Bridges," *Research Report* SETEC CE84-018, Department of Civil Engineering, University of Pittsburgh, 1983.

9. Garevski, M. and Paskalov, T., "Application of FEM Modelling of Cable-Stayed-Bridges," *Proceedings of the 8th European Conference on Earthquake Engineering*, Lisbon, 1986, 6.9/9-6.9/15.

10. Garevski, M., Dumanoglu, A.A. and Severn, R.T., "Dynamic Characteristics and Seismic Behavior of Jindo Bridge, South Korea," *Structural Engineering Review*, Vol. 1, No. 3, September, 1988, 141-149.

11. Gimsing, Nils J., *Cable Supported Bridges Concept and Design, Second Edition* John Wiley & Sons Ltd., Chichester, N.Y., 1997.

12. Goodyear, David and Salamie, Ralph, "Construction of the Clark Cable-Stayed Bridge at Aton, Illinois," *ASCE Structures Congress XII 1994*, Atlanta, Ga., 672–676.

13. Hague, Steven T. and Kruse, Don E., "Earthquake Design Considerations for the Cape Girardeau Cable-Stayed Bridge over the Mississippi River," *Proceedings of the National Seismic Conference on Bridges and Highways: Progress in Research and Practice,* Section 9, 1995, 10-13.

14. HNTB, "Structural Drawings of the Bill Emerson Cable-Stayed Bridge in Cape Girardeau," HNTB Corporation, Kansas City, Missouri, 1994.

15. Khali, M. S., "Seismic Analysis and Design of the Skytrain Cable-Stayed Bridge," *Canadian Journal of Civil Engineering,* No. 23, 1996, 1241-1248.

16. Leonhardt, F. and Zellner W., "Cable-Stayed Bridges-Report on Latest Developments," *Canadian Structural Engineering Conference,* Toronto, Canada, 1970

17. Manabu, Ito, Prof. Takushoku Univ., Tokyo, ,Japan, "The Cable-Stayed Bridges of Meiko," *Journal of Structural Engineering International*, March, 1998, 168-171.

18. Manubu, Ito and Endo, Takeo, "The Tatara Bridge- World's Longest Cable-Stayed Span," *ASCE Structures Congress XII 1994, Atlanta*, Ga., 677–682.

19. Nazmy, A.S. and Sadek, Aly, "Nonlinear Earthquake-Response Analysis of Cable-Stayed Bridges Subjected to Multiple-Support Excitations," *Research Report,* Princeton University, 1987, pp. 1-388.

20. Podolny, Walter and Scalzi, John B., *Construction and Design of Cable-Stayed Bridges, Second Edition*, John Wiley & Sons Inc., Chichester, N.Y., 1986.

21. Poston, Randall W., "Cable-Stay Conundrun, " *Civil Engineering Journal*, August, 1998, 58-61.

22. Reina, Peter and Kosowatz, John J., "Ting Kau Crossing Finishes Hong Kong's Airport Approach," *ENR*, May 18, 1998, 29-32.

23. Taly, Narendra, *Design of Modern Highway Bridges*, McGraw-Hill Inc., New York, N.Y., 1988.

24. Tang, Man-Chung, "Construction of the Baytown Bridge, Houston" *ASCE Structures Congress XII 1994*, Atlanta, Ga., 666–671.

25. Tonias, Demetrios, *Bridge Engineering, Design Rehabilitation, Maintenance of Modern Highway Bridges*, McGraw-Hill Inc., New York, N.Y., 1995.

26. Ulstrup, Carl. C, "Cable-Stayed Bridges," *American Society of Civil Engineering*, New York, N. Y., May, 1988.

27. Virlogeaux, Michael, "The Normandy Bridge," *ASCE Structures Congress XII 1994*, Atlanta, Ga., 1994, 660–665.

28. Walther, Rene, Houriet, Bernard, Isler, Walmar and Moia, Pierre, *Cable Stayed-Bridges*, Thomas Telford, London, GB, 1988.

29. Wilson, J.C. and Gravelle, Wayne "Modeling of Cable-Stayed Bridge for Dynamic Analysis," *Earthquake Engineering and Structural Dynamics,* Vol. 20, 1991, 707-721.

30. Wilson, J.C. and Liu, T. "Ambient Vibration Measurements on a Cable-Stayed-Bridge," *Earthquake Engineering and Structural Dynamics*, Vol. 20, 1991, 723-747.

31. Yamada, Yoshikazu, Toki, Kenzo and Kitzawa, Masahiko, "Earthquake Resistant Design of a Long-Span Cable-Stayed Bridge," *Proceedings from the First U.S.-Japan Workshop on Earthquake Protective Systems for Bridges,* Buffalo, New York, September 4-5, 1991, 531-541.

Appendix

Table 2 Gross Cross Section Properties of H-shape Tower Configuration

Sections	Section I.D.	Width (ft)	Depth (ft)	Area (ft^2)	Moment of Inertia Iz (ft^4)	Moment of Inertia Iy (ft^4)	Section Length (ft)
1	Upper leg	9	22	126.6	1156	6979	119
2	Upper Strut	17	15	255	4127	3339	83
3	Middle Leg	10.5	22	119	1664	6927	121
4	Lower Strut	13	16	208	2929	4437	101
5	Lower Leg	12	22	264	3168	10648	106
6	Footing	22	10	220	8873	1833	89
7	Wall	8	90	-	-	-	-

Table 2.1 Gross Cross Section Properties of A-shape Tower Configuration

Sections	Section I.D.	Width (ft)	Depth (ft)	Area (ft^2)	Moment of Inertia Iz (ft^4)	Moment of Inertia Iy (ft^4)	Section Length (ft)
1	Top Strut	10	8	80	426	666	32
2	Upper leg	9	22	126.6	1156	6979	91.67
3	Upper Strut	17	15	255	4127	3339	66
4	Middle Leg	10.5	22	119	1664	6927	161.08
5	Lower Strut	13	16	208	2929	4437	108
6	Lower Leg	12	22	264	3168	10648	103.25

Table 2.2 Cable Data

Cable Number	Number of 0.6" Strands	Area of one Strand (in^2)	Total Steel Area (in^2)	Pipe Diameter (in)
1	54	0.217	11.718	10.75
2	54	0.217	11.718	10.75
3	50	0.217	10.85	10.75
4	46	0.217	9.982	8.63
5	43	0.217	9.331	8.63
6	41	0.217	8.897	8.63
7	39	0.217	8.463	8.63
8	39	0.217	8.463	8.63
9	35	0.217	7.595	7.13
10	33	0.217	7.161	7.13
11	31	0.217	6.727	7.13
12	29	0.217	6.293	7.13
13	27	0.217	5.859	6.63
14	23	0.217	4.991	6.63
15	21	0.217	4.557	6.63
16	20	0.217	4.34	6.63
17	20	0.217	4.34	6.63
18	21	0.217	4.557	6.63
19	23	0.217	4.991	6.63
20	24	0.217	5.208	6.63
21	28	0.217	6.076	7.13
22	29	0.217	6.293	7.13
23	32	0.217	6.944	7.13
24	34	0.217	7.378	7.13
25	38	0.217	8.246	8.63
26	39	0.217	8.463	8.63
27	42	0.217	9.114	8.63
28	44	0.217	9.548	8.63
29	46	0.217	9.982	8.63
30	49	0.217	10.633	10.75
31	54	0.217	11.718	10.75
32	54	0.217	11.718	10.75

Table 3. Cable Material and Geometric Properties

Cable No.	Number of Strands	Area of one Strand (in^2)	Total Steel Area (in^2)	Pipe Diameter (in)	Weight γ (lb/in^3)	Density (slugs/in^3)	Horiz. length l (in)	Modulus of Elasticity Ee (psi)	Max Stress σ up (psi)	Min Stress σ low (psi)	Stress ratio μ = σlow/σup	σ m (psi)	Equivalent Modulus of Elasticity Eq (psi)
1	54	0.217	11.718	10.75	0.2835648	0.000733863	5537	29000000	118000	70000	0.593220339	94000	28763905.38
2	54	0.217	11.718	10.75	0.0936509	0.000242368	5394	29000000	118000	78000	0.661016949	98000	28979326.02
3	50	0.217	10.85	10.75	0.091811	0.000237606	5250	29000000	116000	86000	0.74137931	101000	28983484.81
4	46	0.217	9.982	8.63	0.0997196	0.000258073	5106	29000000	117000	92000	0.786324786	104500	28983622
5	43	0.217	9.331	8.63	0.0983006	0.000254401	4962	29000000	117000	96000	0.820512821	106500	28985930.92
6	41	0.217	8.897	8.63	0.0968817	0.000250729	4542	29000000	119000	99000	0.831932773	109000	28989346.43
7	39	0.217	8.463	8.63	0.0968817	0.000250729	4122	29000000	120000	99000	0.825	109500	28991331.07
8	39	0.217	8.463	8.63	0.0968817	0.000250729	3702	29000000	119000	94000	0.789915966	106500	28992328.93
9	35	0.217	7.595	7.13	0.1043649	0.000270096	3282	29000000	121000	92000	0.760330579	106500	28992935.22
10	33	0.217	7.161	7.13	0.1022611	0.000264651	2862	29000000	119000	89000	0.74789916	104000	28994435.18
11	31	0.217	6.727	7.13	0.1001823	0.000259271	2442	29000000	119000	91000	0.764705882	105000	28996244.7
12	29	0.217	6.293	7.13	0.0981035	0.000253891	2022	29000000	118000	91000	0.771186441	104500	28997500.93
13	27	0.217	5.859	6.63	0.0989756	0.000256148	1602	29000000	119000	94000	0.789915966	106500	28998500.41
14	23	0.217	4.991	6.63	0.0965425	0.000249851	1182	29000000	118000	89000	0.754237288	103500	28999143.61
15	21	0.217	4.557	6.63	0.0941383	0.000243629	762	29000000	116000	85000	0.732758621	100500	28999627.21
16	20	0.217	4.34	6.63	0.0941383	0.000243629	342	29000000	108000	82000	0.759259259	95000	28999912.01
17	20	0.217	4.34	6.63	0.0941383	0.000243629	342	29000000	101000	74000	0.732673267	87500	28999886.21
18	21	0.217	4.557	6.63	0.0941383	0.000243629	762	29000000	114000	83000	0.728070175	98500	28999603.25
19	23	0.217	4.991	6.63	0.0965425	0.000249851	1182	29000000	118000	87000	0.737288136	102500	28999112.45
20	24	0.217	5.208	6.63	0.0965425	0.000249851	1602	29000000	114000	85000	0.745614035	99500	28998223.66
21	28	0.217	6.076	7.13	0.0981035	0.000253891	2022	29000000	116000	89000	0.767241379	102500	28997348.24
22	29	0.217	6.293	7.13	0.0981035	0.000253891	2442	29000000	118000	92000	0.779661017	105000	28996416.8
23	32	0.217	6.944	7.13	0.1001823	0.000259271	2862	29000000	116000	89000	0.767241379	102500	28994460.37
24	34	0.217	7.378	7.13	0.1022611	0.000264651	3282	29000000	117000	91000	0.777777778	104000	28992759.26
25	38	0.217	8.246	8.63	0.0954457	0.000247013	3702	29000000	114000	88000	0.771929825	101000	28991221.61
26	39	0.217	8.463	8.63	0.0968817	0.000250729	4122	29000000	119000	93000	0.781512605	106000	28990330.25
27	42	0.217	9.114	8.63	0.0983006	0.000254401	4542	29000000	120000	96000	0.8	108000	28988634.98
28	44	0.217	9.548	8.63	0.0997196	0.000258073	4962	29000000	119000	98000	0.823529412	108500	28986317.42
29	46	0.217	9.982	8.63	0.0997196	0.000258073	5382	29000000	120000	98000	0.816666667	109000	28984098.55
30	49	0.217	10.633	10.75	0.091811	0.000237606	5802	29000000	117000	93000	0.794871795	105000	28982374.28
31	54	0.217	11.718	10.75	0.0936509	0.000242368	6222	29000000	121000	93000	0.768595041	107000	28979906.98
32	54	0.217	11.718	10.75	0.0936509	0.000242368	6642	29000000	106000	73000	0.688679245	89500	28959524.17

Table 5 Natural Frequencies from Modal Analysis

Mode	A-shape	A-slab	Box	Composite	Slab
1	0.30016	0.24833	0.34803	0.29817	0.25388
2	0.39647	0.29094	0.58284	0.38861	0.29952
3	0.60637	0.47041	0.63508	0.55803	0.48691
4	0.64203	0.5196	0.85835	0.61679	0.53059
5	0.69742	0.55302	0.86296	0.65139	0.53363
6	0.73886	0.58398	0.86492	0.70067	0.55478
7	0.75208	0.63114	0.96143	0.70789	0.58797
8	0.82677	0.63606	0.9892	0.75345	0.63723
9	0.85786	0.68298	0.98922	0.8388	0.64085
10	0.95336	0.70674	1.0539	0.8556	0.66822
11	0.97905	0.70938	1.1012	0.86218	0.6914
12	1.0666	0.7127	1.1317	0.93273	0.71597
13	1.1023	0.75763	1.4533	0.97999	0.71766
14	1.149	0.80636	1.5262	0.9881	0.76147
15	1.1565	0.82308	1.569	0.98811	0.82868
16	1.1787	0.85403	1.6055	1.0202	0.85569
17	1.1823	0.85583	1.6259	1.0838	0.85739
18	1.2227	0.90461	1.7147	1.1172	0.85868
19	1.283	0.94465	1.8835	1.1348	0.86248
20	1.3298	0.9913	1.9069	1.1641	0.90689
21	1.3688	1.0157		1.1789	0.91353
22	1.4629	1.029		1.1931	0.98787
23	1.5464	1.0384		1.3295	0.98791
24	1.5512	1.0667		1.3651	0.99373
25	1.5843	1.0668		1.3863	0.99918
26	1.6428	1.0997		1.5286	1.024
27	1.7368	1.101		1.5544	1.0345
28	1.7614	1.1974		1.5936	1.0693
29	1.7758	1.2125		1.6503	1.0695
30	1.8142	1.2178		1.6668	1.1025

Table 5.1 Recommendations of Improvements for Original Design

Main Structural Parts	Original Design	Evaluation	Recommendation
Deck	Composite Concrete Steel-Girder	Satisfying	Concrete Box
Towers	H-shape Configuration	Improvable	A-shape Configuration
Cables	-	Improvable	Doubling of Cable Area
Tower-Deck Bearing	Block Rubber Bearings & Damper	Satisfying	Block Rubber Bearings & Damper
Pier Abutment Constraints	No Longitudinal Constraints	Improvable	One End Constaint Longitudinally and One End Free

Table 5.2 Summary of Studies and Comparison to Current Knowledge

Study	Current Knowledge	Investigated Results	Recommendations	Advantages of Recommendations
Non-Linear/Linear Behavior of Cables	Non-Linear Behavior of Cables Negligible for Medium Bridges with Short Cable Length and High Operating Stress levels	Non-Linear Behavior of Cables Negligible for Medium Bridges with Short Cable Length and High Operating Stress levels	Consideration of Non-Linear Cable Behavior only for Long-Span Bridges	Analysis Can be Performed Faster and Less Expensive
Multiple/Single Response-Spectrum Analysis	Multiple Response-Spectrum Analysis Yields in Larger and More Accurate Results	Multiple Response-Spectrum Analysis Yields in Larger and More Accurate Results	Performing of Multiple-Response-Spectrum Analysis, if Multiple-Excitation Data are Available	Analysis Results in Safer and More Accurate Results
Deck	Composite Deck and Concrete Box Deck Configurations are the Most Recommended	Concrete Box and Composite Deck Configurations are the Most Desirable	Preferation of Concrete Box or Composite Deck Configuration	Concrete Box Results in Slightly Less Displacements in Center of Main Span
Towers	A-shape Configuration is Recommended for Long-Span Bridges	A-shape Configuration is Recommended for Medium to Long-Span Bridges	A-shape Tower Configuration is to Prefer to H-Shape Configuration	A-shape Configuration Results in Larger Horizontal Stiffness and Stability of whole Structure
Cables	-	Doubling of Cable Area Results in Lower Displacements	Doubling of Cable Area Should be Considerd, if Decreasing of Displacements is Desirable	Doubling of Cable Area Results in Decreasing of Displacements and Increasing of Stability and Stiffness of Structure
Material Properties	-	Concrete Design Performed Better than Steel Design	Concrete is Preferred	Concrete Design Results in Lower Displacements and Member Forces
Tower-Deck Bearings	Using of Block Rubber Bearings and Damper	Half-Fixed Constraints Resulted in the Least Amount of Displacements and Member Forces	Using of Half-Fixed Constraints for Tower Bearings	Half-Fixed Tower Bearings Result in Lower Displacements, Member Forces and Bending Moments
Pier Abutment Constraints	No Constraints in Longitudinal Direction	One End constraint Longitudinally and one End Free performed the Best	Considering One End Free and One End Fixed Longitudinally For Pier Abutment Constraints	The Special Constraint Case Results in Lower Displacements, Member Forces and Bending Moments

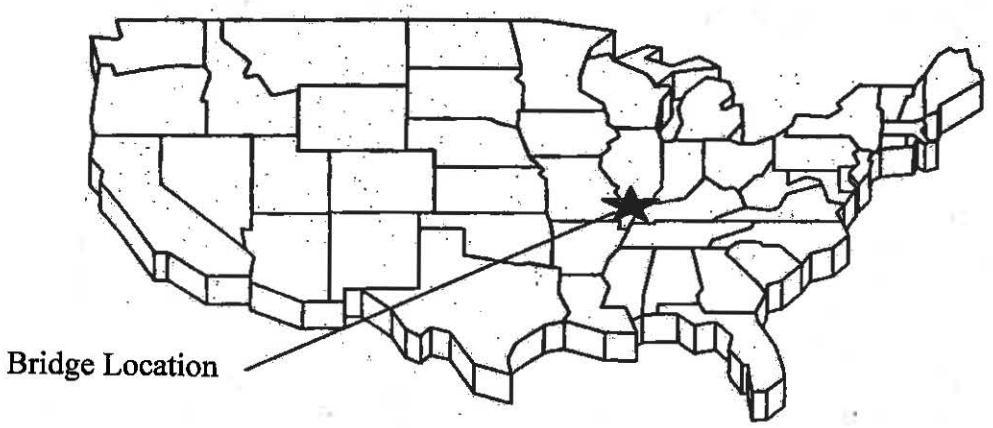

Fig. 1 Location of Bridge

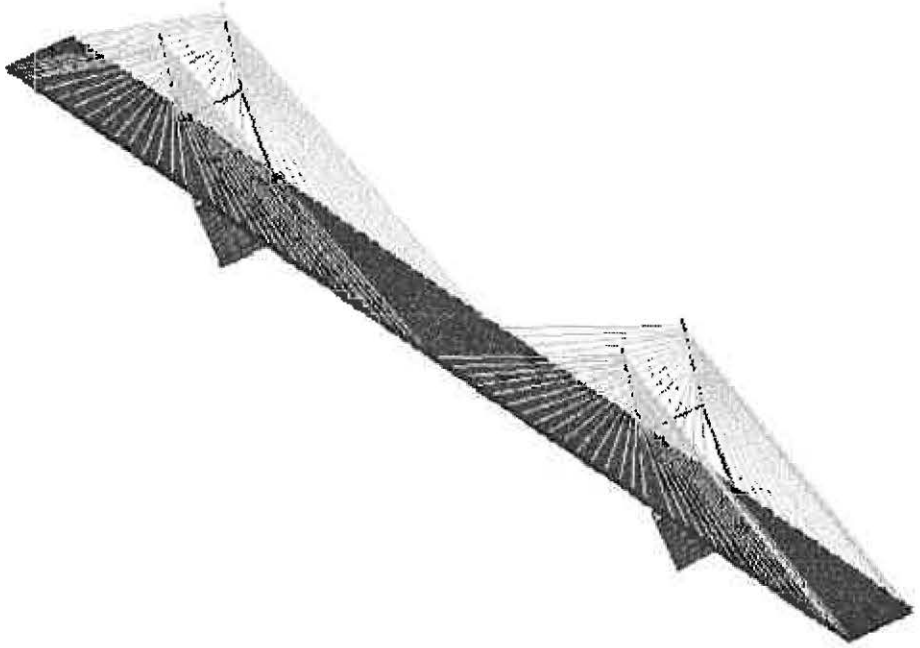

Fig. 1.1 3-D Finite Element Model of Bill Emerson Bridge

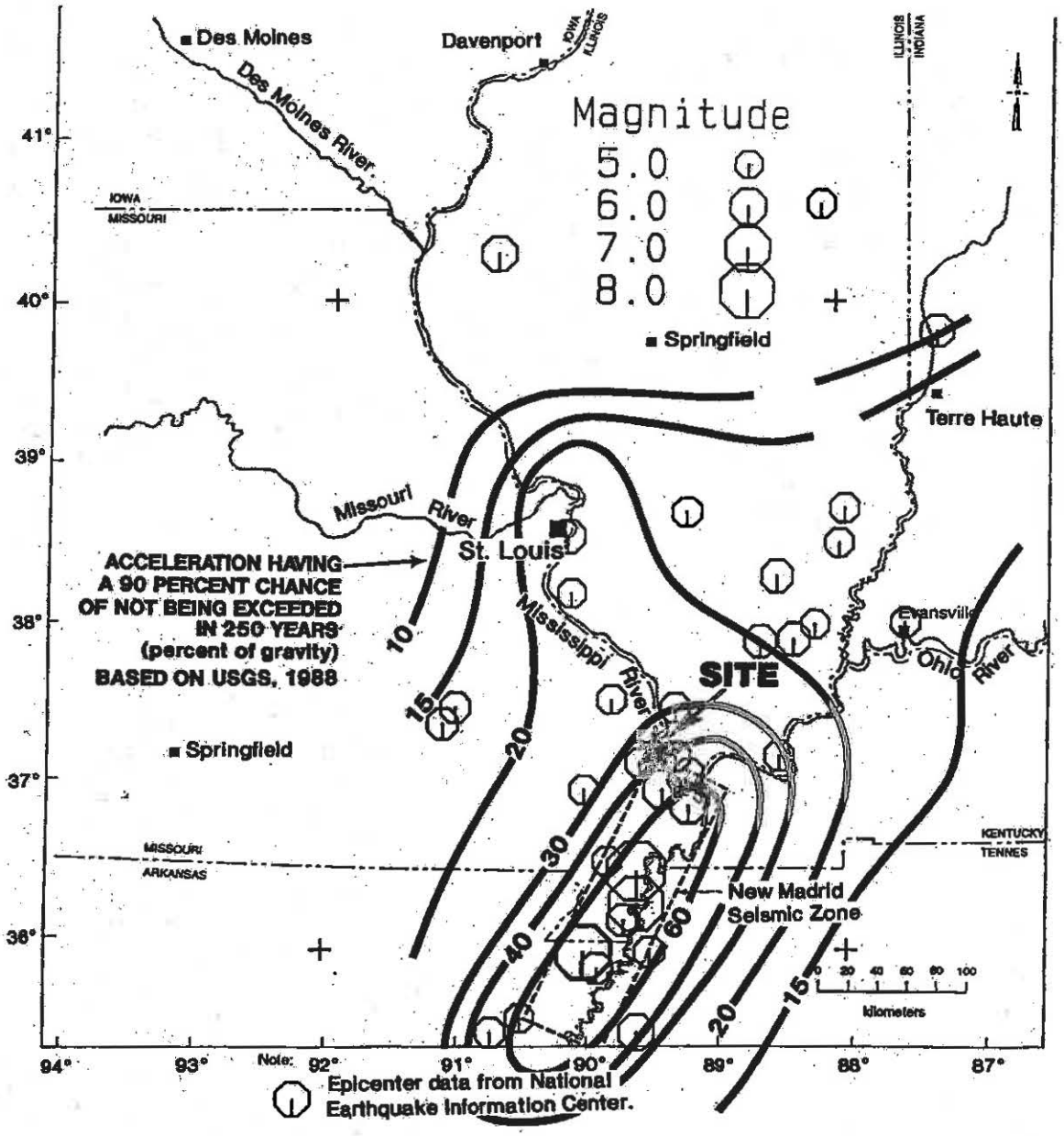

Fig. 1.2 Location of Bridge towards New Madrid Seismic Zone

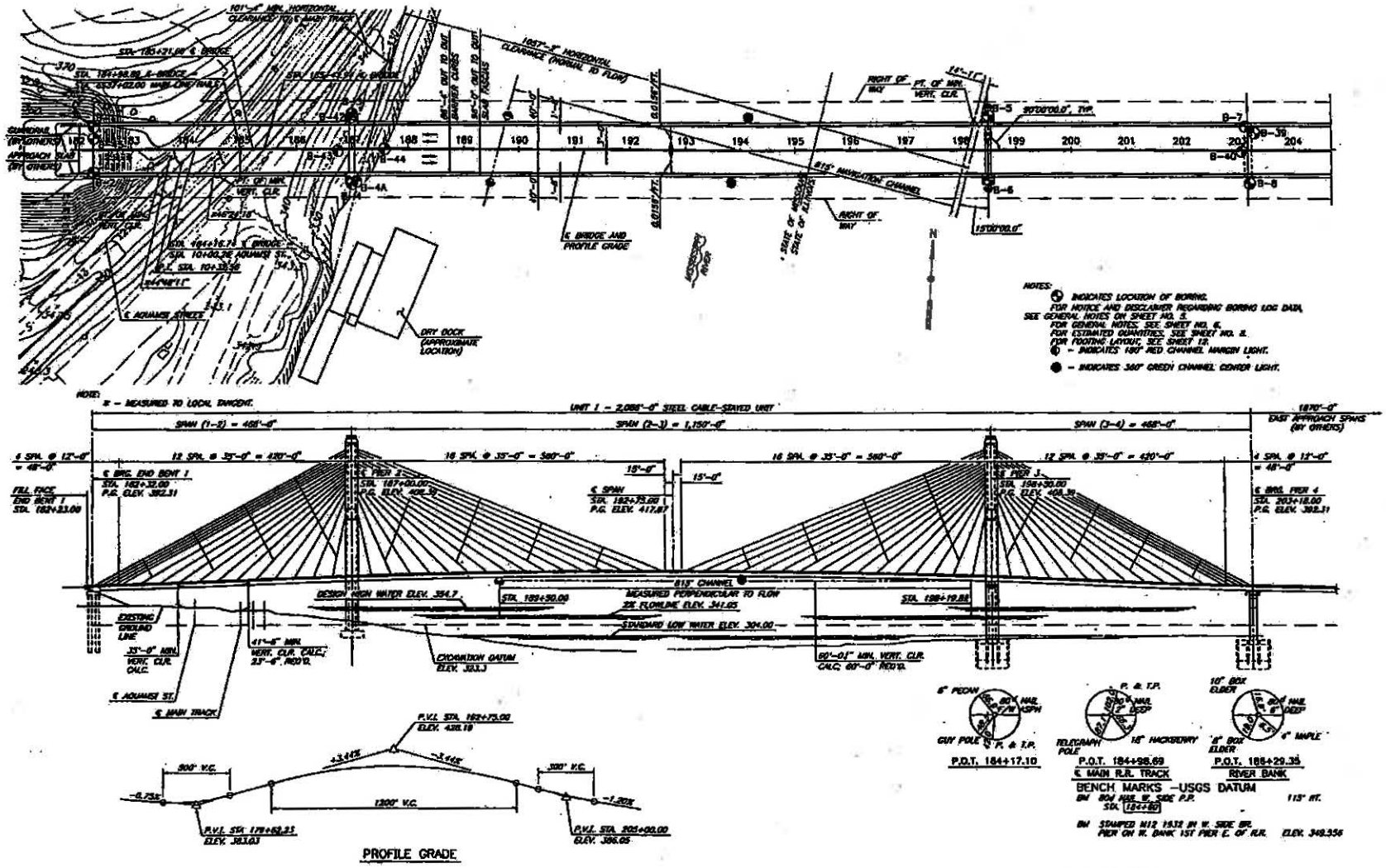

Fig. 1.3 Elevation of the Bill Emerson Bridge

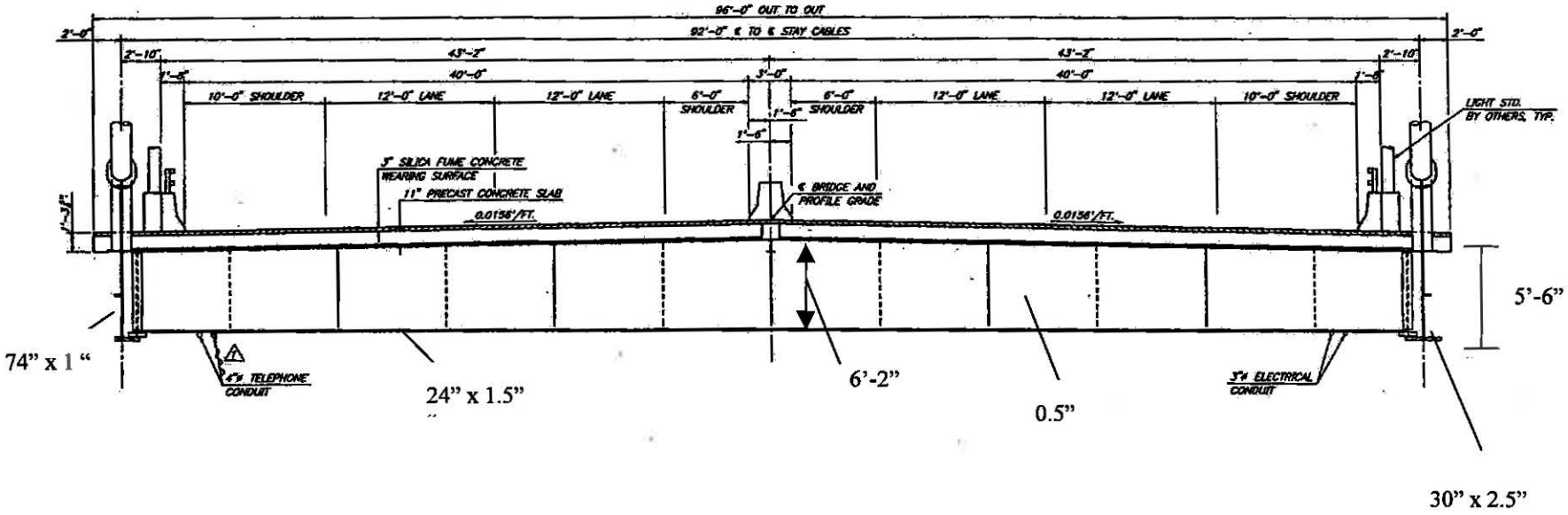

Fig. 1.4 Typical Cross-section of the Bill Emerson Bridge

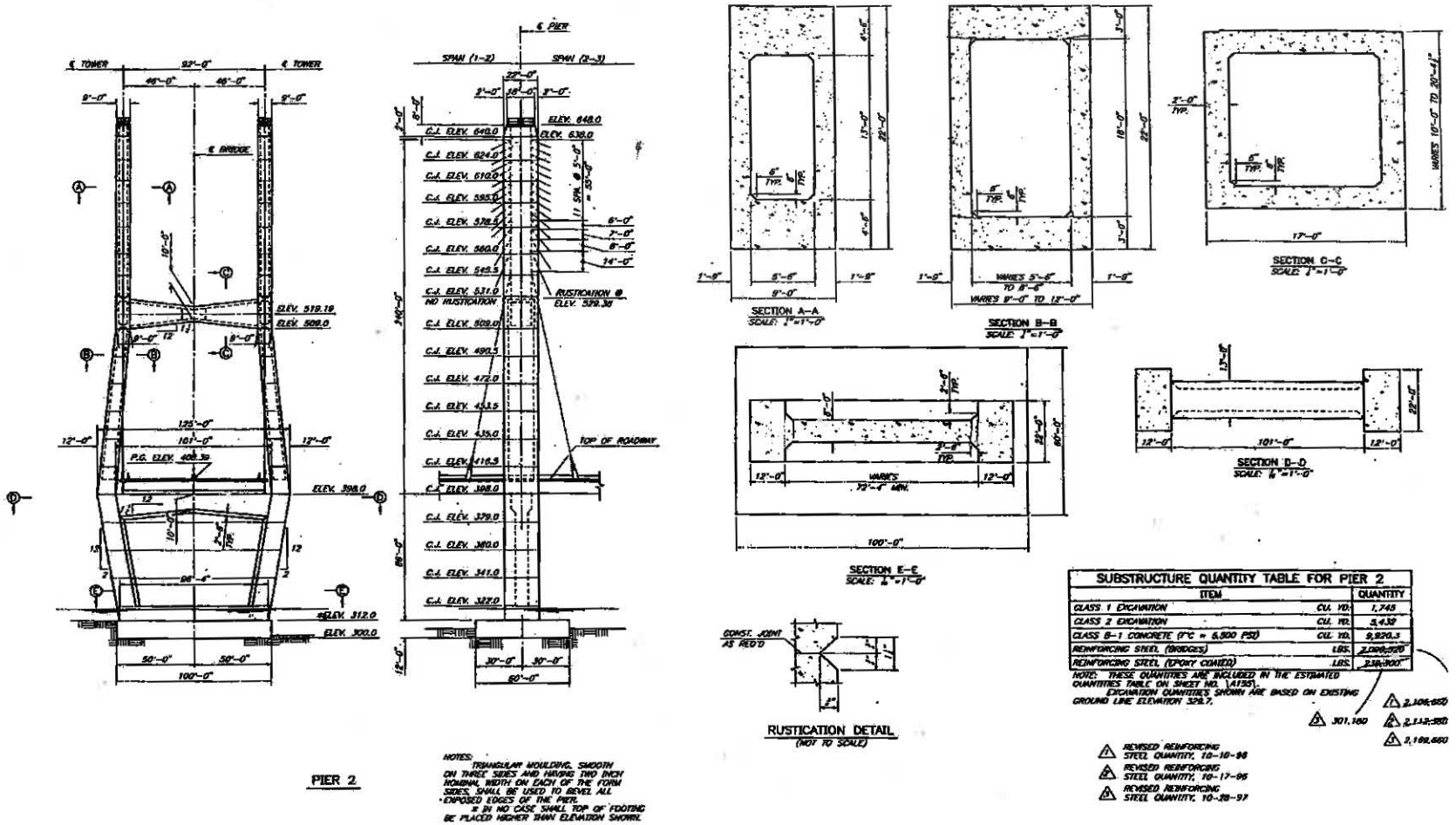

Fig. 1.5 Elevation of Tower 1 at Pier 2

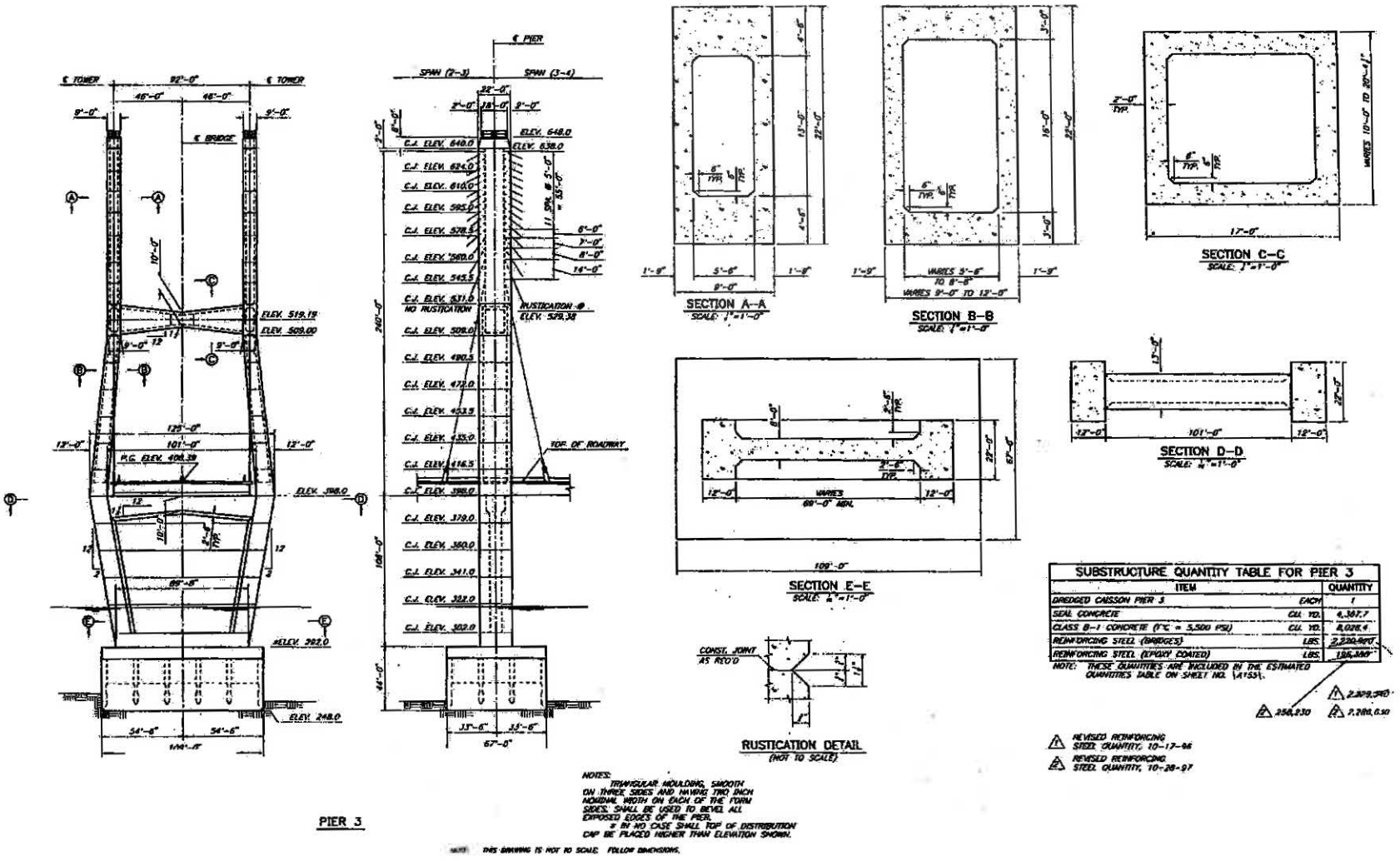

Fig. 1.6 Elevation of Tower 2 at Pier 3

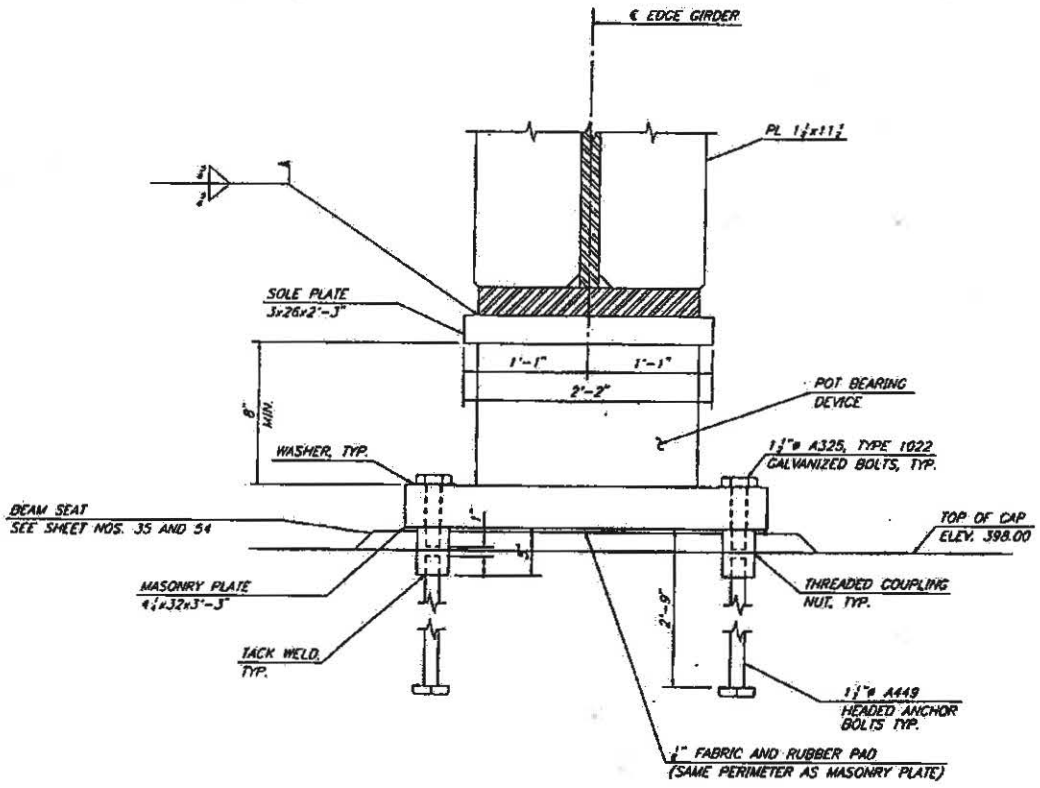

Fig. 1.7 Elevation of Tower-Deck Bearing

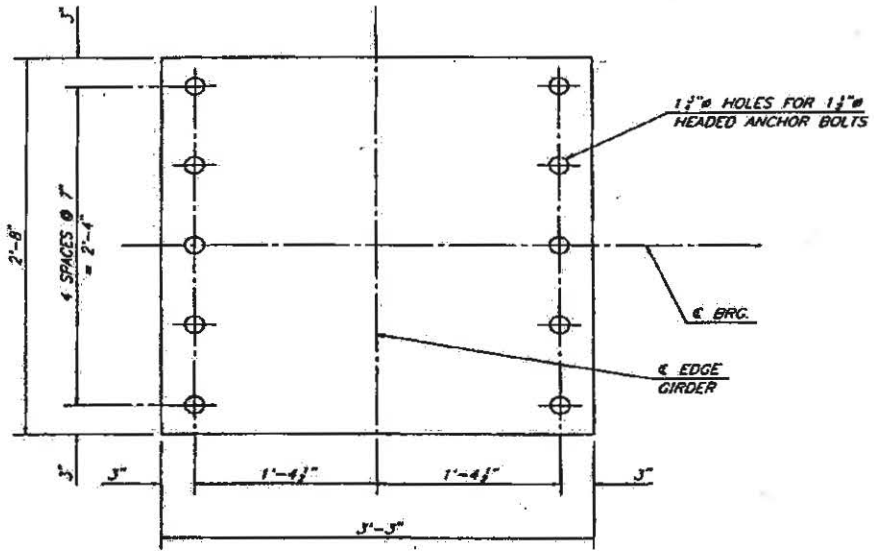

Fig. 1.8 Plan View of Tower-Deck Bearing

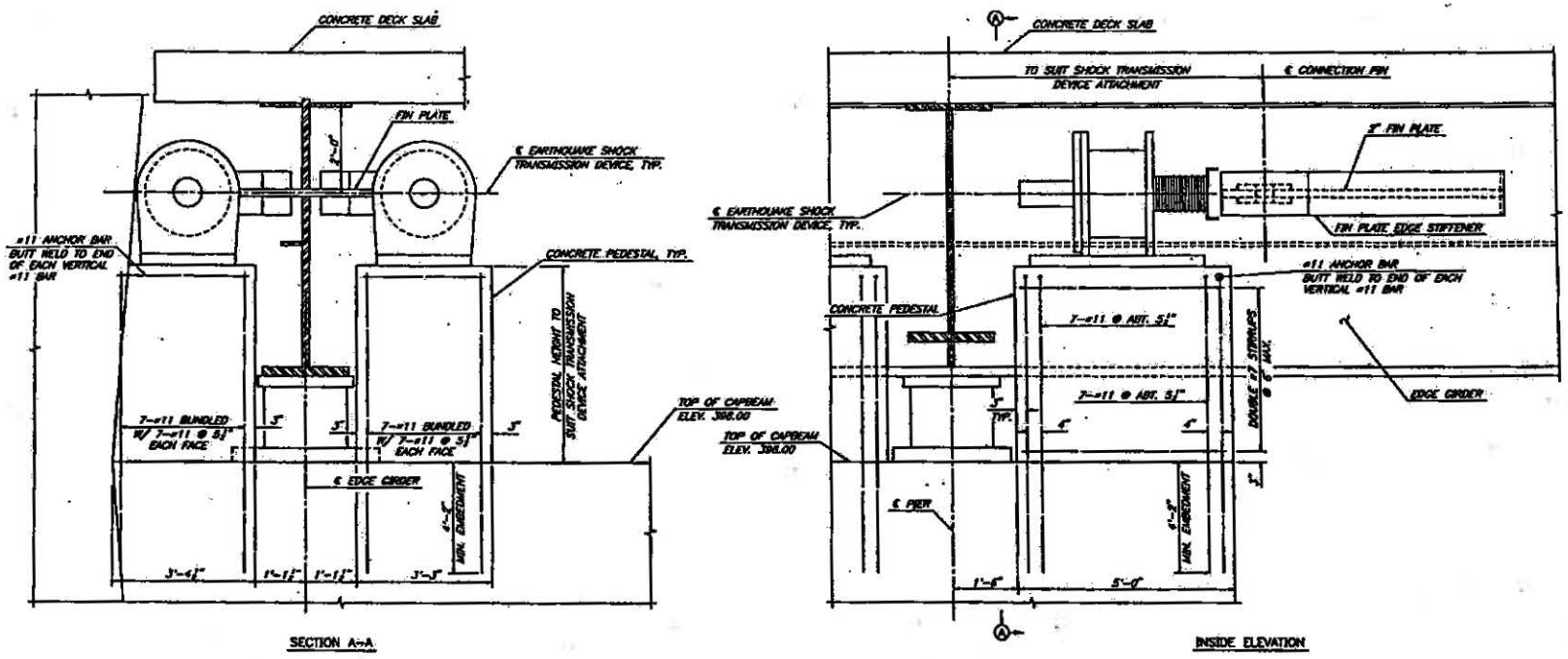

Fig. 1.9 Earthquake Shock Transmission Device

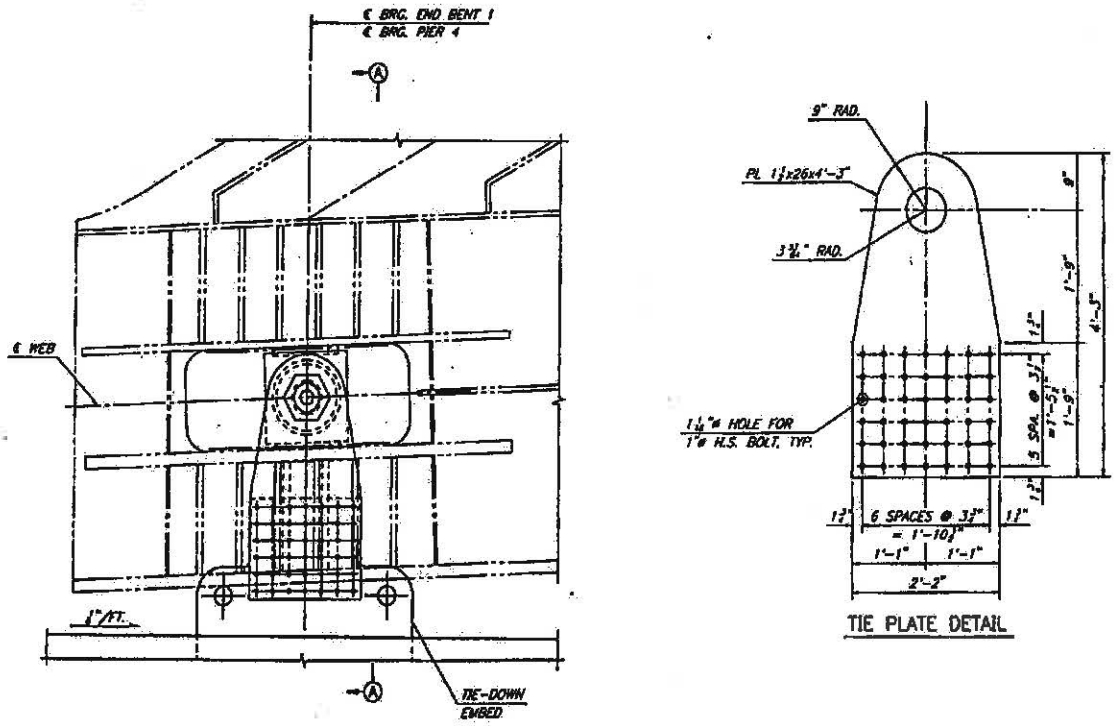

Fig. 1.10 Elevation of Abutment Bearing at Pier 1 and 4

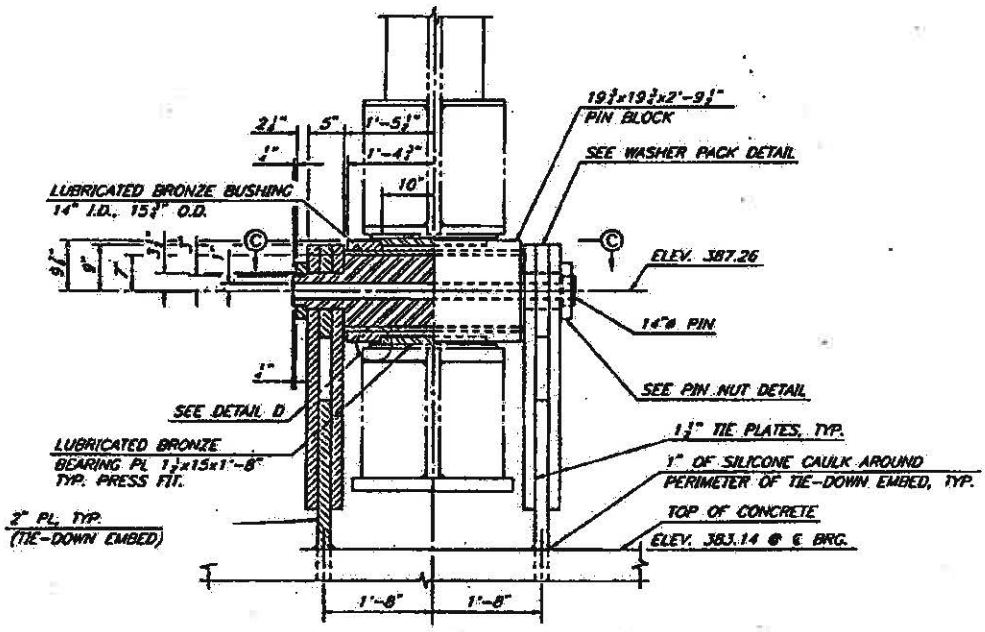

Fig. 1.11 Section View A-A of Abutment Bearing at Pier 1 and 4

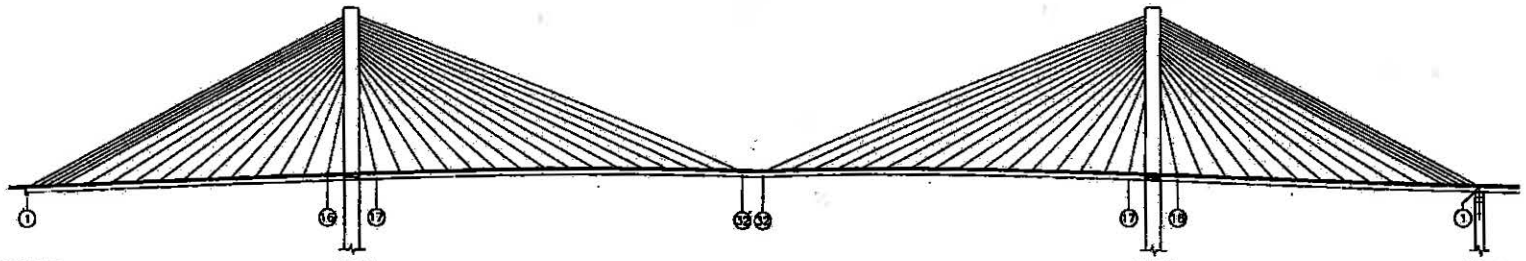

ELEVATION

CABLE NUMBER	CABLE DATA				CABLE FORCES													
								THERMAL LOAD		LIVE LOAD PLUS IMPACT				DESIGN LOAD				
										LANE LOAD		TRUCK LOAD						
	NUMBER OF 0.6"ϕ STRANDS ‡	STEEL AREA	PE PIPE DIAMETER	UNIT WEIGHT OF GROUTED CABLE	INITIAL DEAD LOAD †	LONG TERM LOSSES	FINAL DEAD LOAD †	MAXIMUM	MINIMUM	MAXIMUM	MINIMUM	MAXIMUM	MINIMUM	CABLE FORCE MAXIMUM	CABLE STRESS MAXIMUM	CABLE FORCE MINIMUM	CABLE STRESS MINIMUM	STRESS RANGE (TRUCK)
		(IN²)	(IN)	(LB/FT)	(KIPS)	(KIPS)	(KIPS)	(KIPS)	(KIPS)	(KIPS)	(KIPS)	(KIPS)	(KIPS)	(KIPS)	(KSI)	(KIPS)	(KSI)	(KSI)
1	54	11.72	10.75	102	1045	-26	1019	43	-32	341	-194	84	-67	1386	118	825	70	13
2	54	11.72	10.75	102	1089	-20	1069	37	-26	299	-158	74	-50	1368	118	919	78	11
3	50	10.85	10.75	100	1039	-13	1019	26	-20	231	-83	57	-33	1363	116	928	85	8
4	46	9.98	8.63	70	992	-13	979	19	-14	181	-67	43	-22	1173	117	922	82	7
5	43	9.33	8.63	69	942	-7	935	12	-9	150	-35	33	-15	1082	117	900	96	5
6	41	8.90	8.63	88	893	8	901	6	-4	106	-12	58	-7	1057	119	881	99	7
7	39	8.46	8.63	88	841	14	855	1	-1	159	-5	81	-3	1014	120	836	98	10
8	39	8.46	8.63	88	811	16	827	1	-2	178	-14	92	-3	1005	119	797	94	11
9	35	7.60	7.13	90	724	11	735	2	-3	183	-24	89	-6	918	121	700	92	13
10	33	7.16	7.13	49	663	7	672	3	-4	178	-24	86	-6	850	119	641	89	13
11	31	6.73	7.13	48	633	5	638	2	-3	166	-20	81	-5	802	119	613	91	13
12	29	6.29	7.13	47	589	2	591	1	-2	152	-14	78	-3	743	118	575	91	13
13	27	5.86	8.63	41	564	-3	561	1	0	132	-12	74	-4	696	119	549	94	13
14	23	4.99	8.63	40	475	-12	463	5	-4	116	-17	70	-9	581	118	446	88	16
15	21	4.56	8.63	39	436	-27	409	13	-9	91	-24	59	-14	527	116	385	85	16
16	20	4.34	8.63	39	420	-40	380	23	-17	49	-24	35	-15	469	108	356	82	11
17	20	4.34	8.63	39	390	-40	350	23	-19	50	-28	35	-15	440	101	322	74	11
18	21	4.56	8.63	39	430	-22	408	17	-12	88	-29	58	-14	518	114	379	83	16
19	23	4.99	8.63	40	470	-13	459	7	-6	118	-24	72	-9	568	118	435	87	18
20	24	5.21	8.63	40	485	-1	464	1	-1	131	-20	73	-7	596	114	444	85	15
21	28	6.08	7.13	47	556	3	559	2	-3	144	-17	77	-8	703	116	539	89	14
22	29	6.29	7.13	47	592	3	595	4	-5	148	-16	77	-5	743	118	578	92	13
23	32	6.94	7.13	48	638	2	640	5	-6	163	-18	81	-5	803	116	620	89	12
24	34	7.38	7.13	49	690	1	691	5	-7	174	-19	83	-5	865	117	671	91	12
25	38	8.25	8.63	67	743	4	747	5	-8	194	-21	89	-8	941	114	723	88	12
26	39	8.46	8.63	68	808	5	813	2	-3	193	-20	87	-5	1006	119	788	93	11
27	42	9.11	8.63	69	889	2	891	3	-2	199	-14	89	-4	1090	120	875	96	10
28	44	9.55	8.63	70	941	4	945	12	-9	193	-8	85	-2	1138	119	933	98	9
29	46	9.98	8.63	70	992	1	993	26	-18	207	-16	83	-4	1200	120	976	98	9
30	49	10.63	10.75	100	1021	-2	1019	43	-32	225	-35	80	-9	1246	117	984	93	8
31	54	11.72	10.75	102	1160	-3	1157	68	-49	260	-69	81	-16	1420	121	1088	93	8
32	54	11.72	10.75	102	970	-8	962	83	-63	277	-110	81	-26	1247	106	852	73	9

NOTES:
‡ – NUMBER OF 0.6"ϕ, 7 WIRE STRANDS
† – INITIAL DEAD LOAD AT BEGINNING OF SERVICE LIFE. FINAL DEAD LOAD AFTER LONG TERM CREEP AND SHRINKAGE LOSSES.
NEGATIVE FORCES INDICATE A REDUCTION IN TENSION IN THE CABLE.
① INDICATES STAY CABLE.

Fig. 1.12 Cable Data and Forces

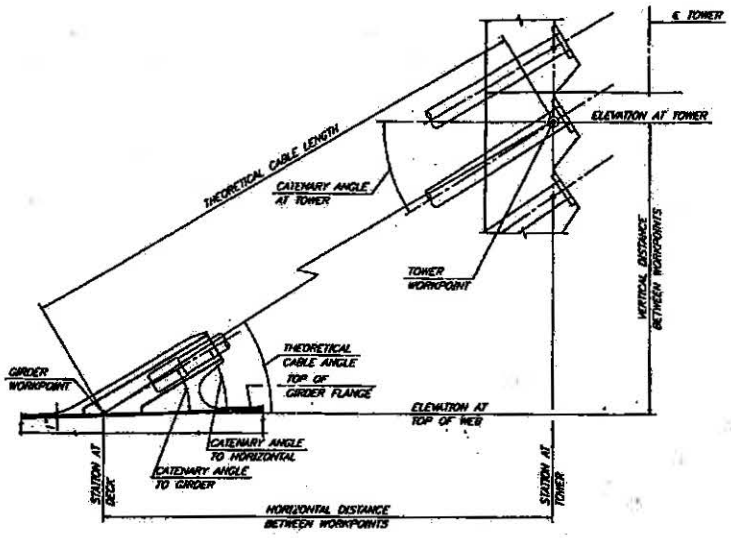

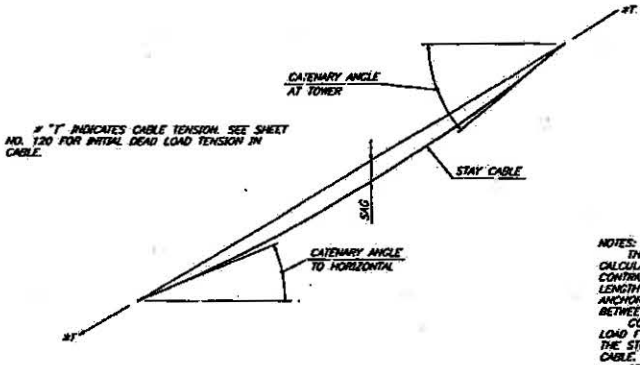

NOTES:
1. THE THEORETICAL CABLE LENGTH SHOWN IS CALCULATED BETWEEN CABLE WORKPOINTS. THE CONTRACTOR SHALL DETERMINE THE REQUIRED LENGTH OF CABLE BASED UPON THE STAY CABLE ANCHORAGE HARDWARE PROVIDED AND THE DISTANCE BETWEEN ANCHORAGE POINTS.
2. COMPUTED SAG IS BASED UPON THE DEAD LOAD FORCE IN THE CABLE UPON COMPLETION OF THE STRUCTURE AND THE GROUTED WEIGHT OF THE CABLE.
3. HORIZONTAL AND VERTICAL DISTANCES, CABLE LENGTH, AND MIDPOINT SAG ARE MEASURED IN FEET.

CABLE DATA – PIER 2

STAY CABLE	GIRDER WORKPOINT STATION AT DECK	GIRDER WORKPOINT ELEVATION AT TOP OF WEB	GIRDER WORKPOINT THEORETICAL CABLE ANGLE	TOWER WORKPOINT STATION AT TOWER	TOWER WORKPOINT ELEVATION AT TOWER	HORIZONTAL DIST B/W WORK POINTS	VERTICAL DIST B/W WORK POINTS	THEORETICAL CABLE LENGTH	CATENARY ANGLE TO HORIZONTAL	CATENARY ANGLE TO GIRDER	CATENARY ANGLE AT TOWER	MIDPOINT SAG
1	182+32.00	390.426	28°12'41.7"	186+93.50	638.000	461.500	247.574	523.713	26°51'23.7"	24°53'11.0"	29°29'20.3"	3.353
2	182+44.00	390.839	28°18'48.4"	186+93.50	633.000	448.500	242.161	510.580	27°02'54.6"	25°04'41.9"	29°30'23.1"	3.055
3	182+56.00	391.252	28°25'10.3"	186+93.50	628.000	437.500	236.748	497.448	27°08'39.8"	25°10'27.1"	29°37'21.7"	3.004
4	182+68.00	391.664	28°31'55.5"	186+93.50	623.000	425.500	231.336	484.321	27°17'49.5"	25°19'36.8"	29°43'17.5"	2.876
5	182+80.00	392.077	28°39'02.8"	186+93.50	618.000	413.500	225.923	471.194	27°44'24.7"	25°46'12.0"	29°30'54.0"	2.042
6	183+15.00	393.281	30°08'06.6"	186+93.50	613.000	378.500	219.719	437.651	26°15'57.0"	27°17'44.3"	30°57'39.2"	1.833
7	183+50.00	394.485	31°51'52.4"	186+93.50	608.000	343.500	213.515	404.452	31°01'44.3"	28°03'31.6"	32°39'10.8"	1.653
8	183+85.00	395.689	33°54'03.6"	186+93.50	603.000	308.500	207.311	371.686	33°07'07.8"	31°08'55.1"	34°38'11.0"	1.450
9	184+20.00	396.893	36°19'38.7"	186+93.50	598.000	273.500	201.107	338.980	35°45'20.5"	33°47'07.8"	36°51'52.2"	0.994
10	184+55.00	398.097	39°15'21.1"	186+93.50	593.000	238.500	194.903	308.009	38°43'22.8"	36°45'10.2"	38°45'12.3"	0.870
11	184+90.00	398.301	42°50'19.7"	186+93.50	588.000	203.500	188.699	277.324	42°22'06.5"	40°23'53.8"	43°18'28.3"	0.725
12	185+25.00	400.505	47°17'00.1"	186+93.50	583.000	168.500	182.495	248.388	46°52'06.8"	44°53'54.1"	47°38'48.6"	0.612
13	185+60.00	401.709	52°42'26.9"	186+93.50	577.000	133.500	175.291	220.139	52°24'01.3"	50°25'50.6"	52°59'05.5"	0.443
14	185+95.00	402.913	59°28'48.5"	186+93.50	570.000	98.500	167.087	193.960	58°12'40.6"	56°14'27.9"	58°40'30.6"	0.398
15	186+30.00	404.117	68°05'24.8"	186+87.50	562.000	63.500	157.883	170.175	67°53'48.1"	65°55'35.4"	66°13'08.8"	0.335
16	186+65.00	405.321	78°42'14.1"	186+93.50	548.000	28.500	143.679	145.498	78°35'33.5"	76°37'42.8"	76°46'46.0"	0.246
17	187+35.00	407.628	78°31'23.8"	187+06.50	548.000	28.500	140.374	143.238	78°24'52.8"	76°26'28.9"	76°36'14.3"	0.235
18	187+70.00	408.674	67°30'11.3"	187+06.50	562.000	63.500	153.326	165.955	67°18'48.4"	65°20'34.8"	67°39'59.8"	0.312
19	188+05.00	409.633	58°26'16.6"	187+06.50	570.000	98.500	160.347	188.185	58°10'33.8"	56°12'56.3"	58°40'30.6"	0.375
20	188+40.00	410.561	51°16'01.6"	187+06.50	577.000	133.500	166.439	213.384	50°54'52.8"	48°29'09.7"	51°35'38.5"	0.440
21	188+75.00	411.398	45°31'21.4"	187+06.50	583.000	168.500	171.602	240.499	45°05'36.3"	43°46'47.5"	45°55'36.3"	0.610
22	189+10.00	412.186	40°49'43.7"	187+06.50	588.000	203.500	176.834	268.942	40°20'48.3"	39°08'31.9"	41°17'14.6"	0.716
23	189+45.00	412.863	37°03'48.5"	187+06.50	593.000	238.500	180.137	298.884	36°31'57.1"	35°26'55.0"	37°34'22.3"	0.838
24	189+80.00	413.490	34°00'16.7"	187+06.50	598.000	273.500	184.510	329.918	33°25'58.7"	32°27'31.1"	34°13'23.1"	0.964
25	190+15.00	414.047	31°29'13.5"	187+06.50	603.000	308.500	188.953	361.767	30°39'53.5"	29°48'38.3"	32°18'51.8"	1.482
26	190+50.00	414.534	29°23'20.8"	187+06.50	608.000	343.500	193.466	394.335	28°52'33.8"	27°48'13.2"	30°12'38.3"	1.634
27	190+85.00	414.950	27°37'15.0"	187+06.50	613.000	378.500	198.050	427.184	26°45'44.1"	26°08'17.8"	28°27'22.0"	1.773
28	191+20.00	415.296	26°06'53.4"	187+06.50	618.000	413.500	202.704	460.512	25°13'08.4"	24°42'34.8"	26°58'23.8"	1.973
29	191+55.00	415.572	24°49'12.8"	187+06.50	623.000	448.500	207.428	494.144	23°54'08.6"	23°30'28.5"	25°43'08.8"	2.151
30	191+90.00	415.778	23°41'53.1"	187+06.50	628.000	483.500	212.222	528.025	22°19'28.4"	22°24'43.6"	25°02'16.2"	3.407
31	192+25.00	415.913	22°43'05.7"	187+06.50	633.000	518.500	217.087	562.111	21°23'29.8"	21°13'37.8"	24°01'00.0"	3.486
32	192+60.00	415.979	21°51'24.6"	187+06.50	638.000	553.900	222.021	596.369	20°10'01.5"	20°07'03.9"	23°30'23.4"	4.681

CABLE DATA – PIER 3

STAY CABLE	GIRDER WORKPOINT STATION AT DECK	GIRDER WORKPOINT ELEVATION AT TOP OF WEB	GIRDER WORKPOINT THEORETICAL CABLE ANGLE	TOWER WORKPOINT STATION AT TOWER	TOWER WORKPOINT ELEVATION AT TOWER	HORIZONTAL DIST B/W WORK POINTS	VERTICAL DIST B/W WORK POINTS	THEORETICAL CABLE LENGTH	CATENARY ANGLE TO HORIZONTAL	CATENARY ANGLE TO GIRDER	CATENARY ANGLE AT TOWER	MIDPOINT SAG
32	192+90.00	415.979	21°51'24.6"	198+43.50	638.000	551.500	222.021	596.369	20°10'01.5"	20°07'03.9"	23°30'23.4"	4.681
31	193+25.00	415.913	22°43'05.7"	198+43.50	633.000	518.500	217.087	562.111	21°23'29.8"	21°13'37.8"	24°01'00.0"	3.486
30	193+60.00	415.778	23°41'53.1"	198+43.50	628.000	483.500	212.222	528.025	22°19'28.4"	22°24'43.6"	25°02'16.2"	3.407
29	193+95.00	415.572	24°49'12.8"	198+43.50	623.000	448.500	207.428	494.144	23°54'08.6"	23°30'28.5"	25°43'08.8"	2.151
28	194+30.00	415.296	26°06'53.4"	198+43.50	618.000	413.500	202.704	460.512	25°13'08.4"	24°42'34.8"	26°58'23.8"	1.973
27	194+65.00	414.950	27°37'15.0"	198+43.50	613.000	378.500	198.050	427.184	26°45'44.1"	26°08'17.8"	28°27'22.0"	1.773
26	195+00.00	414.534	29°23'20.8"	198+43.50	608.000	343.500	193.466	394.335	28°52'33.8"	27°48'13.2"	30°12'38.3"	1.634
25	195+35.00	414.047	31°29'13.5"	198+43.50	603.000	308.500	188.953	361.767	30°39'53.5"	29°48'38.3"	32°18'51.8"	1.482
24	195+70.00	413.490	34°00'16.7"	198+43.50	598.000	273.500	184.510	329.918	33°25'58.7"	32°27'31.1"	34°13'23.1"	0.964
23	196+05.00	412.863	37°03'48.5"	198+43.50	593.000	238.500	180.137	298.884	36°31'57.1"	35°26'55.0"	37°34'22.3"	0.838
22	196+40.00	412.186	40°49'43.7"	198+43.50	588.000	203.500	175.834	268.942	40°20'48.3"	39°08'31.9"	41°17'14.6"	0.725
21	196+75.00	411.398	45°31'21.4"	198+43.50	583.000	168.500	171.602	240.499	45°05'36.3"	43°46'47.5"	45°55'36.3"	0.610
20	197+10.00	410.561	51°16'01.6"	198+43.50	577.000	133.500	166.439	213.384	50°54'52.8"	48°29'09.7"	51°35'38.5"	0.490
19	197+45.00	409.653	58°26'16.6"	198+43.50	570.000	98.500	160.347	188.185	58°10'33.8"	56°12'56.3"	58°40'30.6"	0.375
18	197+80.00	408.674	67°30'11.3"	198+43.50	562.000	63.500	153.326	165.955	67°18'48.4"	65°20'34.8"	67°39'59.8"	0.312
17	198+15.00	407.628	78°31'23.8"	198+43.50	548.000	28.500	140.374	143.238	78°24'52.8"	76°26'28.9"	76°36'14.3"	0.235
16	198+65.00	405.321	78°42'14.1"	198+56.50	548.000	28.500	142.679	145.498	78°35'33.5"	76°37'42.8"	76°46'46.0"	0.246
15	199+30.00	404.117	68°05'24.8"	198+56.50	562.000	63.500	157.883	170.175	67°53'48.1"	65°55'35.4"	66°13'08.8"	0.335
14	199+55.00	402.913	59°28'48.5"	198+56.50	570.000	98.500	167.087	193.960	59°12'40.6"	57°14'27.9"	59°43'01.2"	0.398
13	199+90.00	401.709	52°42'26.9"	198+56.50	577.000	133.500	175.291	220.139	52°24'01.3"	50°25'50.6"	52°59'05.5"	0.443
12	200+25.00	400.505	47°17'00.1"	198+56.50	583.000	168.500	182.495	248.388	46°52'06.8"	44°53'54.1"	47°38'48.6"	0.612
11	200+60.00	399.301	42°50'19.7"	198+56.50	588.000	203.500	188.699	277.324	42°22'06.5"	40°23'53.8"	43°18'28.3"	0.725
10	200+95.00	398.097	39°15'21.1"	198+56.50	593.000	238.500	194.903	308.009	38°43'22.8"	36°45'10.2"	38°45'12.3"	0.870
9	201+30.00	396.893	36°19'38.7"	198+56.50	598.000	273.500	201.107	338.980	35°45'20.5"	33°47'07.8"	36°51'52.2"	0.994
8	201+65.00	395.689	33°54'03.6"	198+56.50	603.000	308.500	207.311	371.686	33°07'07.8"	31°08'55.1"	34°38'11.0"	1.450
7	202+00.00	394.485	31°51'52.4"	198+56.50	608.000	343.500	213.515	404.452	31°01'44.3"	28°03'31.6"	32°39'10.8"	1.653
6	202+35.00	393.281	30°08'06.6"	198+56.50	613.000	378.500	219.719	437.651	29°15'57.0"	27°17'44.3"	30°57'39.2"	1.833
5	202+70.00	392.077	28°39'02.8"	198+56.50	618.000	413.500	225.923	471.194	27°44'24.7"	25°46'12.0"	29°30'54.0"	2.042
4	203+82.00	391.664	28°31'55.5"	198+56.50	623.000	425.500	231.336	484.321	27°37'48.5"	25°39'36.8"	29°23'17.5"	2.076
3	203+94.00	391.252	28°25'10.3"	198+56.50	628.000	437.500	236.748	497.449	27°08'39.8"	25°10'27.1"	29°37'21.7"	3.004
2	204+06.00	390.839	28°18'48.4"	198+56.50	633.000	449.500	242.161	510.580	27°02'54.6"	25°04'41.9"	29°30'23.1"	3.055
1	204+18.00	390.426	28°12'41.7"	198+56.50	638.000	461.500	247.574	523.713	26°51'23.7"	24°53'11.0"	29°29'20.3"	3.353

Fig 1.13 Cable Geometries

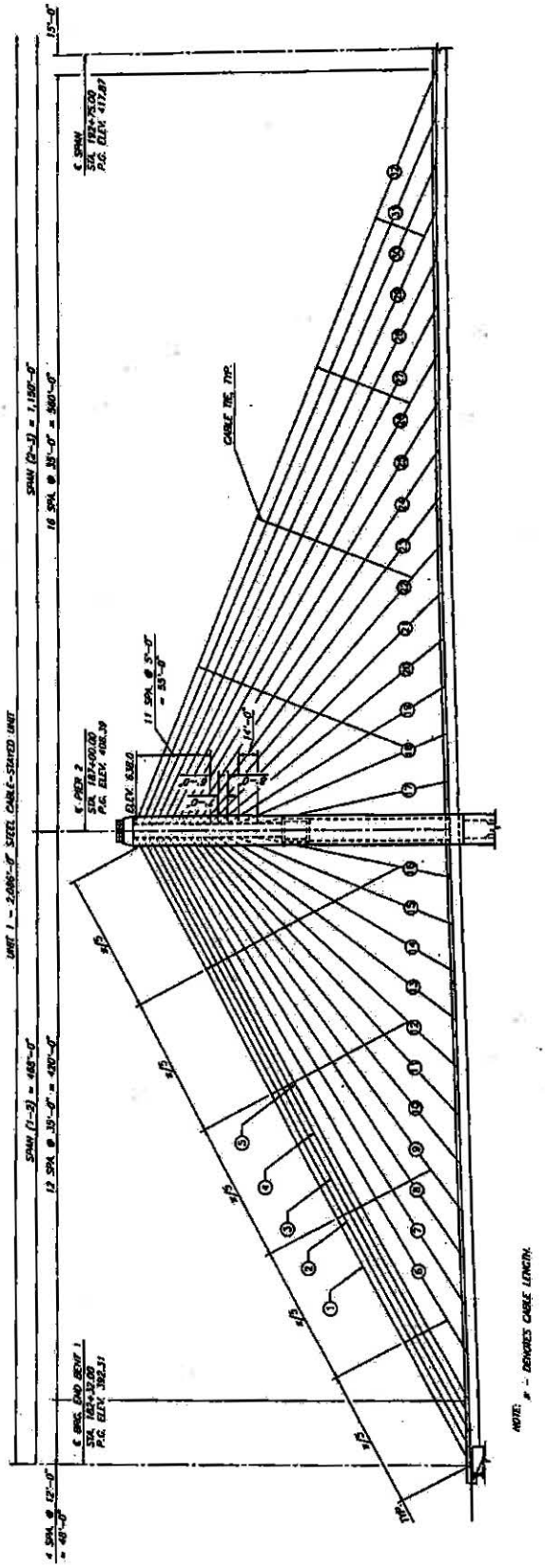

Fig. 1.14 Cable Arrangement at Tower 1

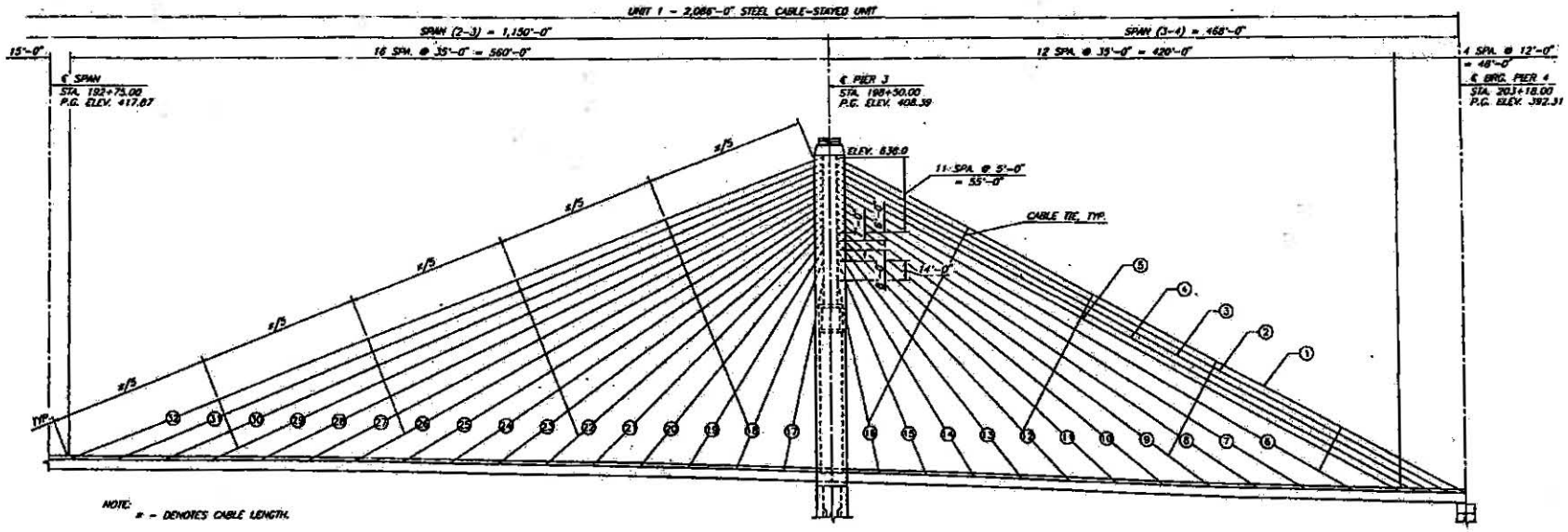

Fig. 1.15 Cable Arrangement at Tower 2

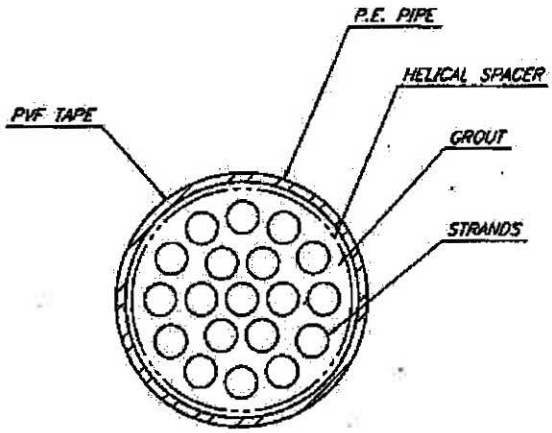

Fig. 1.16 Cable Stay Cross

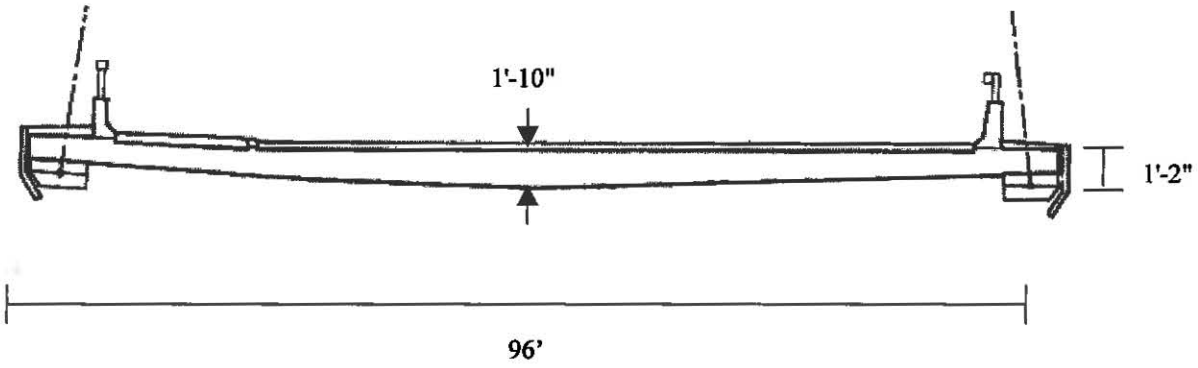

Fig. 2 Cross Section of Precast Concrete Slab Deck Configuration

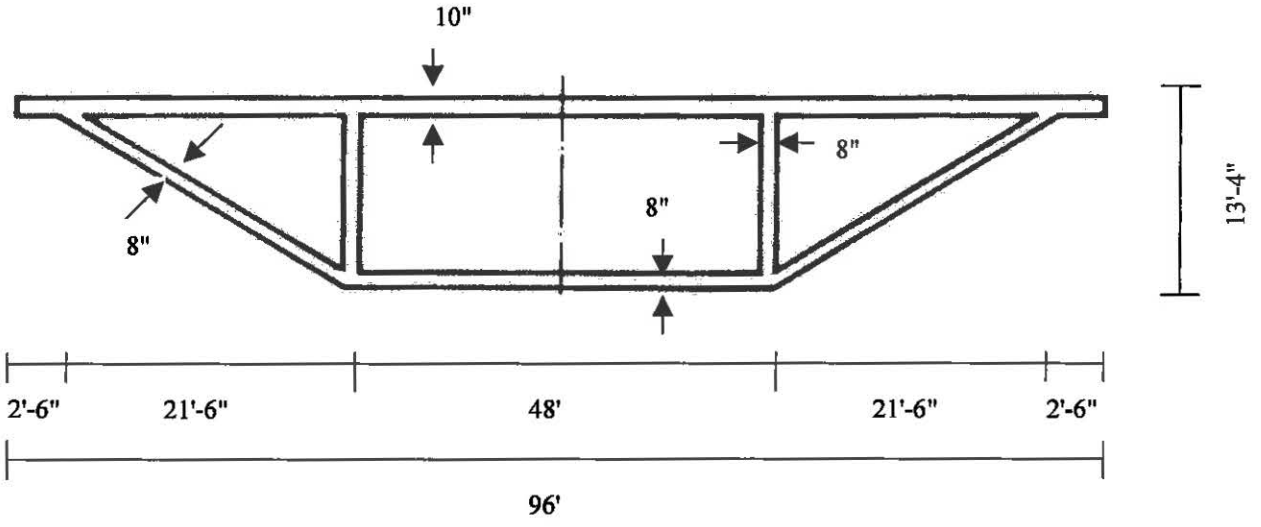

Fig. 2.1 Cross Section of Concrete Box

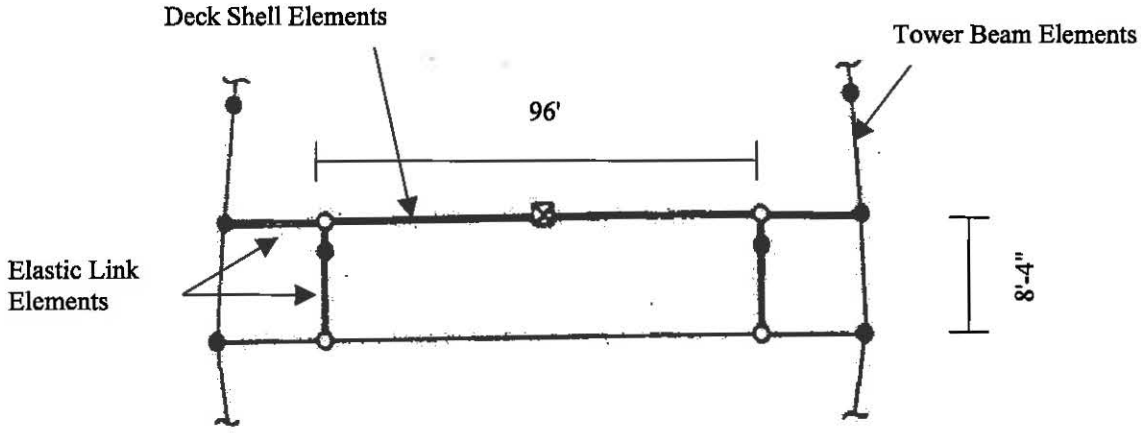

Fig. 2.2 Elastic Links between Tower and Deck

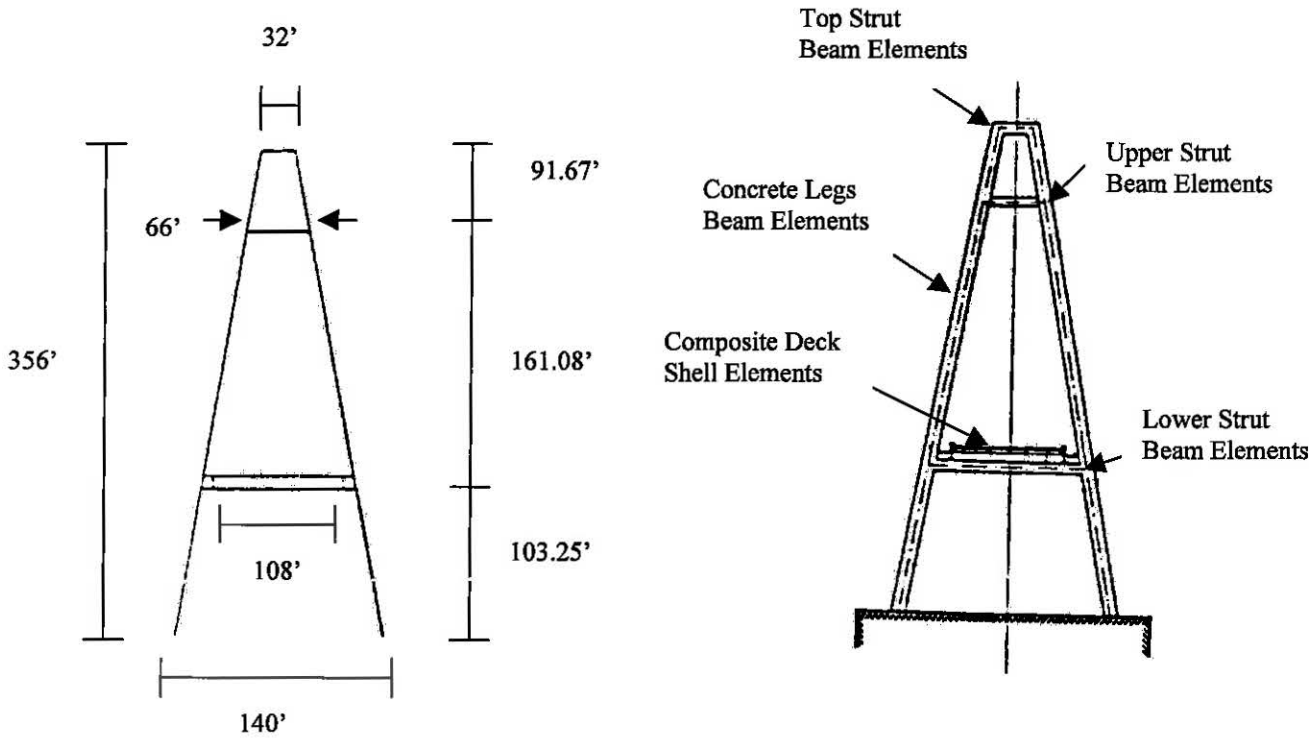

Fig. 2.3 Elevation of A-shape Tower Configuration

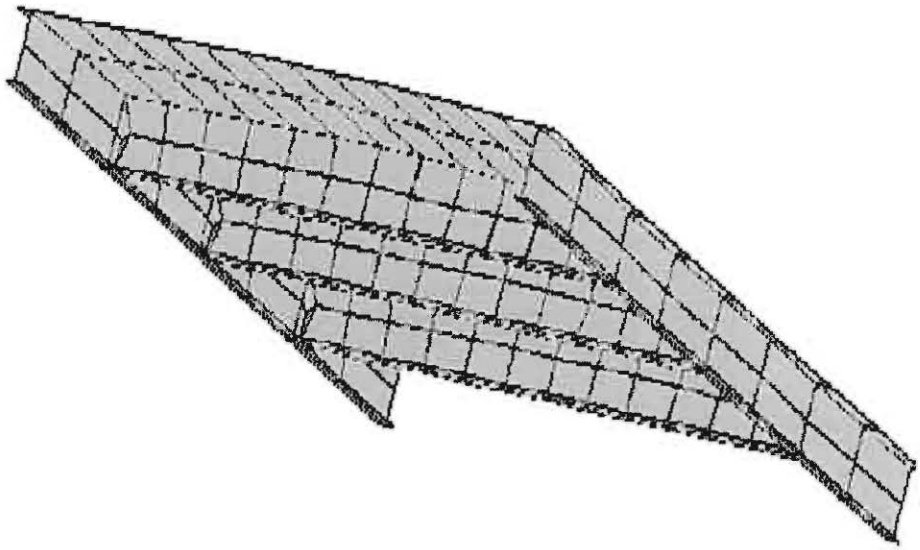

Fig. 2.4 3-D Finite Element Model of the Composite Deck Configuration

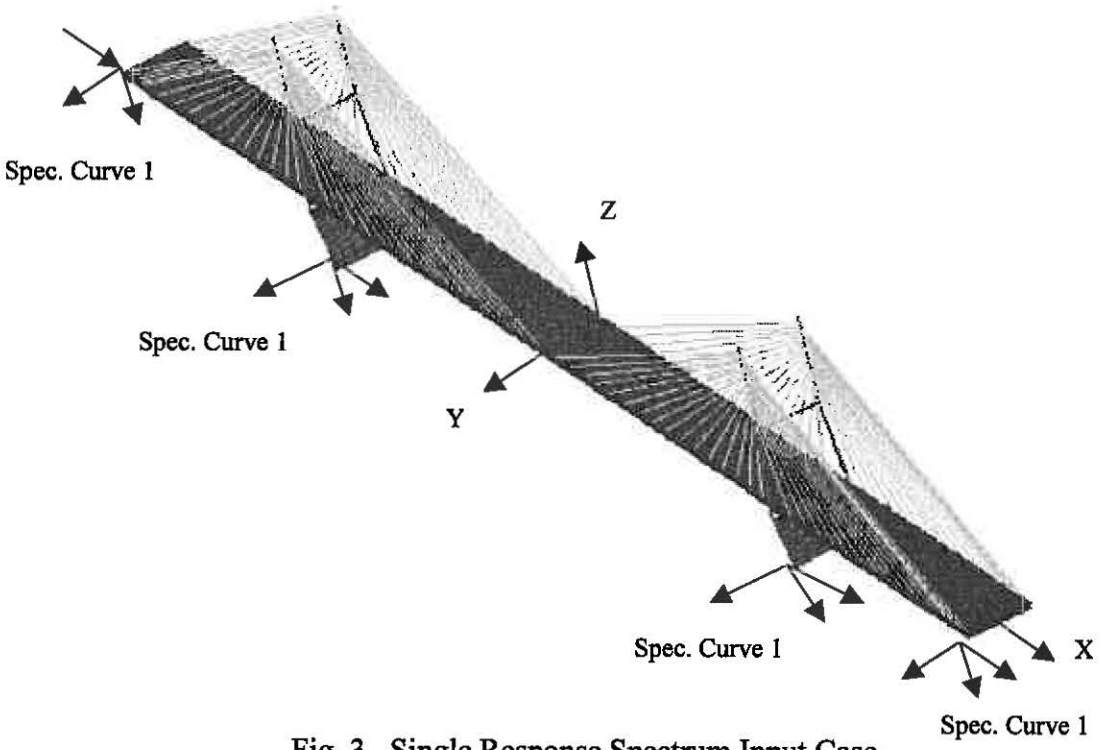

Fig. 3 Single Response Spectrum Input Case

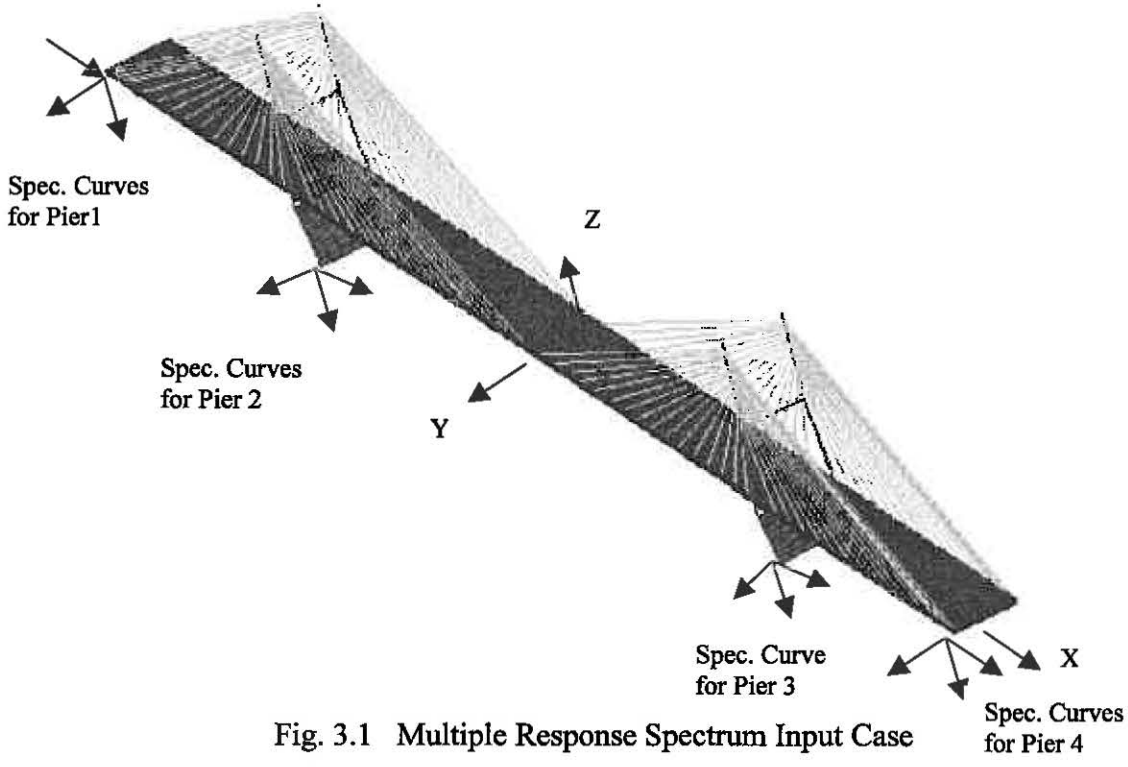

Fig. 3.1 Multiple Response Spectrum Input Case

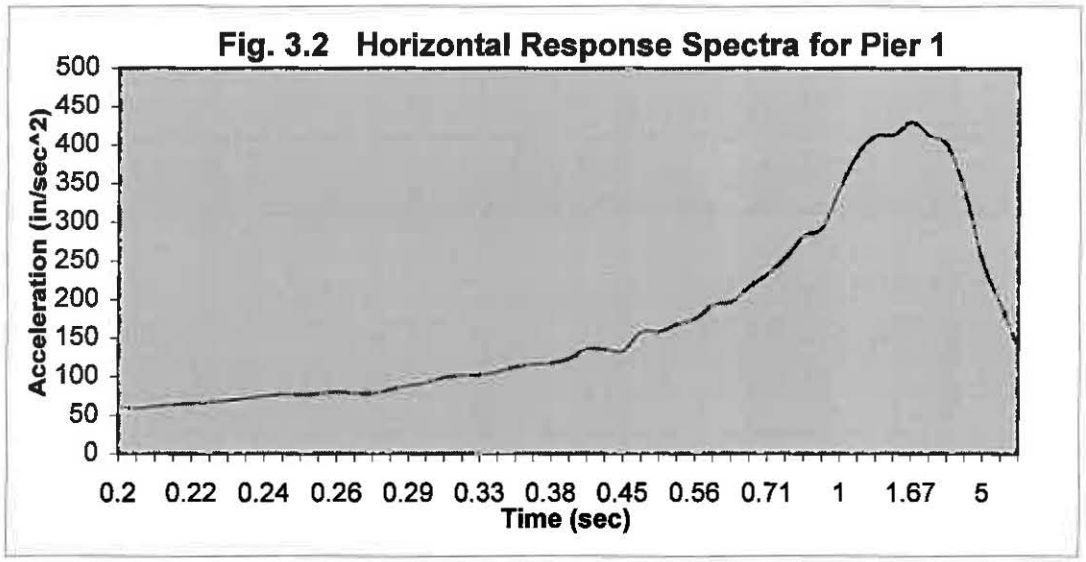
Fig. 3.2 Horizontal Response Spectra for Pier 1
Acceleration (in/sec^2)
500
450
400
350
300
250
200
150
100
50
0
0.2 0.22 0.24 0.26 0.29 0.33 0.38 0.45 0.56 0.71 1 1.67 5
Time (sec)

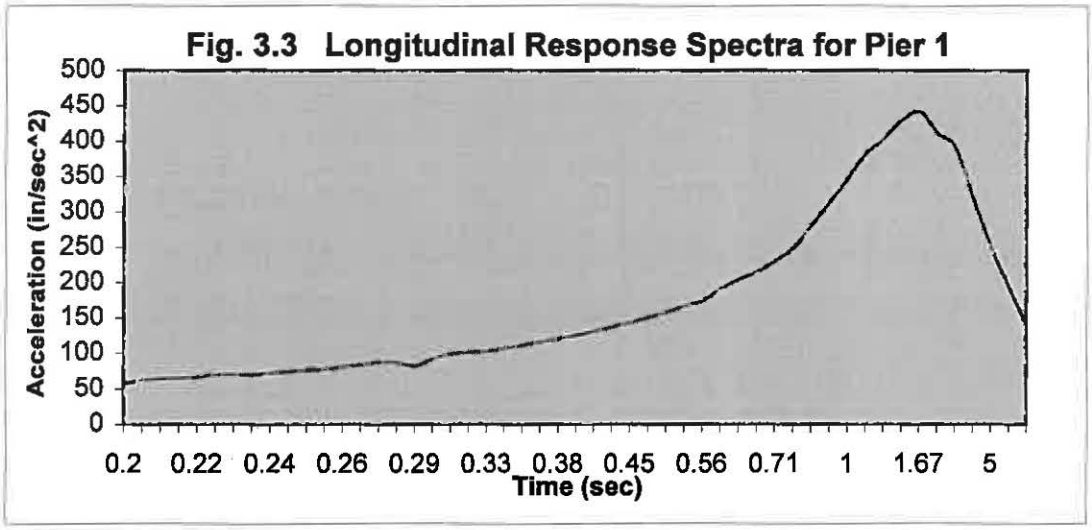
Fig. 3.3 Longitudinal Response Spectra for Pier 1
Acceleration (in/sec^2)
500
450
400
350
300
250
200
150
100
50
0
0.2 0.22 0.24 0.26 0.29 0.33 0.38 0.45 0.56 0.71 1 1.67 5
Time (sec)

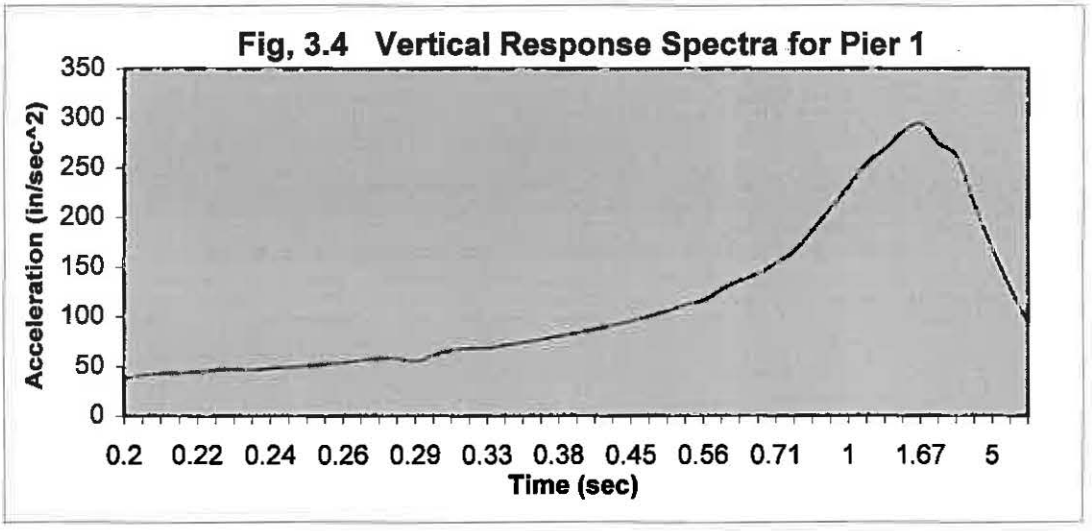
Fig, 3.4 Vertical Response Spectra for Pier 1
Acceleration (in/sec^2)
350
300
250
200
150
100
50
0
0.2 0.22 0.24 0.26 0.29 0.33 0.38 0.45 0.56 0.71 1 1.67 5
Time (sec)

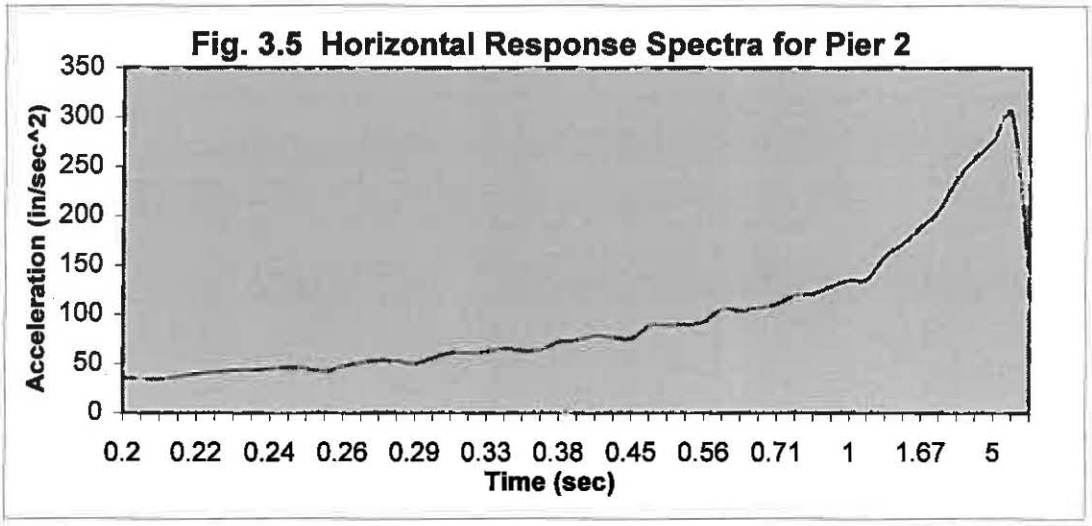
Fig. 3.5 Horizontal Response Spectra for Pier 2
Acceleration (in/sec^2)
350
300
250
200
150
100
50
0
0.2 0.22 0.24 0.26 0.29 0.33 0.38 0.45 0.56 0.71 1 1.67 5
Time (sec)

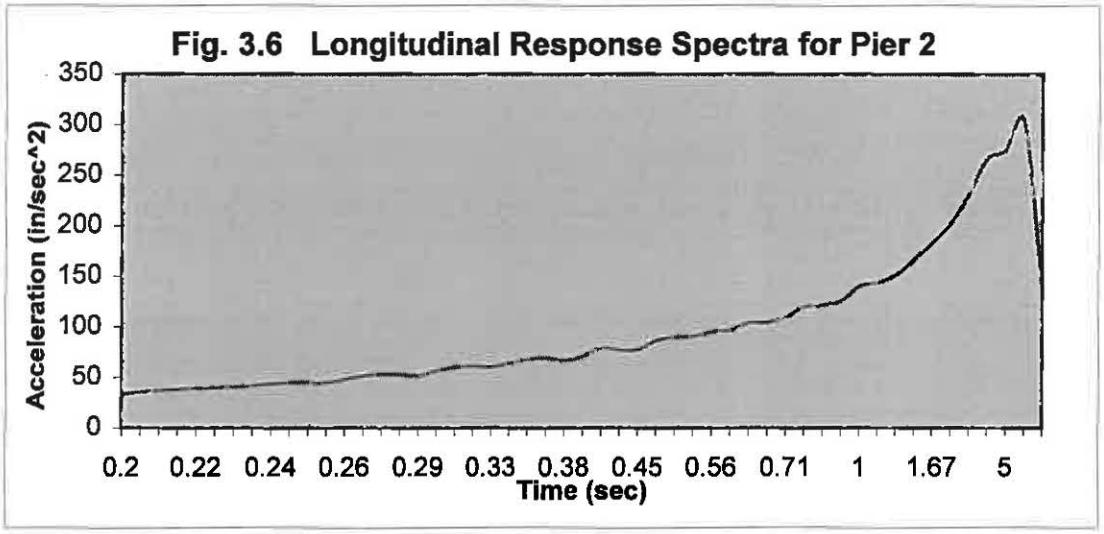
Fig. 3.6 Longitudinal Response Spectra for Pier 2
Acceleration (in/sec^2)
350
300
250
200
150
100
50
0
0.2 0.22 0.24 0.26 0.29 0.33 0.38 0.45 0.56 0.71 1 1.67 5
Time (sec)

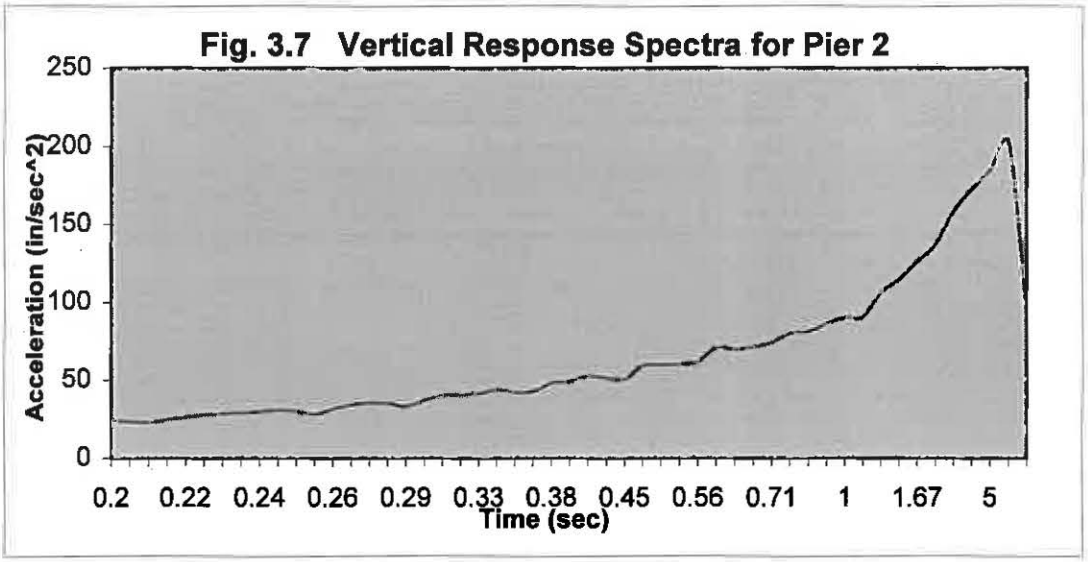
Fig. 3.7 Vertical Response Spectra for Pier 2
Acceleration (in/sec^2)
250
200
150
100
50
0
0.2 0.22 0.24 0.26 0.29 0.33 0.38 0.45 0.56 0.71 1 1.67 5
Time (sec)

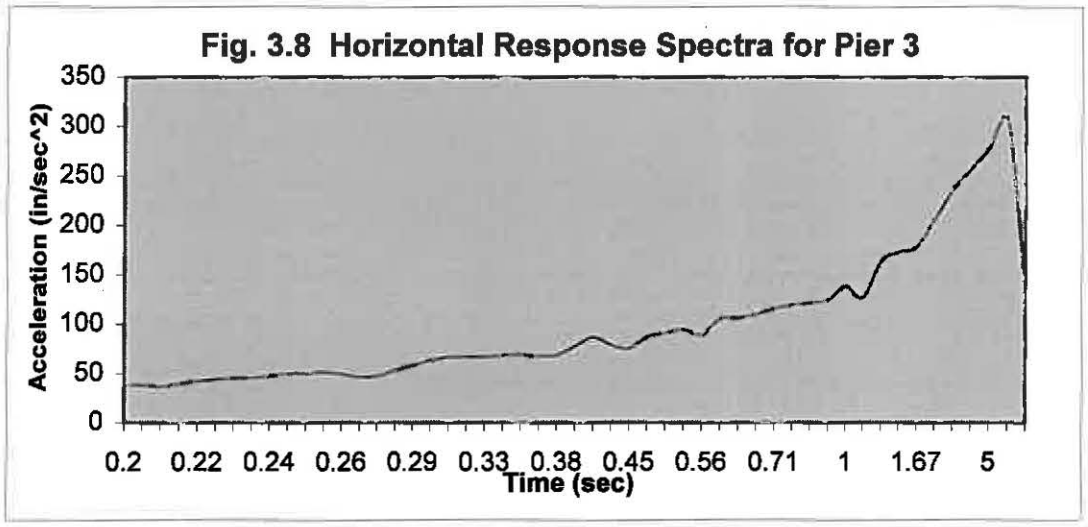
Fig. 3.8 Horizontal Response Spectra for Pier 3
Acceleration (in/sec^2)
350
300
250
200
150
100
50
0
0.2 0.22 0.24 0.26 0.29 0.33 0.38 0.45 0.56 0.71 1 1.67 5
Time (sec)

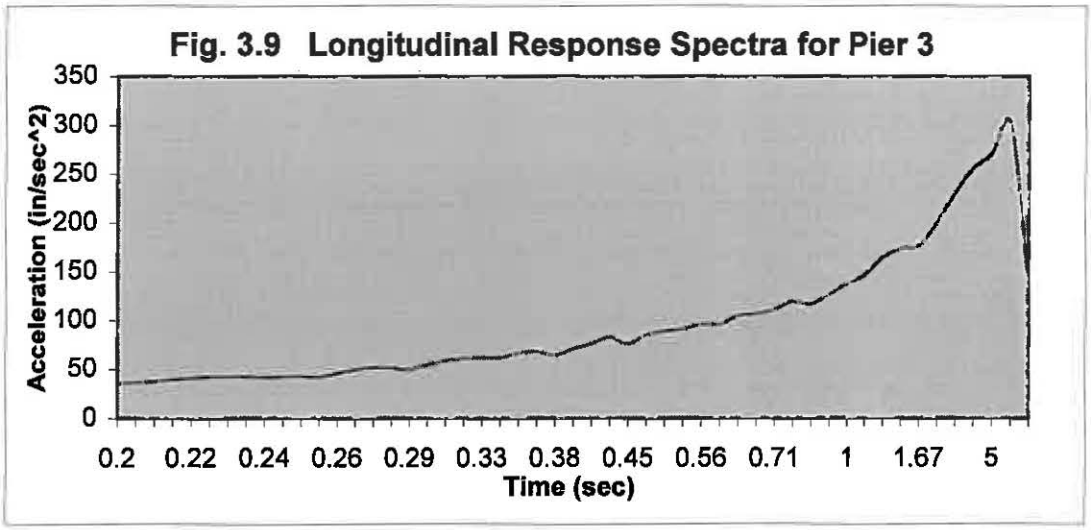
Fig. 3.9 Longitudinal Response Spectra for Pier 3
Acceleration (in/sec^2)
350
300
250
200
150
100
50
0
0.2 0.22 0.24 0.26 0.29 0.33 0.38 0.45 0.56 0.71 1 1.67 5
Time (sec)

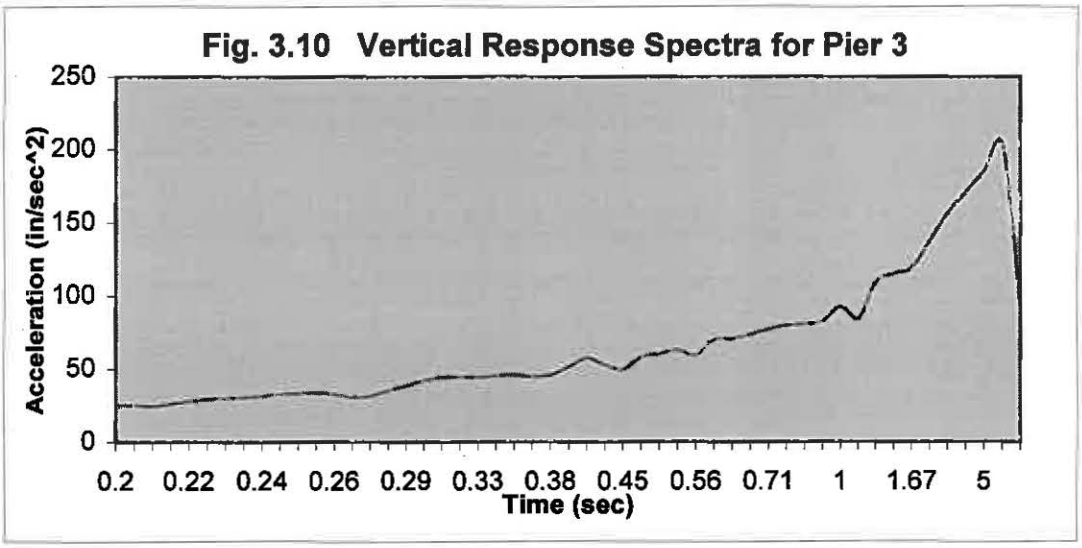
Fig. 3.10 Vertical Response Spectra for Pier 3
Acceleration (in/sec^2)
250
200
150
100
50
0
0.2 0.22 0.24 0.26 0.29 0.33 0.38 0.45 0.56 0.71 1 1.67 5
Time (sec)

Fig. 3.11 Horizontal Response Spectra for Pier 4

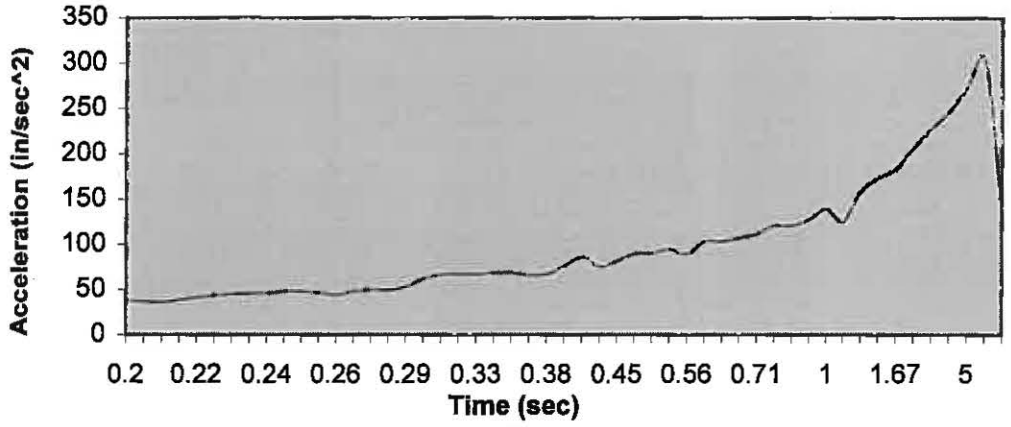

Fig. 3.12 Longitudinal Response Spectra for Pier 4

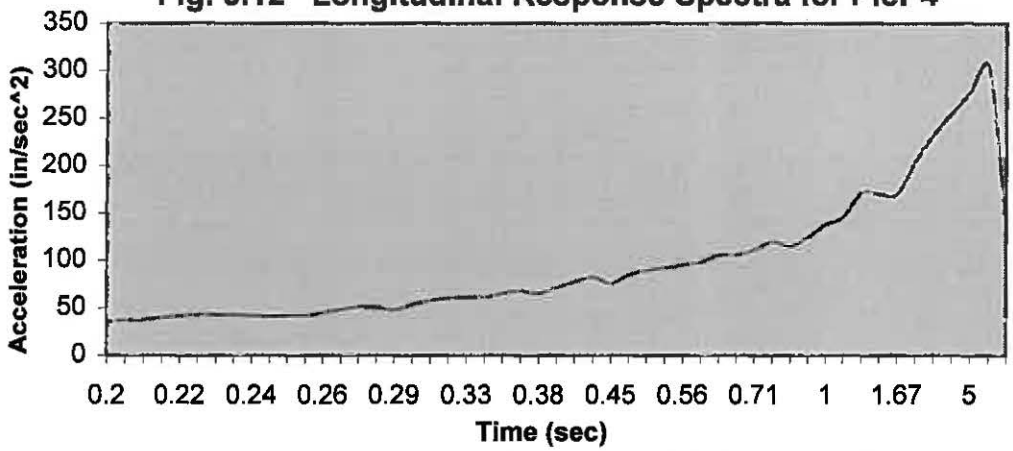

Fig. 3.13 Vertical Response Spectra for Pier 4

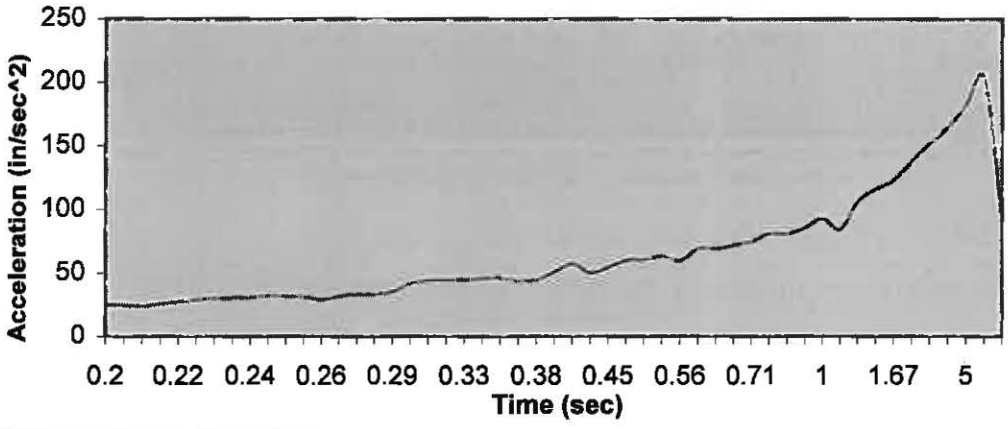

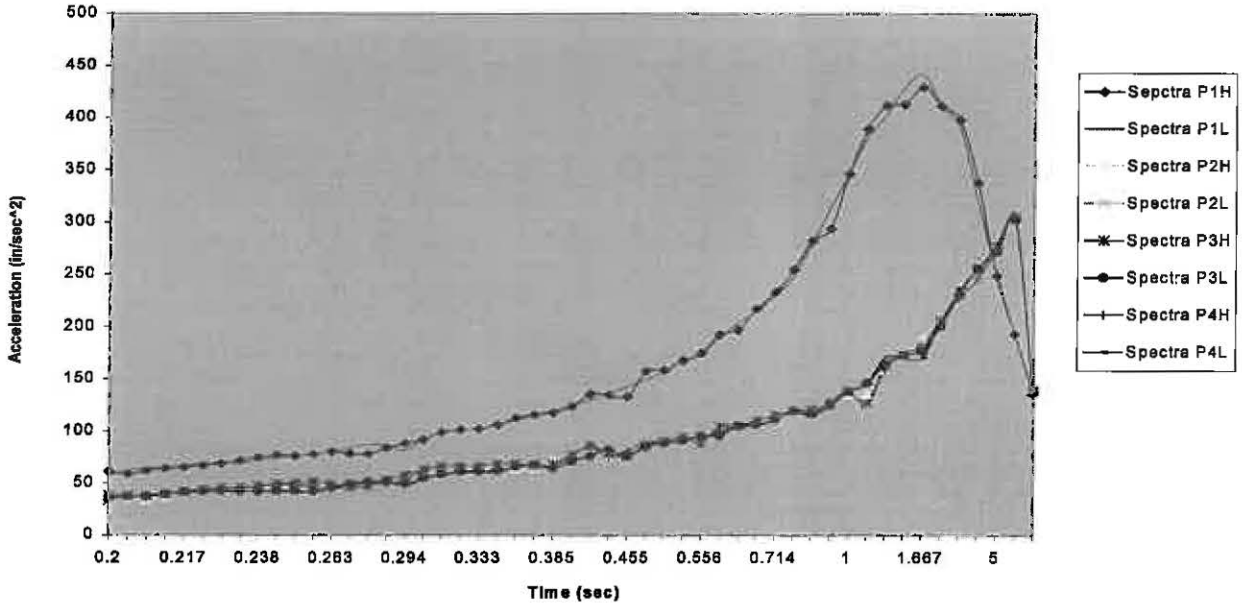

Fig. 3.14 Comparison of Longitudinal and Horizontal Response Spectra

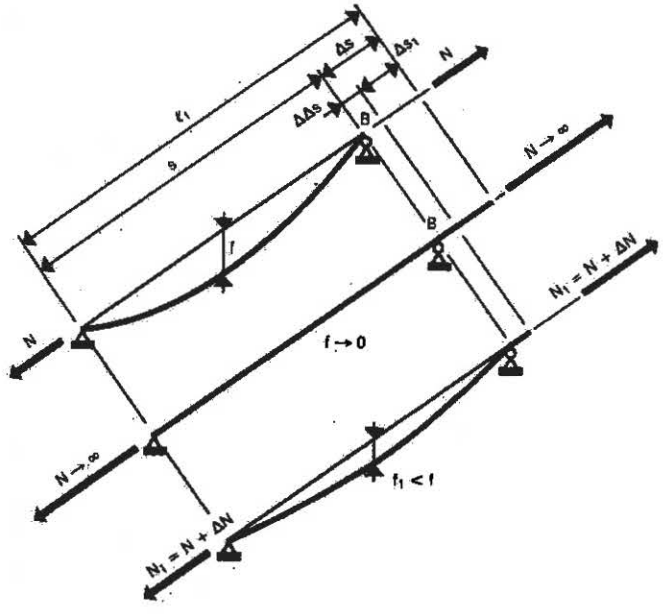

Fig. 3.15 Geometric Behaviour of Cable with Modulus of Elasticity $E = \infty$

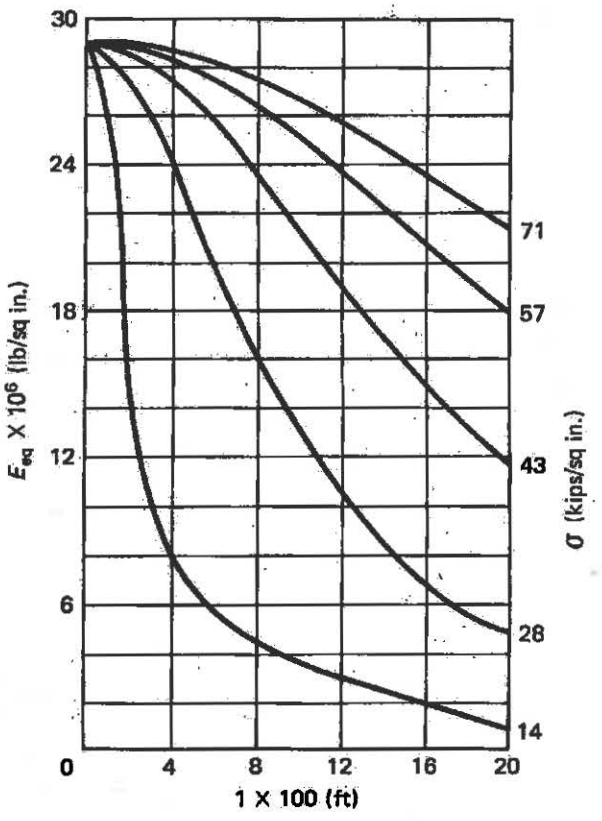

Fig. 3.16 Ernst's Equivalent Modulus of Elasticty

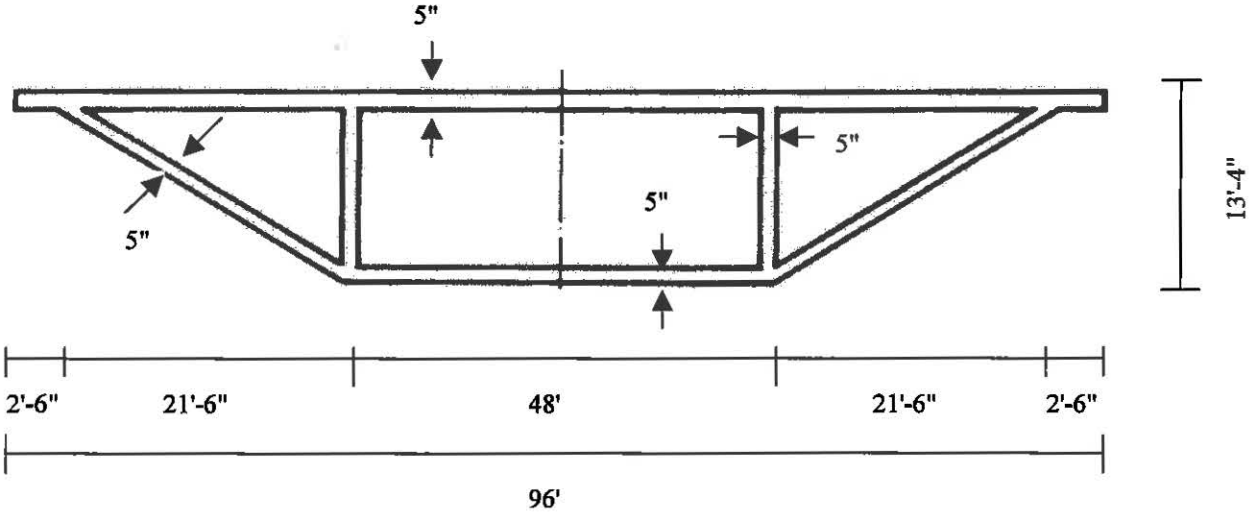

Fig. 4 Cross Section of Steel Box with Concrete Slab on the Top

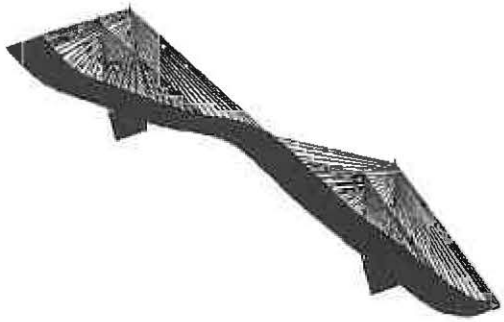

Fig. 5 1. Mode from Modal Analysis

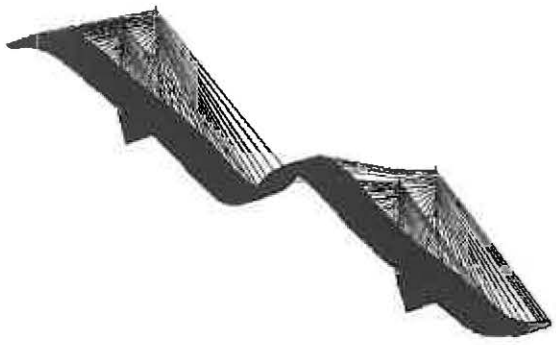

Fig. 5.1 2. Mode from Modal Analysis

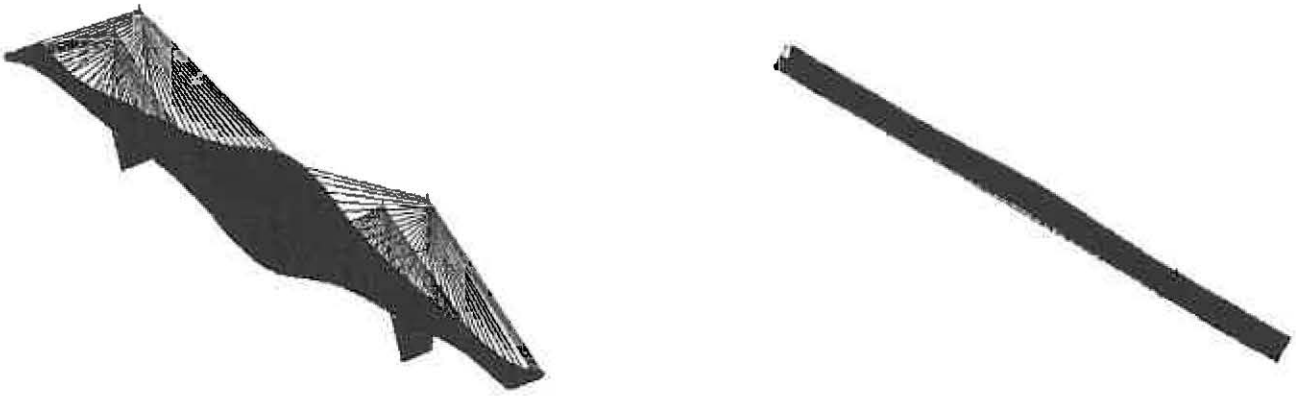

Fig. 5.2 3. Mode from Modal Analysis

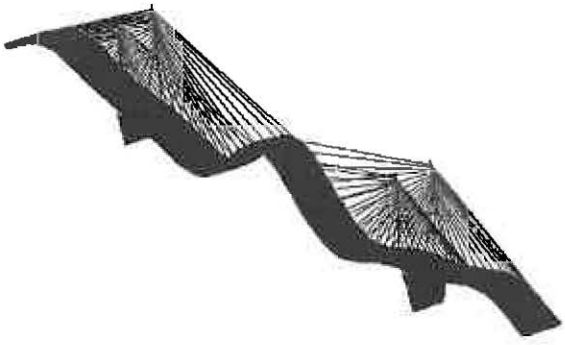

Fig. 5.3 4. Mode from Modal Analysis

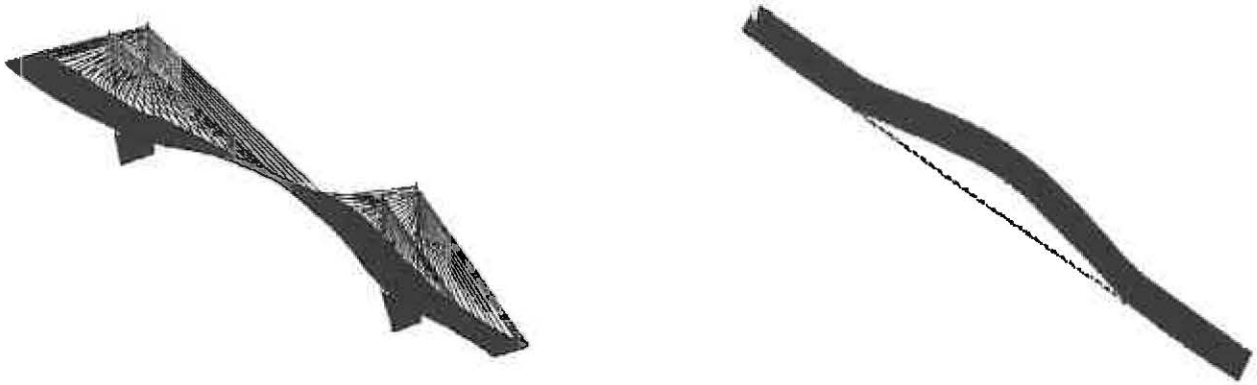

Fig. 5.4 5. Mode from Modal Analysis

Fig. 5.5 6. Mode from Modal Analysis

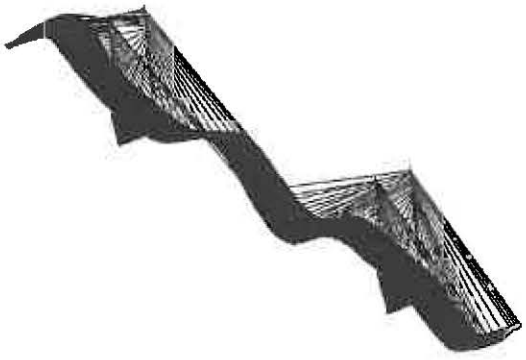

Fig. 5.6 7. Mode from Modal Analysis

Fig. 5.7 8. Mode from Modal Analysis

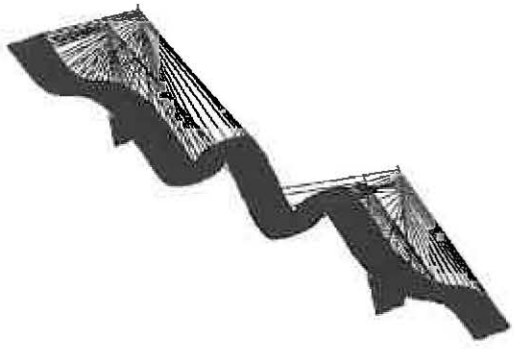

Fig. 5.8 9. Mode from Modal Analysis

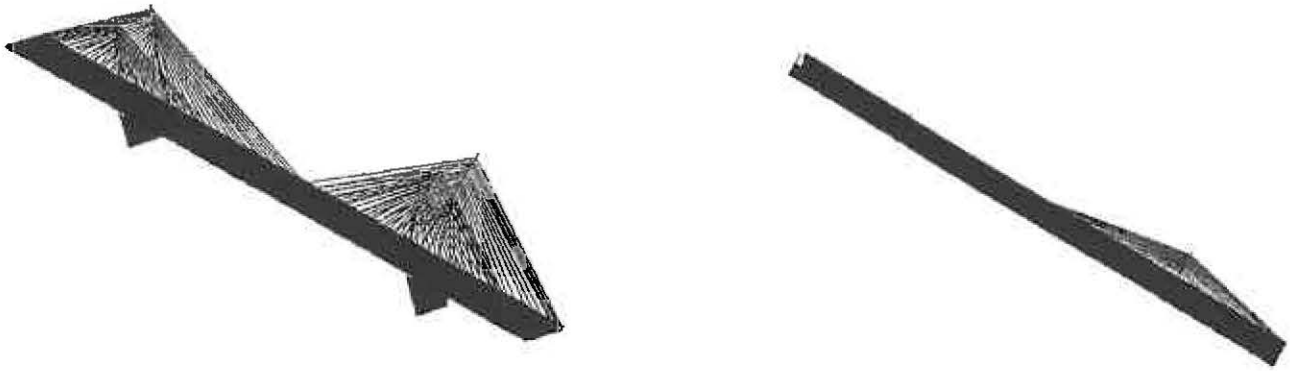

Fig. 5.9 10. Mode from Modal Analysis

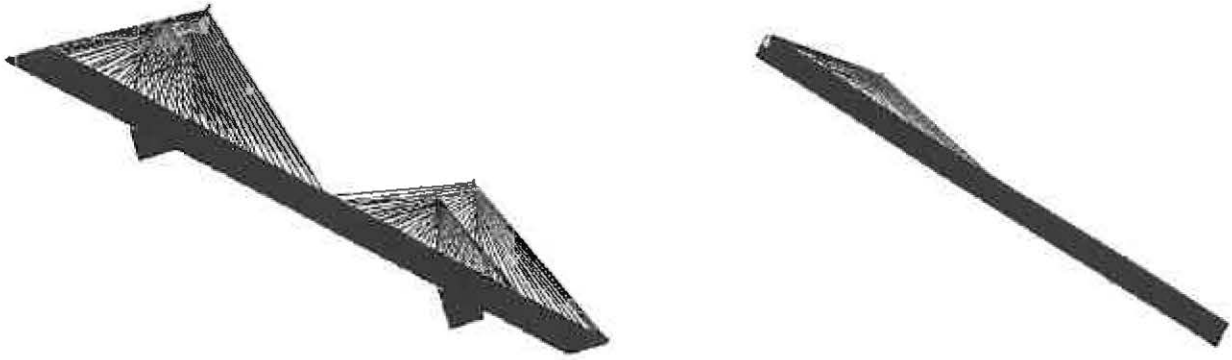

Fig. 5.10 11. Mode from Modal Analysis

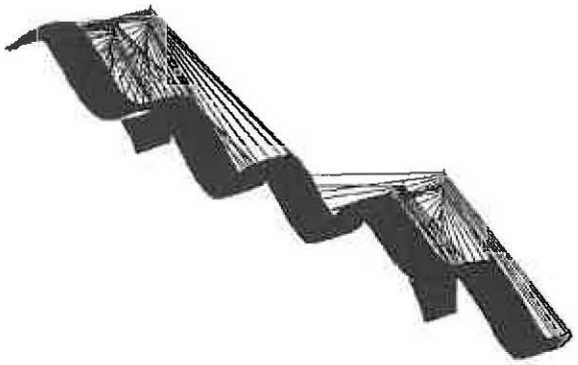

Fig. 5.11 12. Mode from Modal Analysis

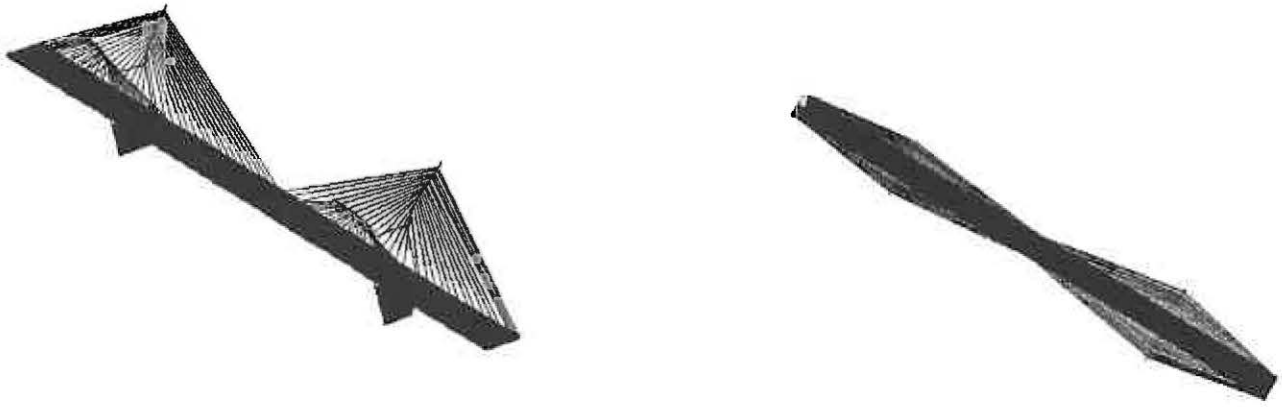

Fig. 5.12 13. Mode from Modal Analysis

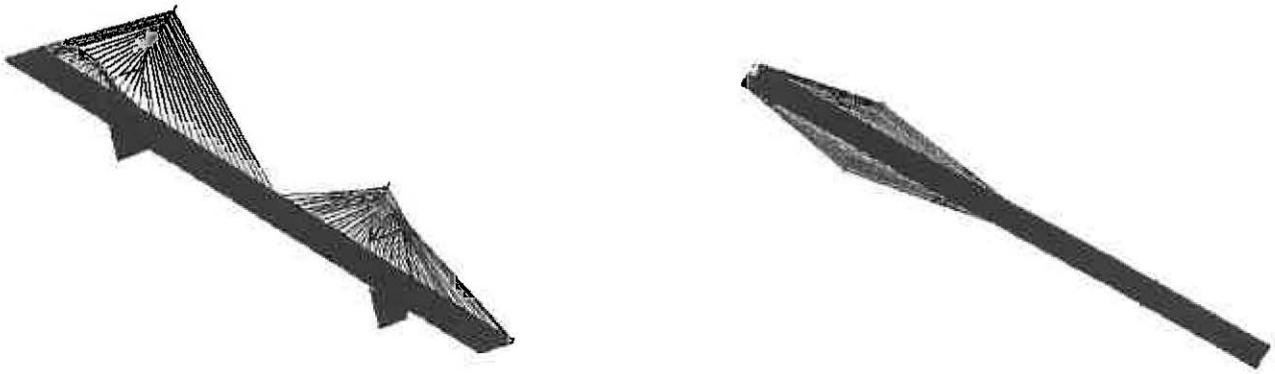

Fig. 5.13 14. Mode from Modal Analysis

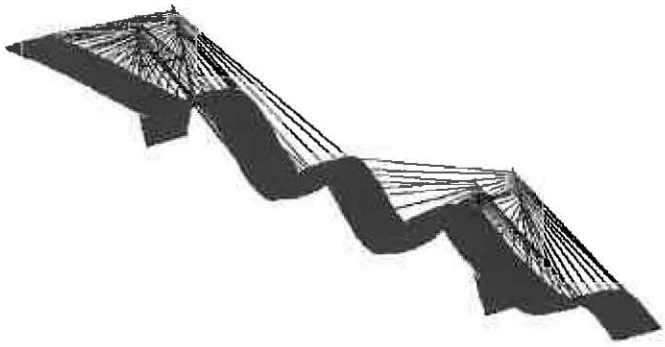

Fig. 5.14 15. Mode from Modal Analysis

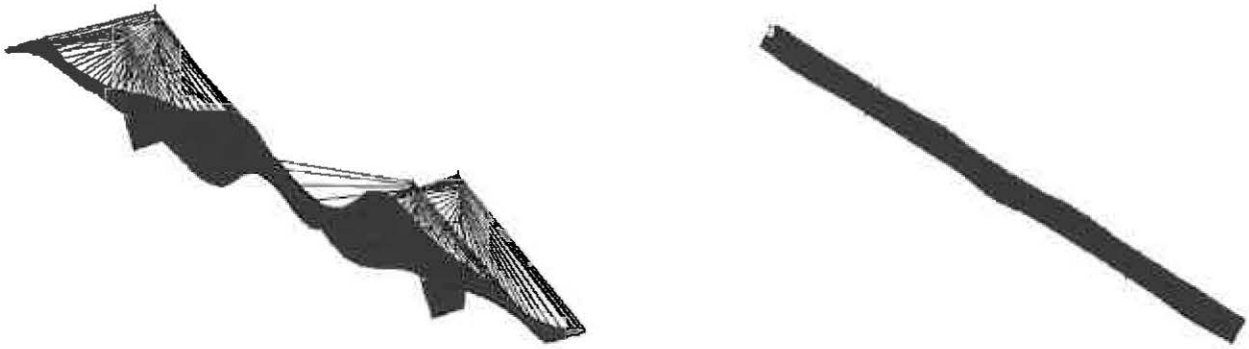

Fig. 5.15 16. Mode from Modal Analysis

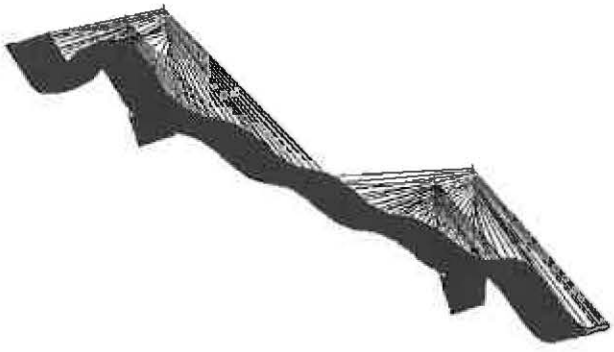

Fig. 5.16 17. Mode from Modal Analysis

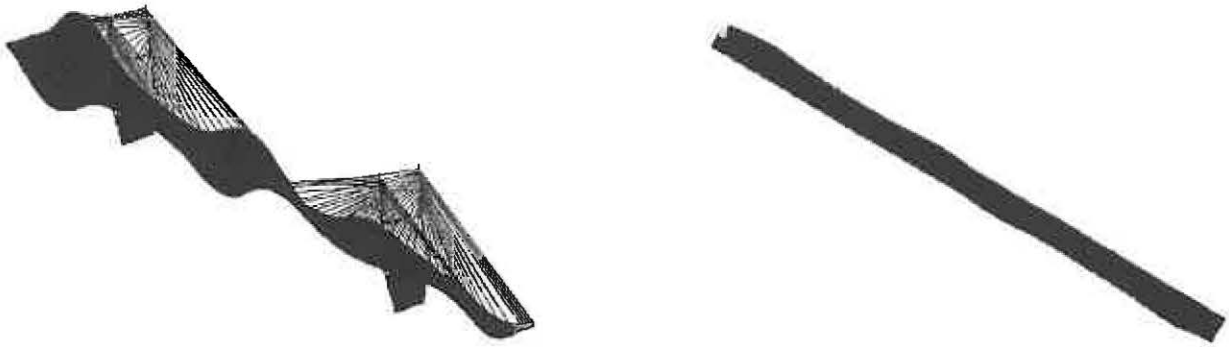

Fig. 5.17 18. Mode from Modal Analysis

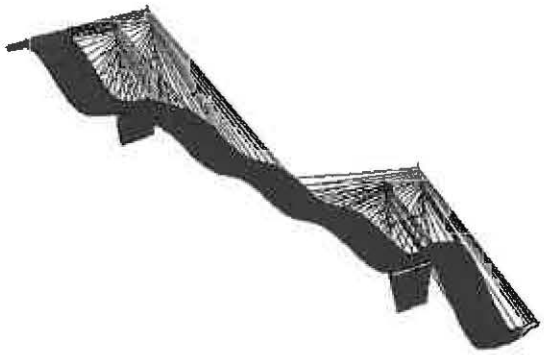

Fig. 5.18 19. Mode from Modal Analysis

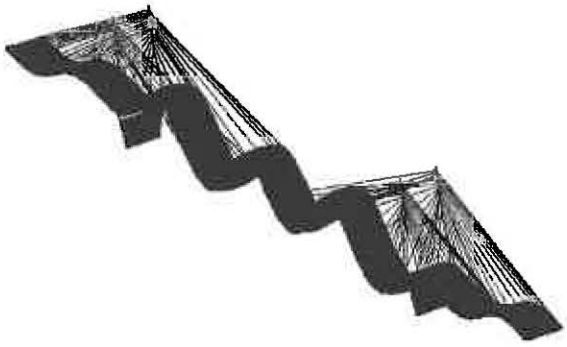

Fig. 5.19 20. Mode from Modal Analysis

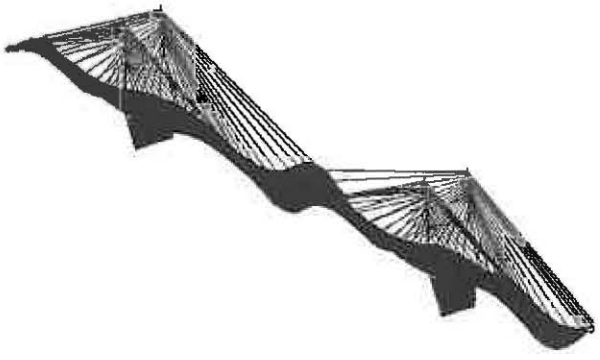

Fig. 5.20 21. Mode from Modal Analysis

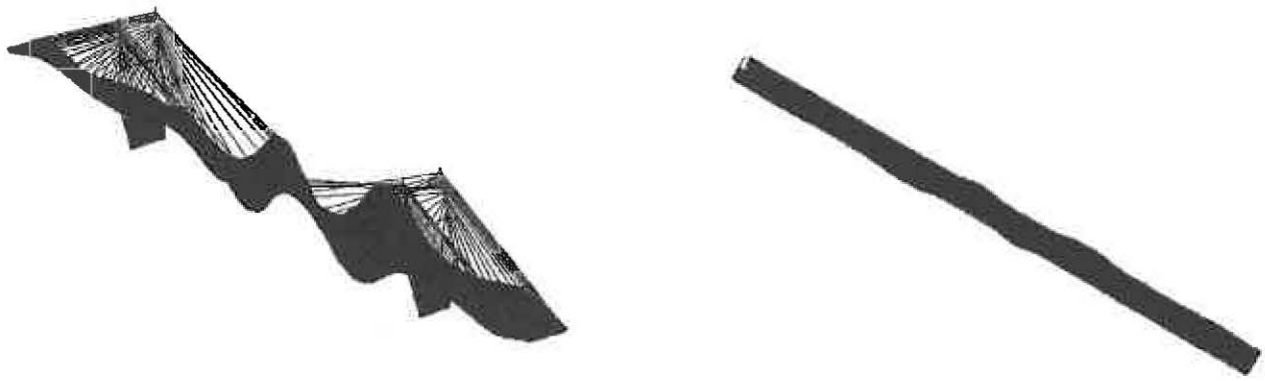

Fig. 5.21 22. Mode from Modal Analysis

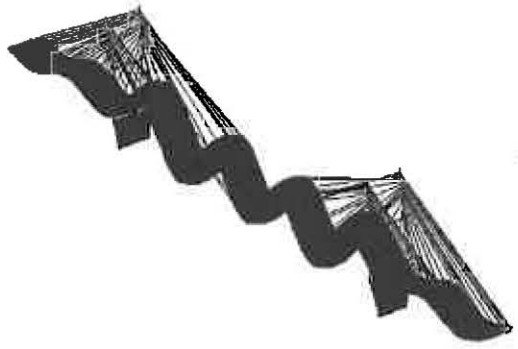

Fig. 5.22 23. Mode from Modal Analysis

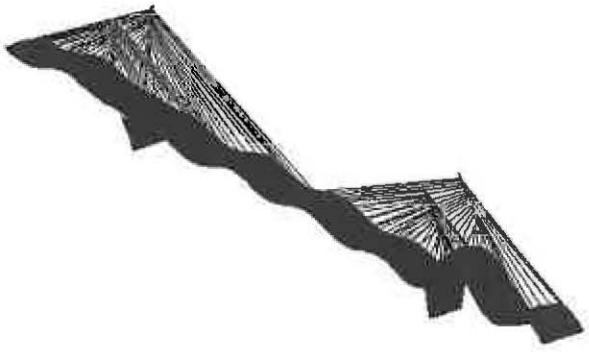

Fig. 5.23 24. Mode from Modal Analysis

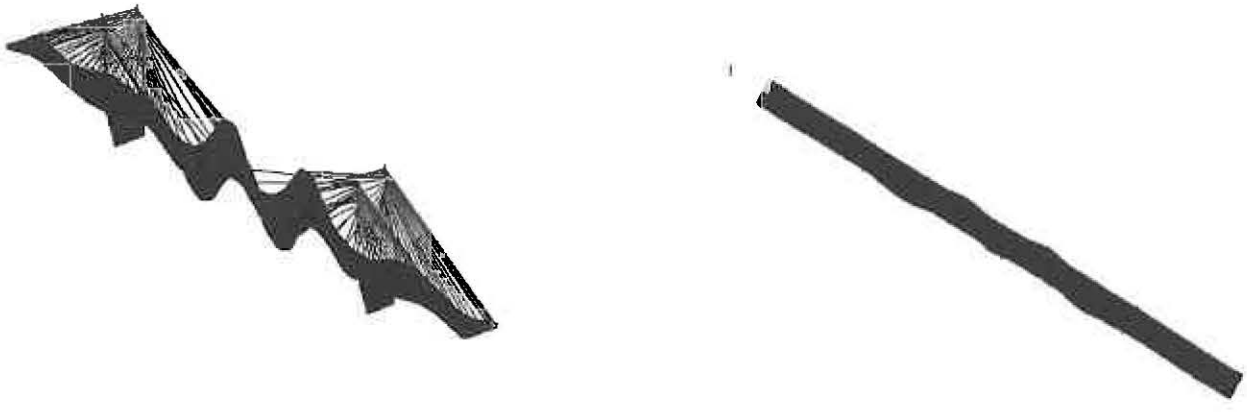

Fig. 5.24 25. Mode from Modal Analysis

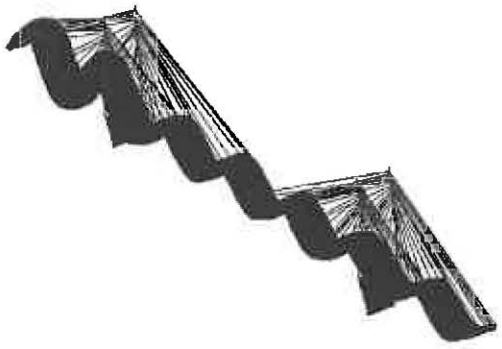

Fig. 5.25 26. Mode from Modal Analysis

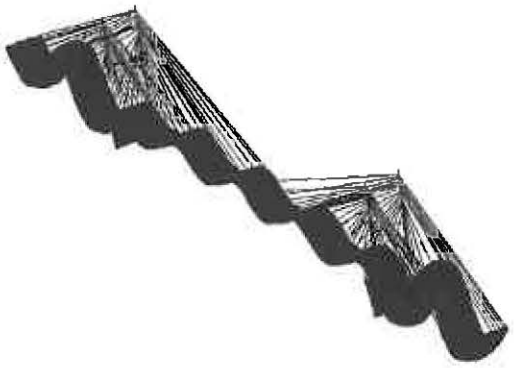

Fig. 5.26 27. Mode from Modal Analysis

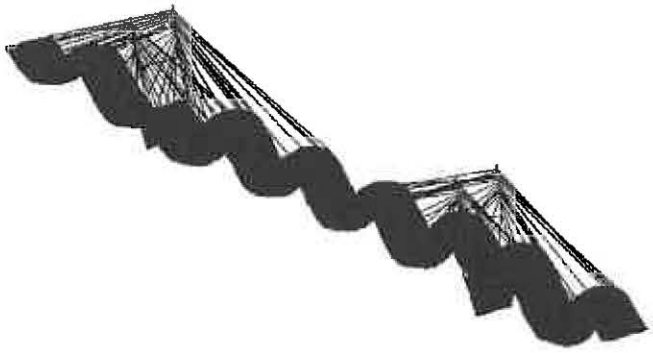

Fig. 5.27 28. Mode from Modal Analysis

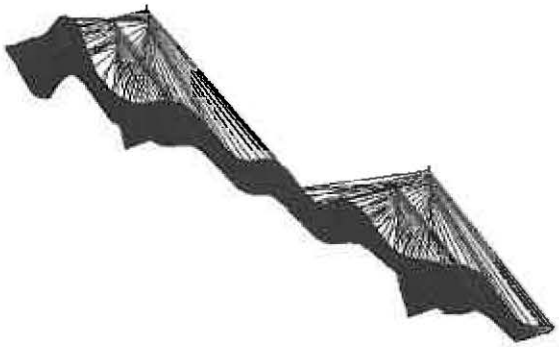

Fig. 5.28 29. Mode from Modal Analysis

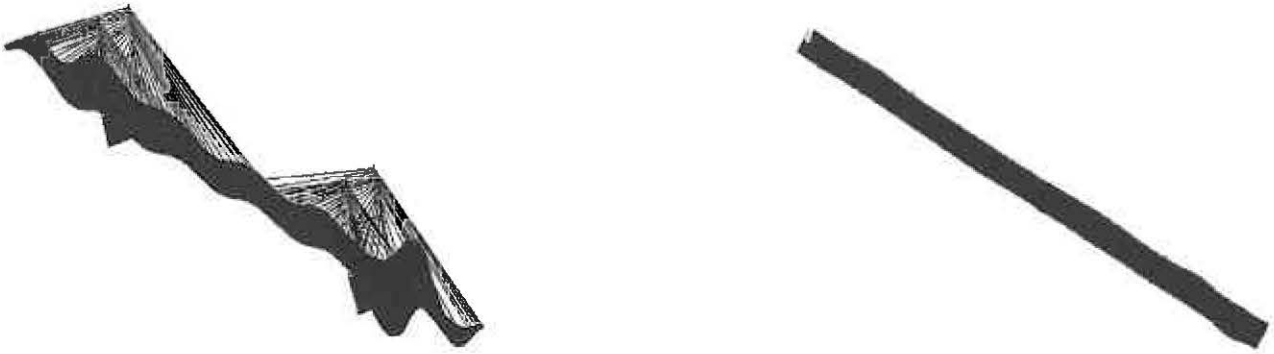

Fig. 5.29 30. Mode from Modal Analysis

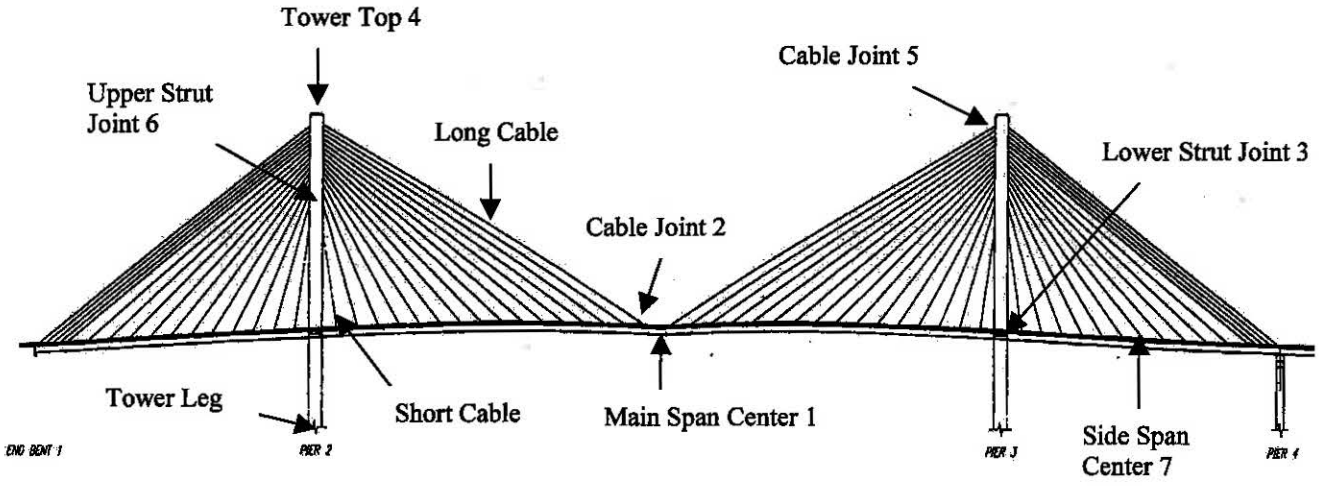

Fig. 5.30 Locations of Calculated Response Quantities

Fig. 5.31 Vertical Displacements from Linear Single Response-Spectrum Analysis

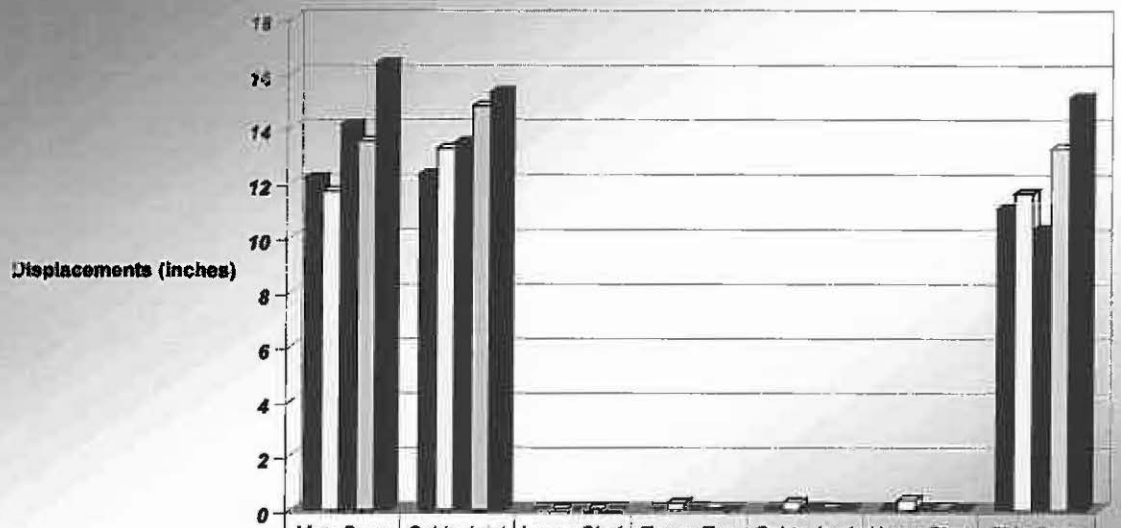

	Main Span Center 1	Cable Joint 2	Lower Strut Joint 3	Tower Top 4	Cable Joint 5	Upper Strut Joint 6	Side Span Center 7
Composite	12 164	12 298	5 50E-02	8 82E-02	8 625-02	6 84E-02	11 054
A-shape	11 674	13 227	6.36E-02	0 25392	0 27599	0 37474	11 609
Box	14 119	13 468	6 52E-02	0 10952	0.10952	9 23E-02	10.305
A-slab	13 497	14 79	4 35E-02	8 05E-02	8 44E-02	0.10276	13.247
Slab	16 363	15 323	6.98E-02	6 67E-02	6.67E-02	5 04E-02	15.124

Nodes

Fig. 5.32 Horizontal Displacements from Linear Single Response-Spectrum Analysis

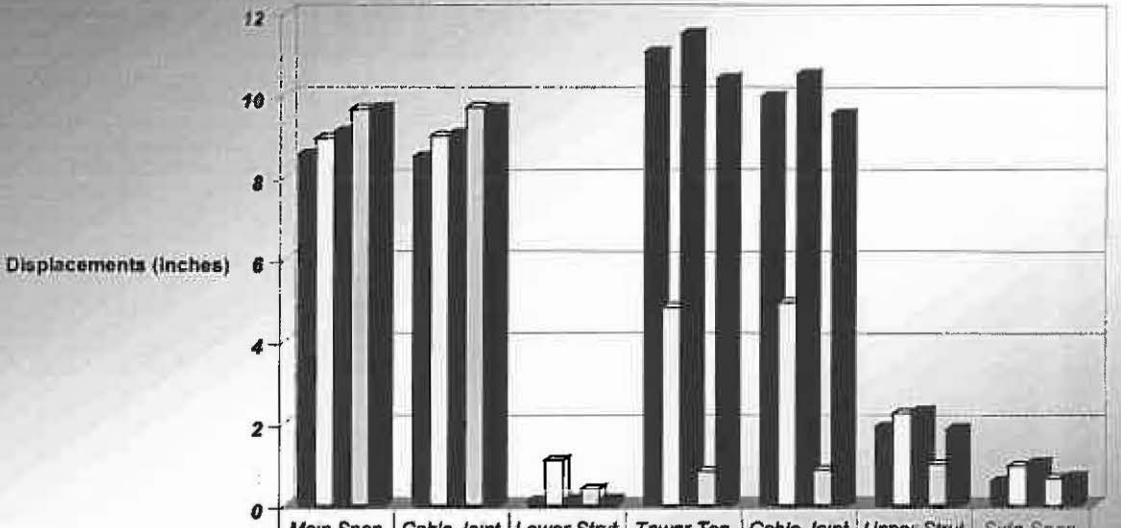

	Main Span Center 1	Cable Joint 2	Lower Strut Joint 3	Tower Top 4	Cable Joint 5	Upper Strut Joint 6	Side Span Center 7
Composite	8 5645	8 5014	0 10769	11 058	9 9771	1 9041	0 5865
A-shape	8 956	9 0051	1.1078	4 8229	4 9372	2 2382	0 96035
Box	9 1124	9 0655	0 13447	11.506	10.512	2 3052	1 0438
A-slab	9 6652	9 7084	0 39775	0 62753	0 85577	0 99492	0 65507
Slab	9 7024	9 6878	0 14311	10 417	9 5524	1 8622	0 71534

Nodes

Fig. 5.33 Longitudinal Displacements from Linear Single Response-Spectrum Analysis

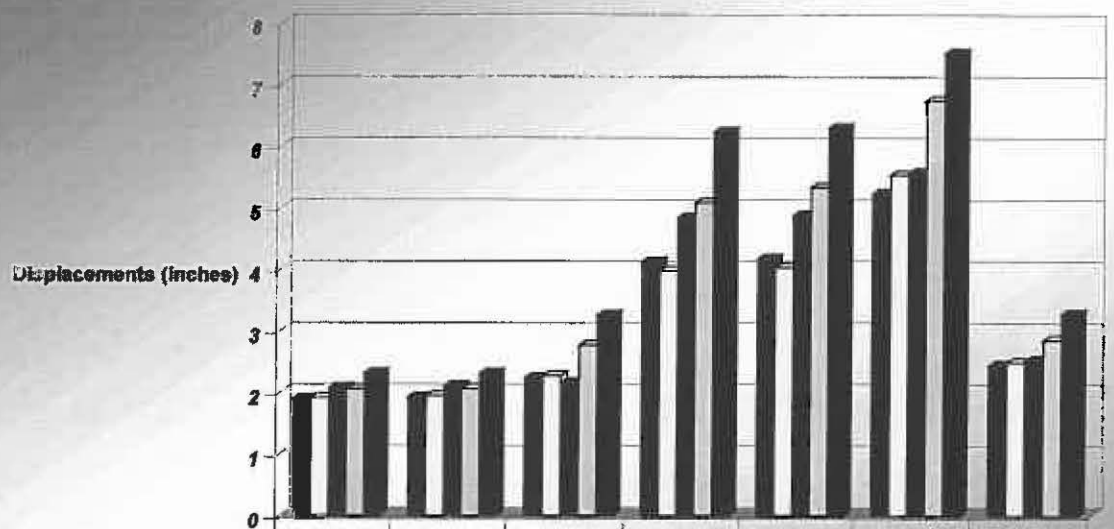

	Main Span Center 1	Cable Joint 2	Lower Strut Joint 3	Tower Top 4	Cable Joint 5	Upper Strut Joint 6	Side Span Center 7
Composite	1.8896	1.9132	2.2296	4.1187	4.1554	5.2261	2.4353
A-shape	1.905	1.9356	2.2642	3.9662	4.0266	5.5283	2.4826
Box	2.0671	2.1004	2.152	4.8323	4.8705	5.5609	2.5168
A-slab	2.0499	2.0516	2.7605	5.0772	5.5272	6.7423	2.8501
Slab	2.3103	2.306	3.2059	6.2326	6.295	7.5122	3.2765

Nodes

Fig. 5.34 Vertical Displacements from Non-Linear Single Response-Spectrum Analysis

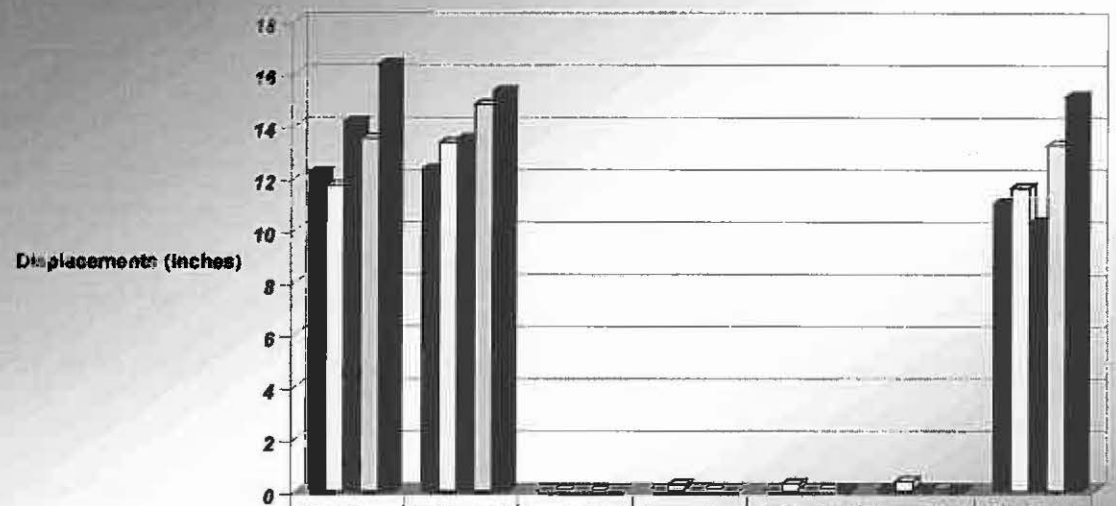

	Main Span Center 1	Cable Joint 2	Lower Strut Joint 3	Tower Top 4	Cable Joint 5	Upper Strut Joint 6	Side Span Center 7
Composite	12.191	12.318	5.50E-02	8.79E-02	8.79E-02	8.79E-02	11.028
A-shape	11.703	13.34	6.36E-02	0.25401	0.27709	0.37491	11.516
Box	14.138	13.488	6.51E-02	0.10944	0.10944	9.23E-02	10.311
A-slab	13.499	14.81	4.35E-02	8.05E-02	8.44E-02	0.10276	13.25
Slab	16.367	15.326	6.98E-02	8.67E-02	6.67E-02	5.04E-02	15.128

Nodes

Fig. 5.35 Horizontal Displacements from Non-Linear Single Response Spectrum Analysis

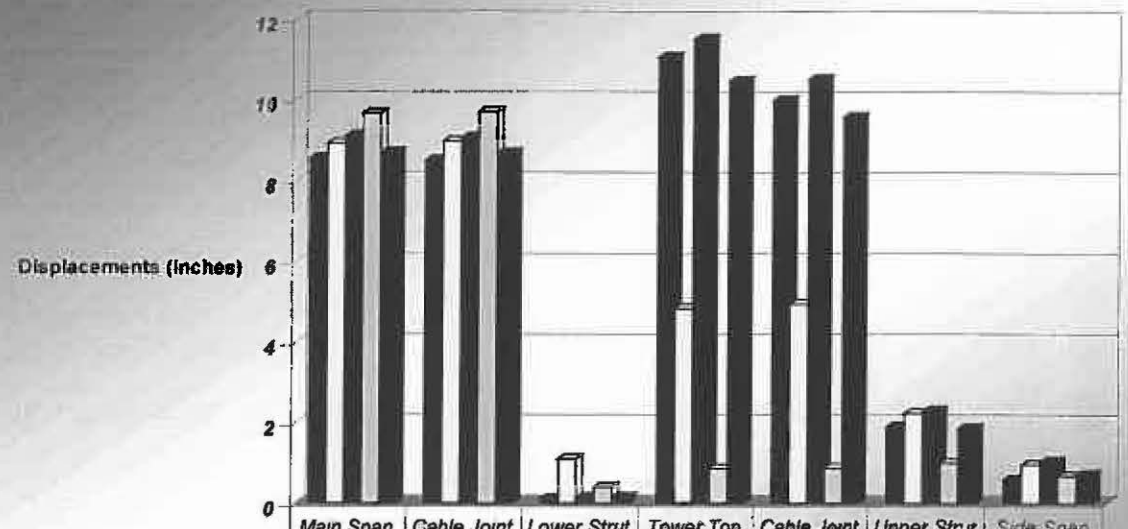

	Main Span Center 1	Cable Joint 2	Lower Strut Joint 3	Tower Top 4	Cable Joint 5	Upper Strut Joint 6	Side Span Center 7
Composite	8 5629	8 4999	0 10769	11 06	9 9787	1 9042	0 58648
A-shape	8 923	8 9727	1 1082	4 8243	4 9387	2 24	0 95894
Box	9 1124	9 0654	0 13445	11 505	10 511	2 3049	1 0438
A-slab	9 667	9 71	0 3979	0 85	0 87	0 995	0 67
Slab	8 703	8 69	0 148	10 46	9 57	1 87	0 715

Nodes

Fig. 5.36 Longitudinal Displacements from Non-Linear Single Response Spectrum Analysis

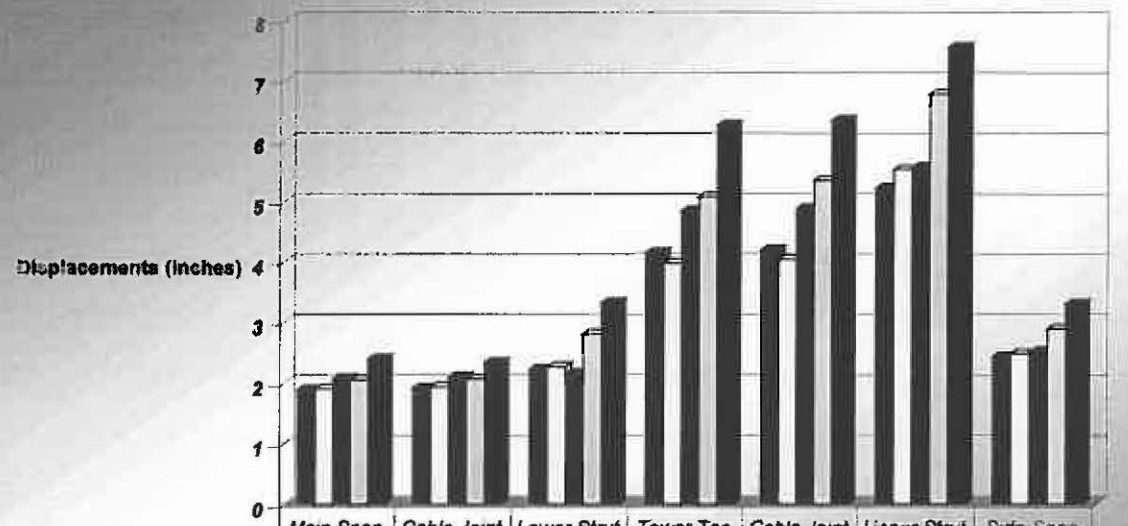

	Main Span Center 1	Cable Joint 2	Lower Strut Joint 3	Tower Top 4	Cable Joint 5	Upper Strut Joint 6	Side Span Center 7
Composite	1 8864	1 9099	2 2266	4 1518	4 1947	5 2245	2 4313
A-shape	1 9037	1 9343	2 2623	3 9753	4 0364	5 5307	2 4809
Box	2 0669	2 1001	2 1521	4 8455	4 8829	5 5648	2 5169
A-slab	2 05	2 06	2 8	5 08	5 35	6 78	2 69
Slab	2 4	2 34	3 32	6 27	6 35	7 56	3 31

Nodes

Fig. 5.37 Comparison between Non-Linear/Linear Vertical Response Displacements of the Composite Design

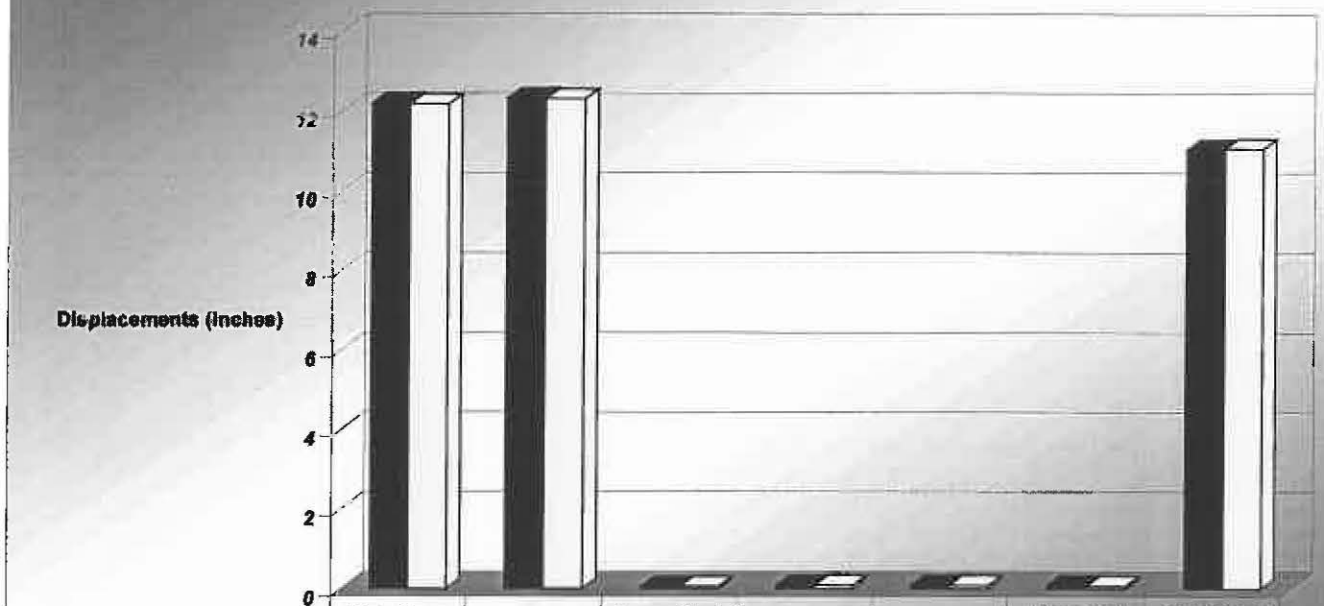

	Main Span Center 1	Cable Joint 2	Lower Strut Joint 3	Tower Top 4	Cable Joint 5	Upper Strut Joint 6	Side Span Center 7
■ Non Linear	12 191	12 318	5 50E-02	8 79E-02	8 79E-02	8 79E-02	11 028
□ Linear	12 164	12 298	8 50E-02	8 82E-02	8 82E-02	6 84E-02	11 054

Nodes

Fig. 5.38 Comparison between Non-Linear/Linear Horizontal Response Displacements of the Composite Design

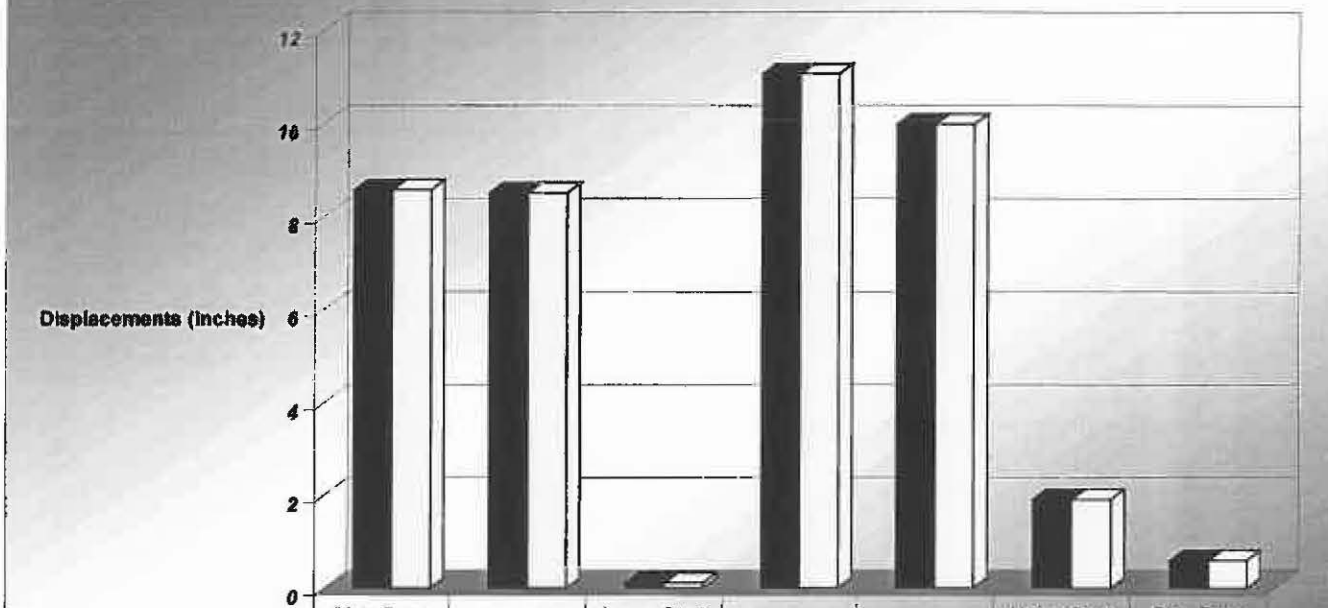

	Main Span Center 1	Cable Joint 2	Lower Strut Joint 3	Tower Top 4	Cable Joint 5	Upper Strut Joint 6	Side Span Center 7
■ Non Linear	8 5629	8 4999	0 10769	11 06	9 9787	1 9042	0 56648
□ Linear	8 5645	8 5014	0 10769	11 053	9 9771	1 9041	0 5665

Nodes

Fig. 5.39 Comparison between Non-Linear/Linear Longitudinal Response Displacements of the Composite Design

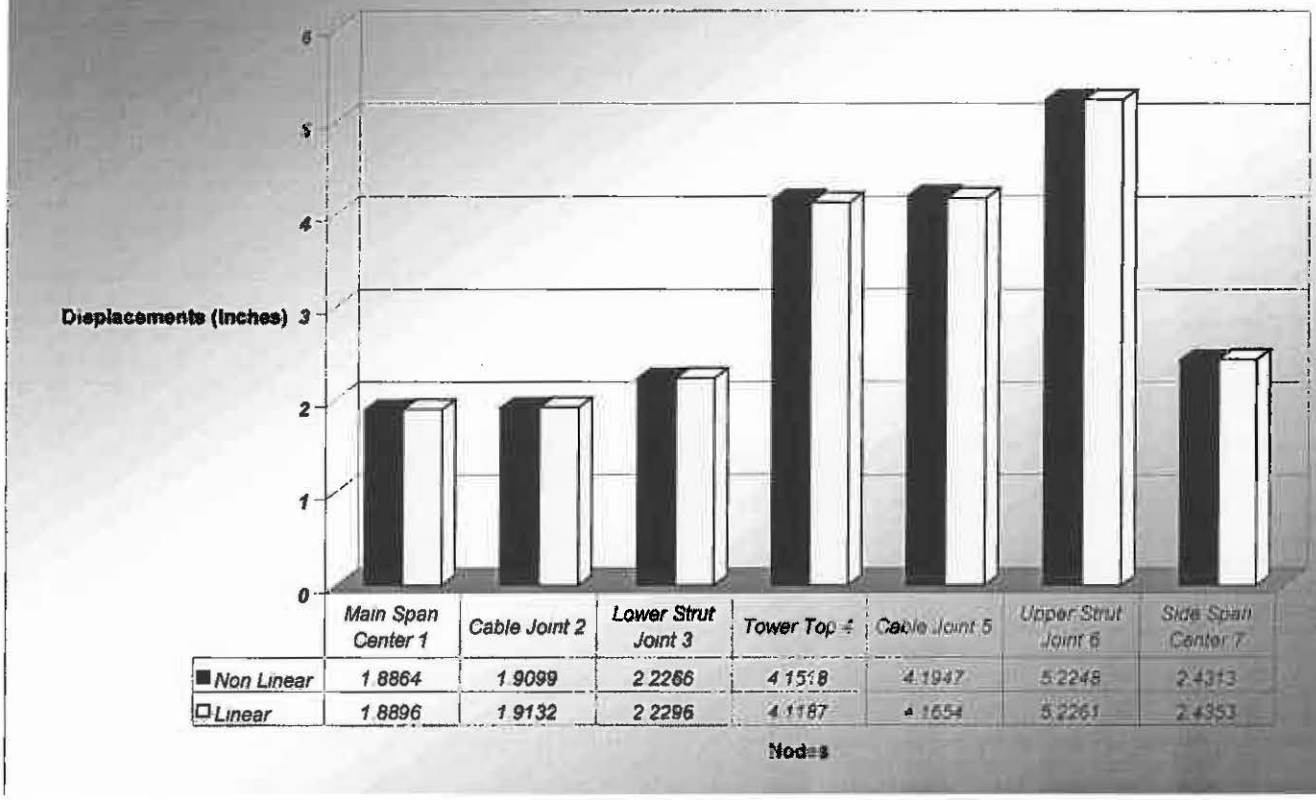

Fig. 5.40 Comparison between Non-Linear/Linear Vertical Response Displacements of the A-shape Design

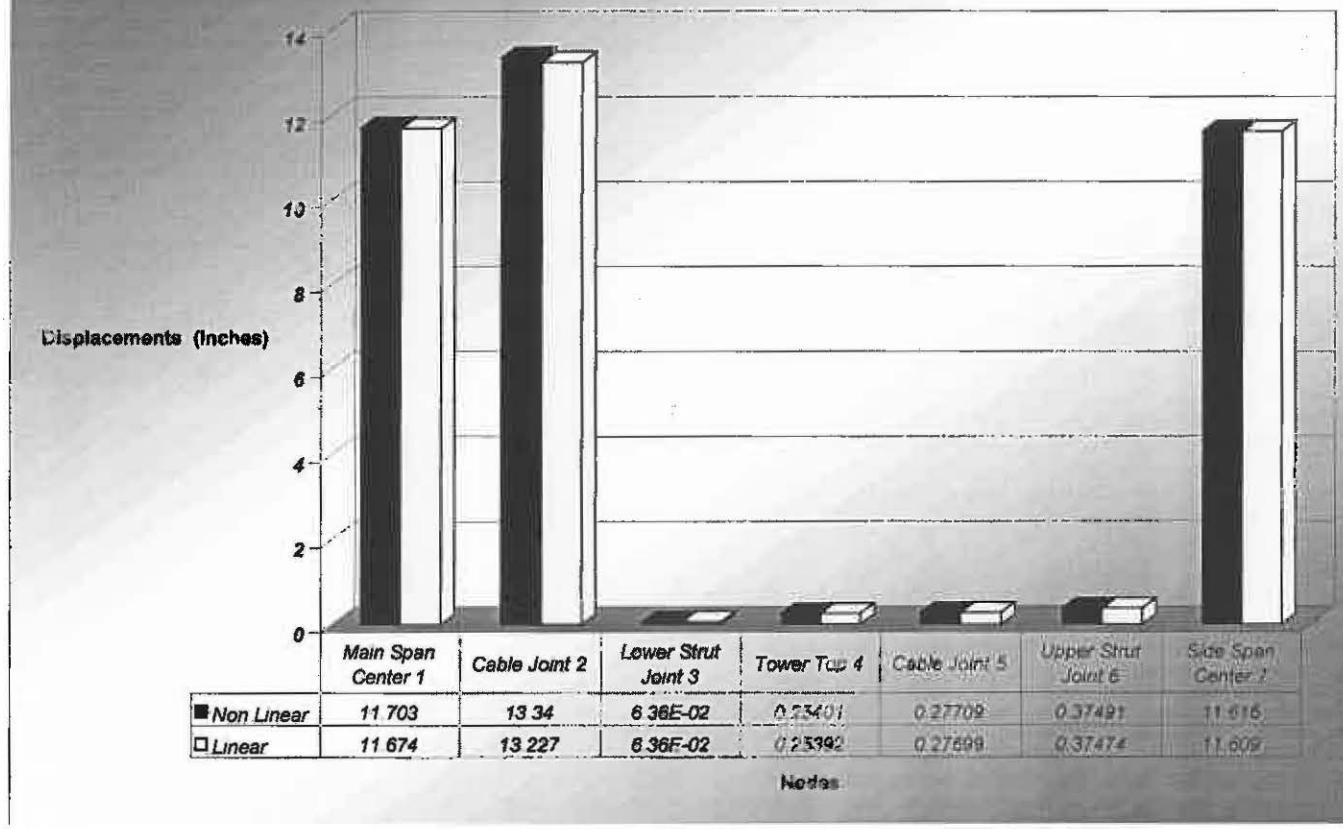

Fig. 5.41 Comparison between Non-Linear/Linear Horizontal Response Displacements of the A-shape Design

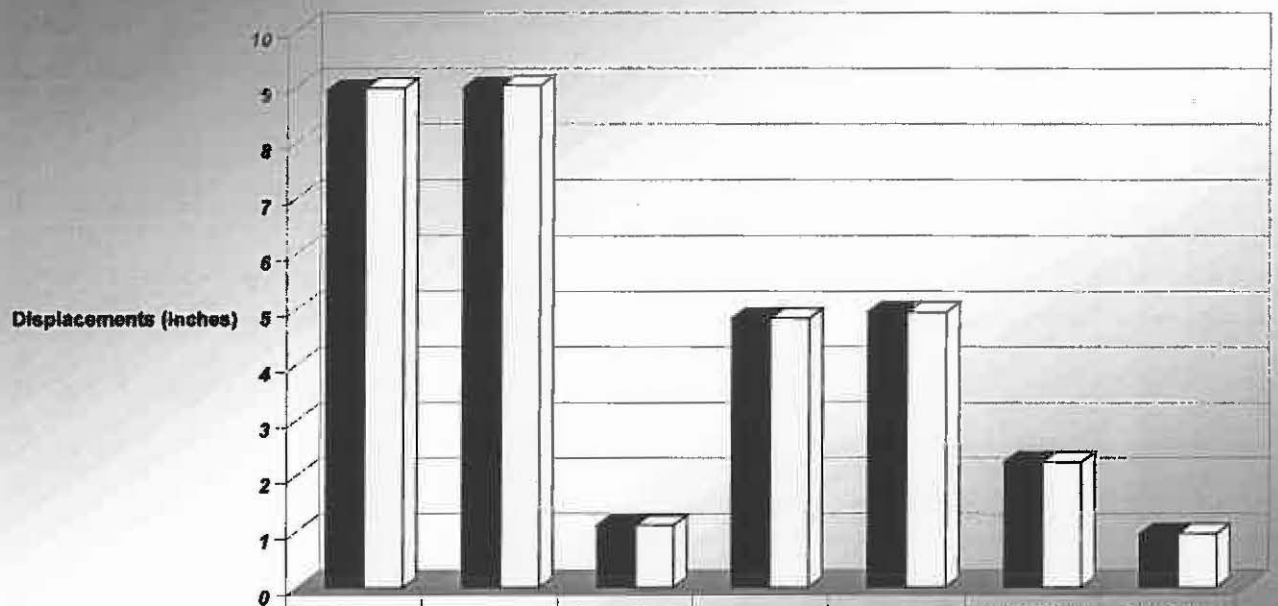

	Main Span Center 1	Cable Joint 2	Lower Strut Joint 3	Tower Top 4	Cable Joint 5	Upper Strut Joint 6	Side Span Center 7
Non Linear	8.923	8.9727	1.1082	4.8243	4.9387	2.24	0.95894
Linear	8.956	9.0051	1.1078	4.5229	4.9372	2.2362	0.96035

Fig. 5.42 Comparison between Non-Linear/Linear Longitudinal Response Displacements of the A-shape Design

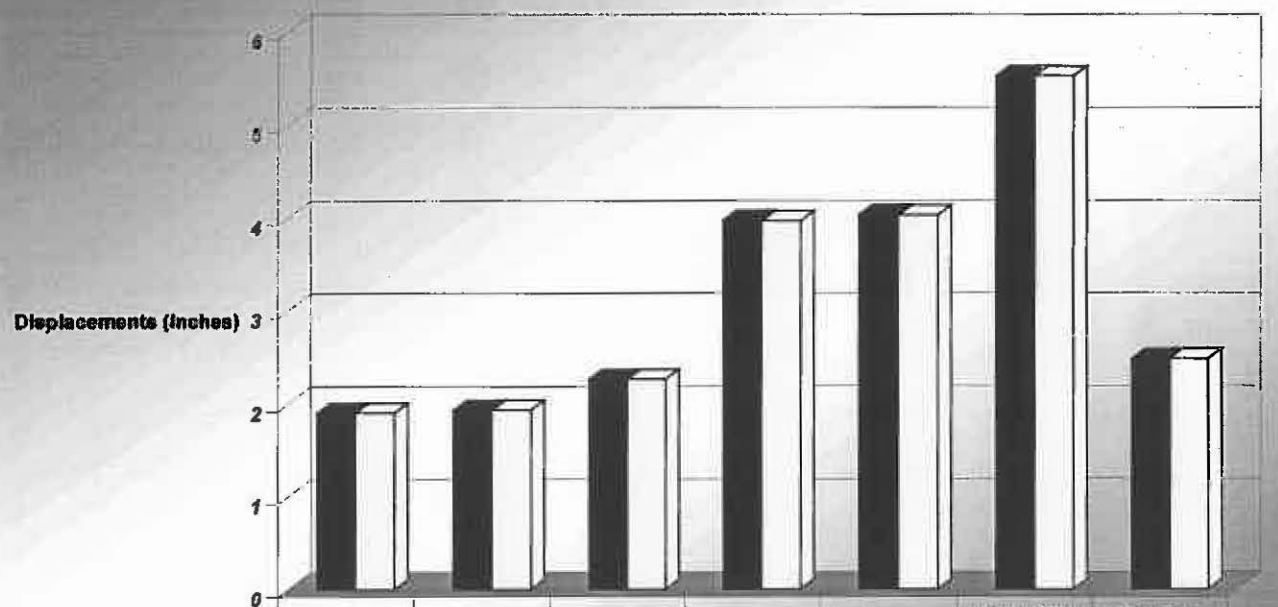

	Main Span Center 1	Cable Joint 2	Lower Strut Joint 3	Tower Top 4	Cable Joint 5	Upper Strut Joint 6	Side Span Center 7
Non Linear	1.9037	1.9343	2.2623	3.9753	4.0364	5.5307	2.4609
Linear	1.905	1.9356	2.2642	3.9552	4.0266	5.5283	2.4626

Fig. 5.43 Comparison between Non-Linear/Linear Vertical Response Displacements of the Box Design

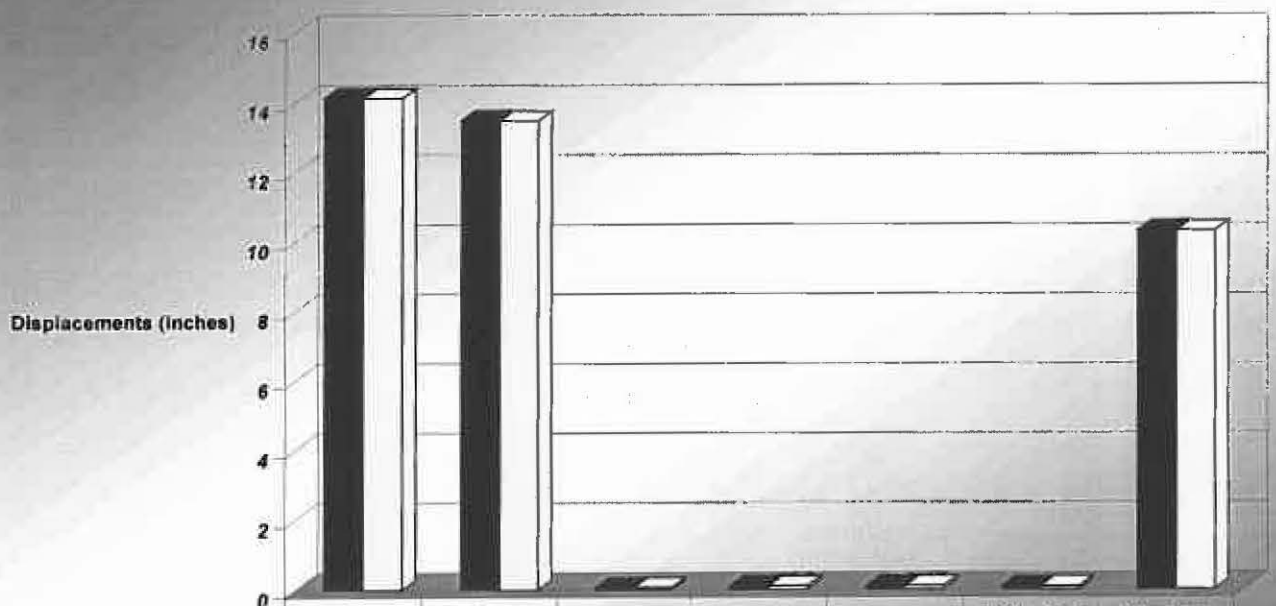

	Main Span Center 1	Cable Joint 2	Lower Strut Joint 3	Tower Top 4	Cable Joint 5	Upper Strut Joint 6	Side Span Center 7
Non Linear	14.138	13.488	6.51E-02	0.10944	0.10944	9.23E-02	10.311
Linear	14.119	13.468	6.52E-02	0.10952	0.10952	9.23E-02	10.305

Nodes

Fig. 5.44 Comparison between Non-Linear/Linear Horizontal Response Displacements of the Box Design

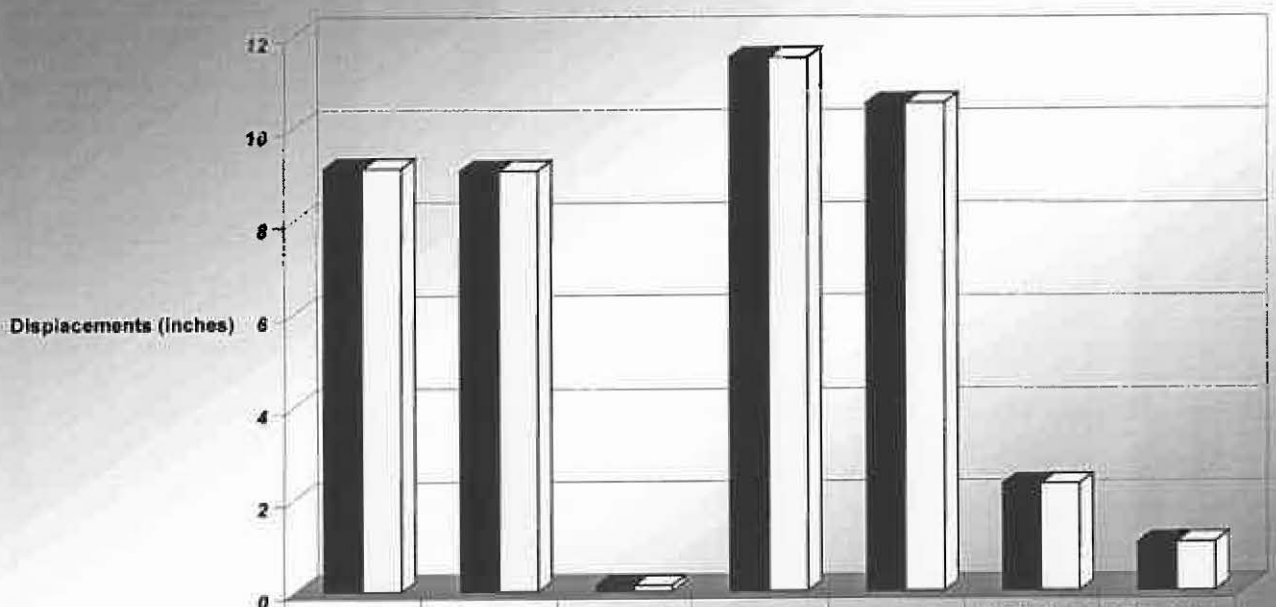

	Main Span Center 1	Cable Joint 2	Lower Strut Joint 3	Tower Top 4	Cable Joint 5	Upper Strut Joint 6	Side Span Center 7
Non Linear	9.1124	9.0654	0.13445	11.505	10.511	2.3049	1.0438
Linear	9.1124	9.0655	0.13447	11.506	10.512	2.3052	1.0438

Nodes

Fig. 5.45 Comparison between Non-Linear/Linear Longitudinal Response Displacements of the Box Design

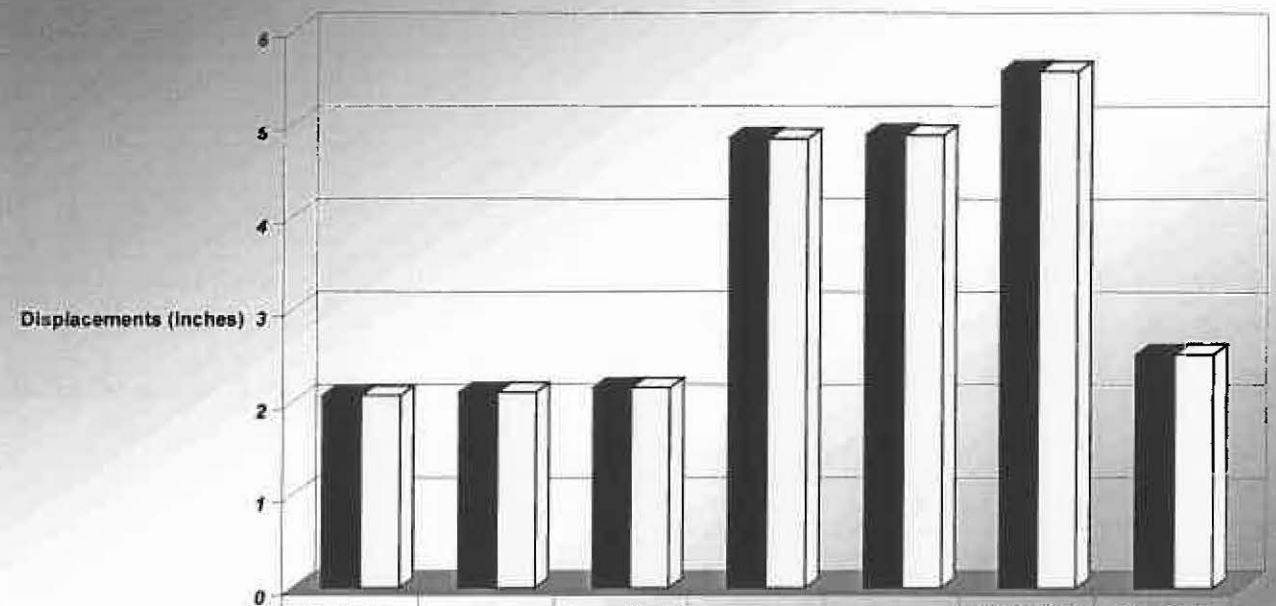

	Main Span Center 1	Cable Joint 2	Lower Strut Joint 3	Tower Top 4	Cable Joint 5	Upper Strut Joint 6	Side Span Center 7
Non Linear	2.0669	2.1001	2.1521	4.8455	4.8629	5.5648	2.5169
Linear	2.0671	2.1004	2.152	4.8323	4.8705	5.5609	2.5168

Nodes

Fig. 5.46 Comparison between Non-Linear/Linear Vertical Response Displacements of the A-slab Design

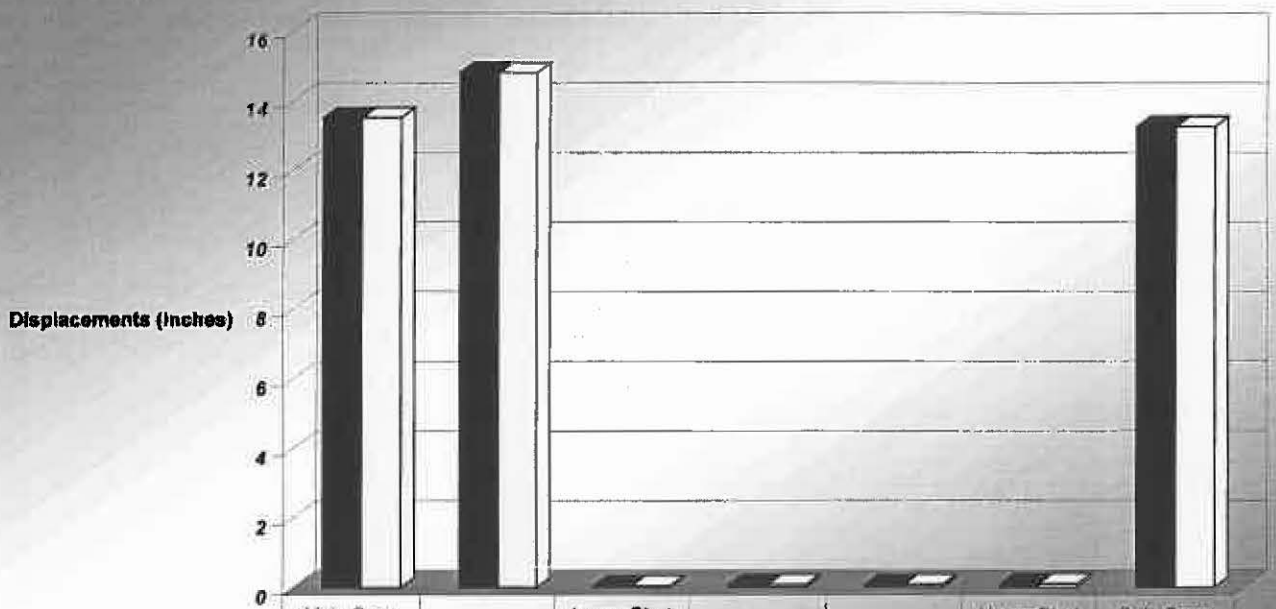

	Main Span Center 1	Cable Joint 2	Lower Strut Joint 3	Tower Top 4	Cable Joint 5	Upper Strut Joint 6	Side Span Center 7
Non Linear	13.499	14.81	4.35E-02	8.05E-02	8.44E-02	0.10276	13.25
Linear	13.497	14.79	4.35E-02	8.05E-02	8.44E-02	0.10276	13.247

Nodes

Fig. 5.47 Comparison between Non-Linear/Linear Horizontal Response Displacements of the A-slab Design

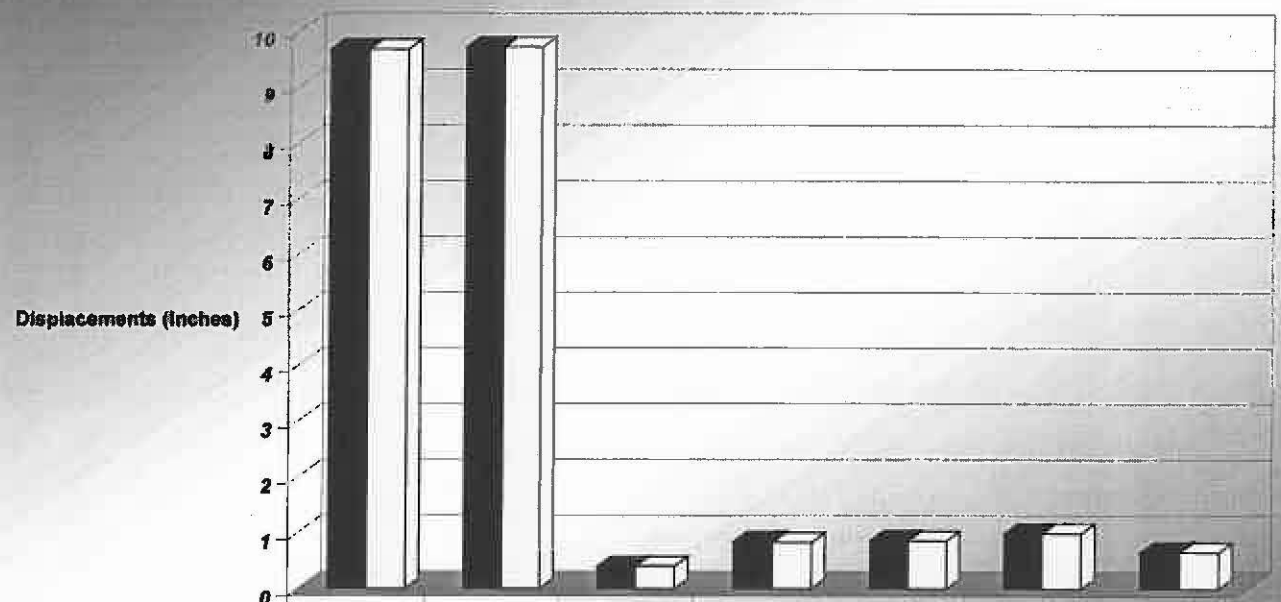

	Main Span Center 1	Cable Joint 2	Lower Strut Joint 3	Tower Top 4	Cable Joint 5	Upper Strut Joint 6	Side Span Center 7
Non Linear	9.667	9.71	0.3979	0.85	0.87	0.995	0.67
Linear	9.6652	9.7084	0.39775	0.82753	0.85577	0.99492	0.66507

Nodes

Fig. 5.48 Comparison between Non-Linear/Linear Longitudinal Response Displacements of the A-slab Design

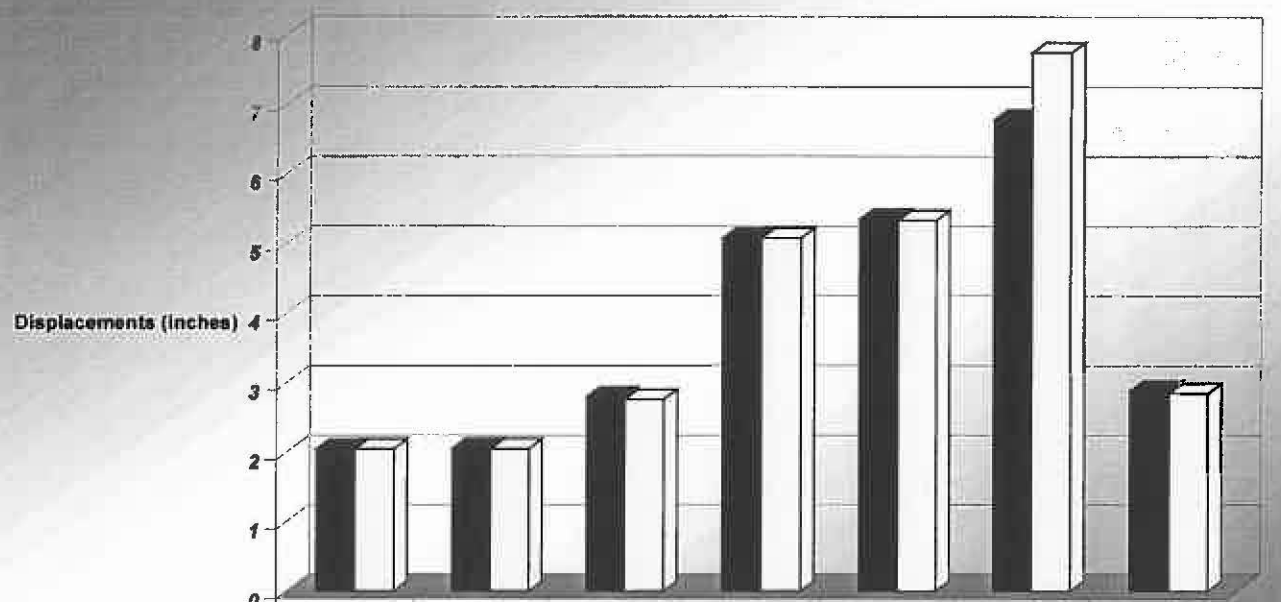

	Main Span Center 1	Cable Joint 2	Lower Strut Joint 3	Tower Top 4	Cable Joint 5	Upper Strut Joint 6	Side Span Center 7
Non Linear	2.05	2.06	2.8	5.03	5.35	6.78	2.89
Linear	2.0499	2.0516	2.7605	5.0172	5.3272	7.7423	2.8501

Nodes

Fig. 5.49 Comparison between Non-Linear/Linear Vertical Response Displacements of the Slab Design

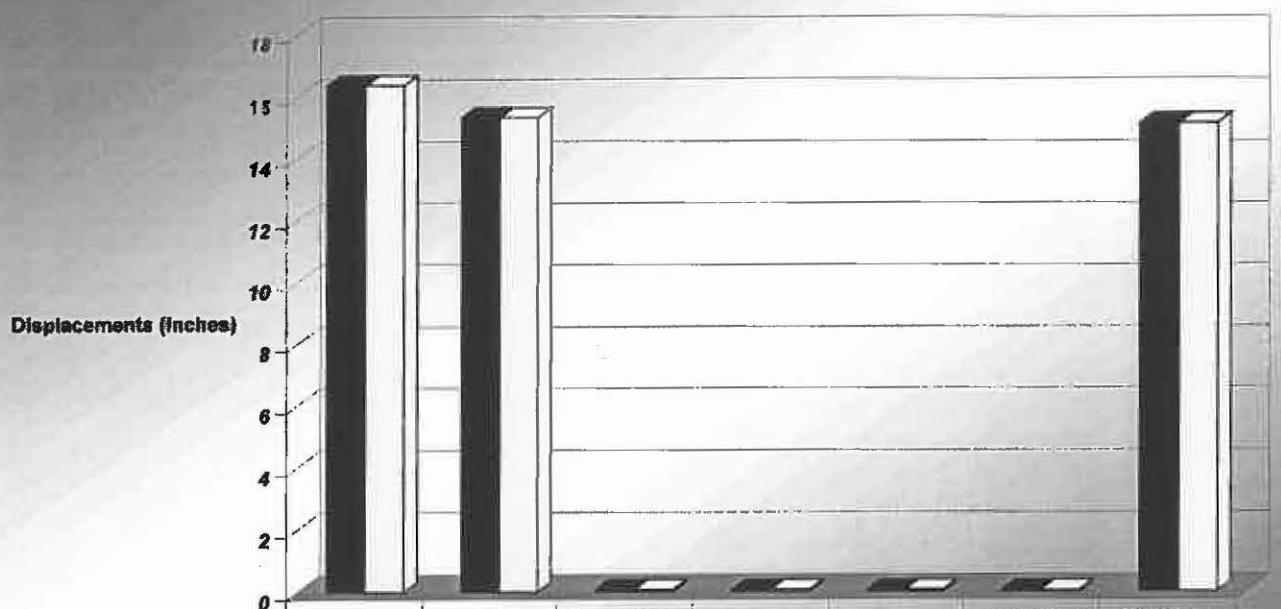

	Main Span Center 1	Cable Joint 2	Lower Strut Joint 3	Tower Top 4	Cable Joint 5	Upper Strut Joint 6	Side Span Center 7
Non Linear	16.367	15.326	6.98E-02	6.67E-02	6.67E-02	5.04E-02	15.128
Linear	16.363	15.323	6.98E-02	6.67E-02	6.67E-02	5.04E-02	15.124

Nodes

Fig. 5.50 Comparison between Non-Linear/Linear Horizontal Response Displacements of the Slab Design

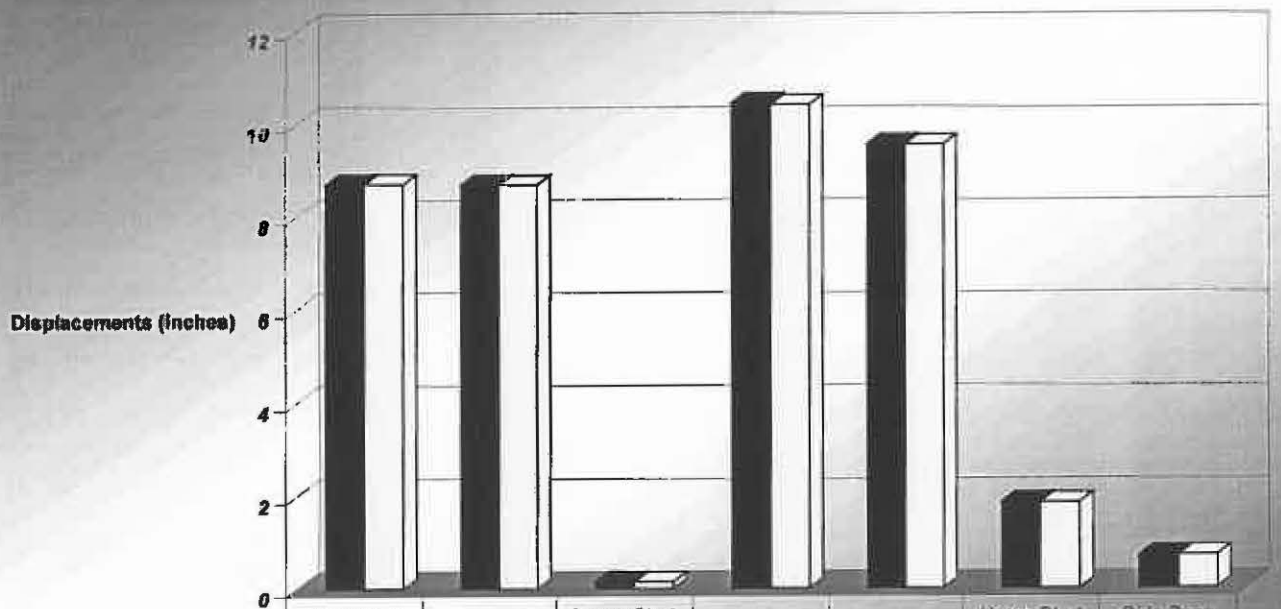

	Main Span Center 1	Cable Joint 2	Lower Strut Joint 3	Tower Top 4	Cable Joint 5	Upper Strut Joint 6	Side Span Center 7
Non Linear	8.703	8.69	0.148	10.46	9.57	1.87	0.715
Linear	8.7024	8.6878	0.14311	10.417	9.5524	1.8622	0.71334

Nodes

Fig. 5.51 Comparison between Non-Linear/Linear Longitudinal Response Displacements of the Slab Design

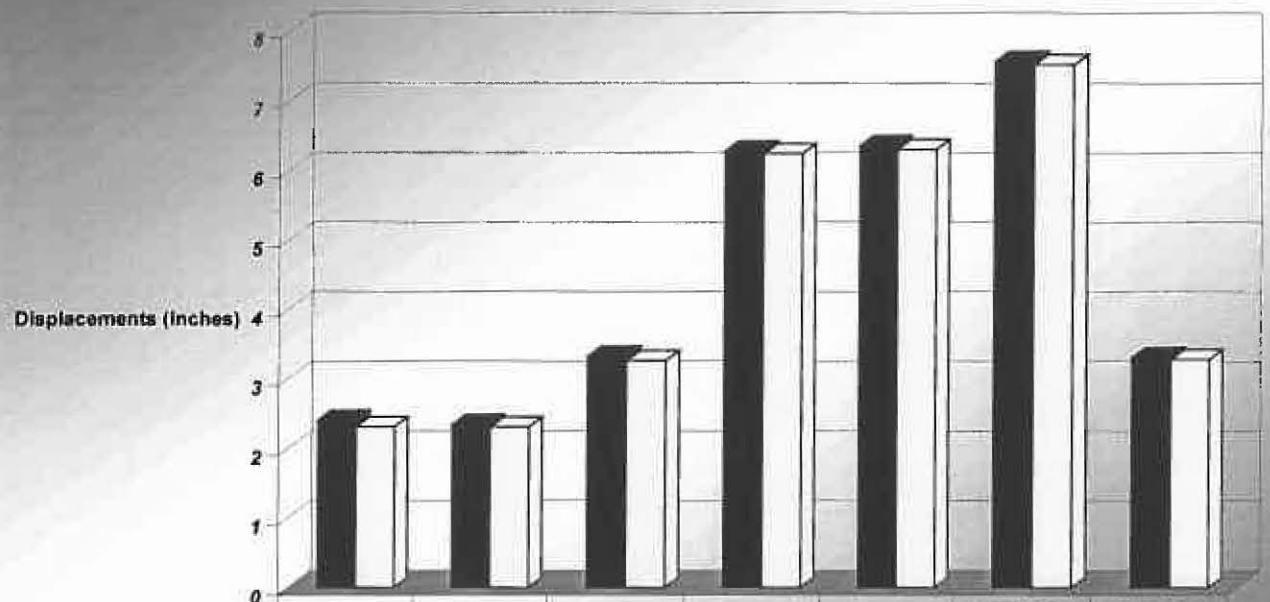

	Main Span Center 1	Cable Joint 2	Lower Strut Joint 3	Tower Top 4	Cable Joint 5	Upper Strut Joint 6	Side Span Center 7
■ Non Linear	2.4	2.34	3.32	6.27	6.35	7.56	3.31
□ Linear	2.3103	2.306	3.2559	6.2325	6.295	7.5122	3.2766

Nodes

Fig. 5.52 Cable Forces from Non-Linear Single Response-Spectrum Analysis

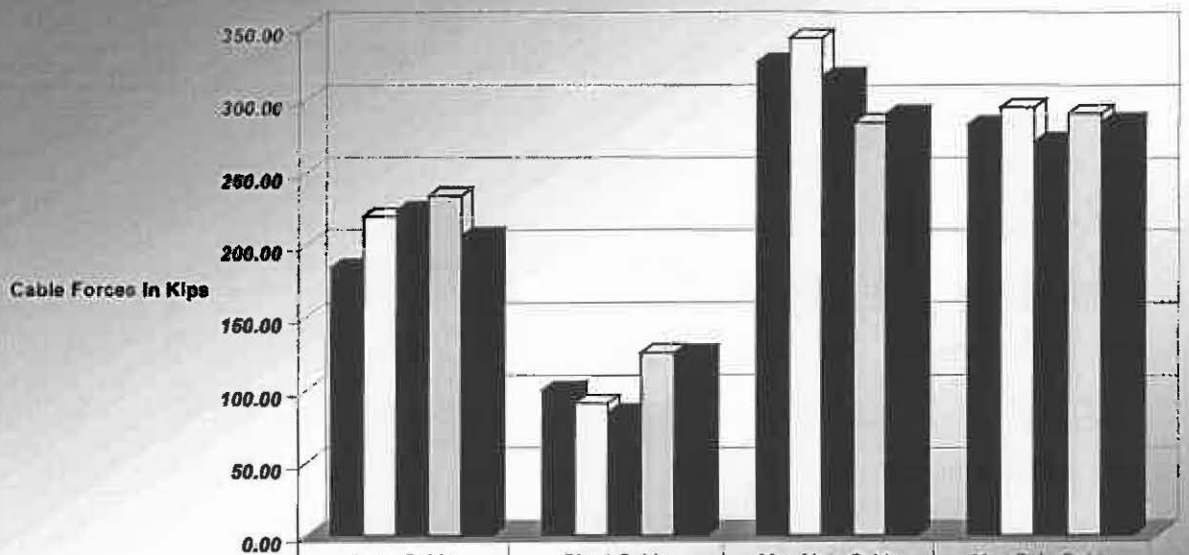

	Long Cable	Short Cable	Max Main Cable	Max Side Cable
■ Composite	184.33	99.825	328.03	283.20
□ A-shape	219.38	90.80	342.49	294.97
■ Box	223.70	84.57	316.20	271.58
□ A-slab	233.79	125.66	284.35	290.76
■ Slab	205.87	125.24	290.33	284.99

Elements

Fig. 5.53 Member Forces from Non-Linear Single Response-Spectrum Analysis

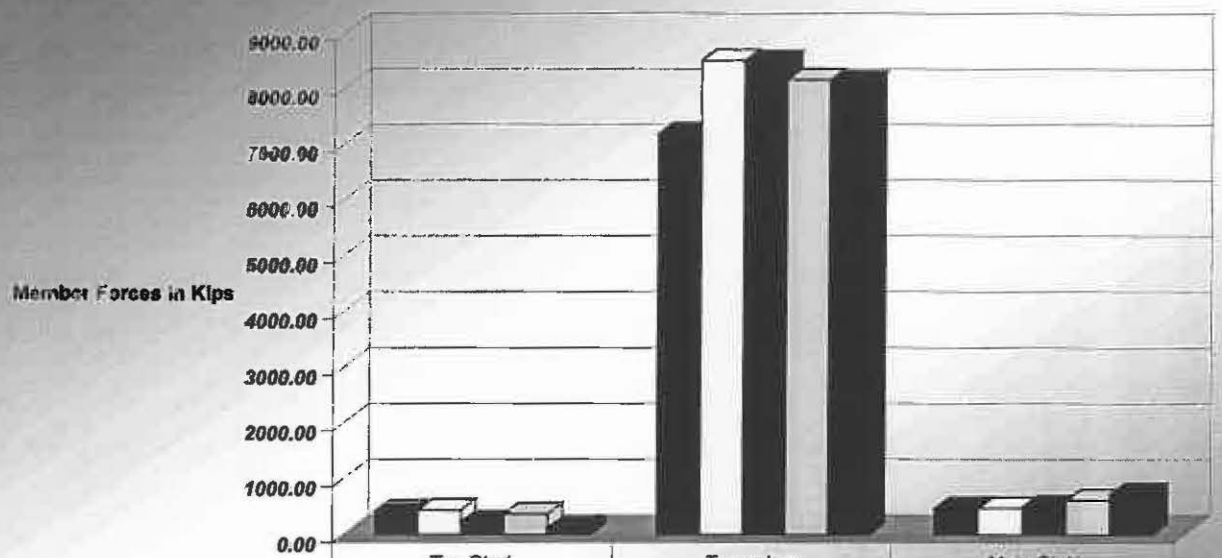

	Top Strut	Tower Leg	Main Slab
Composite	421.76	7177.00	470.11
A-shape	432.17	8507.00	468.05
Box	224.78	8484.10	495.45
A-slab	362.29	8152.10	508.50
Slab	108.58	8111.50	719.02

Elements

Fig. 5.54 Vertical Displacements from Non-Linear Multiple Response-Spectrum Analysis

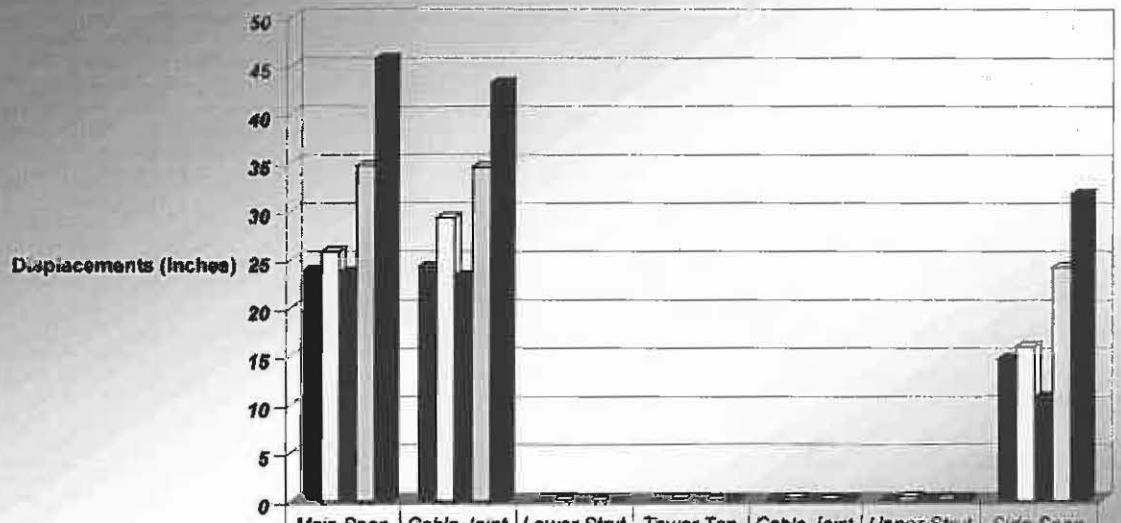

	Main Span Center 1	Cable Joint 2	Lower Strut Joint 3	Tower Top 4	Cable Joint 5	Upper Strut Joint 6	Side Span Center 7
Composite	23.866	24.282	7.31E-02	0.1126	0.11253	8.65E-02	14.727
A-shape	25.801	29.322	7.56E-02	0.27802	0.30219	0.40415	16.019
Box	23.669	23.312	8.98E-02	0.14401	0.14401	0.1251	10.769
A-slab	34.716	34.553	6.30E-02	0.11446	0.11843	0.1341	24.204
Slab	45.77	43.241	9.73E-02	0.11472	0.11472	8.11E-02	31.73

Nodes

Fig. 5.55 Horizontal Displacements from Non-Linear Multiple Response-Spectrum Analysis

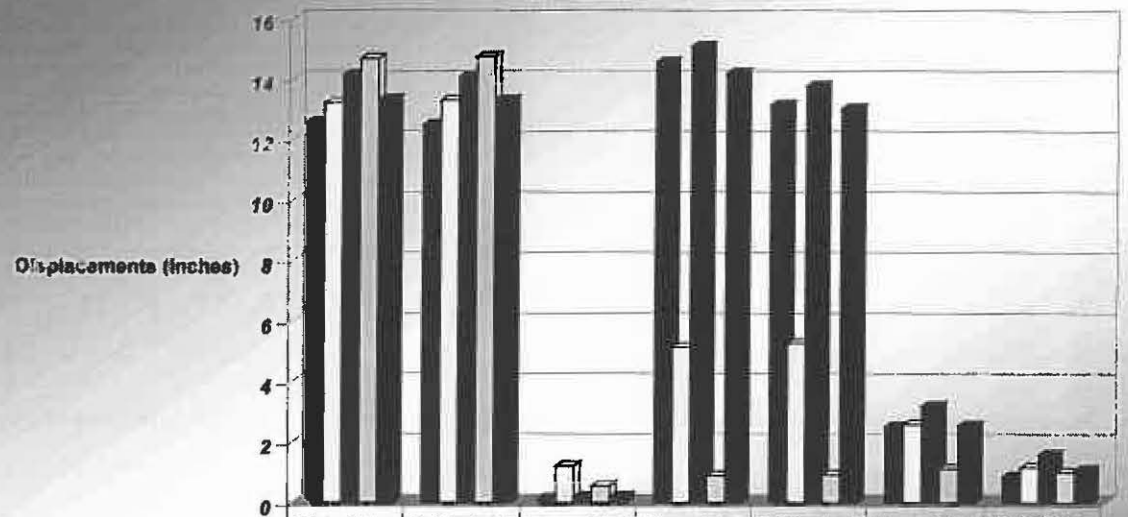

	Main Span Center 1	Cable Joint 2	Lower Strut Joint 3	Tower Top 4	Cable Joint 5	Upper Strut Joint 6	Side Span Center 7
Composite	12.565	12.473	0.14411	14.557	13.135	2.5114	0.85906
A-shape	13.209	13.29	1.2101	5.1319	5.2544	2.5626	1.1618
Box	14.134	14.061	0.19014	15.081	13.783	3.1928	1.5972
A-slab	14.667	14.731	0.54036	0.8744	0.90973	1.1127	0.99448
Slab	13.321	13.299	0.20045	14.19	13.013	2.5466	1.0906

Nodes

Fig. 5.56 Longitudinal Displacements from Non-Linear Multiple Response-Spectrum Analysis

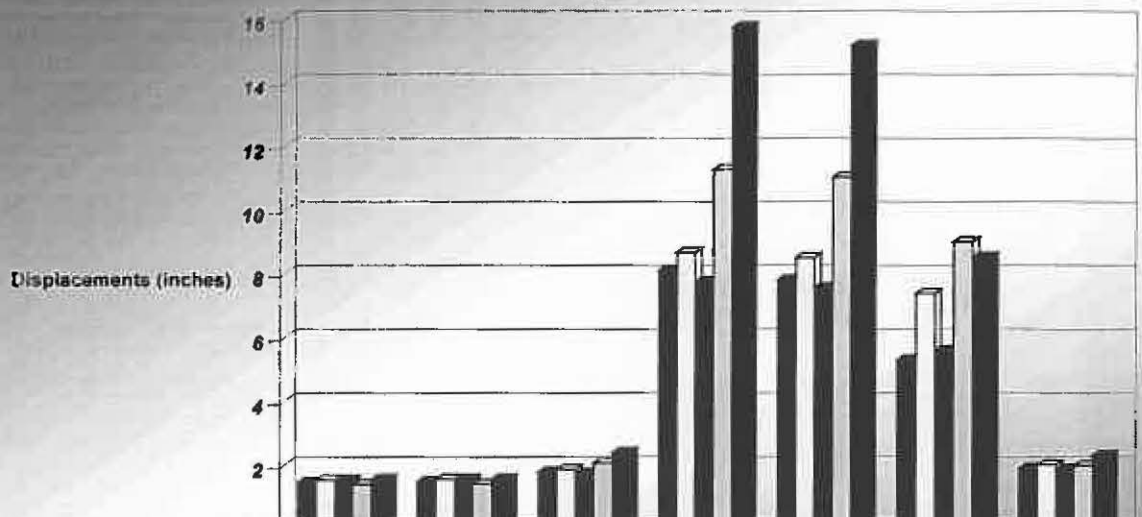

	Main Span Center 1	Cable Joint 2	Lower Strut Joint 3	Tower Top 4	Cable Joint 5	Upper Strut Joint 6	Side Span Center 7
Composite	1.4541	1.4726	1.7733	8.1047	7.8068	5.2852	1.8794
A-shape	1.5194	1.5467	1.8545	8.6704	8.6056	7.3676	1.9941
Box	1.5214	1.5551	1.7265	7.7444	7.5612	5.5847	1.8712
A-slab	1.3816	1.3946	2.0632	11.277	11.032	9.0062	1.9754
Slab	1.5585	1.5668	2.3887	15.765	15.189	8.5261	2.2939

Nodes

Fig. 5.57 Cable Forces from Non-Linear Multiple Response-Spectrum Analysis

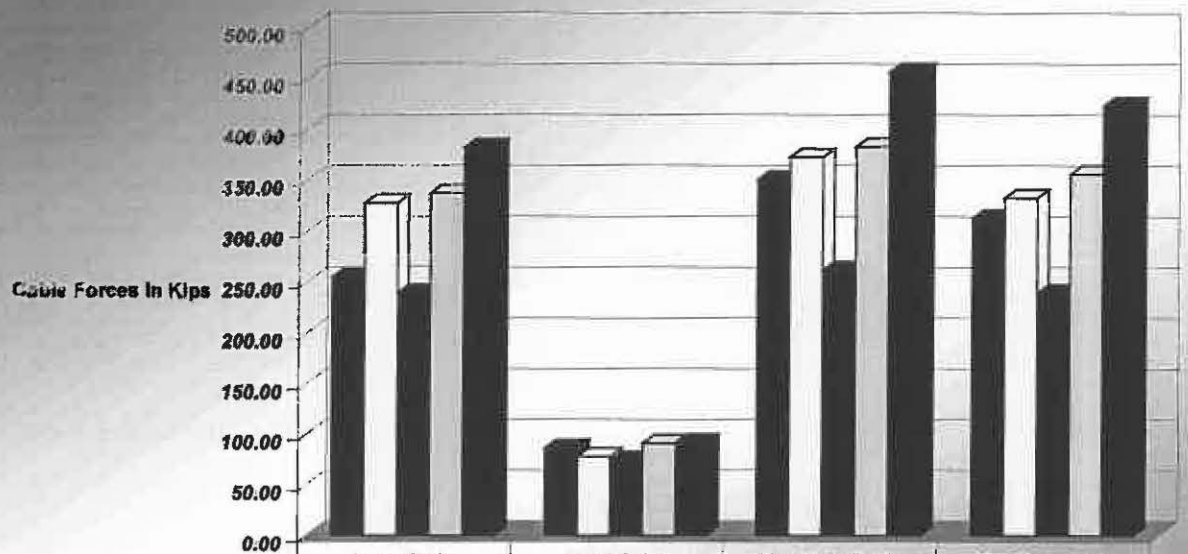

	Long Cable	Short Cable	Max Main Cable	Max Side Cable
Composite	255.15	86.43	350.35	313.05
A-shape	327.52	77.96	372.55	332.98
Box	239.39	74.73	291.82	239.65
A-slab	337.10	91.01	383.08	356.11
Slab	382.16	91.88	456.63	423.70

Elements

Fig. 5.58 Member Forces from Non-Linear Multiple Response-Spectrum Analysis

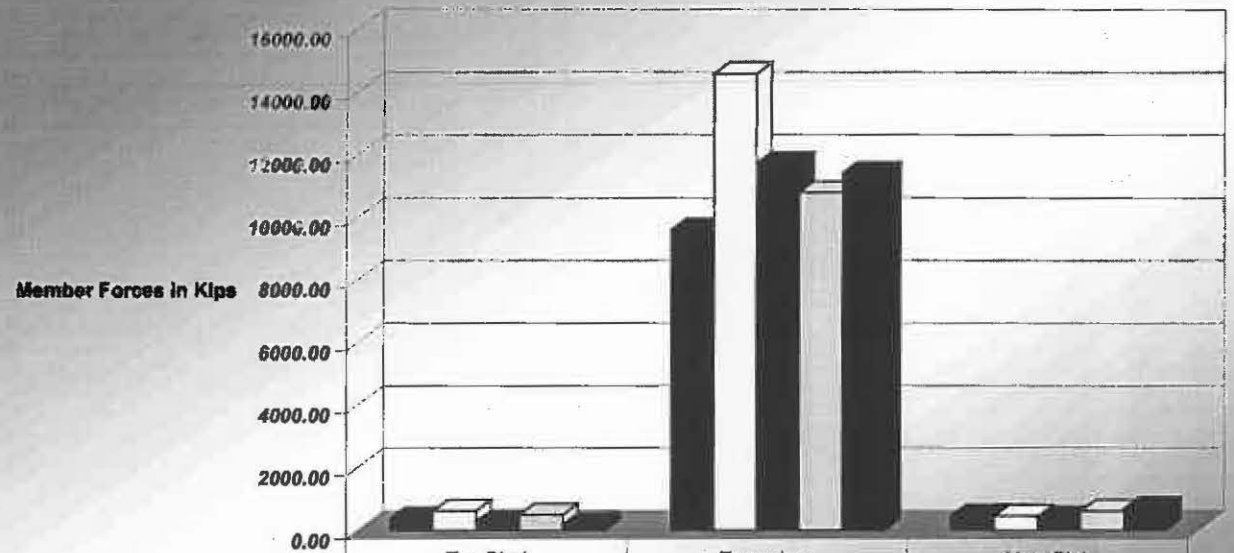

	Top Strut	Tower Leg	Main Slab
Composite	380.75	9611.40	454.05
A-shape	612.75	14572.00	451.81
Box	279.31	11720.00	412.76
A-slab	494.52	10779.50	609.35
Slab	183.17	11409.00	698.51

Elements

Fig. 5.59 Bending Moments from Non-Linear Multiple Response-Spectrum Analysis

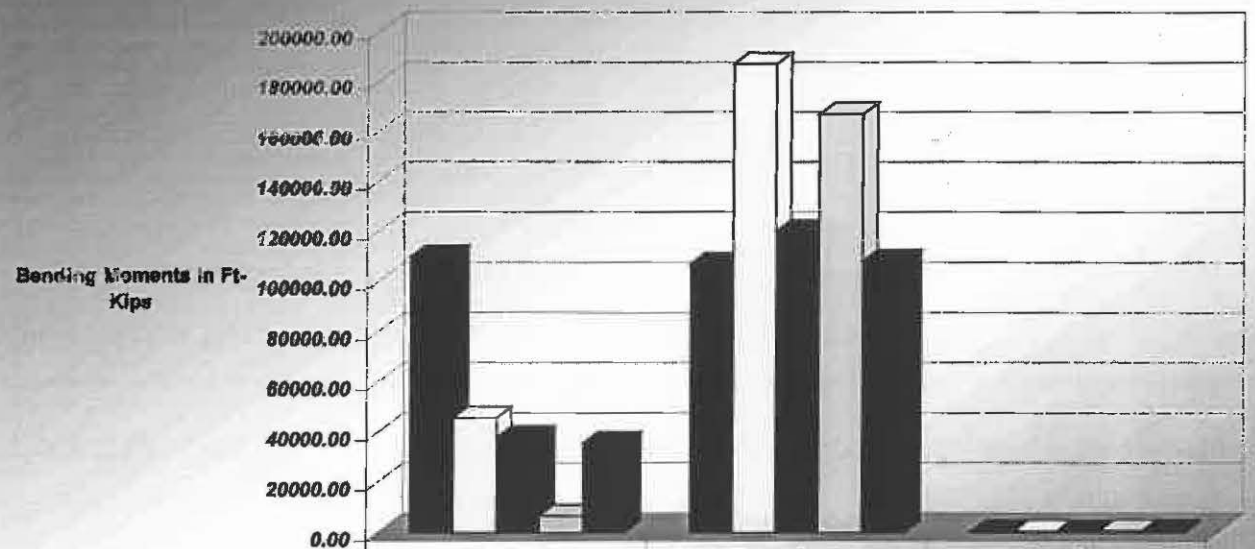

	Top Strut	Tower Leg	Main Slab
■ Composite	110083 33	107058 33	444 80
□ A-shape	45633 33	187008 33	451 53
■ Box	38048 33	120175 00	395 07
□ A-slab	6499 17	193925 00	695 39
■ Slab	35648 33	108275 00	798 29

Elements

Fig. 5.60 Comparison between Vertical Single/Mutiple Response-Spectrum Analysis Results of the Composite Design

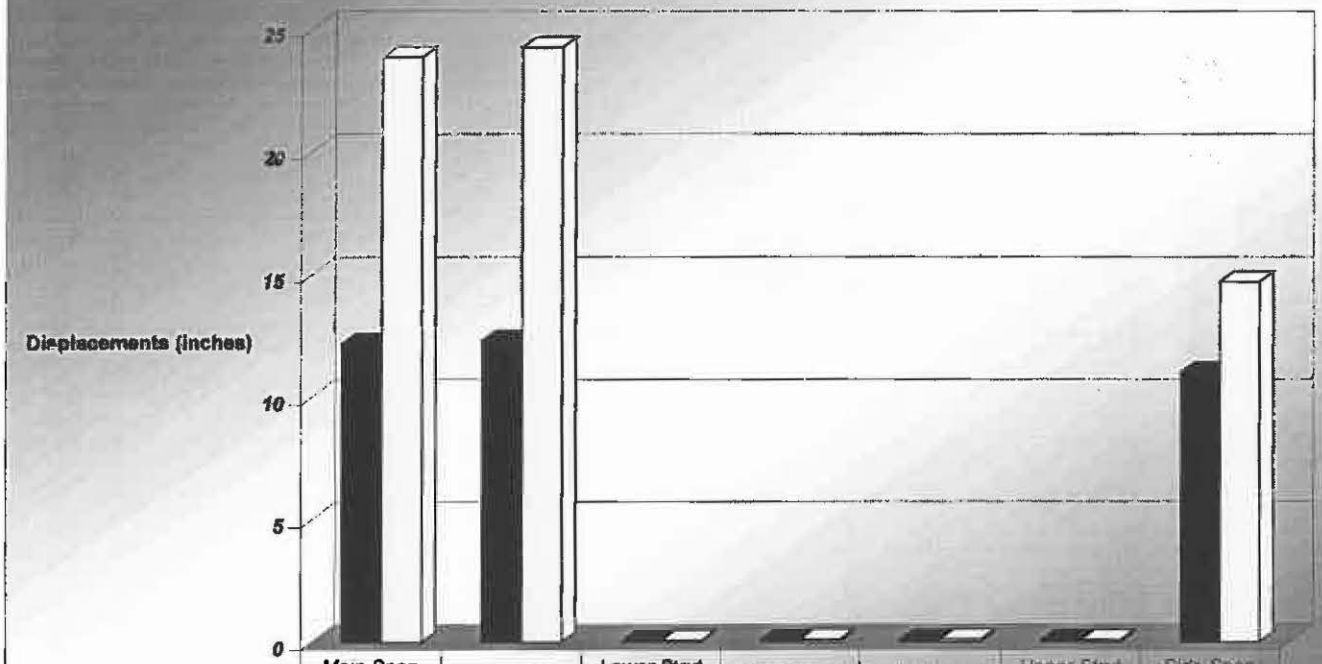

	Main Span Center 1	Cable Joint 2	Lower Strut Joint 3	Tower Top 4	Cable Joint 5	Upper Strut Joint 6	Side Span Center 7
■ Single	12 191	12 318	5 50E-02	8 795-02	9 79E-02	8 79E-02	11 028
□ Multiple	23 866	24 282	7 31E-C2	0 1124	0 11258	8 65E-02	14 727

Nodes

Fig. 5.61 Comparison between Horizontal Single/Mutiple Response-Spectrum Analysis Results of the Composite Design

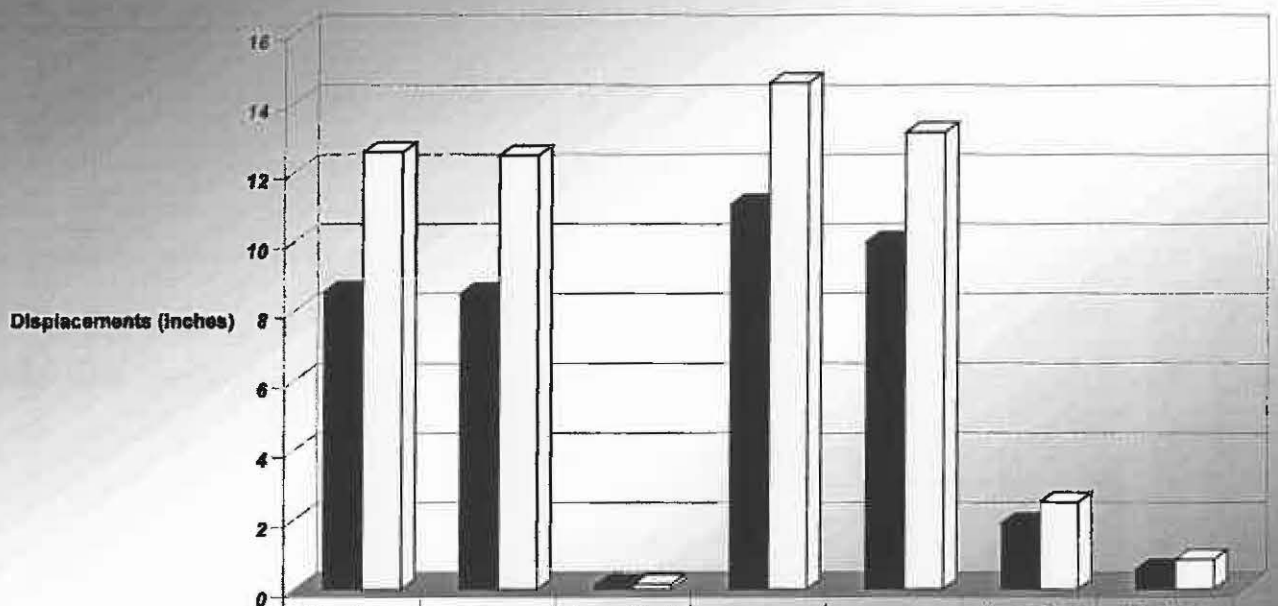

	Main Span Center 1	Cable Joint 2	Lower Strut Joint 3	Tower Top 4	Cable Joint 5	Upper Strut Joint 6	Side Span Center 7
Single	8.5629	8.4999	0.10769	11.06	9.9787	1.9042	0.58648
Multiple	12.565	12.473	0.14411	14.557	13.135	2.5114	0.65906

Fig. 5.62 Comparison between Longitudinal Single/Mutiple Response-Spectrum Analysis Results of the Composite Design

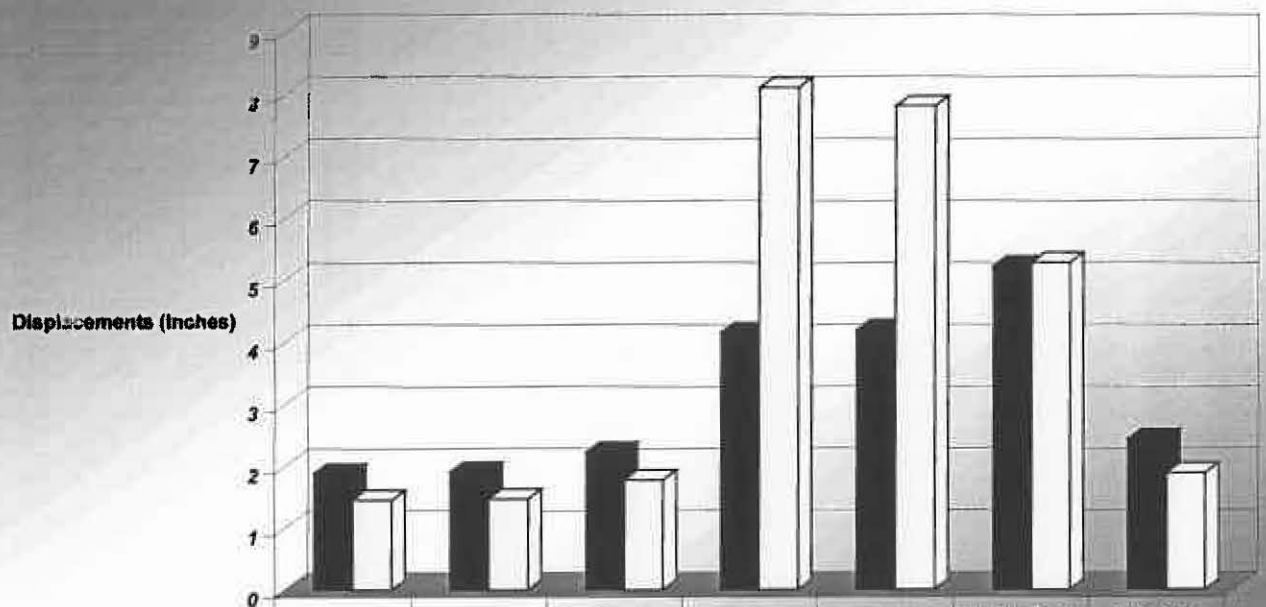

	Main Span Center 1	Cable Joint 2	Lower Strut Joint 3	Tower Top 4	Cable Joint 5	Upper Strut Joint 6	Side Span Center 7
Single	1.8864	1.9099	2.2266	4.1518	4.1947	5.2248	2.4313
Multiple	1.4541	1.4726	1.7733	8.1047	7.6066	5.2552	1.8724

Fig. 5.63 Comparison between Vertical Single/Mutiple Response-Spectrum Analysis Results of the A-shape Design

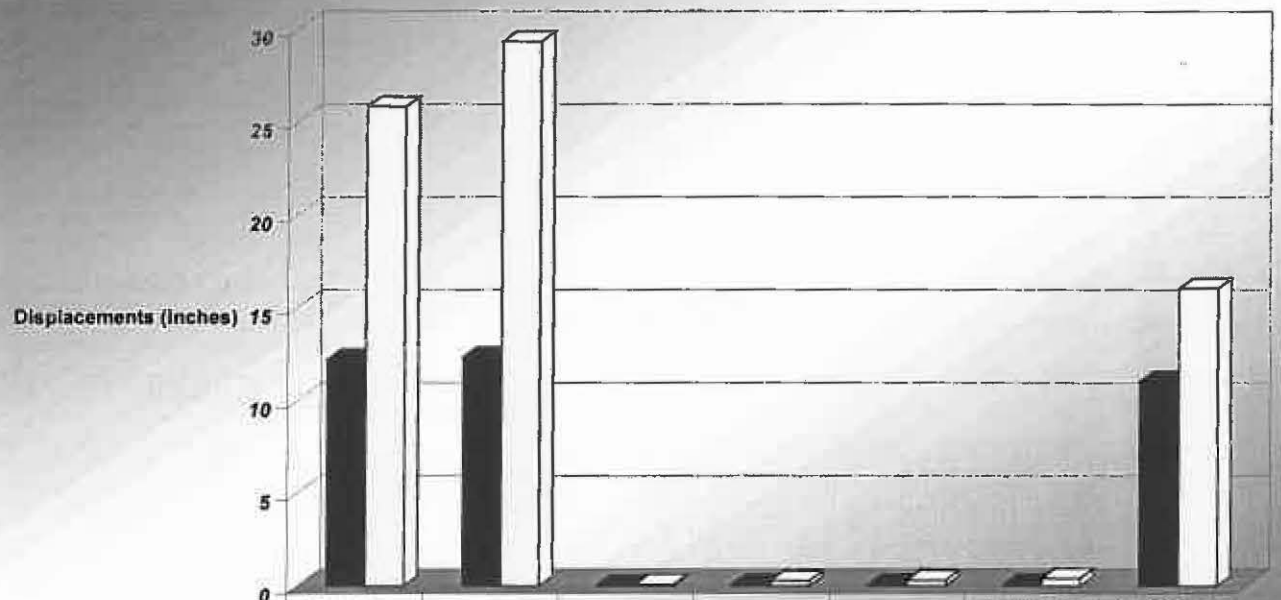

	Main Span Center 1	Cable Joint 2	Lower Strut Joint 3	Tower Top 4	Cable Joint 5	Upper Strut Joint 6	Side Span Center 7
Single	12.191	12.318	5.50E-02	8.79E-02	8.79E-02	8.79E-02	11.028
Multiple	25.801	29.322	7.56E-02	0.27802	0.30219	0.40415	16.019

Nodes

Fig. 5.64 Comparison between Horizontal Single/Mutiple Response-Spectrum Analysis Results of the A-shape Design

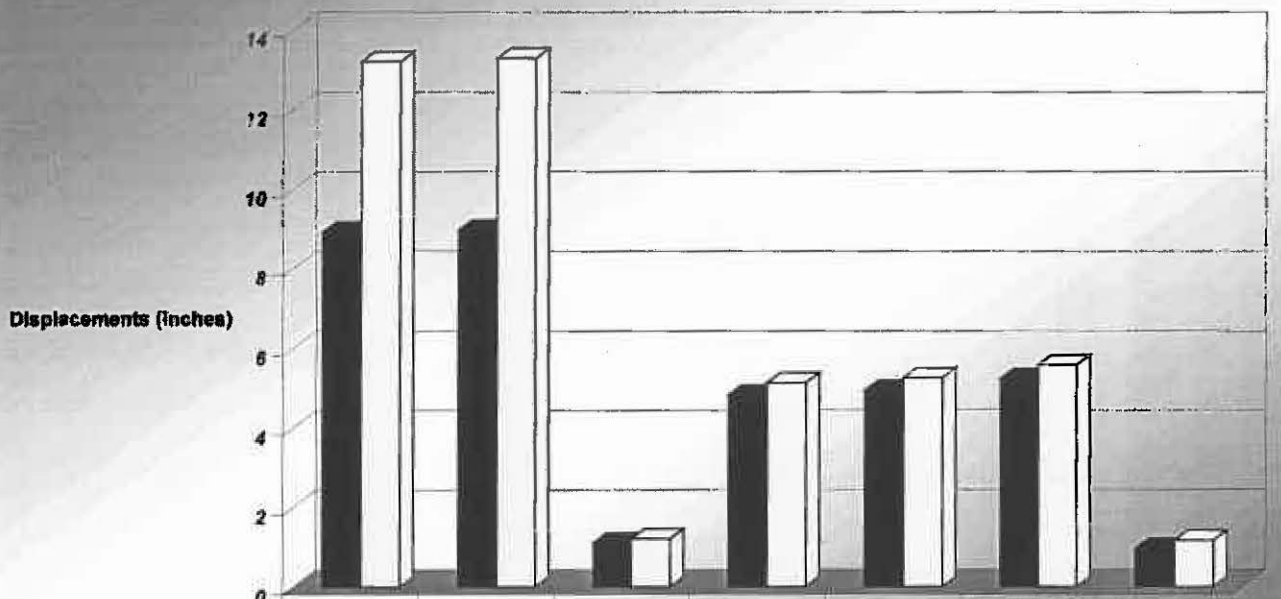

	Main Span Center 1	Cable Joint 2	Lower Strut Joint 3	Tower Top 4	Cable Joint 5	Upper Strut Joint 6	Side Span Center 7
Single	8.923	8.9727	1.1082	4.8243	4.9387	5.24	0.95894
Multiple	13.209	13.29	1.2101	5.1319	5.2544	5.5826	1.1618

Nodes

Fig. 5.55 Comparison between Longitudinal Single/Mutiple Response-Spectrum Analysis Results of the A-shape Design

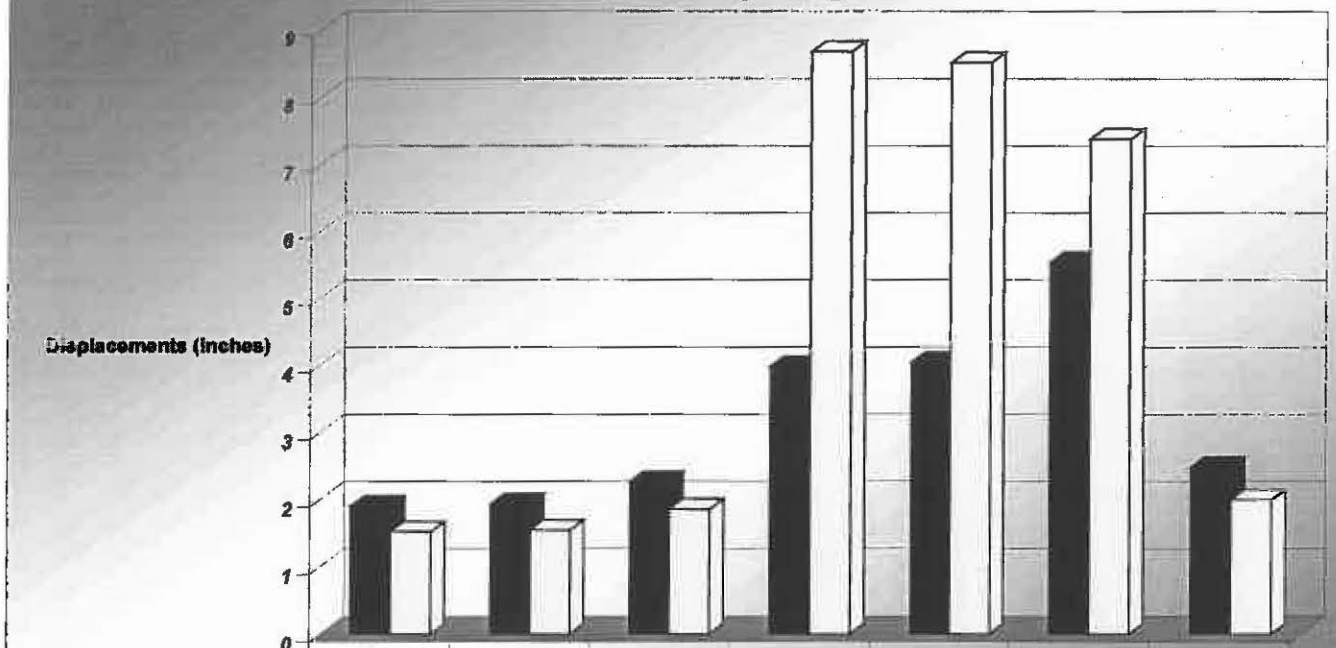

	Main Span Center 1	Cable Joint 2	Lower Strut Joint 3	Tower Top 4	Cable Joint 5	Upper Strut Joint 6	Side Span Center 7
Single	1.9037	1.9343	2.2623	3.9753	4.0364	5.5307	2.4909
Mutiple	1.5194	1.5467	1.8545	8.6704	8.5056	7.3676	1.9941

Nodes

Fig. 5.56 Comparison between Vertical Single/Mutiple Response-Spectrum Analysis Results of the Box Design

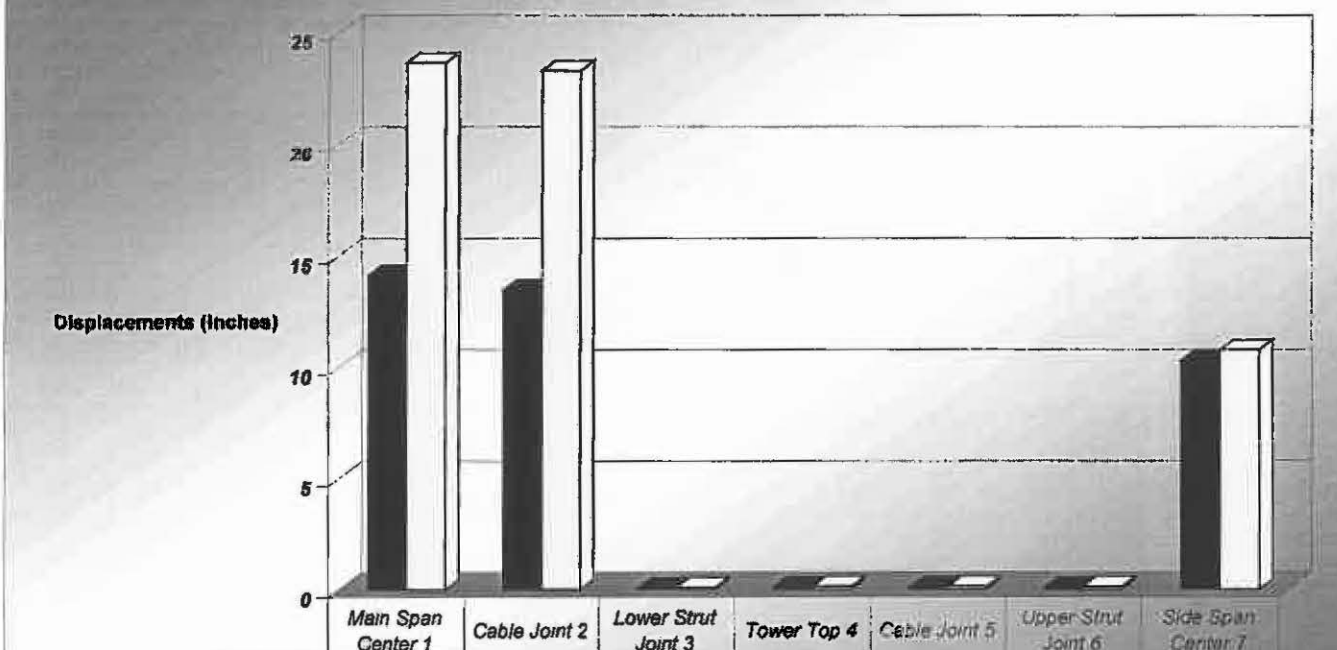

	Main Span Center 1	Cable Joint 2	Lower Strut Joint 3	Tower Top 4	Cable Joint 5	Upper Strut Joint 6	Side Span Center 7
Single	14.138	13.488	6.51E-02	0.10944	0.10944	9.23E-02	10.311
Multiple	23.669	23.312	8.98E-02	0.14401	0.14401	0.1251	10.769

Nodes

Fig. 5.67 Comparison between Horizontal Single/Mutiple Response-Spectrum Analysis Results of the Box Design

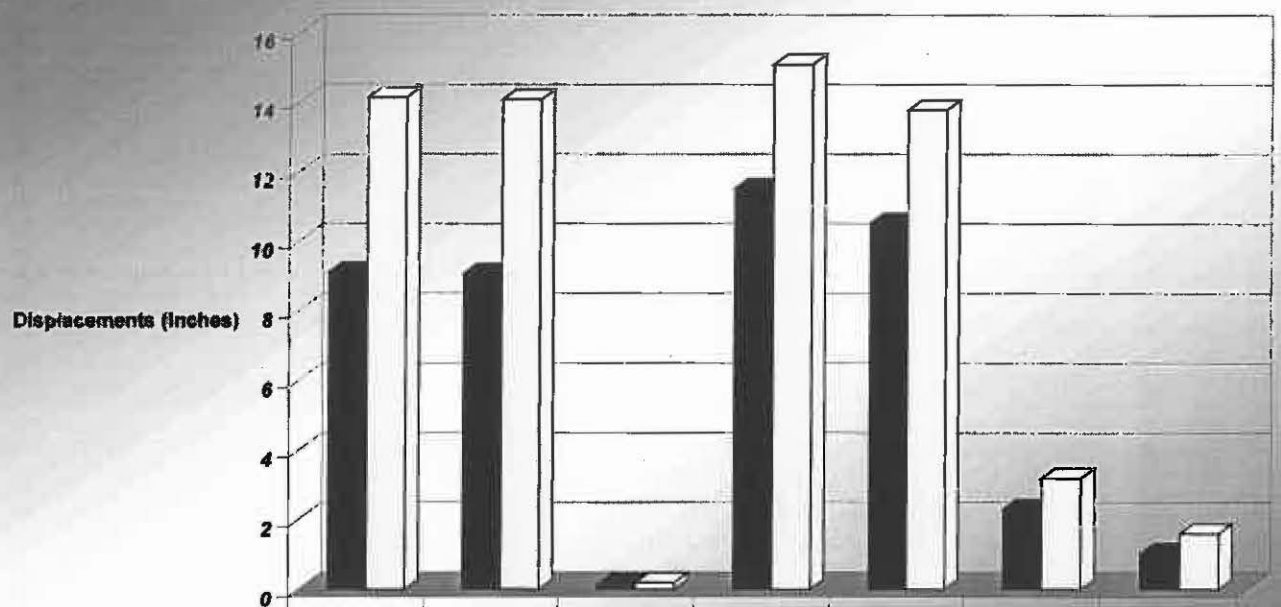

	Main Span Center 1	Cable Joint 2	Lower Strut Joint 3	Tower Top 4	Cable Joint 5	Upper Strut Joint 6	Side Span Center 7
Single	9.1124	9.0654	0.13445	11.505	10.511	2.3049	1.0438
Multiple	14.134	14.061	0.19014	15.061	13.763	3.1928	1.5972

Nodes

Fig. 5.68 Comparison between Longitudinal Single/Mutiple Response-Spectrum Analysis Results of the Box Design

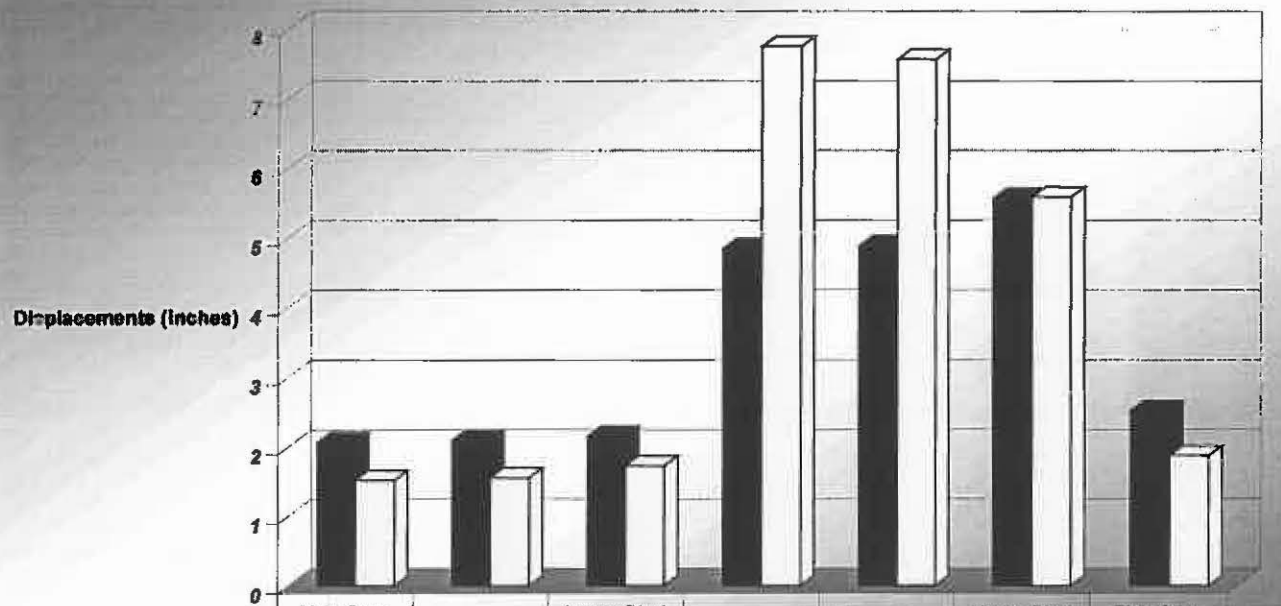

	Main Span Center 1	Cable Joint 2	Lower Strut Joint 3	Tower Top 4	Cable Joint 5	Upper Strut Joint 6	Side Span Center 7
Single	2.0669	2.1001	2.1521	4.8455	4.8829	5.5646	2.5169
Multiple	1.5214	1.5551	1.7265	7.7444	7.5612	5.5847	1.8712

Nodes

Fig. 5.69 Comparison between Vertical Single/Mutiple Response-Spectrum Analysis Results of the A-slab Design

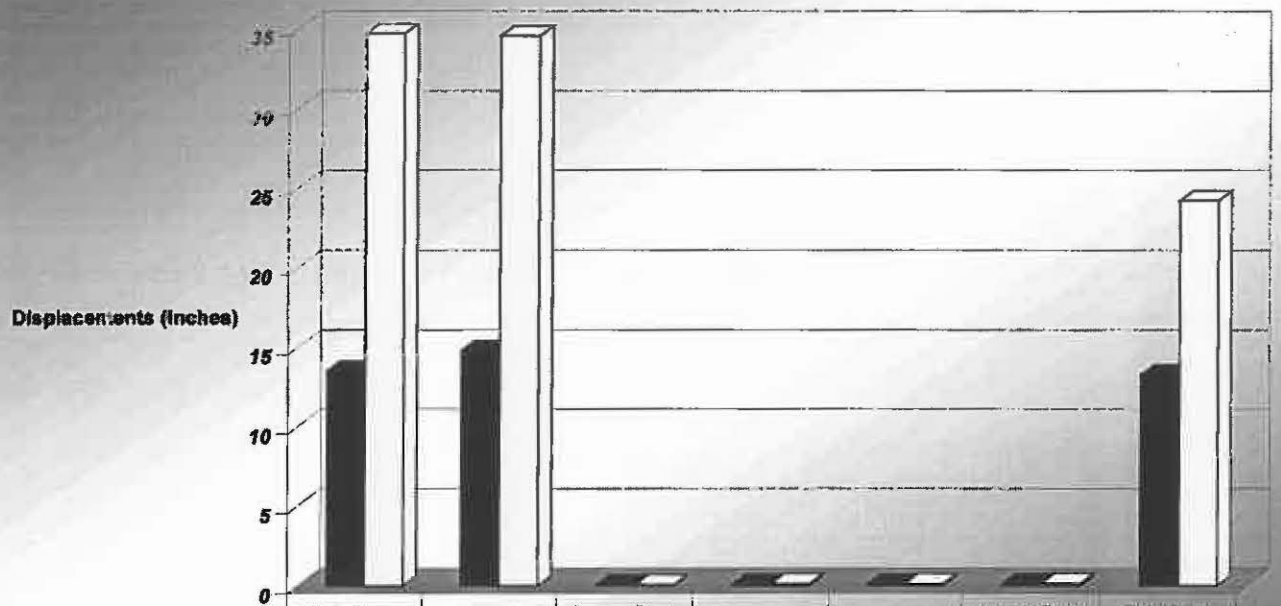

	Main Span Center 1	Cable Joint 2	Lower Strut Joint 3	Tower Top 4	Cable Joint 5	Upper Strut Joint 6	Side Span Center 7
■ Single	13.497	14.79	4.35E-02	8.05E-02	8.44E-02	0.10276	13.247
□ Multiple	34.716	34.553	6.30E-02	0.11446	0.11843	0.1341	24.204

Nodes

Fig. 5.70 Comparison between Horizontal Single/Mutiple Response-Spectrum Analysis Results of the A-slab Design

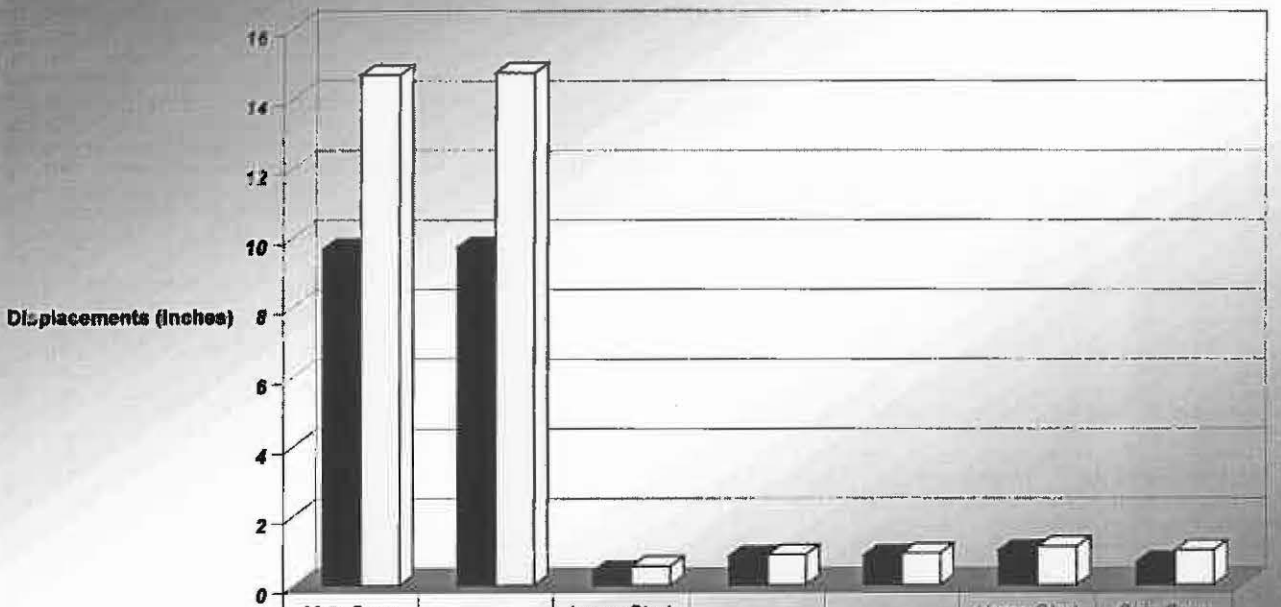

	Main Span Center 1	Cable Joint 2	Lower Strut Joint 3	Tower Top 4	Cable Joint 5	Upper Strut Joint 6	Side Span Center 7
■ Single	9.6652	9.7084	0.39775	0.32753	0.85577	0.99492	0.65507
□ Multiple	14.667	14.731	0.54036	0.8744	0.90973	1.1127	0.99448

Nodes

Fig. 5.71 Comparison between Longitudinal Single/Mutiple Response-Spectrum Analysis Results of the A-slab Design

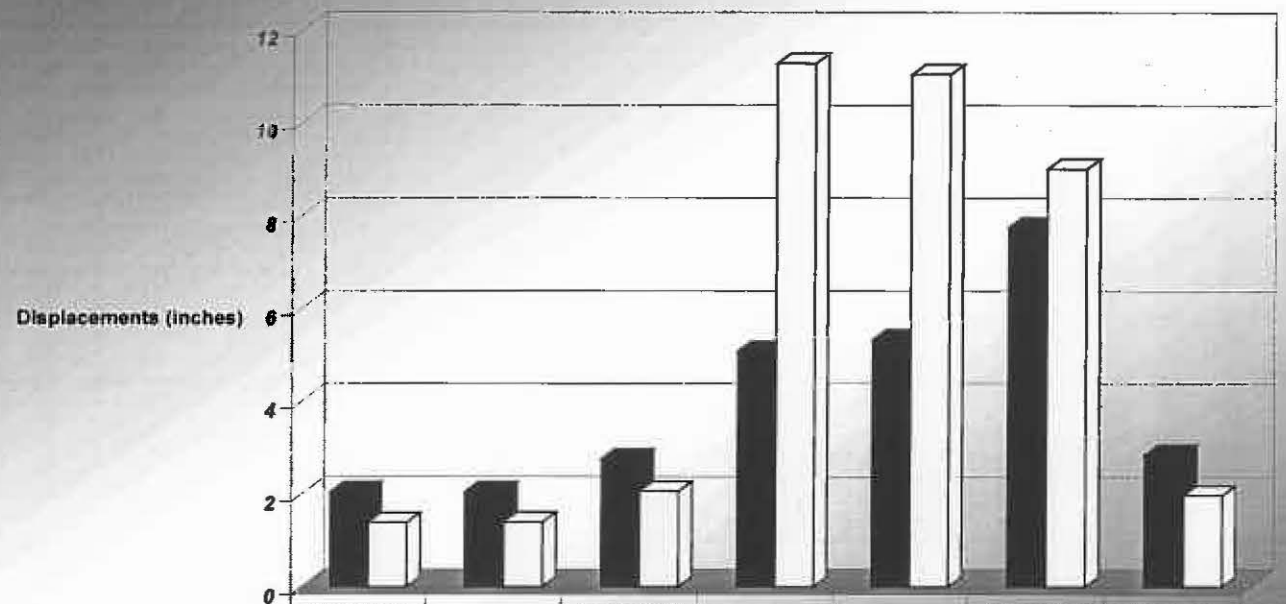

	Main Span Center 1	Cable Joint 2	Lower Strut Joint 3	Tower Top 4	Cable Joint 5	Upper Strut Joint 6	Side Span Center 7
Single	2.0499	2.0516	2.7605	5.0772	5.3272	7.7423	2.8501
Multiple	1.3816	1.3946	2.0632	11.277	11.032	9.0062	1.9754

Nodes

Fig. 5.72 Comparison between Vertical Single/Mutiple Response-Spectrum Analysis Results of the Slab Design

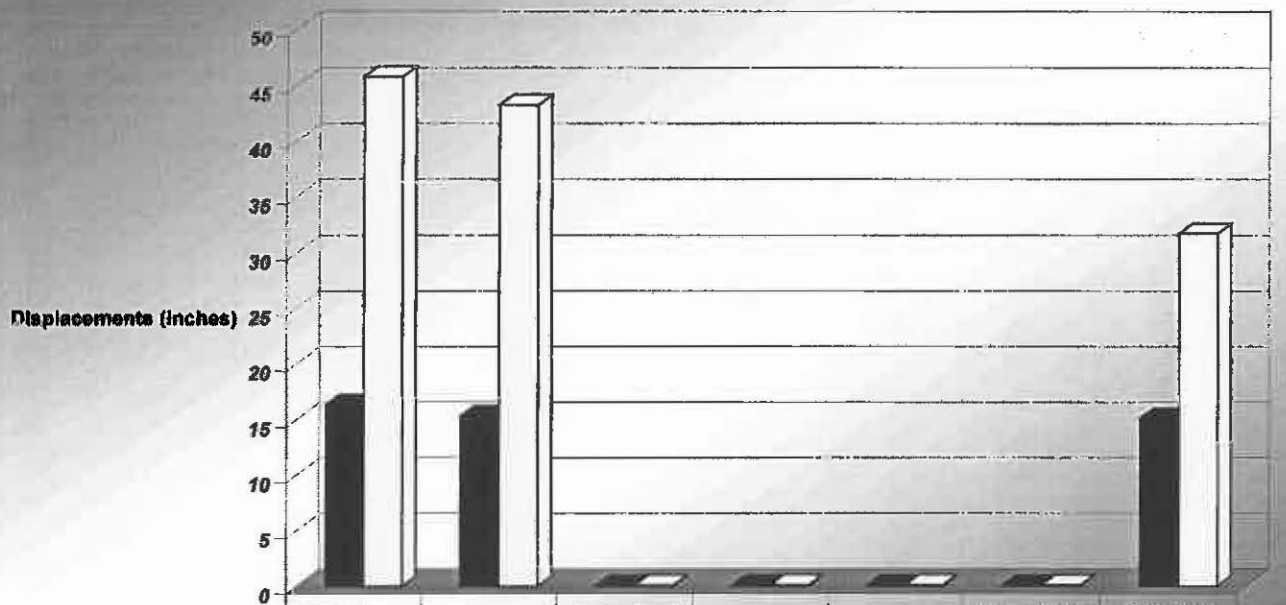

	Main Span Center 1	Cable Joint 2	Lower Strut Joint 3	Tower Top 4	Cable Joint 5	Upper Strut Joint 6	Side Span Center 7
Single	16.363	15.323	6.98E-02	6.67E-02	6.67E-02	5.04E-02	15.124
Multiple	45.77	43.241	9.73E-02	0.11472	0.11472	8.11E-02	31.73

Nodes

Fig. 5.73 Comparison between Horizontal Single/Mutiple Response-Spectrum Analysis Results of the Slab Design

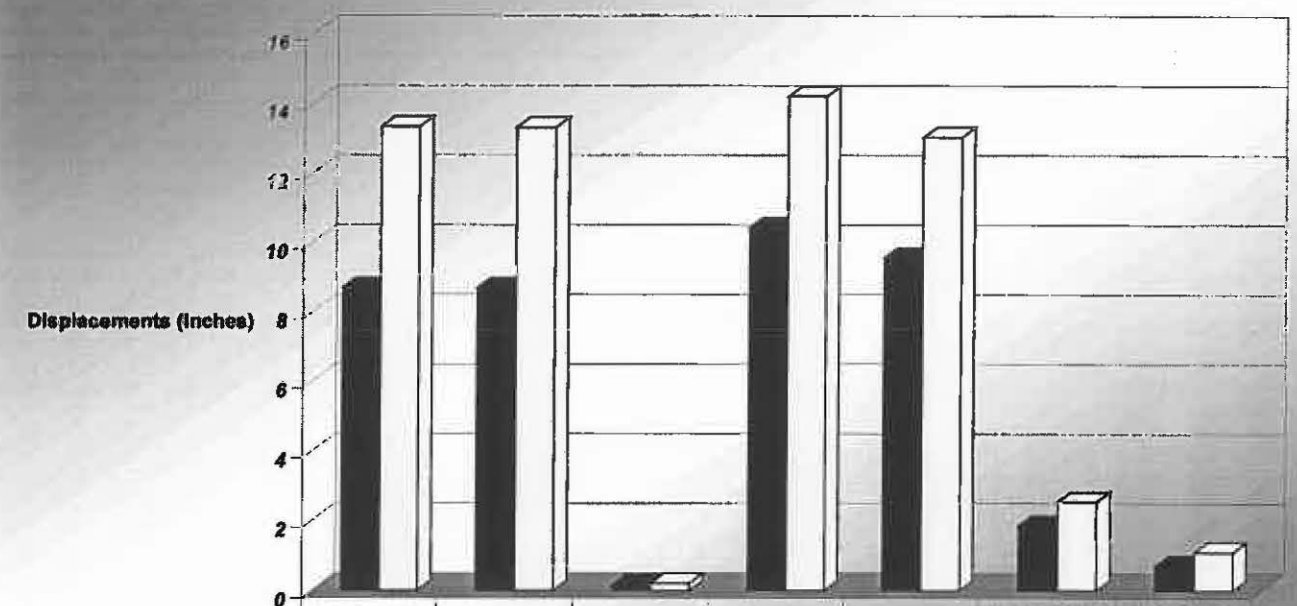

	Main Span Center 1	Cable Joint 2	Lower Strut Joint 3	Tower Top 4	Cable Joint 5	Upper Strut Joint 6	Side Span Center 7
Single	8.7024	8.6878	0.14311	10.417	9.5524	1.8522	0.71334
Multiple	13.321	13.299	0.20045	14.19	13.013	2.5466	1.0908

Nodes

Fig. 5.74 Comparison between Longitudinal Single/Mutiple Response-Spectrum Analysis Results of the Slab Design

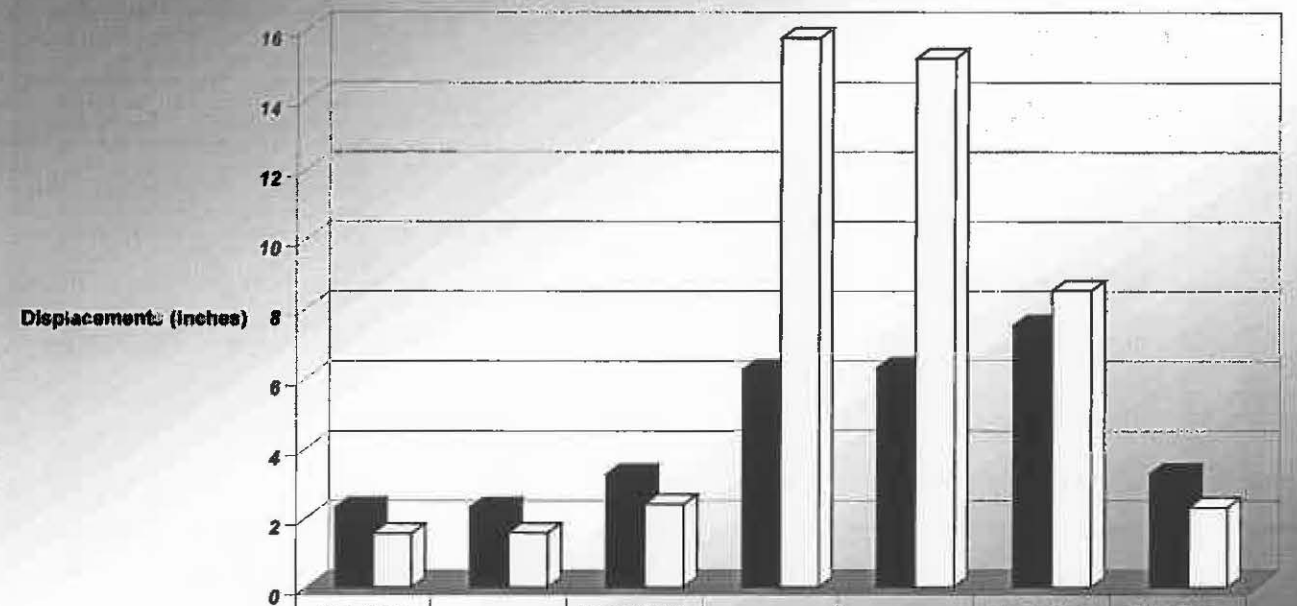

	Main Span Center 1	Cable Joint 2	Lower Strut Joint 3	Tower Top 4	Cable Joint 5	Upper Strut Joint 6	Side Span Center 7
Single	2.3103	2.306	3.2559	6.2325	6.295	7.5122	3.2766
Multiple	1.5585	1.5668	2.3867	13.765	15.183	8.5261	2.2939

Nodes

Fig. 5.75 Comparison between Single/Multiple Cable Force Responses from the Composite Design

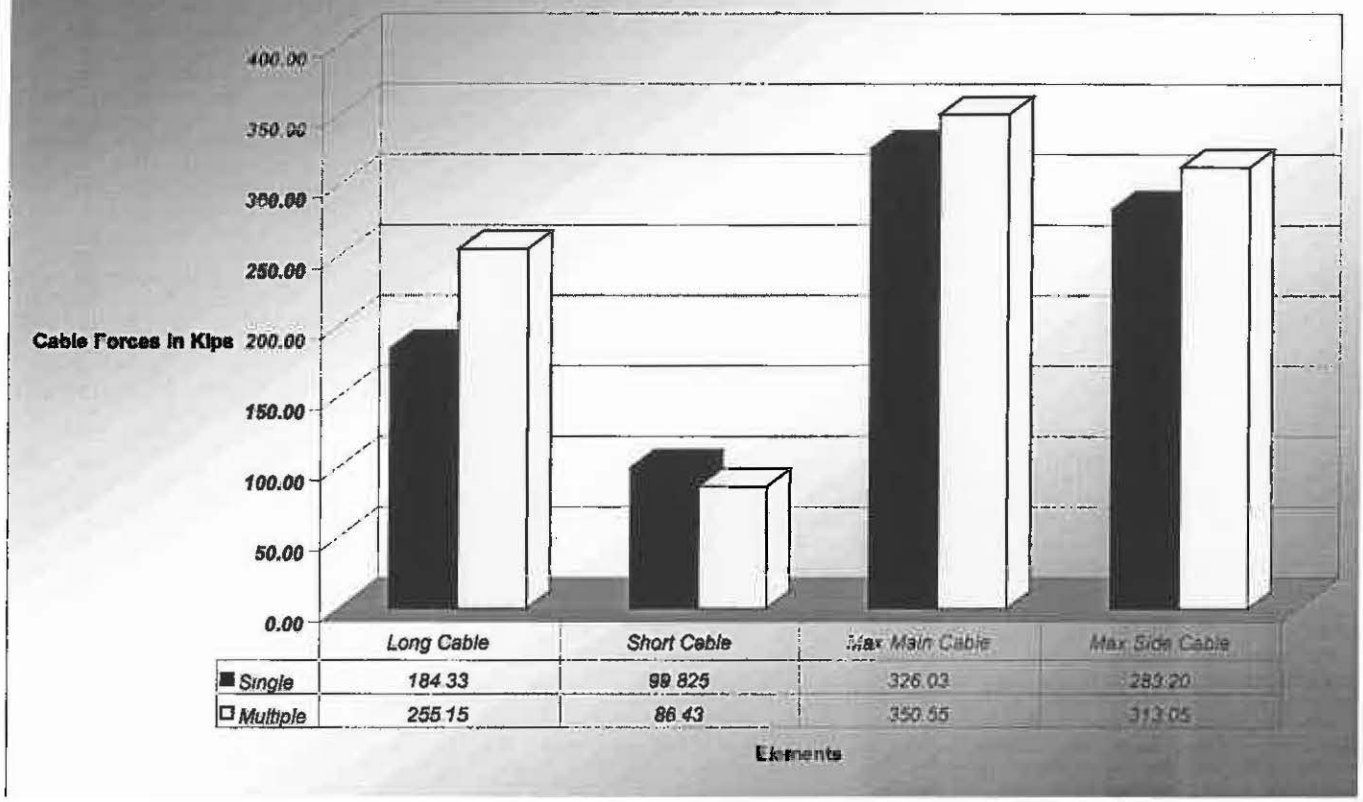

Fig. 5.76 Comparison between Single/Multiple Member Force Responses from the Composite Design

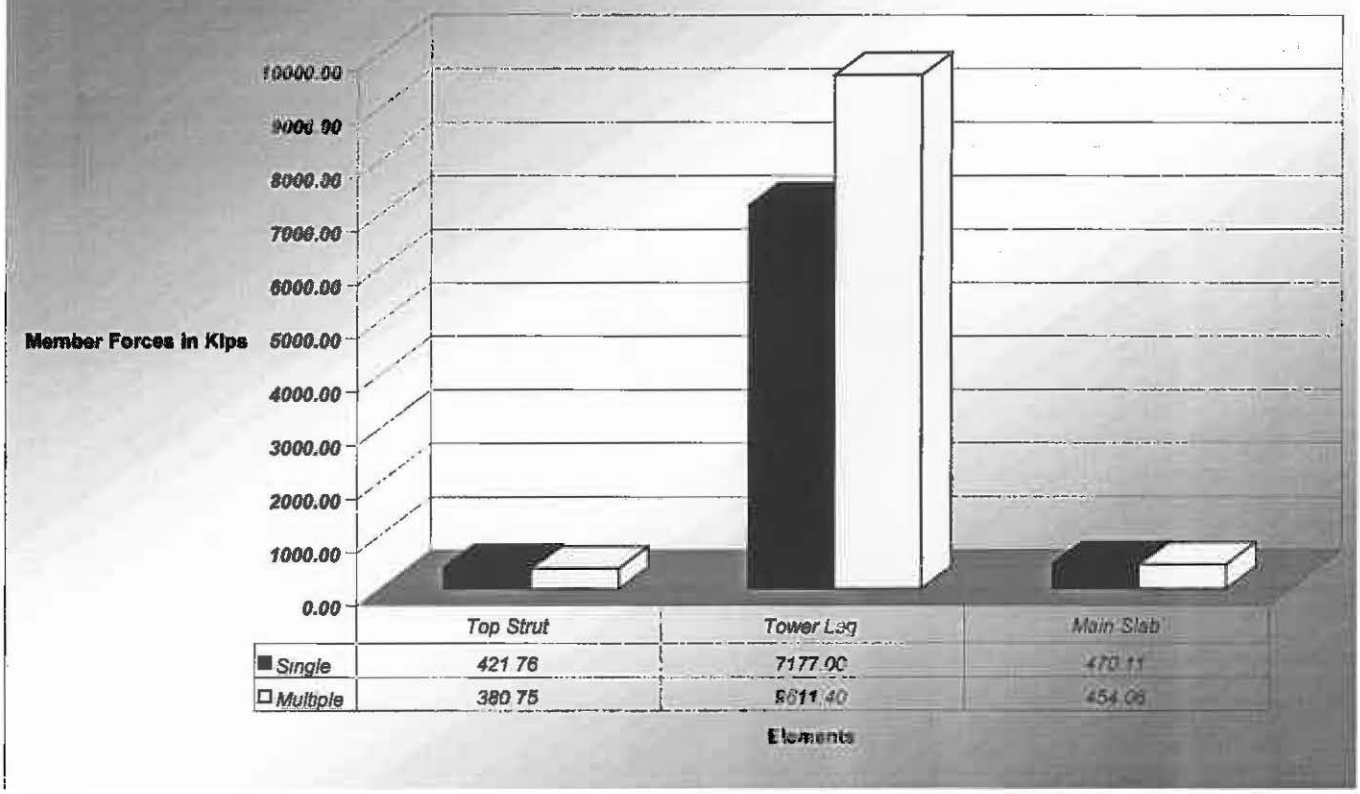

Fig. 5.77 Comparison between Single/Mutiple Cable Force Responses from the A-shape Design

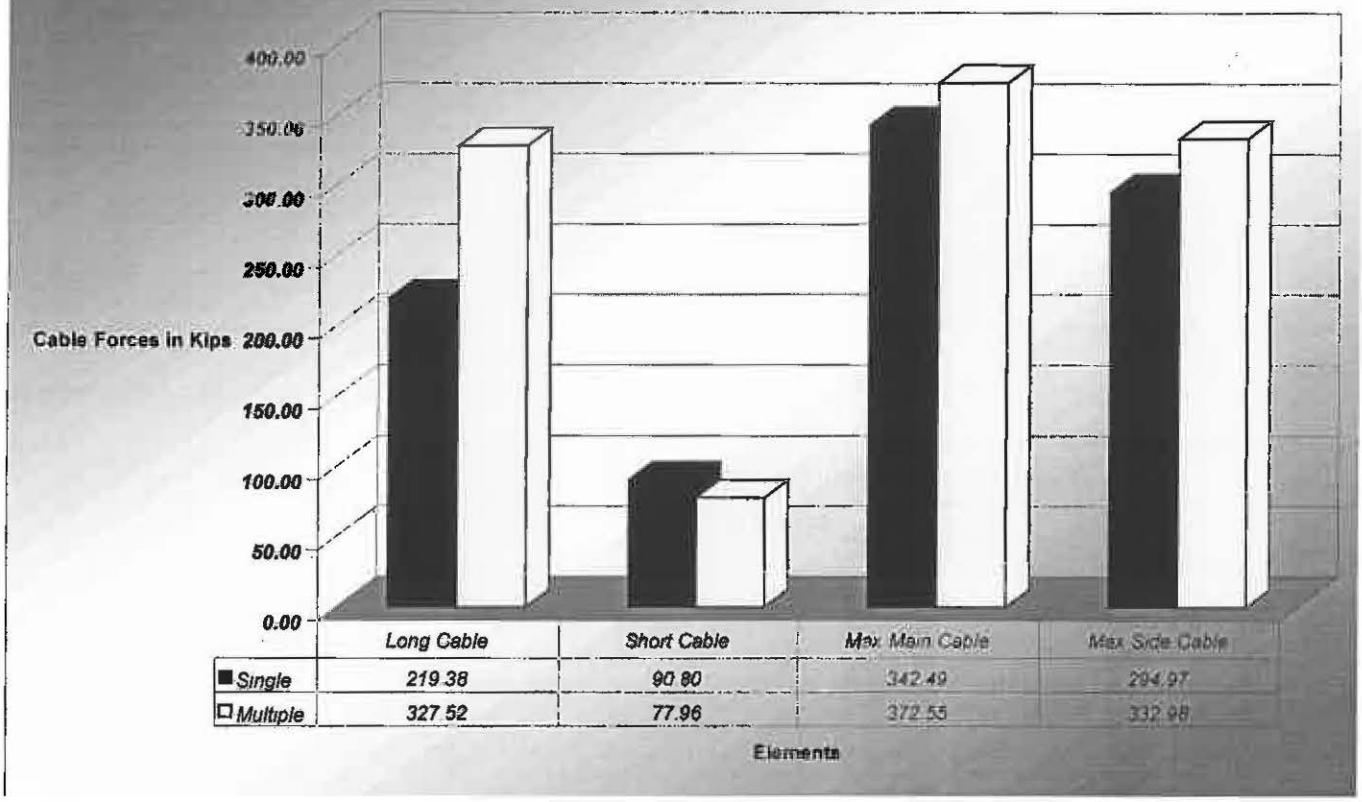

Fig. 5.78 Comparison between Single/Mutiple Member Force Responses from the A-shape Design

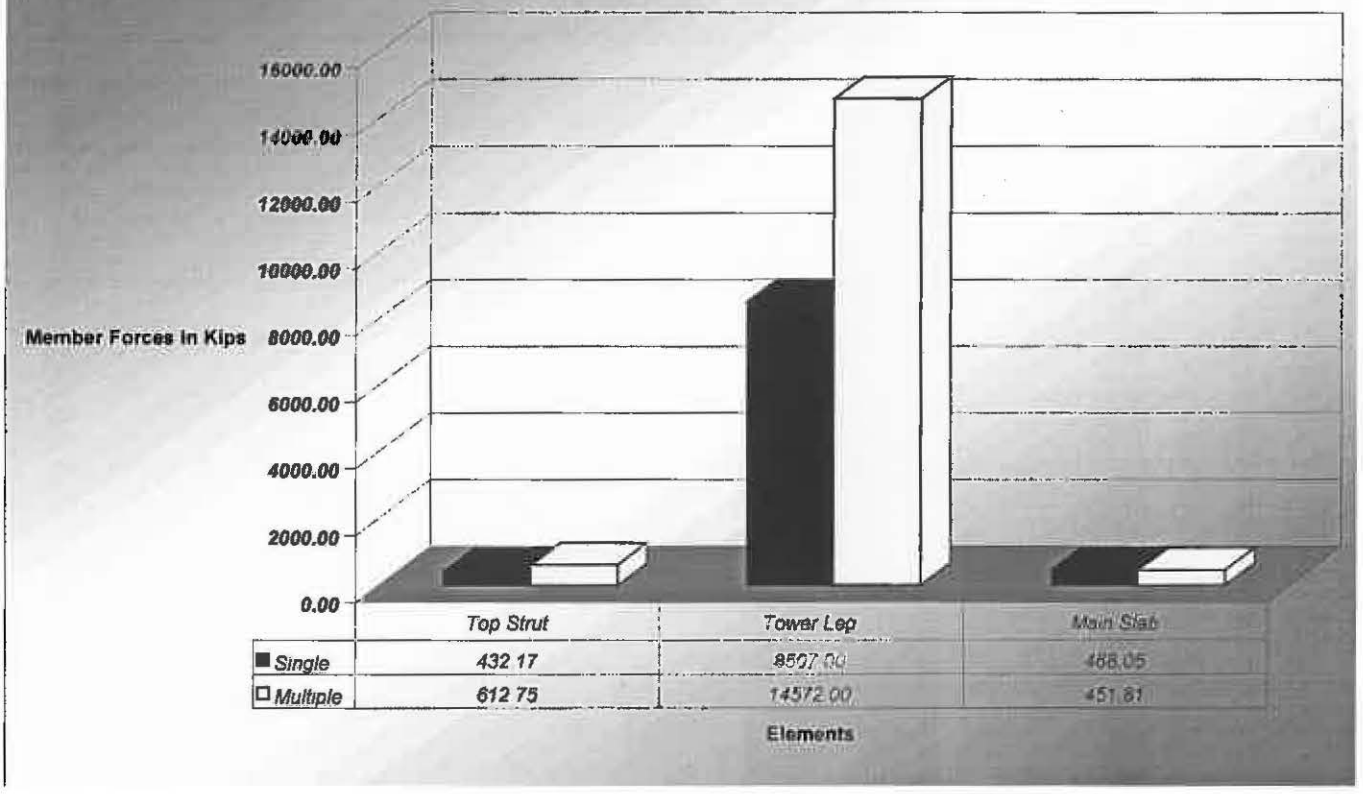

Fig. 5.79 Comparison between Single/Mutiple Cable Force Responses from the Box Design

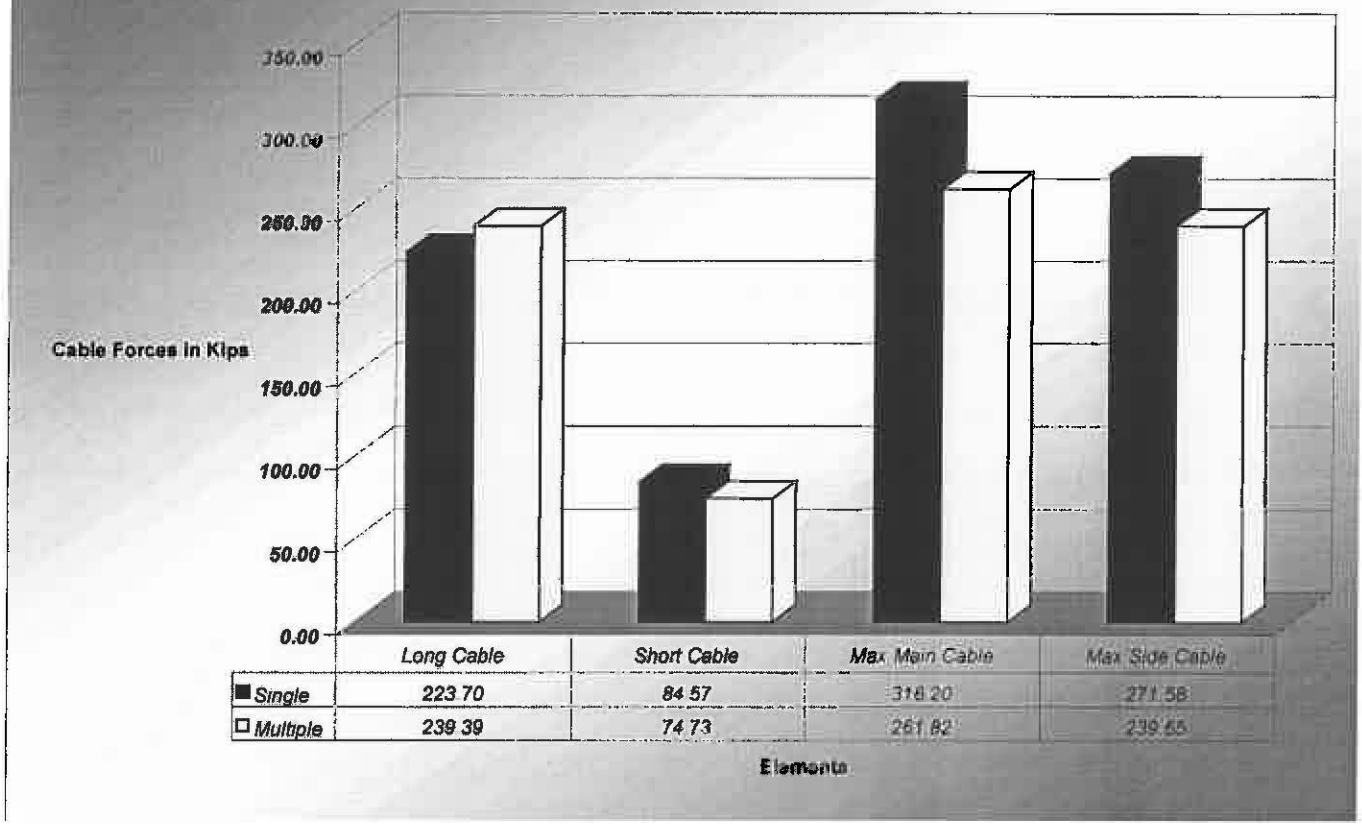

	Long Cable	Short Cable	Max. Main Cable	Max. Side Cable
Single	223.70	84.57	316.20	271.58
Multiple	239.39	74.73	261.82	239.55

Elements

Fig. 5.80 Comparison between Single/Mutiple Member Force Responses from the Box Design

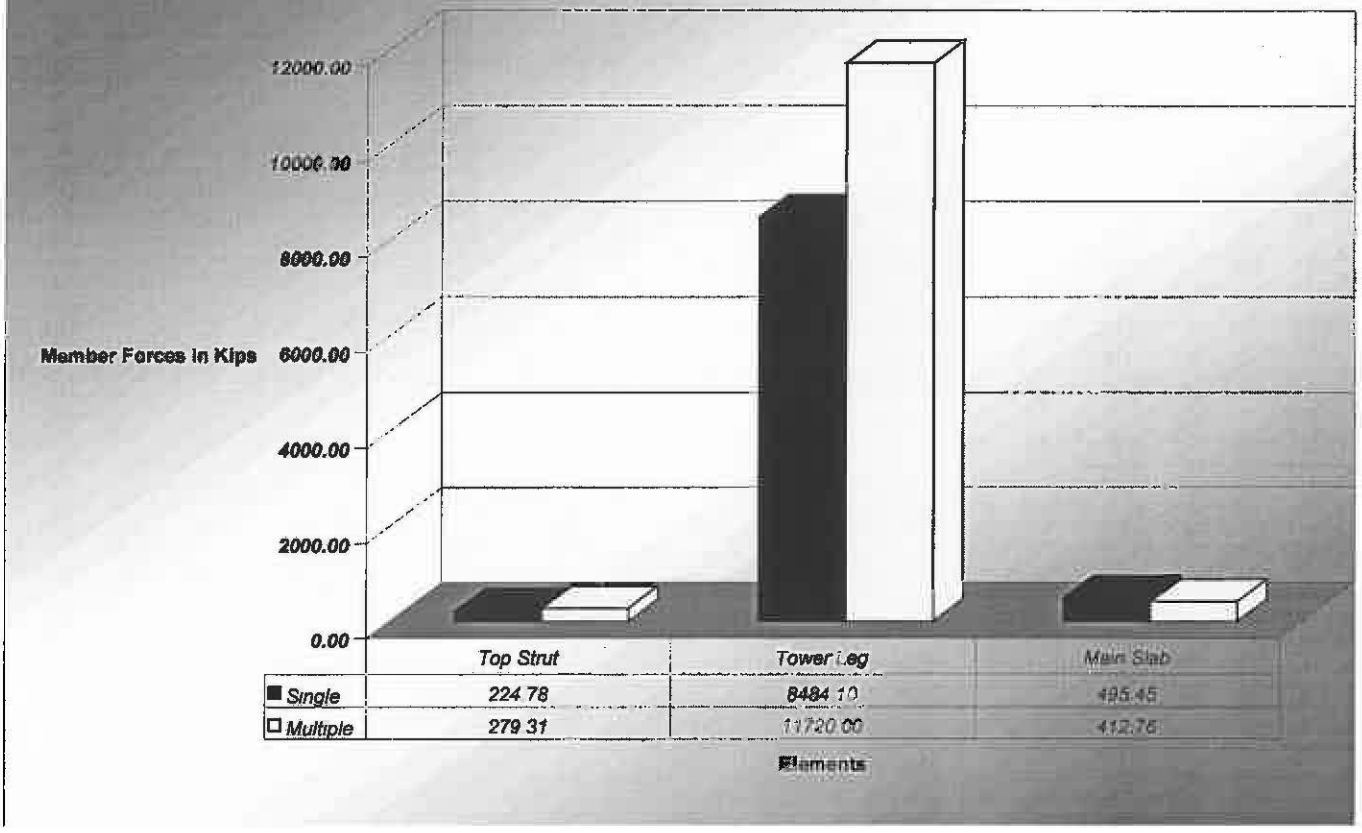

	Top Strut	Tower Leg	Main Slab
Single	224.78	8484.10	495.45
Multiple	279.31	11720.00	412.76

Elements

Fig. 5.81 Comparison between Single/Mutiple Cable Force Responses from the A-slab Design

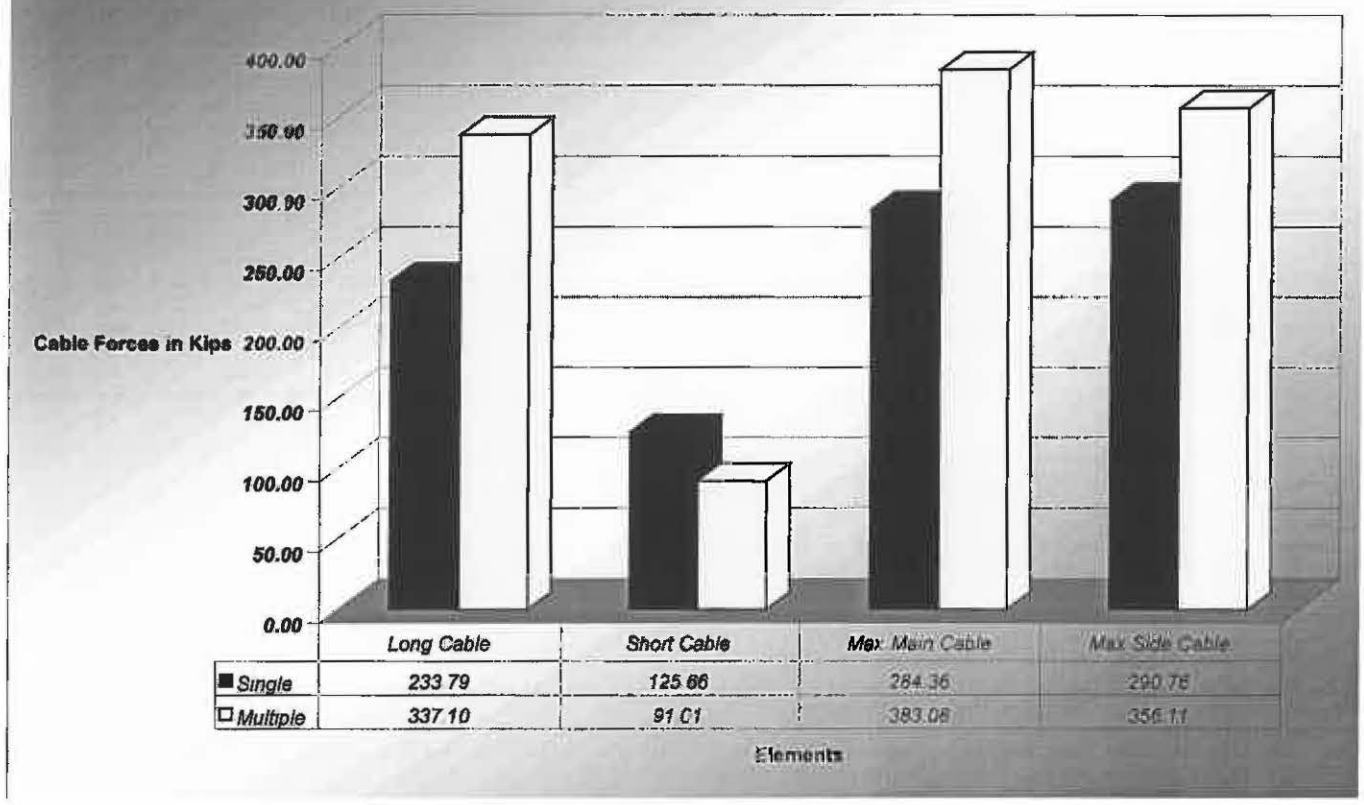

Fig. 5.82 Comparison between Single/Mutiple Member Force Responses from the A-slab Design

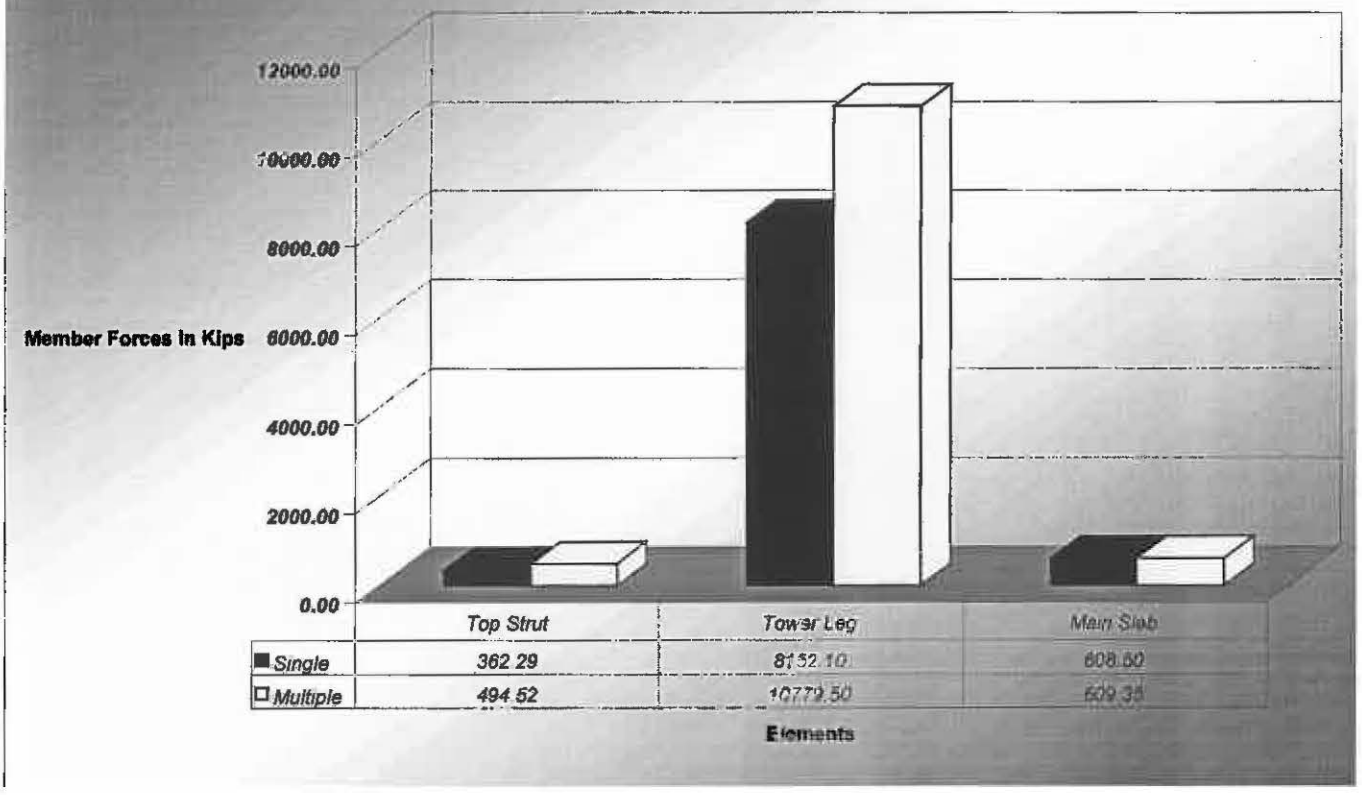

Fig. 5.83 Comparison between Single/Multiple Cable Force Responses from the Slab Design

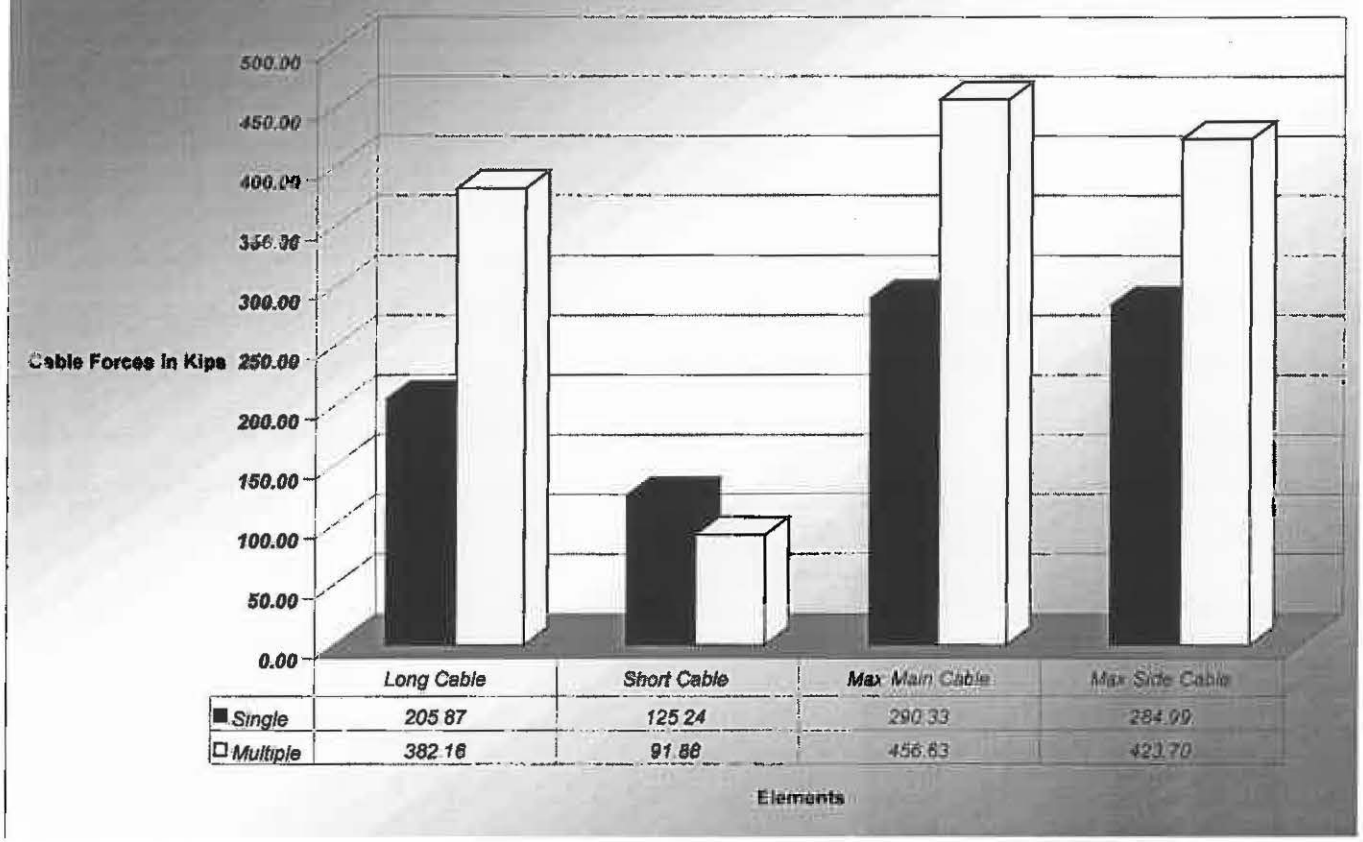

	Long Cable	Short Cable	Max Main Cable	Max Side Cable
Single	205.87	125.24	290.33	284.99
Multiple	382.16	91.86	456.63	423.70

Fig. 5.84 Comparison between Single/Mutiple Member Force Responses from the Slab Design

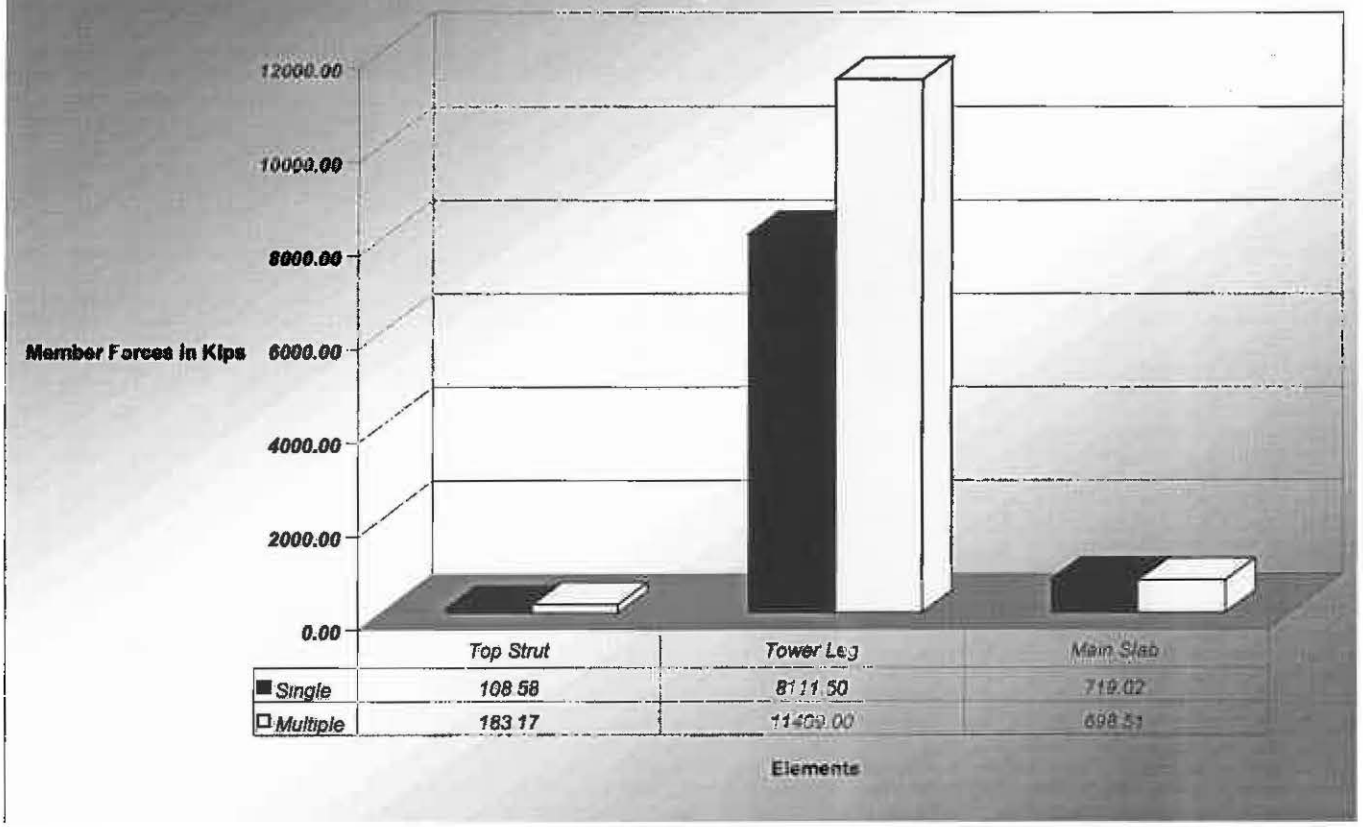

	Top Strut	Tower Leg	Main Slab
Single	108.58	8111.50	719.02
Multiple	183.17	11409.00	698.51

Fig. 5.85 Comparison of Vertical Displacements from Tower Configuration Study

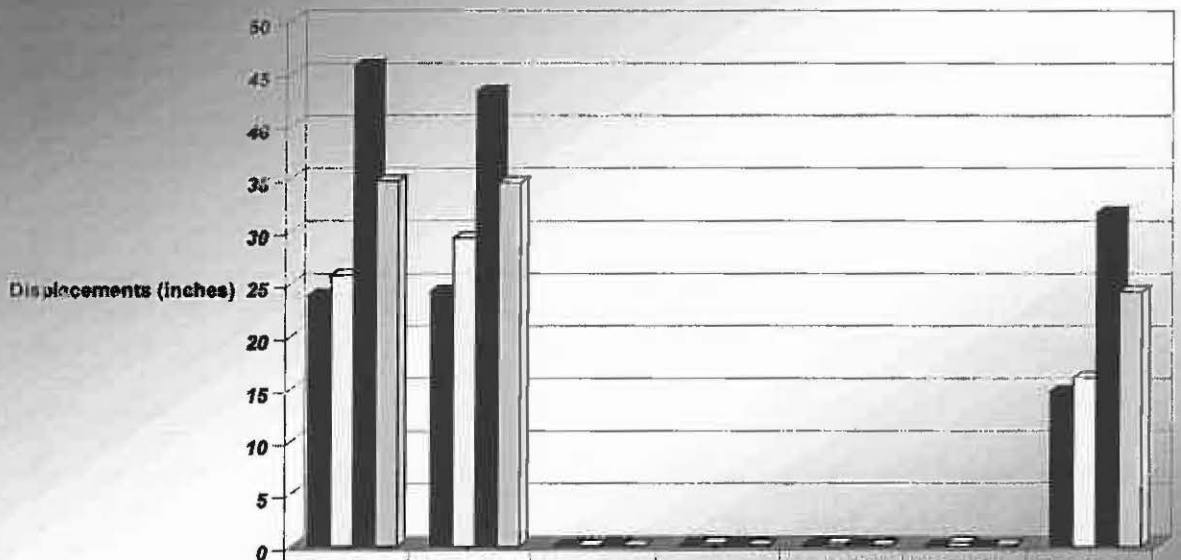

	Main Span Center 1	Cable Joint 2	Lower Strut Joint 3	Tower Top 4	Cable Joint 5	Upper Strut Joint 6	Side Span Center 7
■ Composite	23 866	24 282	7 31E-02	0 1126	0 11258	8 65E-02	14 727
□ A-shape	25 801	29 322	7 56E-02	0 27302	0 30219	0 40415	16 019
■ Slab	45 77	43 241	9 73E-02	0 11472	0 11472	8 11E-02	31 73
□ A-slab	34 716	34 553	6 30E-02	0 11446	0 11843	0 1341	24 204

Nodes

Fig. 5.86 Comparison of Horizontal Displacements from Tower Configuration Study

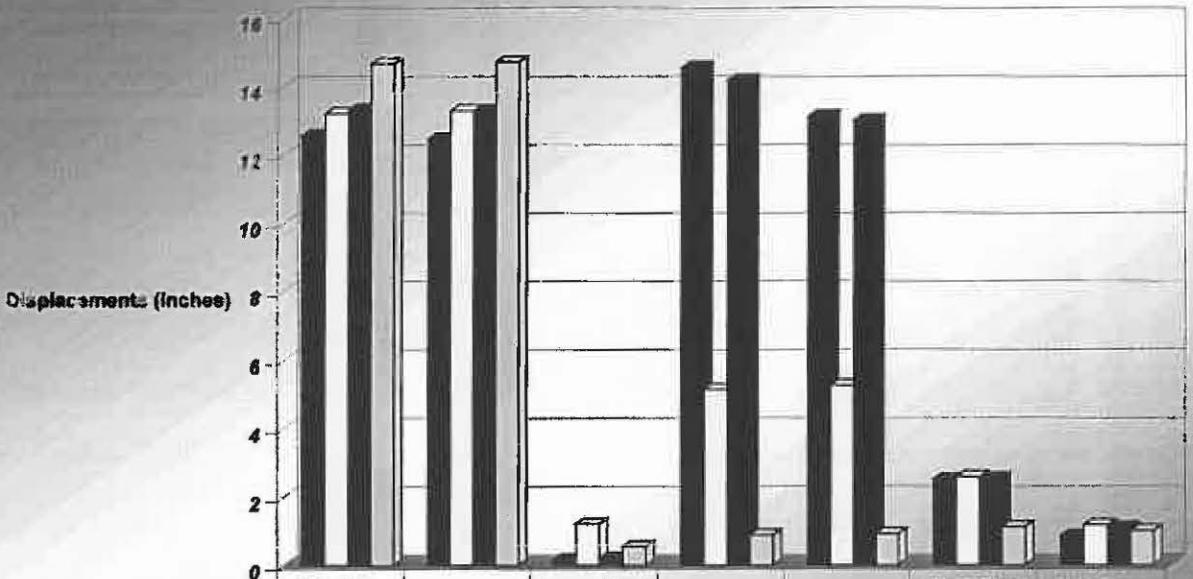

	Main Span Center 1	Cable Joint 2	Lower Strut Joint 3	Tower Top 4	Cable Joint 5	Upper Strut Joint 6	Side Span Center 7
■ Composite	12 565	12 473	0.14411	14 557	13 135	2.5114	0 85906
□ A-shape	13 209	13 29	1 2101	5 1319	5 2544	2 5826	1 1618
■ Slab	13 321	13 299	0 20045	14 19	13 013	2 5466	1 0909
□ A-slab	14 667	14 731	0 54036	0 8744	0 90973	1 1127	0 99445

Nodes

Fig. 5.87 Comparison of Longitudinal Displacements from Tower Configuration Study

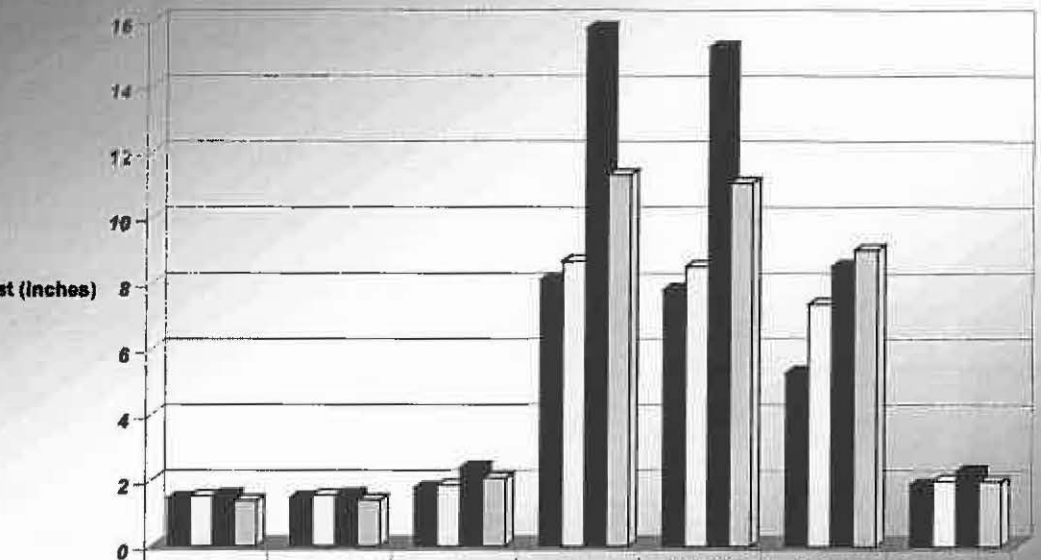

	Main Span Center 1	Cable Joint 2	Lower Strut Joint 3	Tower Top 4	Cable Joint 5	Upper Strut Joint 6	Side Span Center 7
Composite	1.4541	1.4726	1.7733	8.1047	7.8068	5.2852	1.8794
A-shape	1.5194	1.5467	1.8545	8.6704	8.5056	7.3676	1.9941
Slab	1.5585	1.5668	2.3867	15.765	15.163	8.5281	2.2939
A-slab	1.3816	1.3946	2.0632	11.277	11.032	9.0052	1.9754

Nodes

Fig. 5.88 Comparison of Vertical Response Displacements from Cable Area Study

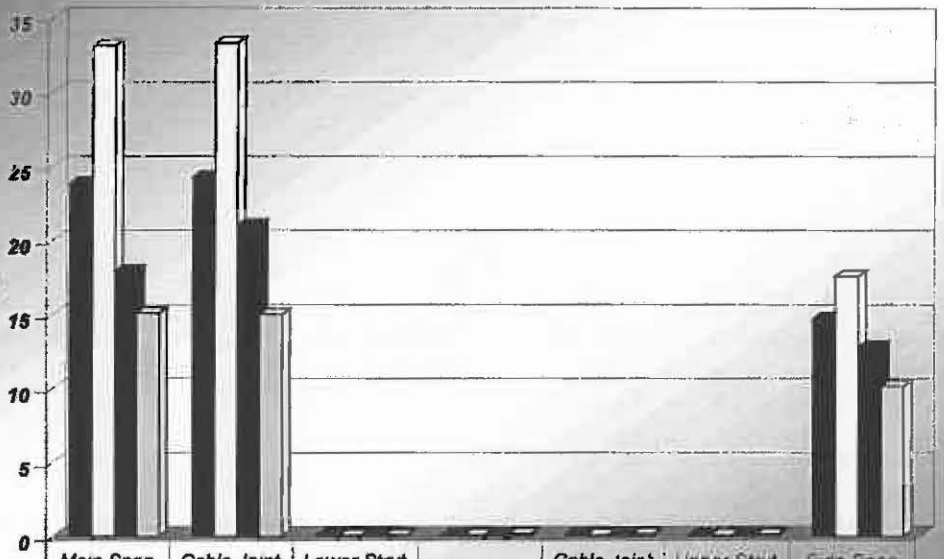

	Main Span Center 1	Cable Joint 2	Lower Strut Joint 3	Tower Top 4	Cable Joint 5	Upper Strut Joint 6	Side Span Center 7
Normal Area	23.866	24.282	7.31E-02	0.1126	0.11258	8.65E-02	14.727
Half Area	33.136	33.336	7.22E-02	9.79E-02	9.79E-02	7.96E-02	17.61
Double Area	17.97	21.064	7.76E-02	0.15242	0.15242	0.11566	12.825
Triple Area	15.085	15.005	9.05E-02	0.16647	0.16645	0.1361	10.172

Nodes

Fig. 5.89 Comparison of Horizontal Response Displacements from Cable Area Study

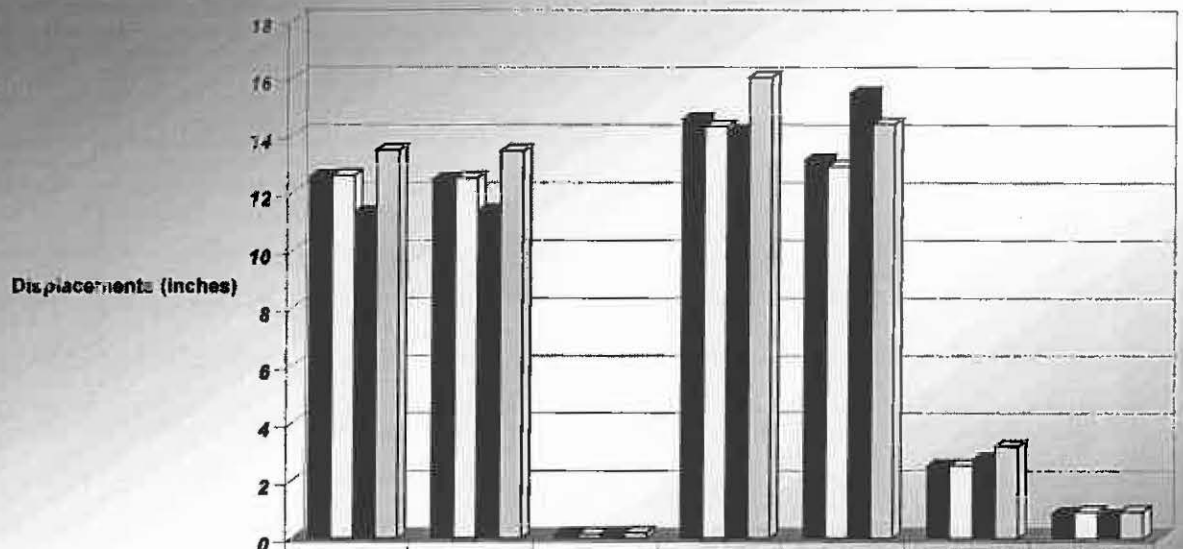

	Main Span Center 1	Cable Joint 2	Lower Strut Joint 3	Tower Top 4	Cable Joint 5	Upper Strut Joint 6	Side Span Center 7
Normal Area	12 565	12 473	0 14411	14 557	13.135	2 5114	0 85906
Half Area	12 6	12 53	0 14474	14 294	12 906	2 5269	0 92319
Double Area	11 335	11 395	0 15678	14 136	15 452	2 7508	0 79528
Triple Area	13 475	13 444	0 18729	16 008	14 374	3 2001	0 93596

Nodes

Fig. 5.90 Comparison of Longitudinal Response Displacements from Cable Area Study

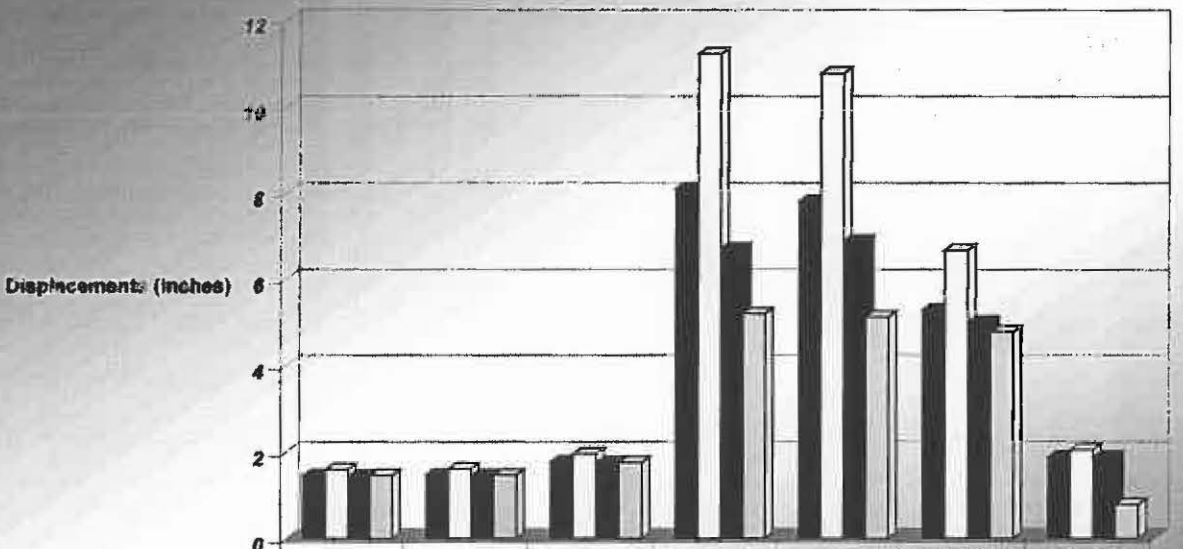

	Main Span Center 1	Cable Joint 2	Lower Strut Joint 3	Tower Top 4	Cable Joint 5	Upper Strut Joint 6	Side Span Center 7
Normal Area	1 4541	1 4726	1 7733	8 1047	7 8068	5 2852	1 8794
Half Area	1 5907	1 6079	1 9483	11 215	10 768	6 6765	2 0446
Double Area	1 4386	1 4571	1 7559	6 7129	6 8938	5 0067	1 8693
Triple Area	1 4587	1 4666	1 7571	5 1927	5 1197	4 7765	0 7841

Nodes

Fig. 5.91 Comparison of Cable Forces from Cable Area Study

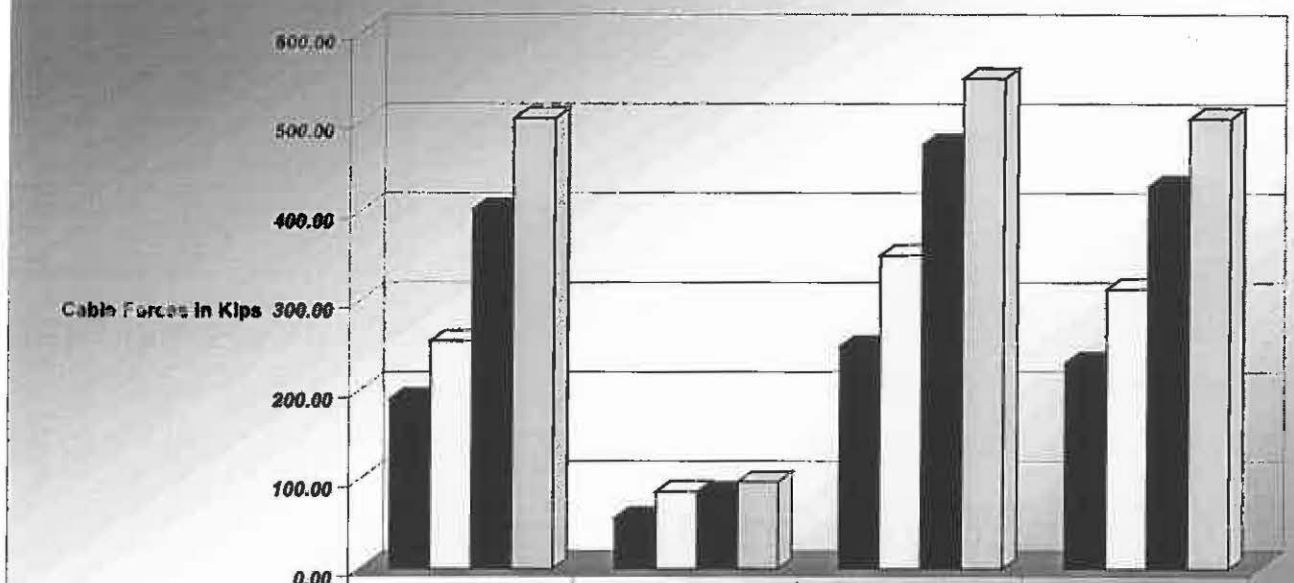

	Long Cable	Short Cable	Max Main Cable	Max Side Cable
Half Area	190 50	57 07	248 90	230 68
Normal Area	255 15	86 43	350 55	313 05
Double Area	402 16	85 45	474 24	428 29
Triple Area	503 69	97 20	548 82	503 60

Elements

Fig. 5.92 Comparison of Member Forces from Cable Area Study

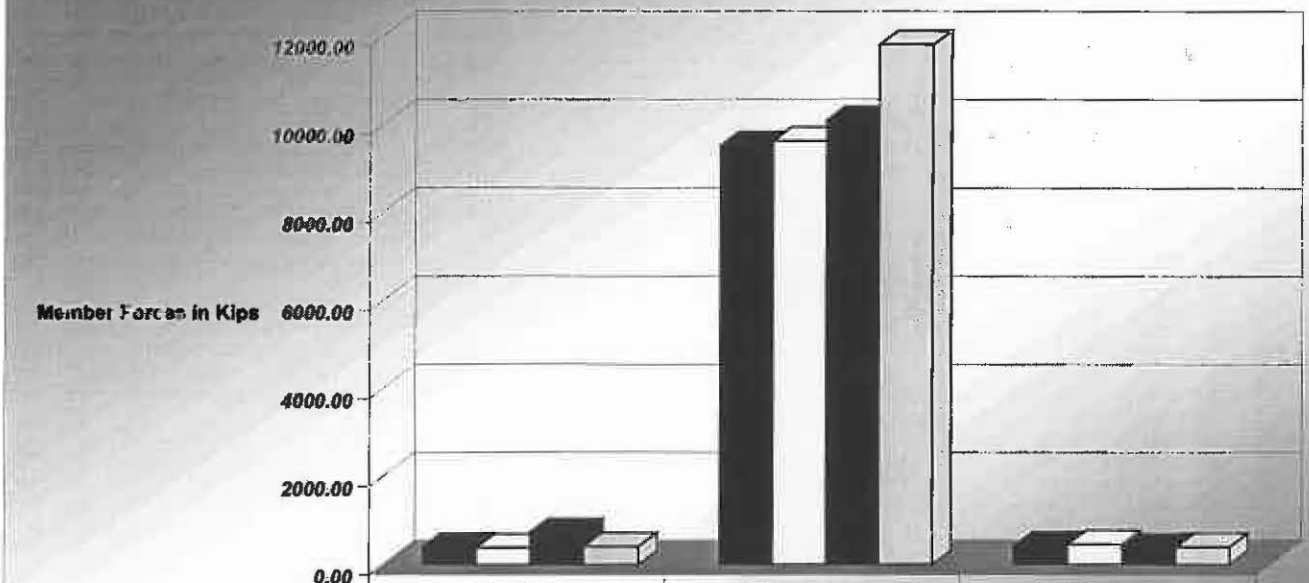

	Top Strut	Tower Leg	Main Slab
Half Area	402 59	9508 70	417 07
Normal Area	380 75	9611 40	454 06
Double Area	732 05	10084 00	379 01
Triple Area	406 31	11793 00	388 15

Elements

Fig. 5.93 Comparison of Bending Moments from Cable Area Study

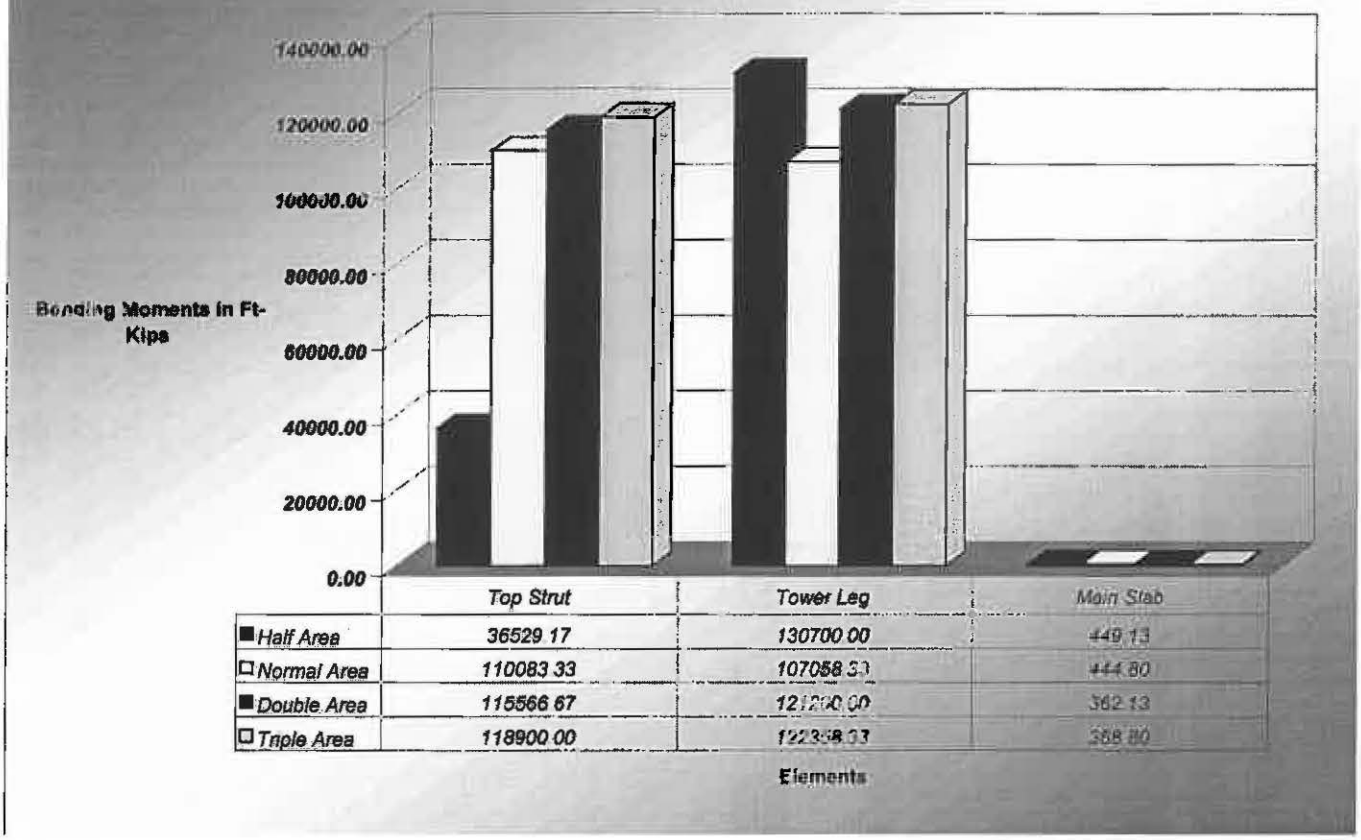

	Top Strut	Tower Leg	Main Slab
Half Area	36529 17	130700 00	449 13
Normal Area	110083 33	107058 33	444 80
Double Area	115566 67	121200 00	362 13
Triple Area	118900 00	122338 33	368 80

Elements

Fig. 5.94 Comparison of Vertical Response Displacements from Material Property Study

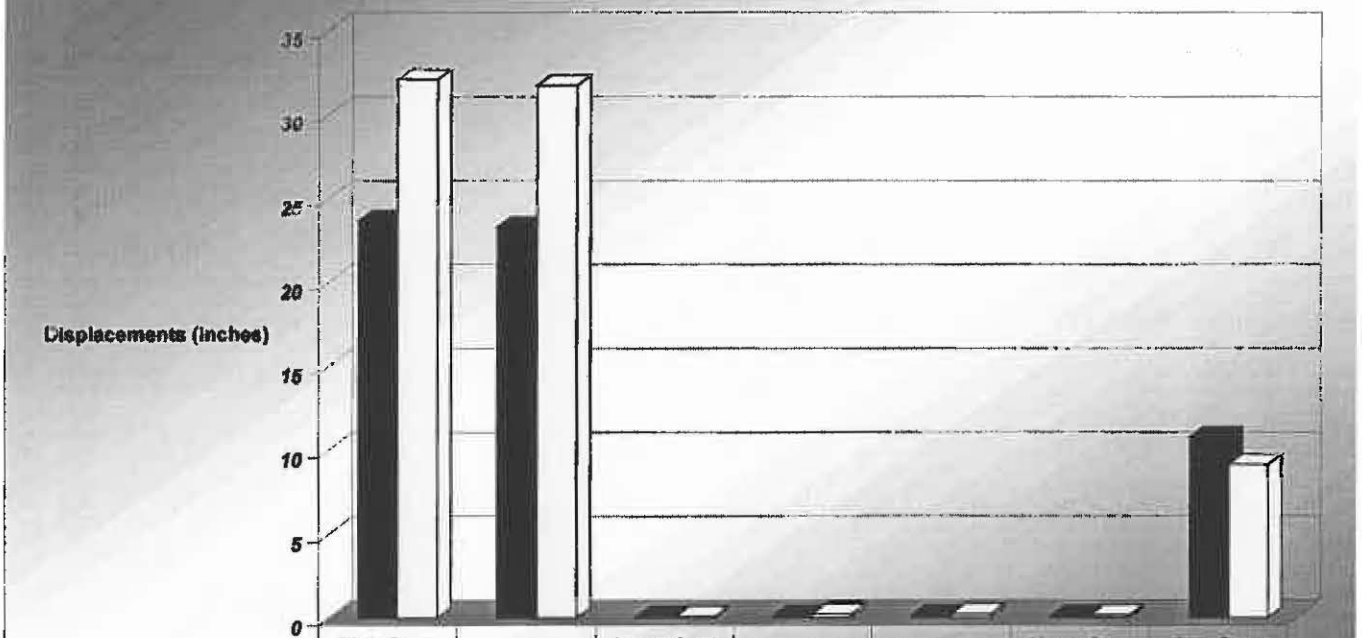

	Main Span Center 1	Cable Joint 2	Lower Strut Joint 3	Tower Top 4	Cable Joint 5	Upper Strut Joint 6	Side Span Center 7
Concrete	23 669	23 312	8 98E-02	0.14401	0 14401	0.1251	10.769
Steel	32 076	31 714	8 97E-02	0 22586	0 22586	0 18427	9.117

Nodes

Fig. 5.95 Comparison of Horizontal Response Displacements from Material Property Study

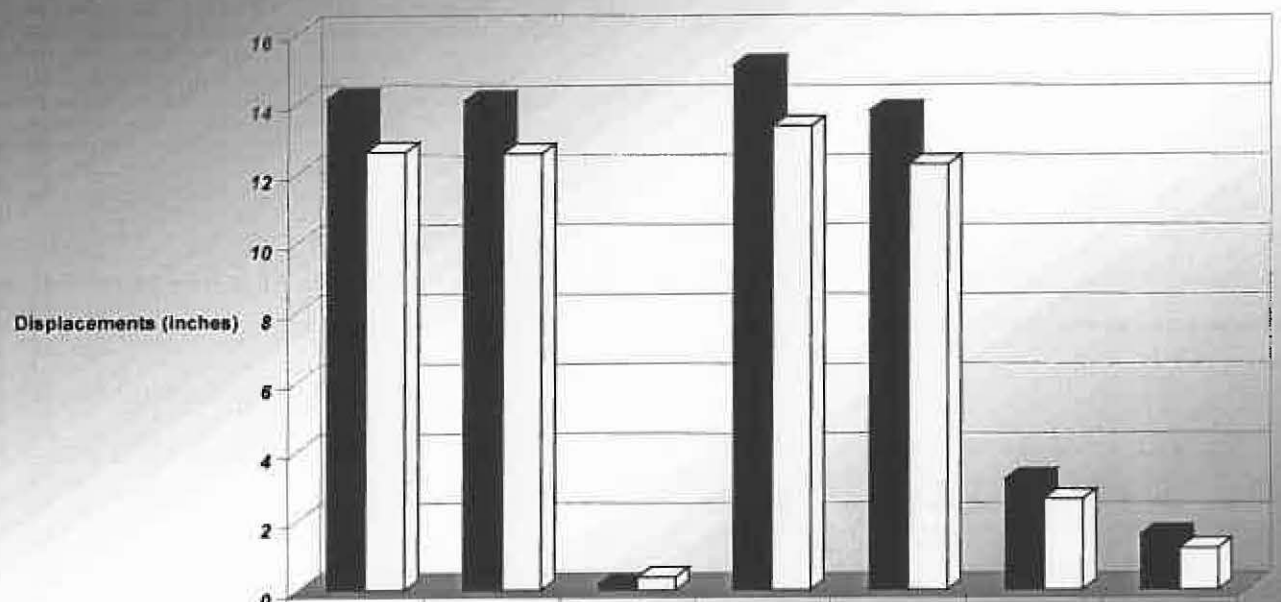

	Main Span Center 1	Cable Joint 2	Lower Strut Joint 3	Tower Top 4	Cable Joint 5	Upper Strut Joint 6	Side Span Center 7
Concrete	14.134	14.061	0.19014	15.081	13.763	3.1928	1.5972
Steel	12.577	12.532	0.37086	13.312	12.212	2.605	1.1041

Nodes

Fig. 5.96 Comparison of Longitudinal Response Displacements from Material Property Study

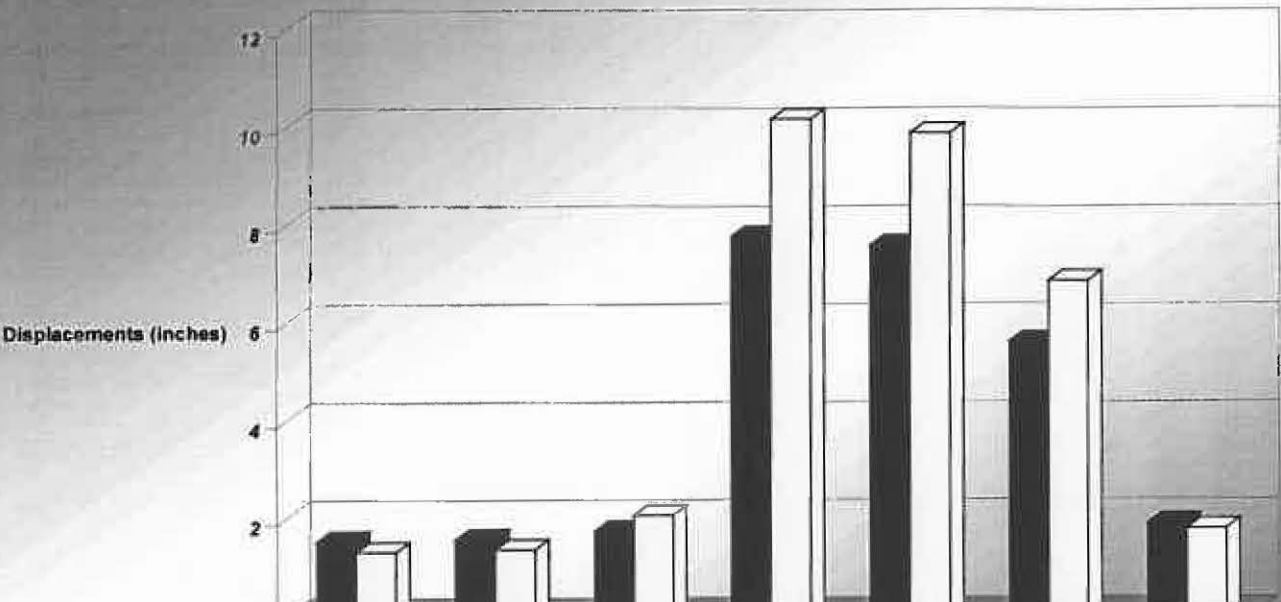

	Main Span Center 1	Cable Joint 2	Lower Strut Joint 3	Tower Top 4	Cable Joint 5	Upper Strut Joint 6	Side Span Center 7
Concrete	1.5214	1.5551	1.7265	7.7444	7.5612	5.5847	1.8712
Steel	1.2999	1.3509	2.0444	10.126	9.8491	6.8303	1.7605

Nodes

Fig. 5.97 Comparison of Vertical Displacements from Slab Thickness Study

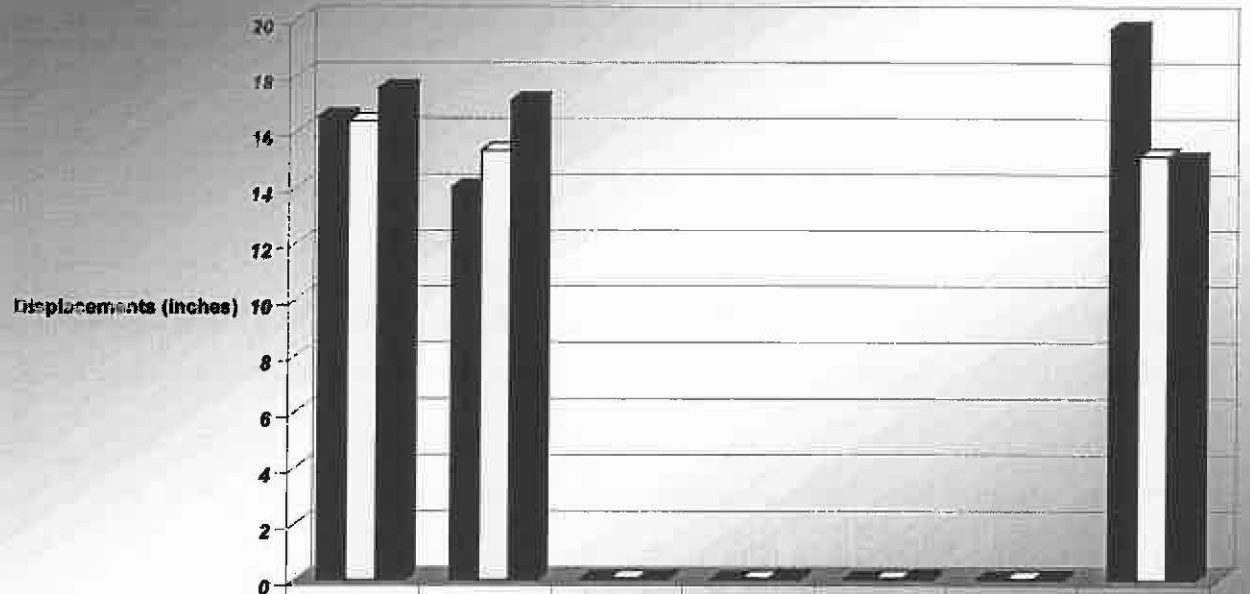

	Main Span Center 1	Cable Joint 2	Lower Strut Joint 3	Tower Top 4	Cable Joint 5	Upper Strut Joint 6	Side Span Center 7
Slab-14	16 538	14 003	6 87E-02	5 58E-02	5 58E-02	4 36E-02	19 672
Slab-18	16 363	15 323	6 98E-02	6 67E-02	6 67E-02	5 04E-02	15 124
Slab-25	17 554	17 118	7.29E-02	8 36E-02	8 36E-02	6 17E-02	15 008

Nodes

Fig. 5.98 Comparison of Horizontal Displacements from Slab Thickness Study

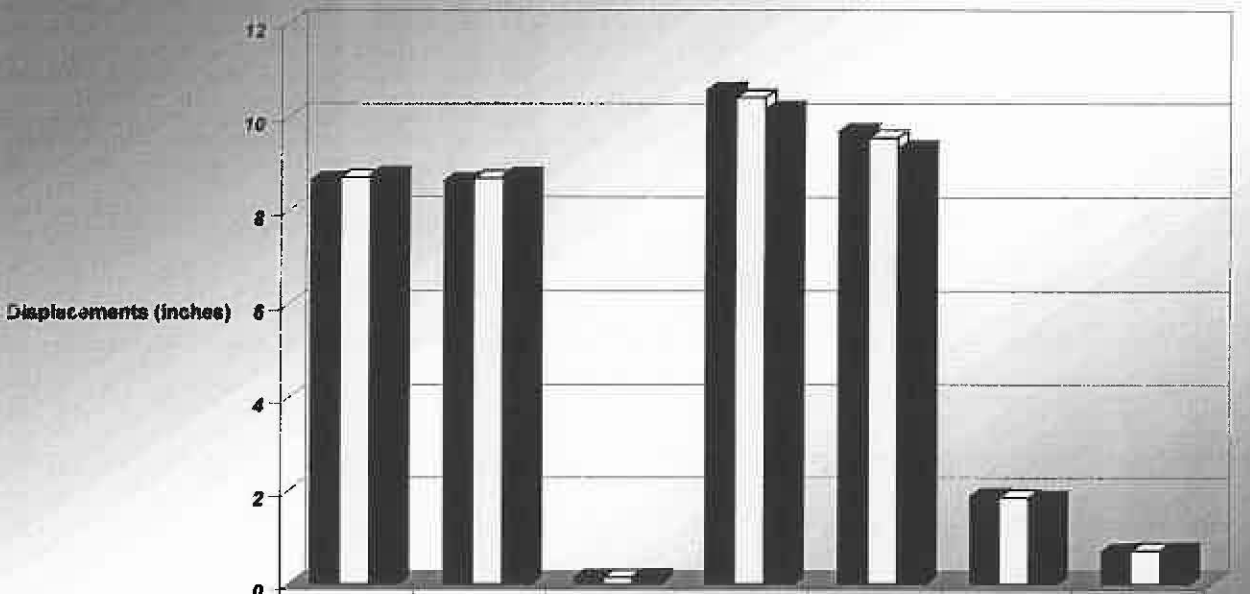

	Main Span Center 1	Cable Joint 2	Lower Strut Joint 3	Tower Top 4	Cable Joint 5	Upper Strut Joint 6	Side Span Center 7
Slab-14	8 6552	8 6357	0 13923	10 57	9 6914	1 8812	0 69213
Slab-18	8 7024	8 6878	0 14311	10 417	9 5524	1 8622	0 71334
Slab-25	8 7649	8 7539	0 1534	10 172	9 329	1 8341	0 72623

Nodes

Fig. 5.99 Comparison of Longitudinal Displacements from Slab Thickness Study

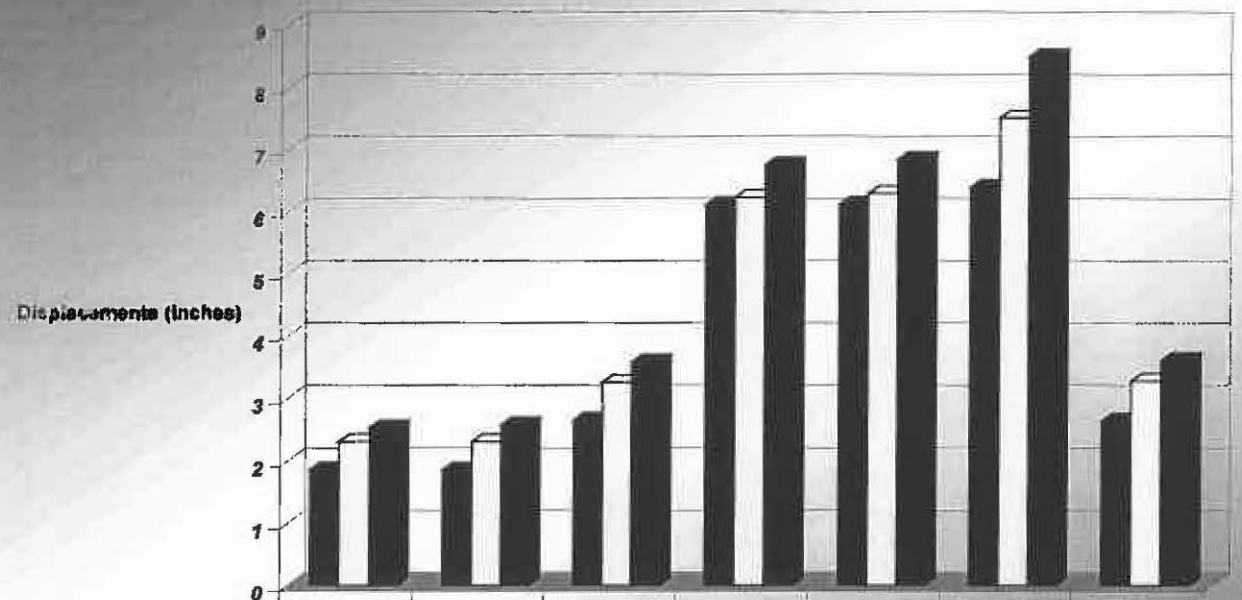

	Main Span Center 1	Cable Joint 2	Lower Strut Joint 3	Tower Top 4	Cable Joint 5	Upper Strut Joint 6	Side Span Center 7
Slab-14	1.8622	1.8588	2.653	6.1125	6.1164	6.3931	2.6472
Slab-18	2.3103	2.306	3.2559	6.2325	6.295	7.5122	3.2766
Slab-25	2.5332	2.5779	3.5621	6.7523	6.8396	8.4997	3.6154

Nodes

Fig. 5.100 Comparison of Vertical Displacements from Tower Bearing Study

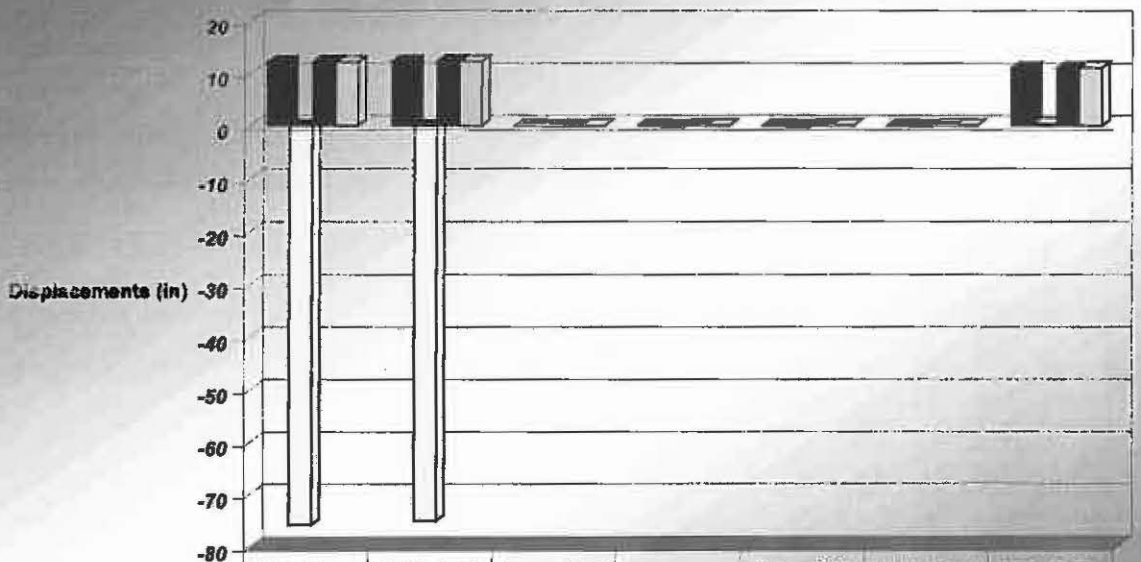

	Main Span Center 1	Cable Joint 2	Lower Strut Joint 3	Tower Top 4	Cable Joint 5	Upper Strut Joint 6	Side Span Center 7
Composite	12.191	12.318	5.50E-02	8.79E-02	8.79E-02	6.83E-02	11.028
Static-Movable	-75.715	-74.963	-4.62E-02	-0.34053	-0.34039	-0.22575	0.37767
Fixed	12.201	12.335	5.43E-02	8.71E-02	8.71E-02	6.71E-02	11.042
Movable	12.123	12.246	5.50E-02	8.79E-02	8.79E-02	6.84E-02	11.119

Nodes

Fig. 5.101 Comparison of Horizontal Displacements from Tower Bearing Study

	Main Span Center 1	Cable Joint 2	Lower Strut Joint 3	Tower Top 4	Cable Joint 5	Upper Strut Joint 6	Side Span Center 7
■ Half-Fixed	8 5629	8 4999	0 10769	11 06	9 9767	1 9042	0 58648
□ Static-Movable	-1 32E-03	2 61E-03	2 11E-02	-0 1558	-0 13815	-2 47E-03	-2 89E-04
■ Fixed	8 4615	8 3978	0 10199	10 964	9 8882	1 8571	0 58317
□ Movable	9 0135	8 9544	0.10858	11 051	9.9717	1 9063	0 53268

Nodes

Fig. 5.102 Comparison of Longitudinal Displacements from Tower Bearing Study

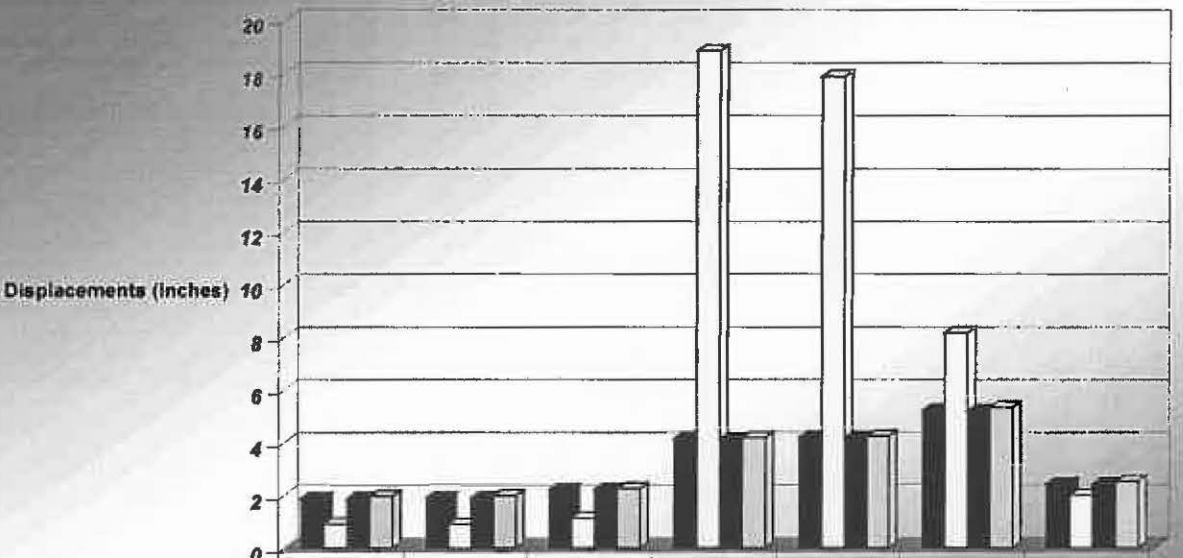

	Main Span Center 1	Cable Joint 2	Lower Strut Joint 3	Tower Top 4	Cable Joint 5	Upper Strut Joint 6	Side Span Center 7
■ Half-Fixed	1 8864	1 9099	2 2266	4 1518	4 1947	5 2248	2 4313
□ Static-Movable	0 91095	0 90982	1 1306	18 83	17 861	8 1711	1 957
■ Fixed	1 8774	1 9008	2 227	4 1336	4 1762	5 2072	2 4198
□ Movable	1 9548	1 9794	2.2424	4 1739	4 23	5 338	2 5165

Nodes

Fig. 5.103 Comparison of Cable Forces from Tower Bearing Study

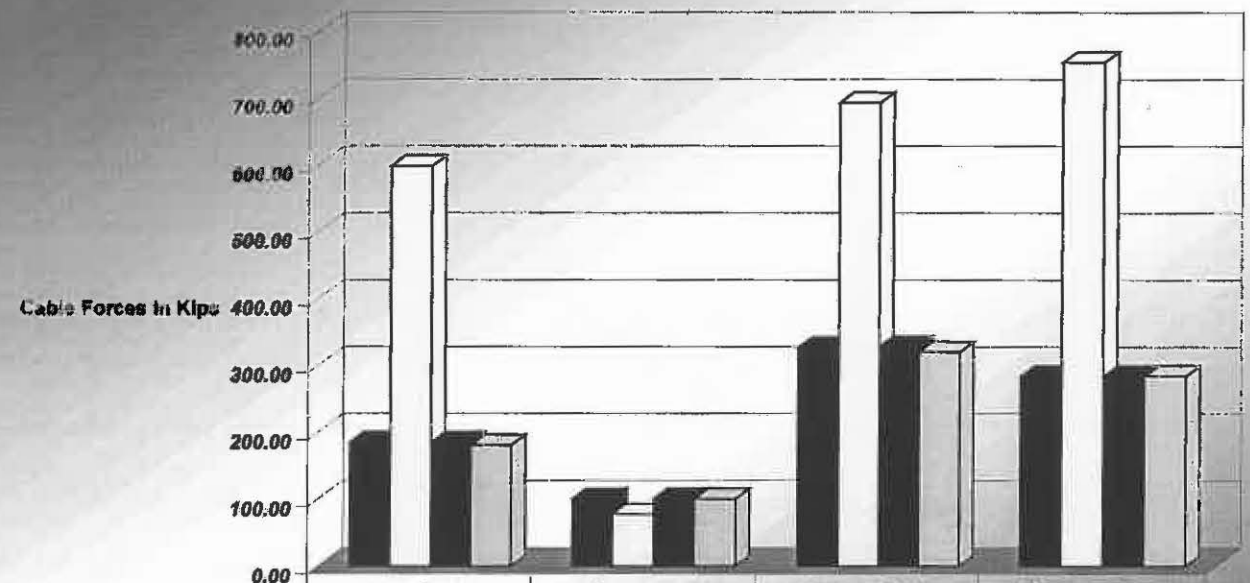

	Long Cable	Short Cable	Max Main Cable	Max Side Cable
Half-Fixed	184.33	99.825	328.03	283.20
Static-Movable	597.63	76.81	621.92	753.23
Fixed	184.47	99.93	327.17	283.19
Movable	180.33	99.70	319.12	283.67

Elements

Fig. 5.104 Comparison of Member Forces from Tower Bearing Study

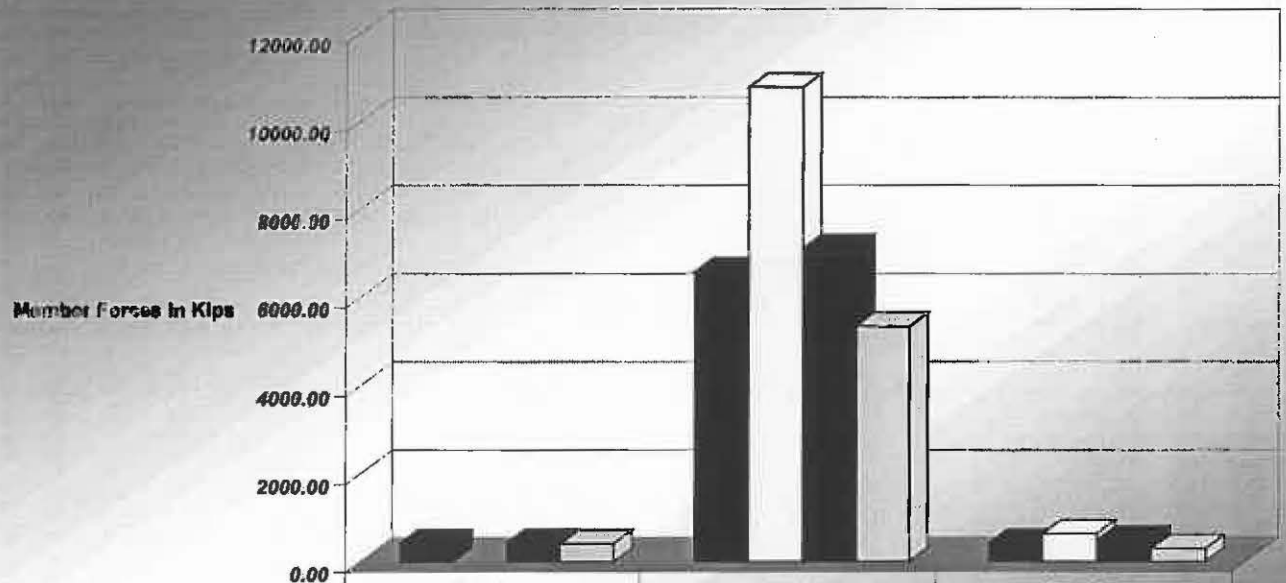

	Top Strut	Tower Leg	Main Slab
Half-Fixed	421.76	6583.00	420.11
Static-Movable		10783.00	630.04
Fixed	430.62	7114.10	489.45
Movable	408.80	5345.00	285.02

Elements

Fig. 5.105 Comparison of Bending Moments from Tower Bearing Study

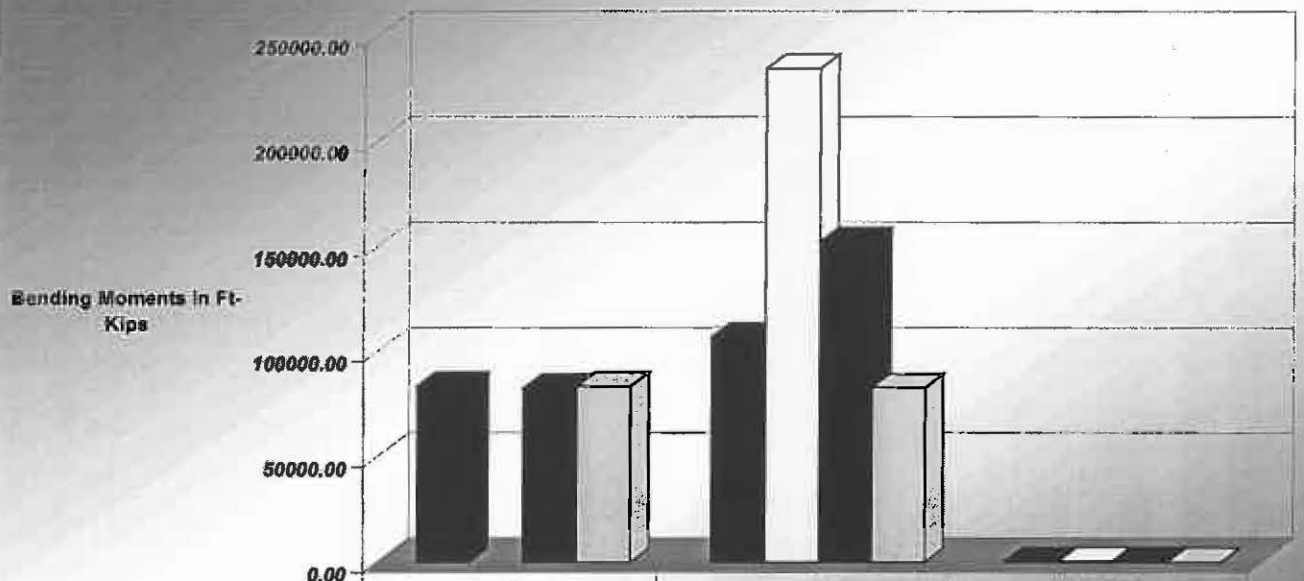

	Top Strut	Tower Leg	Main Slab
Half-Fixed	83566 67	107058 33	444 80
Static-Movable		234456 00	475 03
Fixed	82596 67	152208 33	492 04
Movable	83525 00	82841 00	238 00

Elements

Fig. 5.106 Comparison of Vertical Displacemenet from Abutment Constraints Study

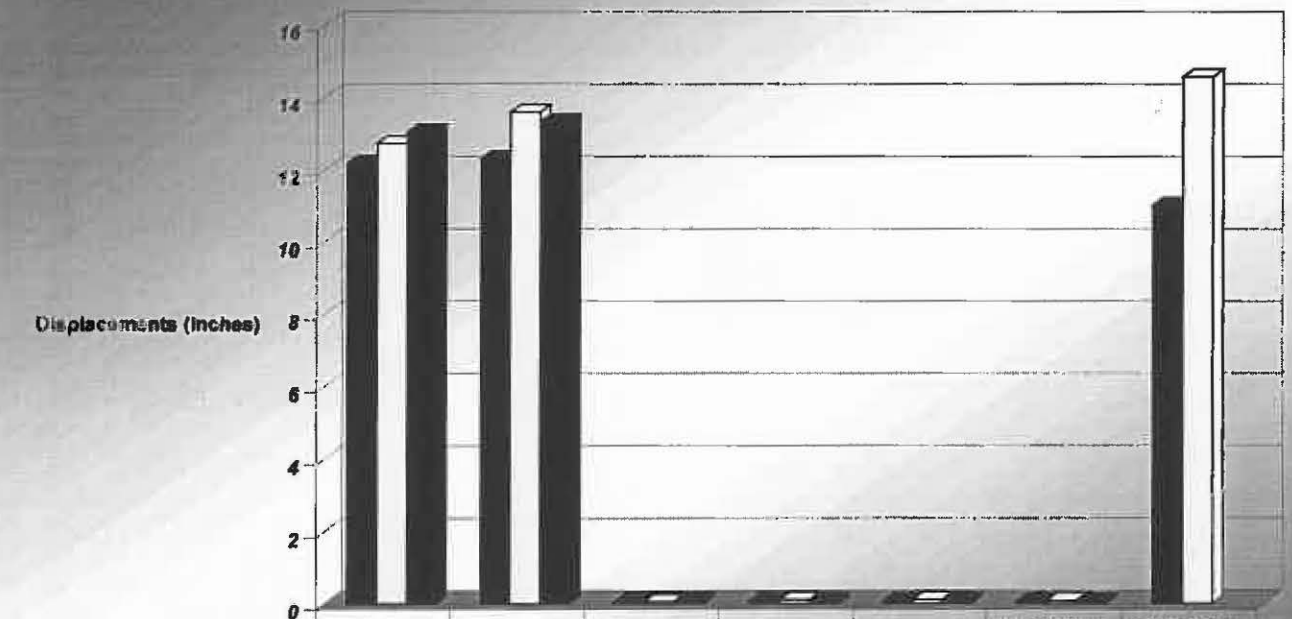

	Main Span Center 1	Cable Joint 2	Lower Strut Joint 3	Tower Top 4	Cable Joint 5	Upper Strut Joint 6	Side Span Center 7
Composite Free-Fixed	12 191	12 318	5 50E-02	8 79E-02	8 79E-02	8 83E-02	11 028
Composite Free	12 726	13 598	5 53E-02	0 10212	0 10271	7 54E-02	14 573
Composite Fixed	13 049	13 342	5 54E-02	8 62E-02	8 62E-02	6 71E-02	

Nodes

Fig. 5.107 Comparison of Horizontal Displacements from Abutment Constraints Study

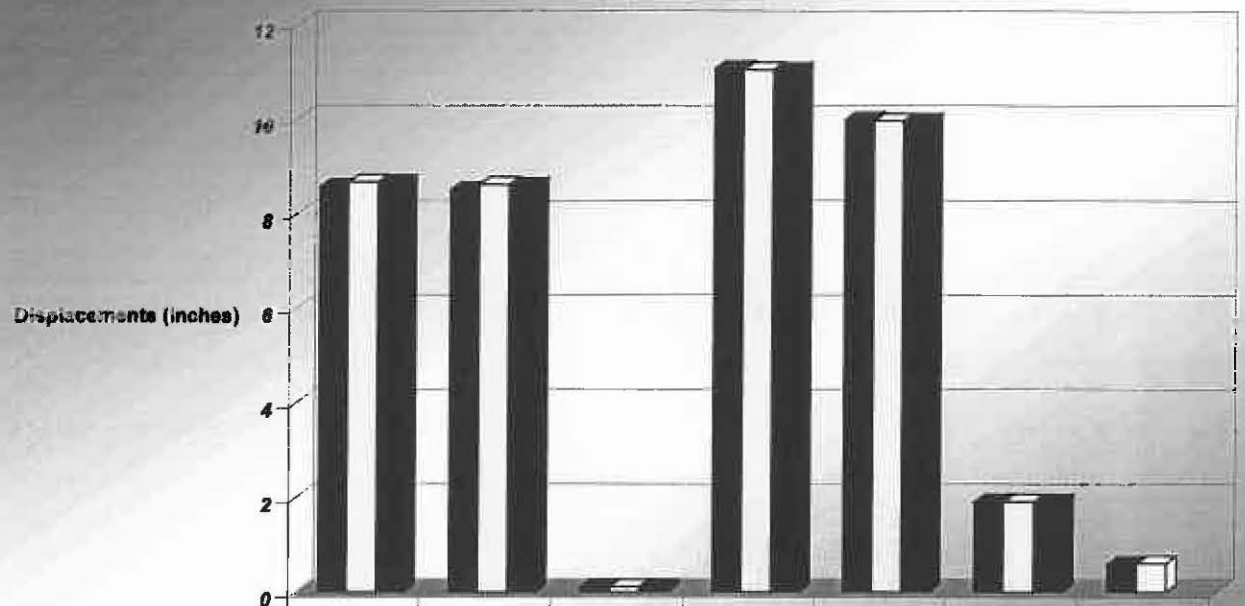

	Main Span Center 1	Cable Joint 2	Lower Strut Joint 3	Tower Top 4	Cable Joint 5	Upper Strut Joint 6	Side Span Center 7
Composite Free-Fixed	8.5629	8.4999	0.10769	11.06	9.9787	1.9042	0.58648
Composite Free	8.659	8.6081	0.10827	11.034	9.9564	1.9058	0.60082
Composite Fixed	8.655	8.5902	0.10896	11.025	9.9484	1.9024	

Nodes

Fig. 5.108 Comparison of Longitudinal Displacements from Abutment Constraints Study

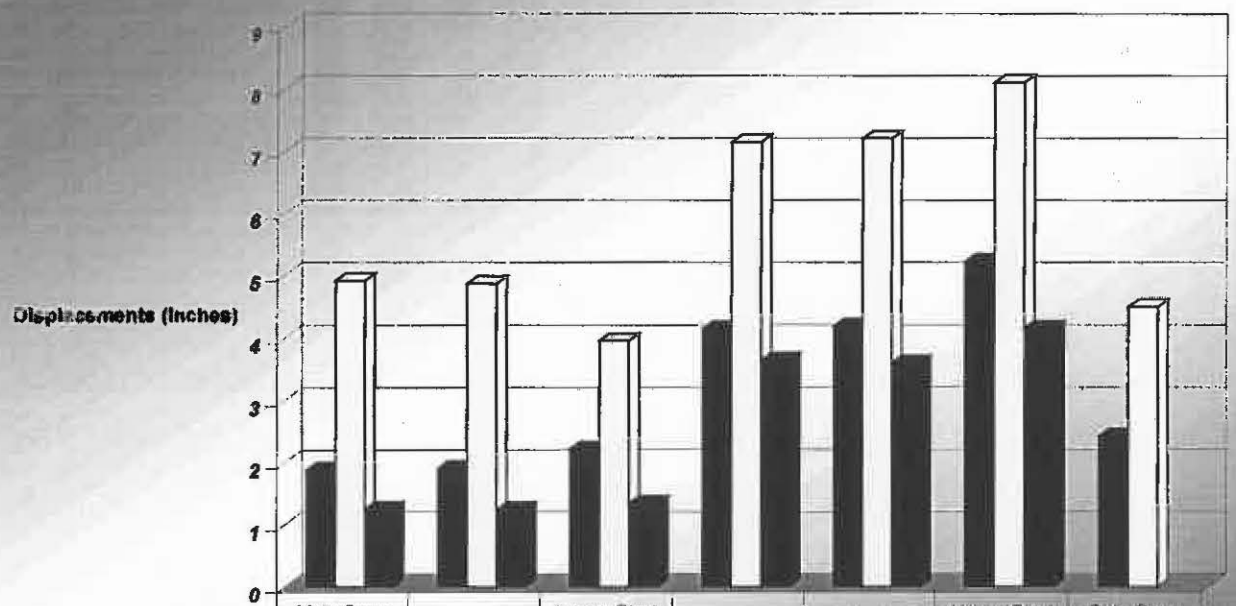

	Main Span Center 1	Cable Joint 2	Lower Strut Joint 3	Tower Top 4	Cable Joint 5	Upper Strut Joint 6	Side Span Center 7
Composite Free-Fixed	1.8864	1.9099	2.2266	4.1513	4.1947	5.2248	2.4313
Composite Free	4.9185	4.8714	3.9624	7.1527	7.2074	8.109	4.5
Composite Fixed	1.2573	1.246	1.349	3.6487	3.6032	4.1617	

Nodes

Fig. 5.109 Comparison of Cable Forces from Abutment Constraints Study

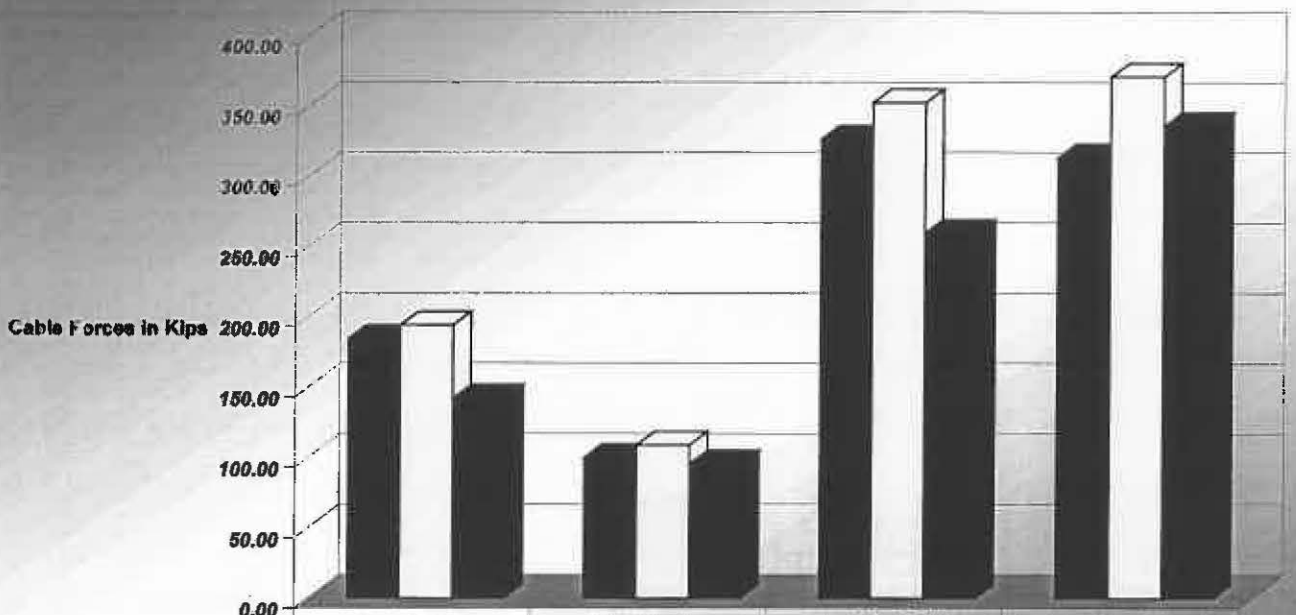

	Long Cable	Short Cable	Max Main Cable	Max Side Cable
Composite Free-Fixed	184.33	99.826	326.03	313.05
Composite Free	193.82	108.62	352.18	370.74
Composite Fixed	141.96	95.317	259.45	335.77

Elements

Fig 5.110 Comparison of Member Forces from Abutment Constraints Study

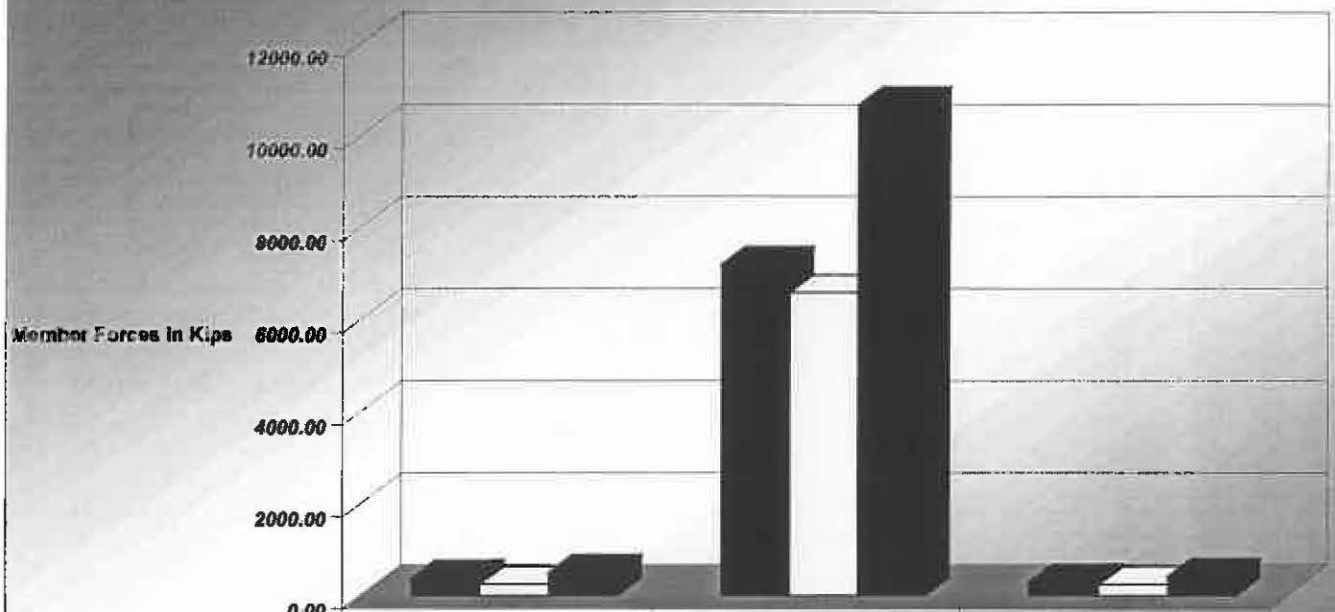

	Top Strut	Tower Leg	Main Slab
Composite Free-Fixed	380.75	7200.10	293.89
Composite Free	253.78	6563.00	245.09
Composite Fixed	507.41	10857.00	420.11

Elements

Fig 5.111 Comparison of Bending Moments from Abutment Constraints Study

	Top Strut	Tower Leg	Main Slab
Composite Free-Fixed	110083.33	107058.33	250.80
Composite Free	83475.00	86041.67	208.06
Composite Fixed	83400.00	181433.00	275.88

Elements

Fig. 5.112 Comparison of Vertical Displacements from Deck Study

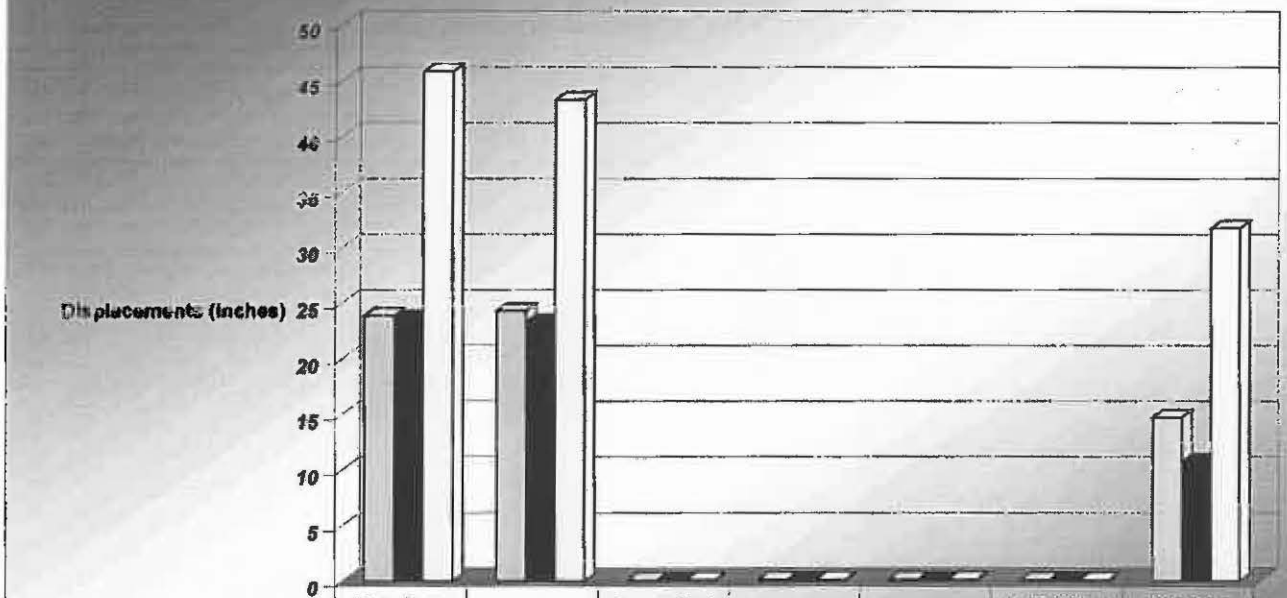

	Main Span Center 1	Cable Joint 2	Lower Strut Joint 3	Tower Top 4	Cable Joint 5	Upper Strut Joint 6	Side Span Center 7
Composite	23.866	24.282	7.31E-02	0.1126	0.11258	8.65E-02	14.737
Box	23.669	23.312	8.98E-02	0.14401	0.14401	0.1251	10.769
Slab	45.77	43.241	9.73E-02	0.11472	0.11472	8.11E-02	31.73

Nodes

Fig. 5.113 Comparison of Horizontal Displacements from Deck Study

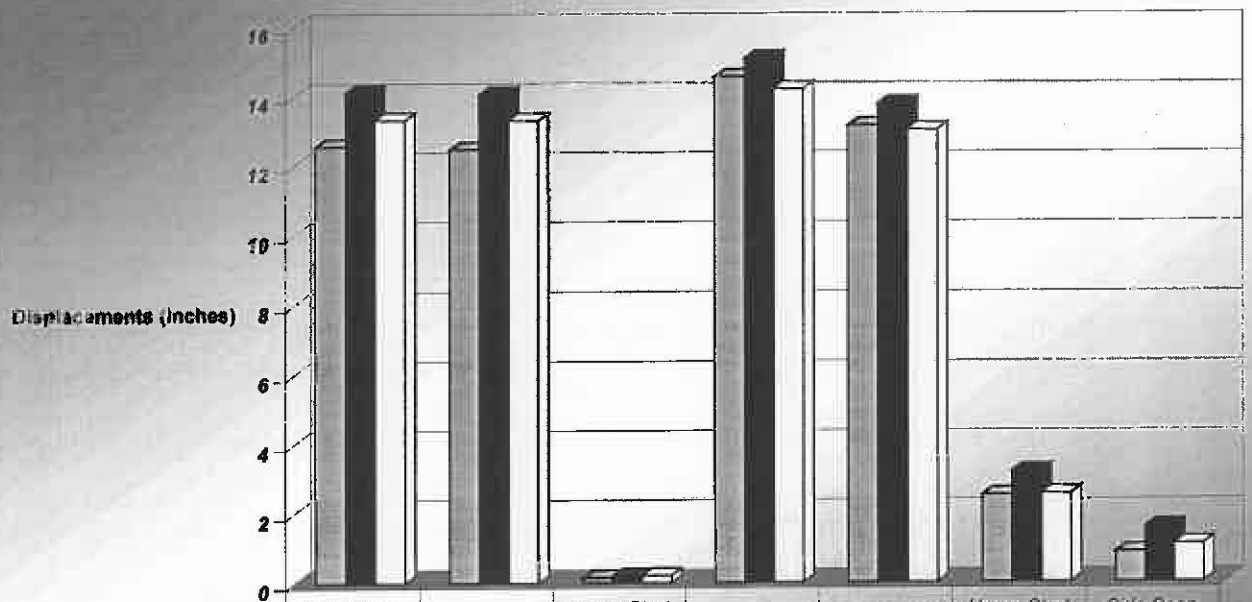

	Main Span Center 1	Cable Joint 2	Lower Strut Joint 3	Tower Top 4	Cable Joint 5	Upper Strut Joint 6	Side Span Center 7
Composite	12 565	12 473	0 14411	14 557	13 135	2 5114	0 85906
Box	14 134	14 061	0 19014	15 081	13 763	3 1928	1 5972
Slab	13 321	13 299	0 20045	14 13	13 013	2 5466	1 0906

Nodes

Fig. 5.114 Comparison of Longitudinal Displacements from Deck Study

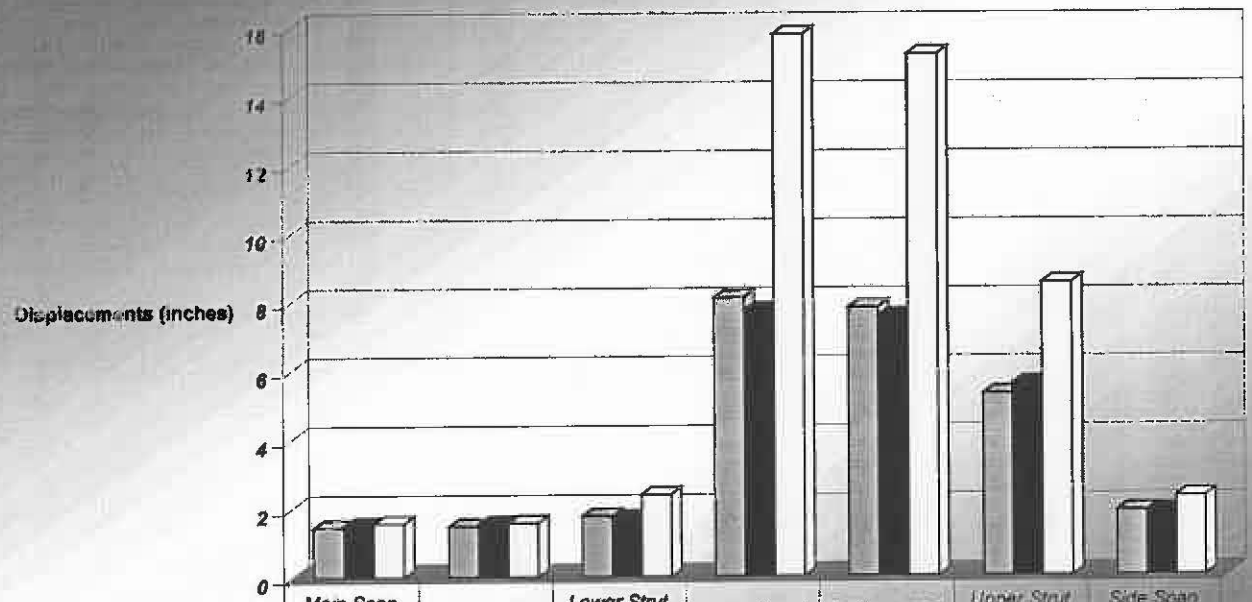

	Main Span Center 1	Cable Joint 2	Lower Strut Joint 3	Tower Top 4	Cable Joint 5	Upper Strut Joint 6	Side Span Center 7
Composite	1 4541	1 4726	1 7733	8 1047	7 8068	5 2852	1 8794
Box	1 5214	1 5551	1 7265	7 7444	7 5612	5 5847	1 8712
Slab	1 5585	1 5668	2 3867	15 765	15 183	8 5281	2 2939

Nodes

Fig. 5.115 Comparison of Cable Forces from Deck Study

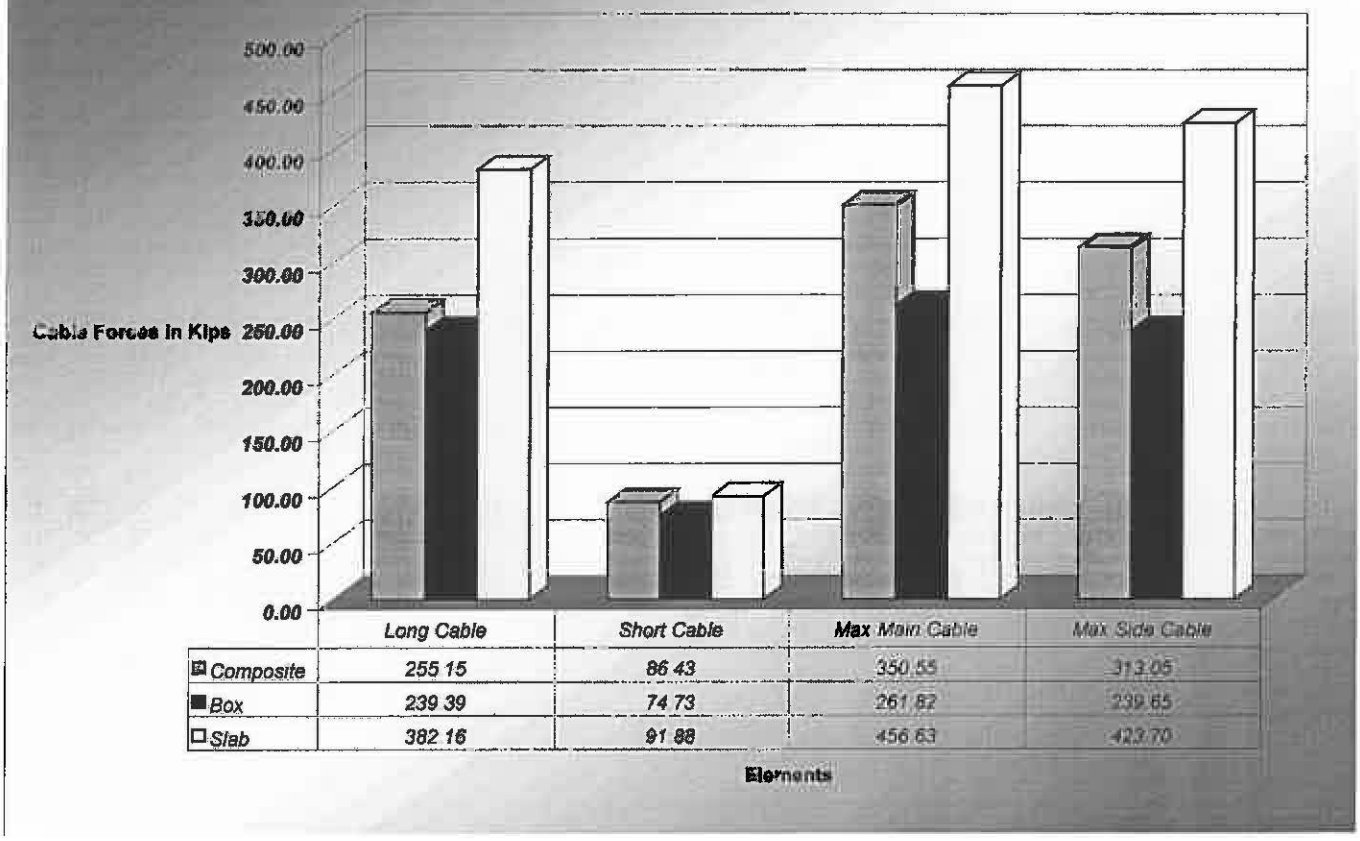

	Long Cable	Short Cable	Max Main Cable	Max Side Cable
Composite	255 15	86 43	350.55	313.05
Box	239 39	74 73	261 82	239.65
Slab	382 16	91 88	456 63	423.70

Fig. 5.116 Comparison of Member Forces from Deck Study

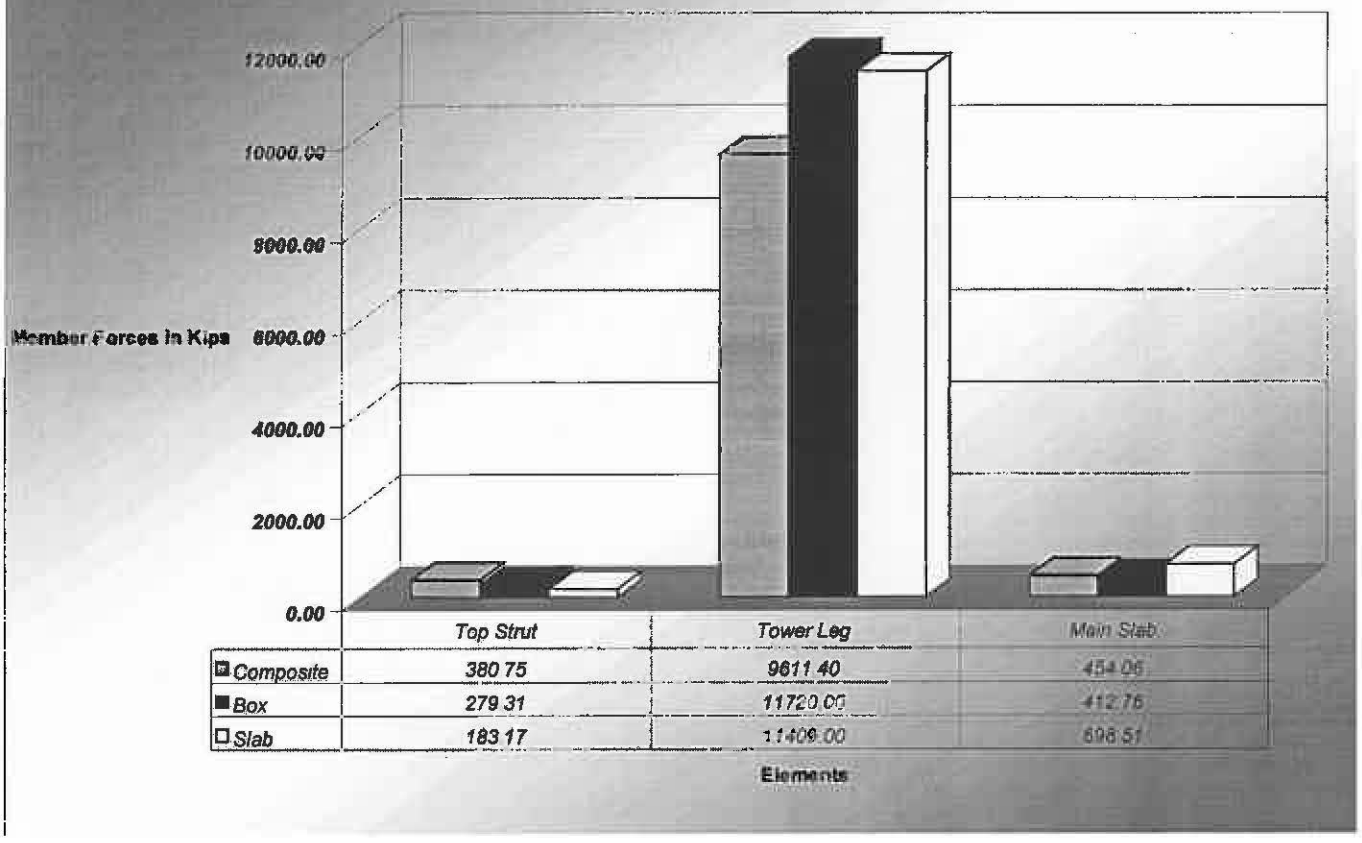

	Top Strut	Tower Leg	Main Slab
Composite	380 75	9611 40	454 06
Box	279 31	11720.00	412.76
Slab	183 17	11409.00	696 51

Fig. 5.117 Comparison of Bending Moments from Deck Study